Universidade Federal de Minas Gerais
Instituto de Ciências Biológicas

LUARA ISABELA DOS SANTOS

Estabelecimento de uma nova terapia antitumoral utilizando parasito transgênico expressando NY-ESO-1 associado ao bloqueio de CTLA-4

Belo Horizonte
2013

LUARA ISABELA DOS SANTOS

Estabelecimento de uma nova terapia antitumoral utilizando parasito transgênico expressando NY-ESO-1 associado ao bloqueio de CTLA-4

Tese apresentada ao Departamento de Bioquímica e Imunologia do Instituto de Ciências Biológicas da Universidade Federal de Minas Gerais, como requisito final para obtenção de título de Doutor em Ciências.

Área de concentração: Imunologia.

Orientador: Prof. Dr. Ricardo Tostes Gazzinelli

Co-orientadora: Dra. Lis Ribeiro do Vale Antonelli

Belo Horizonte

2013

Aos meus familiares e amigos, com carinho.

AGRADECIMENTOS

Gostaria de agradecer a todos que contribuíram de alguma forma para o andamento e finalização. Durante esses quatro anos, muitos passaram pelo meu caminho e vários tiveram contribuição importante neste trabalho. Vale ressaltar os seguintes, aos quais eu presto meus sinceros agradecimentos:

Meu orientador, Dr. Ricardo Gazzinelli, gostaria de agradecer por ter me recebido tão cordialmente em seu laboratório e por me disponibilizar a melhor infraestrutura possível. Também gostaria de agradecer por abrir um mundo novo perante aos meus olhos com os congressos internacionais e por todos os encontros com grandes pesquisadores. Obrigada pelos elogios a este trabalho, pelos puxões de orelha e por todos os conselhos e paciência quando eu nem conseguia fazer um gráfico decente! E, finalmente, agradeço a confiança em mim depositada e pela amizade durante esses anos. A realização desse projeto não foi fácil! Obrigada por tudo.

Minha co-orientadora Dra. Lis Antonelli, gostaria de agradecer por sua contribuição durante a realização desse trabalho, pelos ensinamentos e paciência durante minhas vastas citometria e análises. Tudo que sei de citometria devo à você! Obrigada por estar sempre disposta a discutir comigo todos os dados e os experimentos que eu gostaria de realizar, mesmo quando eu estava perdida. Obrigada pela valorosa amizade, principalmente nos momentos difíceis que enfrentei ao longo desse trabalho. Obrigada por ser uma luz no meu caminho em todos os aspectos da vida.

Ao meu braço direito Bruno Galvão-Filho por me ajudar a conduzir esse projeto, por partilhar comigo todas as alegrias e angústias durante o nosso caminho. Sem você esse trabalho não seria possível. Obrigada em especial também a minha amiga querida Paula Cristina por ser mais que uma colaboradora, a Miriam Dutra por toda a paciência, pelas discussões cientificas, por todos os comentários durante a escrita e pela amizade eterna. A Caroline Junqueira por ter aguentando todos os dias meus dias de TPM e fases pessoais,, pelos conselhos, por toda a companhia dentro e fora do lab, pela paciência e compreensão, pelo incentivo, e principalmente por toda a ajuda cientifica, psicológica e amizade durante todos esses anos.

As meninas do administrativo: Clécia, Lorena, Iara, Marina e Luciana por deixarem sempre o ambiente organizado para nosso trabalho e por me deixarem, na última horinha, acrescentar à lista de importação, aquele reagente indispensável! Obrigada.

Obrigada aos muitos colegas de laboratório: Marco Ataide, Isabella Hirako, Warrisson, Polidoro, Samantha, Barbara, Guilherme, Ana Beatriz, Marina, Natália, Suellen, Pedro, Thales, Marta, Igor pela ótima convivência e por deixarem o ambiente de trabalho tão agradável!

Meus melhores amigos Marcela, Marcelão, Dani, Ariana, Jordanna, Fred, Rafa, Pri, Lucas, Wendell, Andre e Thamis. Obrigada por segurarem as pontas quando precisei, por rirem comigo nos momentos de felicidade e por estarem, sempre presentes, longe ou perto. Obrigada por confiarem em mim, quando confiança me faltava e por fazerem pequenos os problemas, quando eles pareciam maiores do que eu. Vocês são indispensáveis para mim. Obrigada.

Meus familiares que sempre entenderam a minha ausência nas datas importantes, meus momentos de desespero e mau humor. Obrigada também por se alegrarem com minhas felicidade e conquistas. Gostaria de agradecer em especial a meus pais pelo esforço de me fornecerem a melhor educação que puderam. Minha irmã, pelo exemplo na vida científica e por ser no final das contas todo o meu saco de pancadas quando tudo dava errado e ao meu cunhado por sempre me dar suporte. Amo muito vocês.

Meu marido, Stéphano Farias, por estar ao meu lado durante todo o período e mesmo sem entender nada me apoiar sempre. Obrigada por aguentar minhas crises de humor, por me alimentar quando eu não queria nem sair da frente do computador e pela paciência para desenhar todas as células do jeito que eu queria. Te amo!!! A minha segunda família em especial a minha sogra que fez todas as promessas possíveis para que tudo se encaixasse.

Ao meu Deus, e nossa Senhora de Fátima por terem permitido ter fé em mim mesmo, na vida e na ciência mesmo quando nada parecia fazer sentido.
Muito obrigada!

"A vida está cheia de desafios que, se aproveitados de forma criativa, transformam-se em oportunidades." (Maxwell Maltz)

APRESENTAÇÃO

Essa tese foi realizada no departamento de Bioquímica e Imunologia do Instituto de Ciências Biológicas (ICB) da Universidade Federal de Minas Gerais (UFMG), no Centro de Pesquisas René Rachou (CPqRR), da Fundação Oswaldo Cruz (FIOCRUZ). Para a realização desse trabalho, contou-se com a orientação do professor Dr. Ricardo Tostes Gazzineli, do departamento de Bioquímica e Imunologia deste Instituto e a co-orientação da pesquisadora Lis Ribeiro do laboratório de Imunopatologia do CPqRR. Contamos com o suporte das seguintes instituições: Atlantic Philanthropies/Program of Clinical Discoveries a partir do Instituto Ludwig de Pesquisa sobre o Câncer, Fundação de Amparo a Pesquisa de Minas Gerais (FAPEMIG), Fundação Oswaldo Cruz, Instituto Nacional de Ciência e Tecnologia para Vacinas e Conselho Nacional de Desenvolvimento Científico e Tecnológico (CNPq).

RESUMO

O desenvolvimento da imunoterapia contra o câncer é um grande desafio. Embora vários estudos clínicos resultaram no desenvolvimento de resposta imune mensuráveis, apenas uma minoria dos pacientes obtiveram beneficio clínico, tal como a regressão tumoral. A utilização de uma cepa atenuada do *Trypanosoma cruzi* (CL-14) como vetor vacinal expressando o antígeno *cancer testis* NY-ESO-1 (CL-14-NY-ESO-1), proposta pelo nosso grupo, foi capaz de prevenir o crescimento do tumor em um modelo profilático. Neste trabalho nós elucidamos que o CL-14-NY-ESO-1 promove a formação de ambos linfócitos T $CD8^+$ de memória efetora e efetores, que impedem eficazmente o desenvolvimento do tumor. Além disso, o melhor prognóstico correlaciona com a alta produção das citocinas IFN-γ e IL-2 e a presença de maior número de células específicas contra o tumor, inclusive células com perfil citotóxico. No entanto, o efeito terapêutico de tal vacina é bastante limitado. A fim de prolongar a resposta efetora induzida pelo CL-14-NY-ESO-1 nós propomos, em um protocolo terapêutico, o bloqueio dos sinais inibitórios mediados pelo Antígeno Associado ao Linfócito T citotóxico-4 (CTLA-4). Os resultados demonstram o aumento da frequência das células T $CD8^+$ específicas contra o tumor, das células T produtoras de IFN-γ e ainda a promoção da migração dos linfócitos para o infiltrado tumoral. Como resultado, a terapia com CL-14-NY-ESO-1 associado com o anti-CTLA-4 é altamente eficaz no controle do desenvolvimento de melanoma em curso.

ABSTRACT

The development of immunotherapy for cancer has long been a challenge. Although multiple clinical trials have resulted in the development of measurable immune responses only a minority of patients has experienced clinical benefit, such as tumor regression. The use of a transgenic attenuated *Trypanosoma cruzi* strain (CL-14) as a vaccine vector expressing the *cancer testis* antigen NY-ESO-1 (CL-14-NY-ESO-1), proposed by our group, was able to prevent tumor growth in a vaccine model. Here we report that CL-14-NY-ESO-1 induces both memory effector and effector $CD8^+$ T lymphocytes that efficiently prevent tumor development. Additionally, the better prognosis correlates with the high production of cytokines IFN-γ and IL-2 and the presence of greater numbers of specific cells against tumor including cells with cytotoxic profile. However, the therapeutic effect of such vaccine is rather limited. To increase T cell response induced by transgenic parasite we propose, in therapeutic protocol, the blockade of inhibitory signals mediated by Cytotoxic T Lymphocyte-associated Antigen 4 (CTLA-4). The results show the enhanced of the frequency of NY-ESO-1-specific effector $CD8^+$ T cells producing IFN-γ, and promote lymphocyte migration to the tumor infiltrate. As a result, therapy with CL-14-NY-ESO-1 associated with anti-CTLA-4 is highly effective in controlling the development of an ongoing melanoma.

SUMÁRIO

LISTA DE ABREVIATURAS

Ag	Antígeno
B.O.D	Estufa de demanda bioquímica de oxigênio
BCG	Bacilo Calmette-Guérin
CD	Domínio clonal
$CD8^+T_E$	células T CD8 efetoras
$CD8^+T_{EM}$	células T CD8 de memória efetora
$CD8^+T_{CM}$	células T CD8 de memória central
cDNA	Ácido desoxirribonucleico complementar
CEBIO	Centro de bioterismo de produção animal
CETEA	Comitê de ética em experimentação animal
CpG	Citosina-fósforo-guanina
CSF1	Fator estimulador de macrófagos-1
CTA	Antígeno *cancer testis*
CTLA-4	Antígeno associado ao linfócito T citotóxico-4
DC	Célula dendrítica
DNA	Ácido desoxirribonucleico
EGF	Fator crescimento epidermal
ELISA	Ensaio imunoenzimático
ELISPOT	*Enzyme-linked immunosorbent spot*
EYFP	Proteína fluorescente amarela
FGF1	Fator crescimento fibroblasto-1
GIPL	Glicoinositol-fosfolípides
gp100	glicoproteína 100
gp63	glicoproteína de 63 quilo dalton
gzmB	Granzima B
IARC	Agência Internacional para a Pesquisa do Câncer
IFN-γ	Interferon
IL	Interleucina
iNOS	Enzima óxido nítrico sintase
kDa	Quilo Dalton

LIT	Linfócitos infiltrados no tumor
LTCs	Linfócitos T citotóxicos
M1/M2	Macrófagos tipo 1/tipo2
MPL	Monofosforil lipídeo A
mRNA	Ácido ribonucleico mensageiro
NK	Células matadoras naturais
ODN	Oligodeoxinucleotídeo
Pam3Cys	Lipopeptídeo sintético
PBS	Tampão salina fosfato
PD-1	Proteína morte programada-1
R10	Meio RPMI contendo antibióticos e 10% SFB
rNY-ESO-1	Proteína recombinante NY-ESO-1
SFB	Soro fetal bovino
ssRNA	Acido ribonucleico fita simples
TAMs	Macrófagos associados a tumor
TGF-β1	Fator de crescimento transformante-β1
Th1/Th2	Resposta auxiliadora tipo 1/tipo2
TLR	Receptores do tipo Toll
TNF	Fator de necrose tumoral
Treg	Célula T regulatória
VEGF	Fator de crescimento vascular endotelial

LISTA DE FIGURAS E TABELA

1. Introdução

1.1. A história do câncer até os dias atuais

O câncer é uma condição patológica que acomete milhares de indivíduos a cada ano e que atinge a espécie humana desde tempos remotos. O relato mais antigo da doença foi feito por volta de 3000 a.C., em um papiro egípcio chamado Edwin Smith Papiro, parte integrante de um livro egípcio em cirurgia do trauma. Ele descreve oito casos de tumores ou úlceras na mama que foram tratadas pela cauterização com uma ferramenta chamada broca de fogo. A conclusão final sobre o relato dessa doença foi "não há nenhum tratamento" (Acs, 2012).

A origem do termo câncer é atribuída ao médico grego Hipócrates (460- 370 a.C.). Considerado o 'pai da medicina' ele usou os termos *carcinos* e *carcinoma* para descrever tumores devido a semelhança dos vasos sanguíneos desses com o formato das patas dos caranguejos. Em 28-50 a.C., o médico romano Celsus, traduziu o termo grego para câncer, a palavra latina para caranguejo. Posteriormente, Galeno (130-200 d.C.), outro médico romano, usou a palavra *oncos* para descrever tumores, a palavra grega remetia ao inchaço encontrado na patologia. Embora a analogia ao caranguejo de Hipócrates e Celsus ainda seja usada para descrever tumores malignos, o termo de Galeno agora é usado como referência para estudo e tratamento do câncer, a oncologia (Gallucci, 1985; Acs, 2012).

A epidemiologia do câncer é debatida desde os primórdios e várias teorias já surgiram tentando explicar a sua formação. Durante mais de 1300 anos a teoria humoral de Hipócrates predominou. Nela acreditava-se que o corpo humano é constituído de quatro

fluidos humorais (sangue, fleuma, bile amarela e bile negra) e que o equilíbrio entre eles determinava um indivíduo saudável. Por outro lado, o excesso de bile negra era responsável pelo surgimento do câncer. Nesse período, devido à proibição por questões religiosas em realizar estudos com corpo humano, incluindo autópsias, pouco progresso foi obtido nessa área (Hajdu, 2011b; a; 2012).

Entre as teorias que substituíram a teoria humoral do câncer, a teoria linfática foi a mais aceita. Descrita por Stahl e Hoffman, relacionava o movimento contínuo do sangue e da linfa pelo corpo com a saúde do individuo. Descrevia-se que a formação do tumor influenciava diretamente na variação da densidade, acidez ou alcalinidade de tais fluidos. Por volta de 1700 essa teoria ganhou o suporte de um famoso cirurgião escocês da época, John Hunter, e só foi substituída em 1838 pela teoria de blastema.

Responsável pela teoria de blastema, o patologista alemão Johannes Muller, foi o primeiro a descrever que o tumor é constituído de células ao invés dos fluídos corporais. No entanto, ele não acreditava que as células cancerígenas eram originadas a partir das células normais mas a partir de brotamento (blastema) entre os tecidos. Posteriormente, seu aluno Rudolph Virchow (1821-1902), foi quem determinou que o tumor originava a partir de outras células (Acs, 2012) .

A partir de então várias causas foram relacionadas para a modificação das células "saudáveis" do individuo. Dentre elas cita-se: teoria da radiação, teoria do trauma e a teoria da doença infecciosa. No entanto, a primeira descrição de um agente cancerígeno precede à teoria de Muller e é datada em 1761 quando John Hill publicou a influência do uso imoderado do tabaco relacionando ao câncer (Devita e Rosenberg, 2012).

Atualmente, mais de 107 fatores de risco físicos, químicos e biológicos foram

relacionados pela Agência Internacional para a Pesquisa do Câncer (IARC) como carcinogênicos aos humanos (International Agency for Research on Cancer, 2011). Entre os fatores físicos descritos, a exposição à radiação ultravioleta está associada, por exemplo, ao desenvolvimento de câncer de pele (Massari, Kastelan *et al.*, 2007) enquanto que asbestos, hidrocarbonetos aromáticos e o tabaco representam importantes fatores químicos de risco para o desenvolvimento do câncer de pulmão (Veglia, Vineis *et al.*, 2007). Os fatores biológicos incluem vírus como Epstein-Barr culminando na formação do linfoma de Hodgkin, o vírus da Hepatite B e C na formação de hepatocarcinomas e até bactérias *Helicobacter pylori* levando a tumores gástricos, dentre outros (International Agency for Research on Cancer, 2012).

Além dos fatores listados pela IARC , que são os responsáveis por cerca de 95% dos carcinomas, fatores genéticos estão associados a 5% dos cânceres em humanos (Sonnenschein e Soto, 2008). Como exemplo, mutações nos genes BRCA-1 e 2 aumentam a susceptibilidade aos cânceres de mama e ovário (Lynch et al., 2008). Por sua vez, a translocação entre os cromossomos 9 e 22, está relacionada a um tipo específico de câncer, a leucemia mielóide crônica (Nowell e Hungerford, 1960). A relação entre alterações genéticas e o surgimento do câncer foi descrita entre o final do século 19 e o início do século 20 por David Von Hansemann e Theodor Boveri. Em seus estudos, esses pesquisadores observaram a presença de aberrações cromossômicas em células tumorais. Mais tarde, foi demonstrado que agentes mutagênicos e que causam danos no DNA também provocam câncer. Por fim, a relação entre alterações genéticas e câncer foi demonstrada pela conversão de células de fenótipo normal em células cancerígenas por meio da introdução do DNA genômico de células tumorais em células normais (Krontiris e Cooper, 1981; Murray, Shilo *et al.*, 1981).

Entre as teorias atuais de formação das células neoplásicas duas estão em constante debate. A primeira, a teoria da evolução clonal, defende que o surgimento do câncer seja análogo a um processo de evolução Darwiniana. Nesse processo, células somáticas adquirem mutações aleatoriamente e os fenótipos resultantes são gradualmente selecionados. Alguns desses fenótipos são deletérios e as células com a mutação morrem (Greaves e Maley, 2012). Por outro lado, certas mutações podem conferir à célula a capacidade de proliferar mais rapidamente que as demais células do tecido, ou aumentam sua sobrevivência em condições pouco favoráveis ou ainda conferem-lhe capacidade invasiva. Essas alterações resultam, então, na formação de uma neoplasia (Stratton, Campbell *et al.*, 2009).

A segunda teoria explica a formação de tumores e sua resistência aos tratamentos clínicos baseando-se na existência de uma população de células tronco tumorais (Bosly, Haioun *et al.*, 2001). Acredita-se que essas células representariam uma subpopulação de células iniciadoras que dariam origem às células mais diferenciadas da massa tumoral (Mulholland, Xin *et al.*, 2009). Por terem a capacidade de se auto-renovar e por serem pouco diferenciadas, as células tronco tumorais podem dar origem a diferentes tipos celulares. Essas células teriam a apoptose inibida e, portanto, apresentam maior resistência às terapias convencionais. De fato, existem estudos que demonstram a existência de células com características de células tronco em tumores de mama (Al-Hajj, Wicha *et al.*, 2003), próstata (Collins, Berry *et al.*, 2005), cabeça e pescoço (Prince, Sivanandan *et al.*, 2007) e pâncreas (Li, Heidt *et al.*, 2007), entre outros. Diante de todos as evidências é claro que o câncer é uma patologia complexa e considerar apenas uma teoria ou a presença de agentes cancerígenos seria limitar o entendimento da sua formação e por consequência a resolução urgente de tratamentos mais eficazes.

Atualmente, o câncer é uma das principais causas de óbitos em todo o mundo sendo responsável, de acordo com a Organização Mundial de Saúde, por mais de 7,6 milhões de mortes em 2008, cerca de 13% do total anual. Além disso, estima-se que em 2030 ocorra a progressão para mais de 11 milhões de mortes anuais (Who, 2013).

Dentre todos os tipos tumorais, o melanoma é considerado o câncer com pior prognóstico, sendo o seu alto potencial metastático o principal responsável por esse quadro. Originário dos melanócitos, células que produzem o pigmento melanina que confere a cor da pele, esse tumor maligno pode surgir do tecido epitelial intacto ou de lesões pigmentadas pré-existentes. Esse tipo tumoral é mais comum na pele, mas pode surgir em qualquer superfície mucosa ou ainda em outros locais para onde tenham migrado as células da crista neural, as células embrionárias que dão origem a vários tipos celulares incluindo os melanócitos (Kashani-Sabet, Venna *et al.*, 2009; National Cancer Institute, 2013).

Apesar do progresso na pesquisa do câncer, os tratamentos existentes são na maioria, processos debilitantes ao paciente e muitas vezes não levam à cura. Atualmente a terapêutica envolve a remoção do tecido tumoral e dos linfonodos de drenagem por meio da intervenção cirúrgica, radioterapia, terapia hormonal e drogas citotóxicas (Apostolopoulos, 2011). Os maiores avanços na terapia antitumoral tem sido observados recentemente em estudos clínicos que utilizam ferramentas que proporcionam o aumento da resposta do sistema imune do paciente ao tumor. Dessa forma, novas perspectivas estão sendo abertas a partir do estudo e aplicação da imunologia tumoral.

1.2. Imunologia tumoral

A interação entre o sistema imune e o câncer é muito complexa e o papel preciso que as células do sistema imune exercem sobre a maior parte dos tumores ainda não é totalmente compreendido. No entanto estudos demonstram claramente o recrutamento de numerosos tipos celulares para o microambiente tumoral como leucócitos, linfócitos, células dendríticas e células mielóides. Em uma breve descrição, algumas dessas populações serão abordadas.

1.2.1. Macrófagos associados a tumor

A mais bem caracterizada população de células mielóides são os macrófagos associados ao tumor (TAMs). Interessantemente, os TAMs são capazes de produzir tanto a resposta antitumoral quanto podem disseminar o câncer. Seu papel é dependente da polarização dos monócitos em macrófagos tipo M1 ou M2. O processo de polarização está intrinsicamente relacionado ao microambiente tumoral a qual essas células se expõem (Mantovani, Sozzani *et al.*, 2002; Sica, Larghi *et al.*, 2008; Rogers e Holen, 2011; Dannenmann, Thielicke *et al.*, 2013).

Nesse contexto, a ativação dos macrófagos clássicos M1, responsáveis pela resposta efetora dos TAMs com alta atividade bacteriana e tumoricida, ocorre em resposta a produtos microbianos, como LPS, ou pela estimulação com interferon-γ (IFN-γ). Uma vez ativadas, os M1 produzem grande quantidade de citocinas pró-inflamatórias como a interleucina-6 (IL-6), IL-12, IL-1β, IL-23, o fator de necrose tumoral (TNF), além da expressão da enzima óxido nítrico sintase (iNOS) (Rogers e Holen, 2011; Edin, Wikberg *et al.*, 2012; Dannenmann, Thielicke *et al.*, 2013)

Em contraste, os TAMs considerados pró-tumorais, chamados M2, são induzidos por

vários sinais como IL-4, IL-13, IL-10, fator estimulador de macrófagos-1 (CSF-1) ou imunocomplexos em associação com IL-1 ou ligantes de receptores do tipo Toll (TLR). Esses macrófagos responsáveis pelo reparo tecidual e por funções imunoregulatórias são capazes de sintonizar as respostas inflamatórias e a imunidade adaptativa auxiliadora do tipo 2 (Th2) (Sica, Larghi *et al.*, 2008; Edin, Wikberg *et al.*, 2012). Eles favorecem a progressão tumoral pela secreção de citocinas como o fator crescimento epidermal (EGF), o fator crescimento fibroblasto-1 (FGF1) e o fator de crescimento transformante-β1 (TGF-β1). Além disso, estimulam a angiogênese pela alta secreção do fator de crescimento vascular endotelial (VEGF). Adicionalmente também secretam fatores imunoregulatórios, tais como IL-10 e TGF- β1, que reduzem a resposta imune.

TAMs são frequentemente encontrados no fenótipo M2 e tem sido associados com a diminuição da sobrevivência em pacientes com melanoma (Jensen, Schmidt *et al.*, 2009), câncer de pulmão (Tsutsui, Yasuda *et al.*, 2005), rins e bexiga (Edin, Wikberg *et al.*, 2012). No entanto, essa relação não é verdadeira para todos os tipos de tumor, por exemplo tumores de estômago (Haas, Dimmler *et al.*, 2009), e assim a influência dos TAMs permanece controversa.

1.2.2. Células citotóxicas

Outros dois tipos de células abundantes e efetoras na imunidade contra o tumor são as células matadoras naturais (NK) e as células T CD8 citotóxicas (Zitvogel, Tesniere *et al.*, 2006). Em modelos murinos, as células NK são capazes de controlar ambos crescimentos local e metastático do tumor devido a sua habilidade de reconhecer e lisar as células tumorais e ainda secretarem citocinas imunoestimulatórias do tipo Th1 tais como IFN-γ (Levy, Roberti *et al.*, 2011; Wong, Berk *et al.*, 2013). No entanto, em

pacientes com neoplasias avançadas, as células NK não são encontradas em grande quantidade, indicando que elas não seriam importantes contra o crescimento maligno (Levy, Roberti *et al.*, 2011).

Por outro lado, diversos estudos tem demonstrado que a maior frequência dos linfócitos T CD8 nos infiltrados tumorais correlacionam significativamente ao prolongamento da sobrevivência dos pacientes (Naito, Saito *et al.*, 1998; Sato, Olson *et al.*, 2005). Além disso, a transferência adotiva desses linfócitos infiltrados no tumor (LIT), expandidos *ex vivo*, reportou que essas células podem mediar a regressão do tumor quando devidamente ativadas (Klebanoff, Gattinoni *et al.*, 2006). Complementarmente, em um estudo clínico foi observado a completa regressão tumoral em 40% dos pacientes com melanoma metastático que receberam a transferência adotiva autóloga dos LIT associados com a citocina IL-2, após uma linfodepleção (Rosenberg, Yang *et al.*, 2011). Nesse estudo, o autor relatou ainda que entre os vinte pacientes com o quadro favorável, dezenove experimentavam resposta duradoura entre três a sete anos.

1.2.2.1. A expansão da resposta imune mediada pelas células T CD8

A típica resposta mediada pelas células T CD8 envolve três principais estágios de desenvolvimento: (1) uma fase de ativação inicial caracterizada por uma expansão clonal de células antígeno específicas, secreção de citocinas efetoras e atividade citolíticas; (2) fase de contração das células efetoras ($CD8^+T_E$) caracterizada por uma extensa apoptose e (3) a estabilização e manutenção da população de memória (Kaech, Tan *et al.*, 2003; Klebanoff, Gattinoni *et al.*, 2006). As células T CD8 de memória são comumente classificadas em células de memória central ($CD8^+T_{CM}$) ou células de memória efetora ($CD8^+T_{EM}$) de acordo com os marcadores fenotípicos que denotam sua

migração para tecidos linfoides ou periféricos, respectivamente (Bixby e Tarleton, 2008; Vasconcelos, Dominguez *et al.*, 2012).

Nos camundongos, as células efetoras de vida-curta (T_E) expressam baixas quantidades da cadeia alpha do receptor IL-7 (CD127) e regulam para baixo a expressão da L-selectina (CD62L) (Huster, Busch *et al.*, 2004). As Células T de memória, consideradas de vida longa, são caracterizadas pela expressão constitutiva de CD127. O CD62L é usado para melhor discriminar T_{CM} ($CD62L^{high}$) das T_{EM} ($CD62L^{low}$). A marcação com CD44 é comumente utilizada para determinação das células T $CD3^+CD8^+$ ativadas ($CD44^{high}$) (Figura 1).

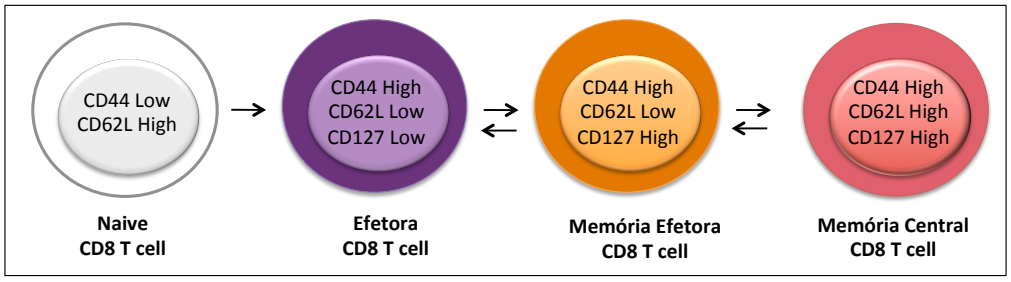

Figura 1. Células CD8 e seus subtipos. Os diferentes subtipos das células T CD8 podem ser caracterizadas de acordo com a intensidade de expressão dos seus marcadores de superfície CD44, CD62L e CD127. Dessa forma as células $CD3^+CD8^+$ podem ser fenotipadas em Células Naive (CD62LHighCD44Low), Células Efetoras (CD62LLowCD127Low), Células de Memória Efetora (CD62LLowCD127High) e Células de Memória Central (CD62LHighCD127High).

Não há um consenso como ocorre a conversão para os subtipos celulares, ou seja se são geradas de maneira linear ($CD8^+T_E \rightarrow CD8^+T_{EM} \rightarrow CD8^+T_{CM}$) ou se as células T_{EM} podem ser convertidas para células T_{CM} (Figura 2*a*). Sob condições normais, ambos subtipos de célula de memória contribuem para a proteção do hospedeiro perante a uma reinfecção.

No caso de uma infecção crônica ou em alguns tumores, o padrão normal de produção

das células T CD8 pode ser alterado (Figura 2 *b,c*). Linfócitos com características de células T_{CM} ou células T_{EM} são encontradas em frequência maior que o esperado, sugerindo o recrutamento de novas células de memória a partir das pré-existentes ou pela estimulação de células naive, ou ambos (Bustamante, Bixby *et al.*, 2008). No entanto, apesar de presentes em grande frequência, infecções crônicas são caracterizadas por diferentes graus de comprometimento funcional das células T CD8 patógeno-específicas, presumivelmente devido a uma resposta de exaustão das células T mediante a estimulação constante (Angelosanto e Wherry, 2010; Wherry, 2011).

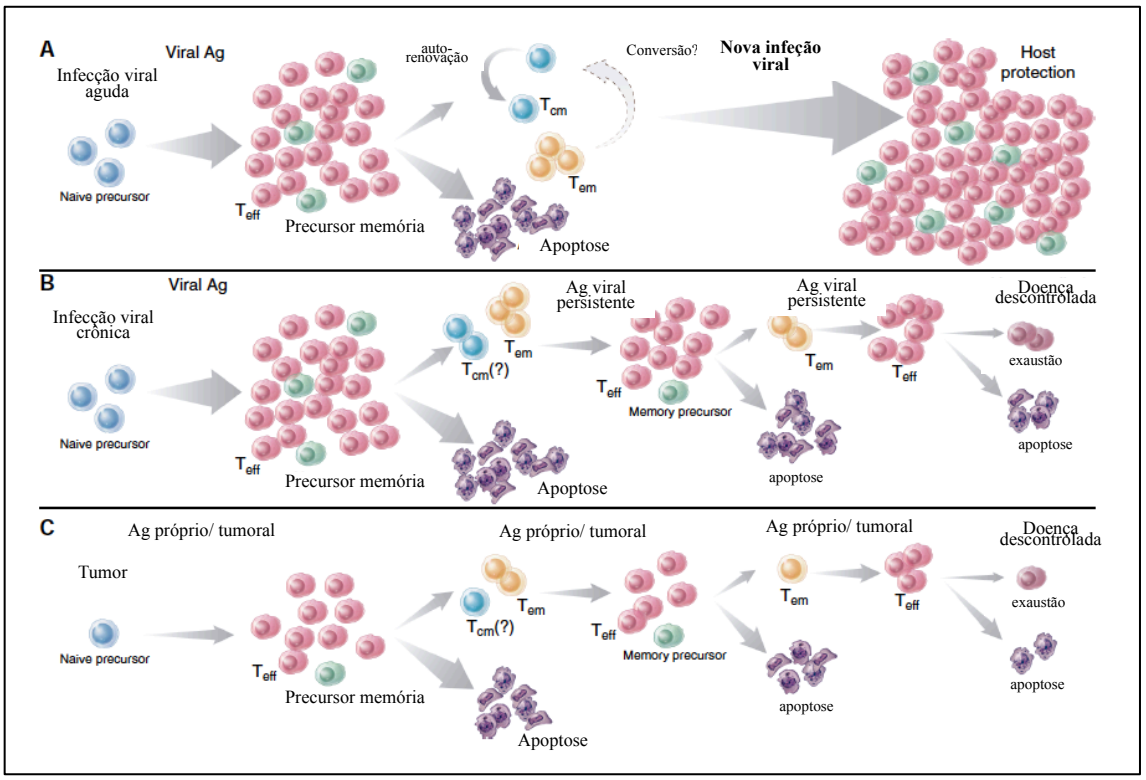

Figura 2. Comparação dos estágios de diferenciação das célula T CD8. A expansão das células CD8 em uma infecção aguda (A), infecção crônica (B) ou em um estado tumoral (C) começa quando a população naive (células azuis) é estimulada a expandir perante a exposição a um antígeno (Ag). A medida que essas células se dividem, elas adquirem atributos fenotípicos e funcionais de células T efetoras (T_E) (células vermelhas). Com a conclusão da primeira resposta, a maioria das células morrem por apoptose; uma limitada subpopulação de células T_E (em verde) formam um *pool* estável de células de memória T CD8. Esse *pool* de memória é heterogêneo e pode ser dividido em T_{CM} e T_{EM}. As células roxas representam a exaustão celular perante a exposição prolongada ao antígeno (Klebanoff, Gattinoni *et al.*, 2006).

1.2.3. A regulação da resposta imune e a resposta antitumoral

A resposta efetiva contra o tumor frequentemente entra em choque com os mecanismos regulatórios do sistema imune. Evidências no estudo do câncer sugerem que as células T denominadas como regulatórias (T_{reg}) naturais ($CD4^{+}FoxP3^{+}CD25^{+}$) não só exercem a manutenção da tolerância imunológica aos antígenos próprios como também impedem a imunovigilância contra as células tumorais (Ko, Yamazaki *et al.*, 2005). Apesar do papel dessas células no microambiente tumoral ainda não ser completamente esclarecido, vários estudos demonstraram o aumento da resposta antitumoral por meio da depleção das T_{reg} com o uso do anticorpo anti-CD25. Dessa forma aumenta-se a resposta conduzida pelas células T CD4 e CD8 conforme ilustrado na Figura 3 (Beyer e Schultze, 2006; Quezada, Peggs *et al.*, 2006; Mitsui, Nishikawa *et al.*, 2010).

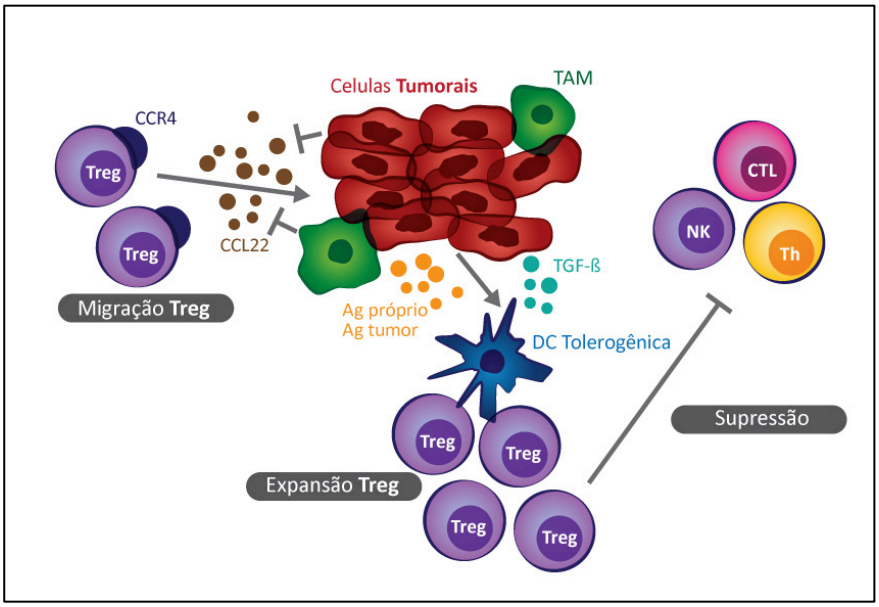

Figura 3. Células Tregs suprimem a resposta imune antitumoral. CCL22 produzido pelos tumores e macrófagos infiltrados no tumor (TAM) recrutam células regulatórias (Treg) que expressam CCR4 (migração Treg). As células Tregs acumuladas via CCR4-CCL22 reconhecem antígenos-próprios e antígenos associados ao tumor e proliferam (Expansão Treg). Células dendríticas (DC) tolerogênicas induzidas por TGFβ, derivado das células tumorais, aumentam a expansão das Treg. Essas Tregs suprimem células efetoras antitumorais. Embora essa figura esteja focada no sítio tumoral, a expansão das Treg também ocorre nos linfonodos drenantes. NK: células matadoras naturaisCTL: células T CD8 citotóxica; Th: Célula CD4 T Helper; Ag: antígeno (Nishikawa e Sakaguchi, 2010).

A inibição da resposta efetora é controlada principalmente pelo antígeno associado ao linfócito T citotóxico (CTLA-4) e a proteína conhecida como morte programada-1 (PD-1), ambos agonistas do receptor B7 (Leach, Krummel *et al.*, 1996; Mangsbo, Sandin *et al.*, 2010). Tais antígenos expressos normalmente pelas células T efetoras na fase de contração, tem a função de impedir a exaustão da resposta imune, mas por outro lado inibem a função efetora dessas células ocasionando a diminuição da resposta imune e do controle tumoral. Estudos recentes demonstraram a presença de um dos ligantes do PD-1, o PD-L1, na superfície de algumas células tumorais, proporcionando assim a inibição da função efetora das células T diretamente pelo tumor (Yamazaki, Akiba *et al.*, 2002; Nishikawa e Sakaguchi, 2010; Lyford-Pike, Peng *et al.*, 2013).

Resultados clínicos limitados tem sido obtido pelo uso do PD-1 e/ou PD-L1 em pacientes com diferentes tipos tumorais. Em 2012 foi descrito que o uso do anti-PD-1 obteve resultados clínicos positivos (regressão parcial ou completa do tumor) nas taxas de 19 – 41% para pacientes com melanoma, 24 – 31% para pacientes com câncer renal e cerca de 18% para pacientes com um determinado tipo de câncer pulmonar. No entanto, nos casos em que o tumor não expressava o PD-L1 não foi obtida nenhuma melhora objetiva (Topalian, Hodi *et al.*, 2012).

Outro alvo de interesse é o CTLA-4, homólogo à molécula coestimulatória CD28, o CTLA-4 liga aos ambos receptores B7-1 e B7-2 com afinidade muito maior do que o CD28 é acoplado (Leach, Krummel *et al.*, 1996). O anticorpo monoclonal anti-CTLA-4 tem demonstrado respostas promissoras em estudos clínicos com pacientes com melanoma em estágio avançado e devido à essas respostas o anticorpo humano Ipilimumab foi aprovado nos Estados Unidos e Europa como imunoterapia (Yuan, Adamow *et al.*, 2011; Yuan, Ginsberg *et al.*, 2011; Scott, Allison *et al.*, 2012). No

entanto, além dos mecanismos não estarem completamente esclarecidos, os resultados precisam ser aprimorados tanto quanto ao controle tumoral quanto aos efeitos adversos decorrentes dessa terapia (Fellner, 2012). Uma estratégia para minimizar os efeitos secundários da terapia com anti-CTLA-4 seria a estimulação específica da resposta imune em uma terapia combinada com adjuvantes imunológicos ou uma vacina tumoral-específica.

1.3. Antígenos tumorais

Visando uma resposta específica, durante os últimos quinze anos, numerosos antígenos humanos associados a tumores tem sido identificados, seja por triagem de bibliotecas de cDNA, originadas a partir de soros de pacientes com câncer (SEREX) ou pelo uso de linfócitos T respondedores aos peptídeos tumorais associados a HLA específicos. O grupo de antígenos tumorais que teve maior expansão foi dos antígenos *cancer testis* (CTA), os quais não estão expressos nos tecidos normais, exceto em células germinativas, oogônias e placenta (Van Rhee, Szmania *et al.*, 2005; Nicholaou, Chen *et al.*, 2011). Esse padrão de expressão restrito ao tumores, juntamente com sua forte imunogenicidade *in vivo*, identificaram os CTA como alvos ideais para abordagens imunoterapêuticas específicas contra o tumor, e levou ao desenvolvimento de vários ensaios clínicos (Fratta, Coral *et al.*, 2011).

Até o momento, foram descritos ao menos 70 famílias de CTA, representando globalmente cerca de 140 membros (Cheng, Wong *et al.*, 2011). Apesar da maioria desses CTA serem expressos durante a espermatogênese, nenhum deles foi bem caracterizado quanto a sua função nas células germinativas, e também, nas células

cancerígenas (Scanlan, Simpson *et al.*, 2004; Fratta, Coral *et al.*, 2011). Os primeiros membros dessa classe de antígenos tumorais descritos, MAGE, BAGE e GAGE, foram identificados em pacientes com melanoma e até hoje mostram resultados clínicos limitados a certos tipos tumorais (Simpson, Caballero *et al.*, 2005; Fratta, Coral *et al.*, 2011) . A tabela 1 sumariza algumas famílias de CTA.

Família CTA	Número de genes	Cromossomo	Imunidade espontânea induzida em pacientes
MAGE-A		Xq28	Cellular and Humoral
MAGE-B	17	Xp21	Cellular
BAGE	2	4, 13	Cellular
GAGE-A	8	Xp11.4	Cellular
SSX-2	5	Xp11.2	Cellular and Humoral
NY-ESO-1	3	Xq28	Cellular and Humoral
SCP-1	3	1p12-p13	Humoral
CT7/MAGE-C1	7	Xq26–27	Humoral
HOM-TES-85	1	Xq24	Humoral
CT9/BRDT	1	1p22.1	Not Known
CT10	1	Xq27	Humoral
CTp11/SPAN-X-C1	3	Xq27	Not known
SAGE	1	Xq28	Not Known
OY-TES-1	1	12p13	Humoral
cTAGE-1	1	18p11.2	Humoral
CT15/Fertilin beta	30	8p11.2	Not known
CT16	2	Xp11.2	Not Known
CT17	1	21q11	Not Known
MMA-1	1	21q22.2	Not Known
CAGE	1	Xp22	Humoral

Tabela 1: Algumas famílias de CTA conhecidas. (Scanlan, Gure *et al.*, 2002)

O NY-ESO-1 é considerado o mais imunogênico dos CTA e teve seu mRNA encontrado em aproximadamente 20 - 40% dos tumores (Jungbluth, Chen *et al.*, 2001; Van Rhee, Szmania *et al.*, 2005). Além disso, apesar da expressão dos antígenos tumorais variarem de indivíduo para indivíduo, a frequência da expressão desse CTA em alguns tipos tumorais tais como melanoma, câncer de pulmão, câncer de esôfago e sarcomas sinoviais pode chegar a 80% dos pacientes que apresentam esses tumores (Gnjatic et al., 2006).

Diante desses achados, o NY-ESO-1, uma proteína hidrofóbica de 22 kD codificada por um gene na região Xq28, tornou-se uma valiosa ferramenta na indução da resposta imune tumoral sendo extensivamente estudado e utilizado com diversas combinações,

em inúmeros estudos vacinais e terapêuticos, incluindo estudos clínicos avançados (Jungbluth, Chen *et al.*, 2001; Nicholaou, Chen *et al.*, 2011).

Visando caracterizar a resposta imune induzida pelo NY-ESO-1, Daisuke Muraoka em 2010 desafiou camundongos BALB/c com tumores singênicos expressando esse CTA e analisou protocolos, profilático e terapêutico, comparando um peptídeo NY-ESO-1 ou uma vacina de DNA do mesmo CTA. Confirmou-se, nesse estudo, que a utilização somente do peptídeo CTA ou do seu DNA não é capaz de estimular o sistema imune o suficiente para controlar o crescimento tumoral em nenhum dos dois protocolos, sendo necessário a sua combinação com um adjuvante (Muraoka, Kato *et al.*, 2010).

Em 2012 um estudo comparou o uso potencial da proteína recombinante NY-ESO-1 associada a diferentes agonistas de TLR, frente ao controle do crescimento tumoral (Junqueira, Guerrero *et al.*, 2012). Foram utilizados o monofosforil lipídeo A (MPL) derivado de bactéria, lipopetídeo sintético (Pam3Cys) e diversos oligodeoxinucleotídeo (ODN) contendo motivos CpG não metilados derivados de *T. cruzi*. Todos foram associados ao hidróxido de alumínio, único adjuvante comercialmente disponível para uso humano. Os melhores resultados foram obtidos na utilização do CpG ODN derivado do protozoário, em especial o B344 (TCGACGTTTGGATCGGT) que induziu uma resposta antígeno-específica. No entanto, efeitos colaterais, como dor no local da imunização foram observados nos animais e o controle completo do crescimento tumoral não foi obtido (Junqueira, Guerrero *et al.*, 2012).

Vislumbrando a construção de uma nova ferramenta adjuvante, Junqueira e colaboradores, em 2011, propuseram a construção de parasitos transgênicos

expressando NY-ESO-1 como agentes indutores da resposta Th1 considerada ideal para o controle tumoral.

1.4. O uso do *Trypanosoma cruzi* no combate ao câncer

1.4.1. A ação tumoricida do Trypanosoma cruzi

A ação tumoricida do *T. cruzi* foi sugerida pela primeira vez por Roskin em 1946 (Klyueva e Roskin, 1946; Roskin, 1946). Nos seus estudos camundongos infectados com tripanosoma eram simultaneamente desafiados com carcinoma de Ehrlich, um tipo de tumor mamário. Os resultados demonstraram que, apesar da infecção ter levado o camundongo à morte, a regressão tumoral foi observada em cerca de 60% dos camundongos testados (Klyueva e Roskin, 1946; Roskin, 1946; Klyueva, 1947). Acreditava-se que toxinas produzidas pelo protozoário eram as responsáveis pelo prognóstico favorável contra o câncer. Seguindo o mesmo propósito várias pesquisas foram conduzida como os estudos com a toxina de Coley (Coley, 1893; Nauts e Mclaren, 1990) e o BCG (Old, Clarke *et al.*, 1959) mas os resultados foram insatisfatórios e a ação tumoricida permaneceu desconhecida (Malisoff, 1947; Hauschka e Goodwin, 1948; Belkin e Hardy, 1957).

Mais efetivamente em 2006, os cientistas Kallinicova, Batmonkh e colaboradores, observaram a inibição do crescimento de adenocarcinoma em ratos a partir do uso do lisado de epimastigotas de diferentes grupos genéticos de *T. cruzi.* No entanto, o mecanismo de ação inibitória do parasito ainda não foi desvendado (Batmonkh, Kallinikova *et al.*, 2006; Kallinikova, Borisova *et al.*, 2006). Sugere-se contudo, que a

ativação inicial das células do sistema imune inato por componentes do parasito poderia contribuir para o desenvolvimento de imunidade protetora contra o tumor.

1.4.2. Imunidade mediada pelo *T. cruzi*

A infecção por *T. cruzi* é caracterizada por uma fase aguda, na qual ocorre uma elevada parasitemia e parasitismo tecidual acompanhada por vasta ativação do sistema imune, com aumento de citocinas circulantes e ativação de linfócitos B e T. A ativação do sistema imune é responsável pelo controle da parasitemia e do parasitismo, podendo ocorrer a eliminação total dos parasitos ou evoluir para a fase assintomática, que é caracterizada pela difícil detecção de parasitos no organismo (Garg, Nunes *et al.*, 1997; Bixby e Tarleton, 2008; Bustamante, Bixby *et al.*, 2008).

O controle da infecção por *T. cruzi* durante os estágios iniciais da infecção é dependente tanto da imunidade inata quanto da imunidade adquirida (Golgher e Gazzinelli, 2004). Inicialmente, células dendríticas (DCs) e macrófagos infectados pelo parasito produzem IL-12 e TNF-α, citocinas essas responsáveis pela ativação de linfócitos e células NK, respectivamente. Dentre os mecanismos efetores, a produção de IFN-γ pelas células NK ativa mais macrófagos, que por sua vez, produzem espécies reativas de oxigênio e nitrogênio responsáveis pela eliminação dos parasitos. Adicionalmente, as DCs apresentam antígenos aos linfócitos T, fazendo a ligação com a imunidade adquirida. A produção de IL-12 pelas DCs, assim como o IFN-γ pelas células NK estimula a diferenciação do fenótipo dos linfócitos T $CD4^+$ para Th1, favorecendo desta forma, mecanismos efetores dependentes de linfócitos T $CD8^+$ citotóxicos. A Figura 4 ilustra os mecanismos imunológicos acima descritos.

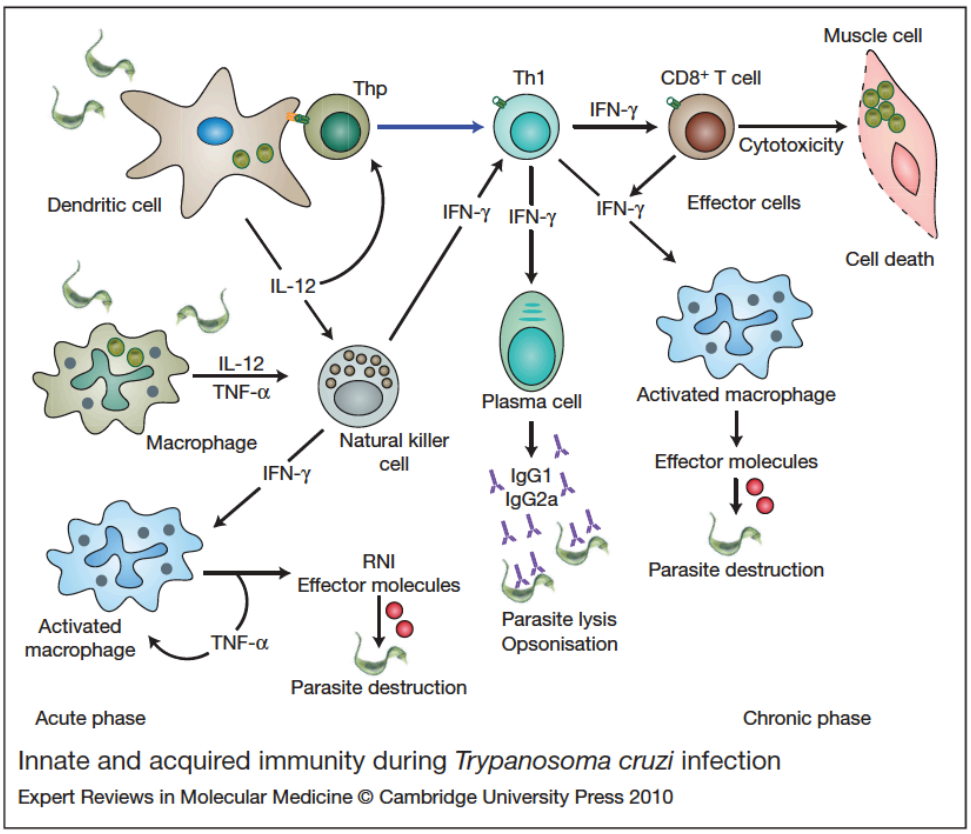

Figura 4. Representação esquemática dos mecanismos imunológicos que medeiam a resposta imune inata e adquirida contra o *T. cruzi*. Na fase inicial do estágio de invasão do *T. cruzi*, a imunidade inata tem um papel crucial na resistência do hospedeiro à infecção: atuando como primeira barreira, as células do sistema imune inato (macrófagos, NK e DC) produzem citocinas (IL-12, TNF-α e IFN-γ). Ao mesmo tempo, células da imunidade inata, particularmente células dendríticas, fazem a ponte entre o sistema imune inato e adquirido, produzindo citocinas (IL-2) necessárias para a diferenciação e expansão clonal das células T helper 1 (Th1) CD4 assim como células T CD8 e células B. O IFN-γ produzido pelas Th1 CD4 ou T CD8 ativam mecanismos efetores nos macrófagos que destroem ambos amastigotas e tripomastigotas fagocitados. Os anticorpos produzidos pelas células B provocam a lise da forma tripomastigota extracelular ou facilitam a fagocitose dos parasitos opsonizados com IgG.

Um problema frequentemente debatido e controverso acerca do uso de parasitos como vetores vacinais seria a sua capacidade de induzir autoimunidade. De um lado estão pesquisadores que suportam a idéia de que a doença de Chagas teria uma etiologia autoimune sugerindo que a resposta inflamatória nas lesões chagásicas não são diretamente induzidas para ou contra o *Trypanosoma cruzi*, mas são específicas para outros antígenos, porventura antígenos-próprios. Apoiando essa teoria alguns estudos observaram a presença de anti-auto-anticorpos e linfócitos em pacientes infectados com o parasito (Cunha-Neto, Coelho *et al.*, 1996; Leon e Engman, 2003). Outras

características da doença, incluindo o início tardio e a especificidade órgão-específica também são consistentes com a etiologia autoimune (Kalil e Cunha-Neto, 1996; Cunha-Neto, Teixeira *et al.*, 2011).

Por sua vez, do outro lado alguns pesquisadores sustentam a teoria que a autoimunidade não está envolvida no processo da doença de Chagas. Dessa maneira, a presença do *T. cruzi*, particularmente nos locais da doença, é que seria responsável e suficiente para desencadear o processo patológico sem ser necessário invocar a autoimunidade. Nessa teoria considera-se que mesmo se houver um componente autoimune da doença de Chagas seria induzido pela presença efetiva do parasito (Tarleton e Zhang, 1999; Tarleton, 2003). Baseado nessa teoria alguns modelos foram propostos utilizando o parasito para desencadear uma resposta imune vacinal.

Em 2011, Junqueira *et al* construíram parasitos transgênicos expressando NY-ESO-1 a partir da cepa atenuada CL-14. Essa cepa teria sido escolhida por ser cerca de quatro vezes menos infectiva que a cepa parental CL (Atayde, Neira *et al.*, 2004) e por não causar parasitemia e parasitismo tecidual, nem mesmo em animais neonatos (Paiva, Castelo-Branco *et al.*, 1999). Foram desenvolvidos três parasitos: (a) CL-14-NY-ESO-1 sem calda de histidina; (b) CL-14-NY-ESO-1 com calda de histidina (His+); (c) CL-14-NY-ESO-1 com peptídeo sinal da glicoproteína 63 (gp63).

Após duas doses vacinais com os parasitos CL-14 e CL-14 expressando NY-ESO-1, animais C57BL/6 foram desafiados com tumores singênicos, expressando ou não o *cancer testis* NY-ESO-1, e os resultados demonstraram que os parasitos transgênicos contendo o CTA em duas construções, tanto contendo a His+ quanto o peptídeo sinal gp63, foram capazes de controlar totalmente o crescimento tumoral (Junqueira, 2011).

Interessantemente, foi avaliado o uso dos parasitos CL-14-NY-ESO-1 gp63 mortos após choque térmico e não foi obtido o mesmo resultado satisfatório observado com o parasito vivo. Observou-se ainda que os *T. cruzi* transgênicos induziram de maneira dependente de Myd88 e IL-12 a produção de IFN-γ e a resposta específica ao crescimento tumoral. No entanto, esse parasito transgênico mostrou-se parcialmente eficiente em protocolo terapêutico.

Dentro desse contexto, surgiram várias questões relacionadas ao uso dos parasitos transgênicos no controle do crescimento tumoral: Qual seria o mecanismo celular envolvido? Há uma resposta duradoura da vacina contra o tumor? Seria possível adotar um protocolo terapêutico usando o parasito transgênico? Dentre tantas outras. Visando responder essas questões propusemos, no presente trabalho, desenvolver um novo protocolo terapêutico e compreender os mecanismos envolvidos perante um dos tumores mais agressivos relatados na literatura, o melanoma.

2. Justificativa

A melhora da qualidade de vida de pacientes com doenças tão devastadoras como o câncer só será possível após entendermos os caminhos a serem trilhados para a indução de uma resposta imune efetora. Nosso grupo se empenha para decodificar essa área do conhecimento tão fragmentada e estamos adquirindo embasamento científico que contribuirá para a formação de um pensamento crítico concreto sobre o câncer e ainda utilizar instrumentos únicos que poderão fornecer novos e relevantes avanços na pesquisa clínica tumoral.

Perante a observação de dados promissores de uma nova ferramenta vacinal de combate ao câncer, faz-se necessário o entendimento dos mecanismos imunológicos envolvidos a fim de aplicá-los em uma nova terapia. A compreensão do processo antitumoral é o caminho para o desenvolvimento de terapias alternativas capazes de prevenir e curar essa patologia. Dessa forma, o aprendizado conquistado levará a novos rumos, deixará de ser apenas um anseio e passará a ser uma realidade terapêutica alcançada por milhares de famílias.

.

3. Objetivos

3.1. Objetivo geral

Desenvolver uma terapia antitumoral com o uso de *T. cruzi* transgênicos expressando o CTA NY-ESO-1.

3.2. Objetivos específicos

- Avaliar a capacidade de internalização do parasito transgênico pelas células do sistema imune.
- Avaliar a necessidade de aplicação de dose de reforço frente a capacidade de indução da resposta imune contra o tumor.
- Caracterizar a resposta imune das células T $CD8^+$ totais e específicas ao NY-ESO-1 induzidas após as vacinação com parasito transgênico.
- Avaliar a capacidade de produção de citocinas pelas células de resposta específica ao tumor.
- Desenvolver nova imunoterapia antitumoral utilizando a associação dos parasitos transgênicos contendo a proteína NY-ESO-1 com anticorpos que prolongam a resposta imune induzida.
- Estudar os mecanismos envolvidos na terapia antitumoral, inclusive na região do infiltrado tumoral.

4. Materiais e métodos

4.1. Meios de cultura

4.1.1. Meio de cultura para células de melanoma murino

A linhagem celular B16-NY-ESO-1 é um melanoma derivado de camundongos C57BL/6 e foram gentilmente cedidas pelo Dr. Jonathan Cebon do LICR-Melbourne. O cultivo dessas células foi realizado em meio RPMI 1640 suplementado com 100 unidades de penicilina G/mL, 100 unidades de estreptomicina/mL, 10% de soro fetal bovino inativado (SFB) (Gibco) (R10), 1 μg/ml tylosin, em estufa a 37°C e 5% CO_2. A fim de selecionar as células que expressam o NY-ESO-1, foram adicionados 250 μg/ml de geneticina (Gibco).

4.1.2. Meio de cultura do hibridoma 9D9

Células do clone 9D9 foram cultivadas para a obtenção do anticorpo monoclonal anti-CTLA-4. A manutenção das células foi feita em estufa a 37°C e 5% CO_2, em meio RPMI 1640 acrescido de 100 unidades de penicilina G/mL, 100 unidades de estreptomicina/mL, 10% SFB (Gibco) e 50 μM 2-mercaptoethanol.

4.2. Cultivo de *Trypanosoma cruzi*

Os clone de *T. cruzi* foram mantidos em meio de cultura *Liver Infusion Tryptose* suplementado com 10% SFB, penicilina a 100 U/ml e estreptomicina a 100 U/ml em estufa de demanda bioquímica de oxigênio (B.O.D.) a 28˚C. A fim de selecionar os

parasitos que expressam NY-ESO-1, foram adicionados 250 µg/ml de geneticina (Gibco).

4.3. Obtenção e manutenção de camundongos para experimentação

A execução dos experimentos *in vivo* foi aprovado pelo Comitê de Ética em Experimentação Animal (CETEA) da Universidade Federal de Minas Gerais pelo número de protocolo 19/2008 (Anexo A).

Os animais selvagens C57BL/6 foram adquiridos no biotério de produção animal da UFMG (CEBIO) e os animais gzmBCreER^{T2}/ ROSA26EYFP foram cedidos pelo Dr. Douglas T. Fearon da Universidade de Cambridge (Bannard, Kraman *et al.*, 2009). O background genético desses animais é o C57BL/6.

Todos os experimentos *in vivo* foram realizados no biotério de experimentação do Centro de Pesquisas René Rachou/FIOCRUZ, o qual é credenciado como NB2. Animais β2-microglobulin$^{-/-}$ (deficientes em células T CD8) foram adquiridos nessa mesma instituição. Todos os animais foram acondicionados em micro-isoladores com maravalha, ração e água autoclavados.

4.4. Realização do protocolo profilático em camundongos

Animais C57BL/6 e gzmBCreER^{T2}/ ROSA26EYFP foram imunizados com o inóculo de 10^7 parasitos/camundongo na forma tripomastigota metacíclica, via intraperitoneal. Os grupos foram comumente distribuídos em: CL-14-NY-ESO-1, CL-14 e PBS. Para a

realização de vacinações com o parasito CL-14-NY-ESO-1 morto procedeu-se a repetição de 5 choques térmicos em freezer -70 e estufa a 37˚C. As duas doses homólogas do parasito transgênico foram administradas com o intervalo de 30 dias. De acordo com o tempo de análise, os animais foram sacrificados por deslocamento cervical e, após preparação, os esplenócitos foram utilizados de acordo com cada experimento.

4.5. Avaliação da migração dos parasitos

Um total de 2 x 10^7 formas metacíclicas do *T.cruzi* foram incubadas com 5 μM CFSE por 10 minutos a 37°C e 5% CO_2 (Souza, Rocha *et al.*, 2004), Os parasitos marcados foram lavados 3 vezes com RPMI por centrifugação a 3000 rpm e inoculados via intraperitoneal em um volume de 200 μl/animal. Após 1 hora, 20 horas e 3 dias da infecção, os camundongos foram submetidos a lavagem intraperitoneal. Adicionalmente, o linfonodo mesentérico e o baço foram coletados. As células foram processadas por vigorosa maceração utilizando seringa de 3 mL seguida por passagem em um filtro de 0.45 μm. Procedeu-se a marcação com os anticorpos anti-CD11b-PE-Cy7, anti-F4/80-PerCP-Cy5.5, anti-CD11c-AlexaFluor700, anti-MHCII-APC, anti-B220-PerCP-Cy5.5, anti-DX5-APC, anti-CD3-APC (todos eBioscience) e aquisição de pelo menos 200.000 eventos em FACSAria, ou LSRFortessa. A análise foi realizada por meio do software FlowJo.

4.6. Desafio de camundongos com células de melanoma murino

Camundongos C57BL/6 foram desafiados com 5 x 10^4 células do melanoma B16-NY-ESO-1 pela via subcutânea na região dorso posterior. O crescimento tumoral foi acompanhado duas vezes por semana, por um período de 40 dias e a sobrevivência por 50 dias. A medida dos tumores foi realizada com paquímetro e foi dada como a área em mm^2.

4.7. Cultivo de esplenócitos

A fim de obter os esplenócitos, os baços dos animais imunizados foram coletados, macerados e lavados em meio de cultura celular RPMI 1640 contendo 5% SFB, 100 unidades de penicilina G/mL e 100 unidades de estreptomicina/mL. As células foram centrifugadas a 1200 rpm, 4°C por 10 min e, em seguida, submetidas a lise das hemácias em tampão composto de 150 mM de NH_4Cl, 1 mM de $KHCO_3$ e 100 μM de Na_2-EDTA. Os esplenócitos remanescentes foram lavados mais 2 vezes em meio RPMI, e finalmente, ressuspendidos em 1 ml de RPMI 1640 acrescido de 10% SFB e 20 ng/mL de IL-2 recombinante (RD systems). Os esplenócitos foram diluídos em Azul de Tripan 0,4% (Gibco) para contagem em câmara de Neubauer.

Para a cultura, 5x10^6 esplenócitos foram plaqueados em placas de 24 poços na presença ou ausência de proteína recombinante NY-ESO-1 (rNY-ESO-1) (Produção GMP – LICR/Cornel University) na concentração de 10 μg/mL ou Concanavalina A (Sigma-Aldrich) na concentração de 5 μg/ml, para controle positivo. As placas foram mantidas em estufa com 5% CO_2 a 37°C por 48 horas, para posterior coleta dos sobrenadantes da cultura de células e dosagem de citocinas por ensaio imunoenzimático (ELISA).

Na preparação para a análise por citometria, 1 x 10^6 esplenócitos foram colocados em cada poço em uma placa de 96 poços. Foram realizadas marcações para avaliação do perfil celular induzido e/ou a estimulação por 18 horas com rNY-ESO-1 visando avaliar a produção de citocinas sob estímulo específico.

4.8. Aferição das citocinas

Os sobrenadantes das culturas de esplenócitos, coletados após 48 horas de estimulação, foram submetidos ao ELISA sanduíche para dosagem de IFN-γ e IL-2. O procedimento foi realizado de acordo com manual do kit DuoSet (R&D Systems). Para determinar as concentrações de citocinas no soro e peritôneo dos camundongos foi utilizado o kit BD Cytometric Bead Array Mouse Inflammation (BD Biosciences), de acordo com a indicação do fabricante. O total de 1800 eventos dentro do gate de beads foi adquirido no citômetro BD FACScan™ (BD Bioscience). A concentração de citocinas em cada amostra foi calculada usando o programa BD FCAP Array™, versão 1.0.1 (BD Biosciences) e o GraphPad Prism, versão 5.0b foi usado para as representações gráficas.

4.9. Caracterização da resposta celular T CD8 por citometria de fluxo

Para realização da marcação de superfície, a placa de 96 poços contendo 1 x 10^6 esplenócitos/poço foi centrifugada a 1400 rpm por 10 minutos e, à cada amostra, foi adicionado 0,3 μg do anticorpo bloqueador de receptores inespecíficas FcII/III (FcRII/III), CD16/CD32 (BD Biosciences Pharmingen). Imediatamente após, realizou-se a incubação com os anticorpos monoclonais marcados com fluoresceína por 30

minutos, sob o abrigo da luz, a 4ºC. As células foram lavadas duas vezes com a solução de lavagem "A" (0,5% de Albumina Bovina Sérica, 2mM de azida em solução salina tamponada (PBS), e ressuspendidas em PBS contendo 2% de formaldeído para fixação. Para marcações intracelulares a fixação é realizada com Citofix/Citoperm (BD Bioscience), de acordo com o protocolo do fabricante, e após lavagem com tampão Perm/Wash (BD Bioscience), é realizada a incubação com o anticorpo por 30 minutos. Segue-se duas lavagens com Perm/Wash e a amostra é ressuspendida em tampão "A" para realização da leitura das amostras.

A análise da especificidade da resposta imune celular foi realizada também pela marcação com tetrâmeros por 30 minutos, à temperatura ambiente. A especificidade do parasito foi analisada pelo TSKB20 ($H2K^b$ ANYKFTLV) enquanto para o tumor foram utilizados os tetrâmeros NY-ESO-1 (87-94) ($H\text{-}2K^b$ LLEFYLAM) e/ou gp100 (25-33) ($H\text{-}2D^b$ EGSRNQDWL) (todos LICR Facility). Os tetrâmeros consistem em quatro moléculas de MHC associadas com peptídeo e com um fluorocromo, permitindo a identificação dos linfócitos T específicos gerados que serão capazes de reconhecer esse peptídeo por meio do complexo TCR-peptídeo-MHC.

Os marcadores de superfície anti-CD3-APC-Cy7, anti-CD4-AlexaFluor700, e anti-CD8-PE ou anti-CD8-FITC ou anti-CD8-PECy5.5 foram utilizados para determinação das células T, de acordo com a combinação dos anticorpos do experimento. O perfil naive, efetor e de memória, efetora ou central, pôde ser definido com a associação dos marcadores de superfície anti-CD44-PerCP-Cy5.5, anti-CD62L-APC e anti-CD127-PE-Cy7. A glicoproteína de superfície CD44 é utilizada comumente para identificação de células T ativadas, já que em células naive é observado a baixa expressão desse marcador ($CD44^{low}$), enquanto que em células maduras, devido a função adesiva e

migratória dessa glicoproteína, temos a sua expressão aumentada ($CD44^{high}$). Por outro lado, complementando a determinação do subtipo celular, é sabido que, em camundongos, as células T efetoras expressam baixas quantidades da cadeia alpha do receptor para IL-7 (CD127) enquanto as células de memória são caracterizadas pela expressão constitutiva do CD127. A expressão da L-selectina (CD62L) foi usada para discriminar células efetoras e de memória efetora ($CD62^{low}$) das células de memória central ($CD62L^{high}$).

Para avaliação da produção da citocina IFN-γ, a cada poço foram adicionados 100 µl de meio R10 acrescido de 10 µg/ml da proteína *cancer testis* rNY-ESO-1, como estímulo. No controle negativo foi utilizado somente o meio R10. O volume de 0,2µl de Brefeldina A ("GolgiPlug Protein Transport Inhibiton") (BD Bioscience) foi adicionada a cada poço, para permitir a concentração de citocinas no interior da célula. Após 18h horas de estímulo na presença de Brefeldina A, as células foram marcadas para moléculas de superfície e para a citocina intracelular utilizando anti-IFN-γ-APC (todos os anticorpos utilizados foram obtidos a partir da Ebioscience).

Os camundongos transgênicos gzmBCreER^{T2}/ ROSA26EYFPA foram utilizados para a avaliação das células citotóxicas granzima B^+ (gzmB). Essa linhagem de animais foi construída por Oliver Bannard e colaboradores, em 2009, no qual a expressão da proteína fluorescente amarela (EYFP) está associada a transcrição do gene *gzmB*. Dessa forma, podemos detectar as células $gzmB^+$ pelas fluorescência emitida após a ativação dessas células. Foram adquiridos 200.000 eventos em FACScalibur ou FACSAria, ou LSRFortessa sendo a análise realizada por meio do software FlowJo.

4.10. Imunoterapia

A fim de avaliar a capacidade terapêutica, animais C57BL/6 desafiados com melanoma foram tratados com parasitos transgênicos em associação com anticorpos monoclonais anti-CTLA-4 e anti-CD25, que auxiliam na manutenção da resposta efetora.

4.9.1. Produção do anticorpo monoclonal anti-CTLA-4

Células 9D9, cedidas pelo Dr. James P. Allison do Memorial Sloan-Kettering Câncer, são hibridomas capazes de produzir e secretar no sobrenadante o anticorpo monoclonal anti-CTLA-4. As células foram cultivadas aproximadamente por duas semanas, até atingirem o crescimento exponencial, sem a realização da coleta do sobrenadante. Após esse período o hibridoma passou a ser repicado na proporção de 1:10 e cultivado por quatro a cinco dias, em estufa úmida à 37ºC e 5% de CO_2, quando então as células foram centrifugadas e o sobrenadante coletado e congelado.

Com o objetivo de purificar o anti-CTLA-4, os sobrenadantes de cultura foram submetidos a diálise em membrana de celulose (Sigma-Aldrich) que retém proteínas de peso molecular maior que 120 kDa e, posteriormente, à cromatografia de afinidade. A coluna de polipropileno Hitrap proteína G (GE Healthcare) foi utilizada de acordo com protocolo do fabricante e a concentração do anticorpo foi medida no aparelho Nanodrop 1000 (Thermo Scientific).

4.9.2. Anticorpo monoclonal anti-CD25

Gentilmente cedido pelo pesquisador Policarpo Ademar Sales Junior, o anticorpo monoclonal anti-CD25 IL-2Rα foi produzido à partir do hibridoma PC61.

4.9.3. Protocolo terapêutico

Foram realizados três diferentes protocolos terapêuticos sendo que a inoculação das células do melanoma foi considerada, em todos os protocolos, como o dia 0. O primeiro tratamento iniciou-se com 400 μg de anti-CD25 intraperitoneal, 200 μl/animal, 4 dias antes do desafio tumoral (Quezada, Peggs *et al.*, 2006). No dia 14, foram inoculados 1 x 10^7 parasitos tripomastigotas juntamente com a primeira dose de 100 μg do anticorpo monoclonal anti-CTLA-4, administrados intraperitonealmente (Quezada, Peggs *et al.*, 2006). Outras quatro aplicações do anti-CTLA-4 ocorreram com o intervalo de três dias enquanto a segunda dose do parasito foi datada no dia 21 (Figura 5).

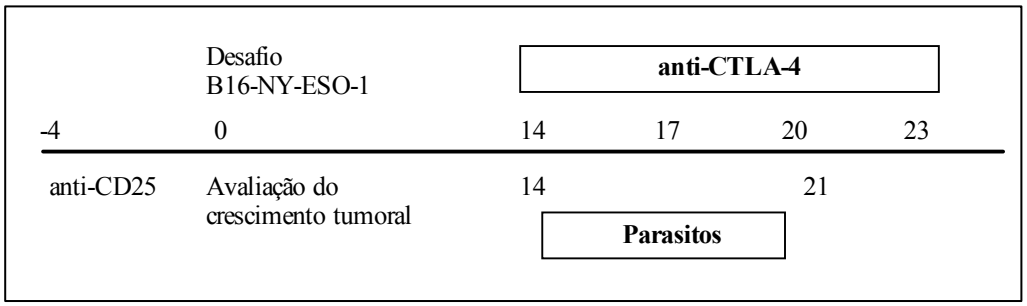

Figura 5. Representação esquemática do primeiro protocolo terapêutico proposto. O desafio com células tumorais expressando o CTA, considerado no dia zero, aconteceu quatro dias após a inoculação de 400 μg do anticorpo anti-CD25. À partir do dia 14 seguiu-se com duas doses de parasitos transgênicos (1 x 10^7 tripomastigotas metacíclicos) com intervalo de 5 dias e cinco doses de 100 μg de anti-CTLA-4. O acompanhamento da progressão do tumor foi realizada durante todo o tempo.

No segundo protocolo, iniciado no dia 11, o intervalo de três dias para o anti-CTLA-4 foi mantido por estar bem estabelecido na literatura. O tratamento com os parasitos, na mesma dose do tratamento anterior, realizou-se nos dias 12 e 17 (Figura 6).

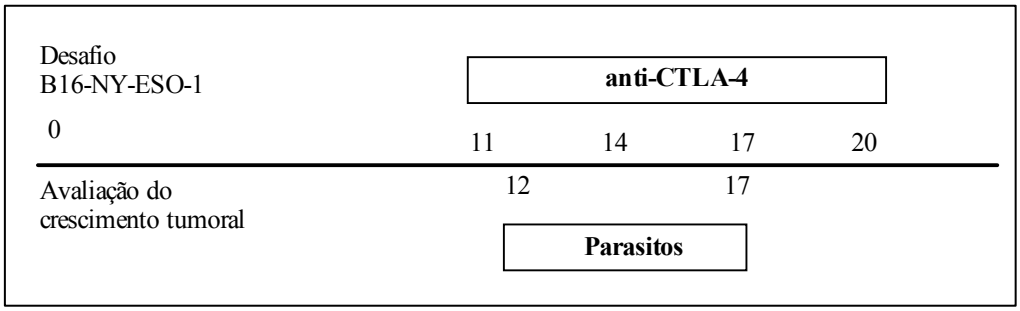

Figura 6. Segundo protocolo terapêutico utilizado. O desafio com células tumorais B16 expressando o NY-ESO-1 foi marcado como dia zero. No dia 11 foi realizada a primeira dose de anti-CTLA-4 seguida de mais 4 doses. O tratamento com o parasito foi iniciado no décimo primeiro dia e repetido no dia 17. O crescimento tumoral foi avaliado durante todo o tempo.

O terceiro tratamento começou mais precocemente, sendo aplicado três doses de parasitos nos dias 4, 9 e 14 enquanto o anti-CTLA-4 foi administrado nos dias 3, 6, 9, 12 e 15 (Figura 7).

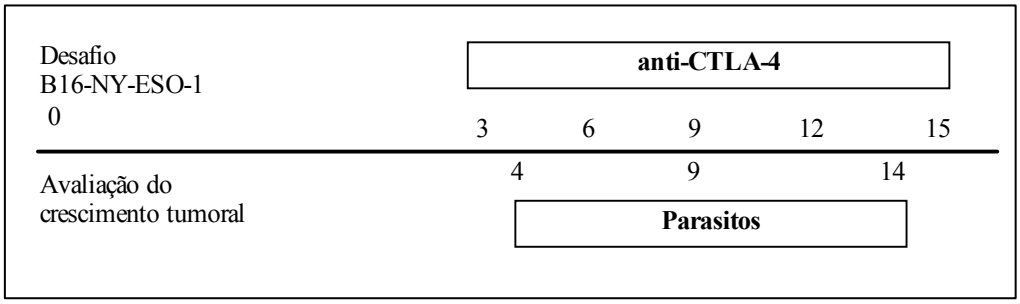

Figura 7. Terceiro modelo terapêutico adotado. O protocolo foi iniciado no dia zero com o desafio com as células tumorais B16-NY-ESO-1. No terceiro dia foi inoculada a primeira dose do anti-CTLA-4 e no dia seguinte foi realizada a primeira dose do parasito transgênico. Seguiu-se com mais duas doses de parasitos transgênicos (1 x 10^7 tripomastigotas metacíclicos) com intervalo de 5 dias e quatro doses de 100 μg de anti-CTLA-4. O crescimento tumoral foi avaliado durante todo o tempo.

4.11. ELISPOT

Para a realização do ensaio de "Enzyme-linked immunosorbent spot" (ELISPOT), no primeiro dia, placas de cultura celular MultiScreen - HA (Millipore) de 96 poços foram sensibilizadas com anticorpos de captura anti-IFN-γ de um dia para o outro a 4°C. No dia seguinte, as placas foram lavadas com PBS, bloqueadas com R10 por 2 horas e lavadas três vezes com meio de cultura RPMI. Em seguida, 5 x 10^4 esplenócitos foram

plaqueados em cada poço em meio R10 contendo 20 ng/mL IL-2 recombinante (RD systems) e os seguintes estímulos: 10 μM CD4-NY-ESO-1 (FYLAMPFATPMEAEL), 10 μM CD8-NY-ESO-1 (LLEFYLAM), 10 μg/mL rNY-ESO-1, 10 μM TSKB20. O controle positivo usado foi 5μg/mL de Concanavalina-A e, como controle negativo, foi utilizado meio R10. As placas foram mantidas em estufa por 24 h, com 5% CO_2 a 37°C. Após o período de cultivo, as células foram descartadas, as placas lavadas com PBS tween 20 (2 vezes) e incubadas por 2 horas com anticorpo biotinilado anti-IFN-γ. Em seguida, foram novamente lavadas e incubadas com streptavidina-ALP (Roche Applied Science, Penzberg, Alemanha) por 1 hora. O ensaio foi revelado com substrato bromocloroindol fosfato em conjunção com nitroblue tetrazoluim (BCIP/NTB) diluído em água. A reação cromogênica foi paralisada com água corrente. Os *spots* foram quantificados em leitor de ELISPOT ImmunoSpot (CTL).

4.12. Processamento do infiltrado tumoral

Para coletar as células do infiltrado tumoral, o melanoma foi retirado e tratado com 1 mg/mL de colagenase IA (Sigma) em Solução Balanceada de Hank´s (HBSS) (0,4 g/L de KCl, 0,06 g/L KH_2PO_4, 8 g/L NaCl, 0,05 g/L Na_2HPO_4, 1 g/L D-glucose, 0,35 g/L $NaHCO_3$, pH 7,4) por 90 minutos a temperatura ambiente seguido por passagem em um filtro de 0.45 μm (Mitsui, Nishikawa *et al.*, 2010). As células foram marcadas para análise por citometria de fluxo, como previamente descrito.

5. Resultados

A gama de funções e respostas das células T incluem a capacidade de proliferar ou induzir a proliferação de outras células (através da secreção de fatores de crescimento), auxiliar respostas imune antígeno-específicas, realizar diretamente funções efetoras (como matar as células infectadas através de mecanismos citolíticos ou pela secreção de citocinas) e, ainda, desenvolver a memória imunológica para a posterior defesa rápida do organismo (Seder, Darrah *et al.*, 2008). Procuramos analisar os aspectos relacionados à resposta imune de maneira ampla no controle do crescimento tumoral seja na vacinação ou na terapia proposta com parasitos transgênicos.

No trabalho desenvolvido em nosso grupo, por Junqueira e colaboradores, animais C57BL/6 imunizados com duas doses de parasitos transgênicos foram desafiados 21 dias após a última dose, com 5 x 10^4 células tumorais B16 expressando ou não o CTA NY-ESO-1(Junqueira, Santos *et al.*, 2011). Os dados apresentados pelos autores, demonstrado na Figura 8, indicaram que os parasitos transgênicos foram capazes de inibir o crescimento tumoral de maneira antígeno-específica para o antígeno NY-ESO-1, assim como proporcionaram o aumento da sobrevida dos animais.

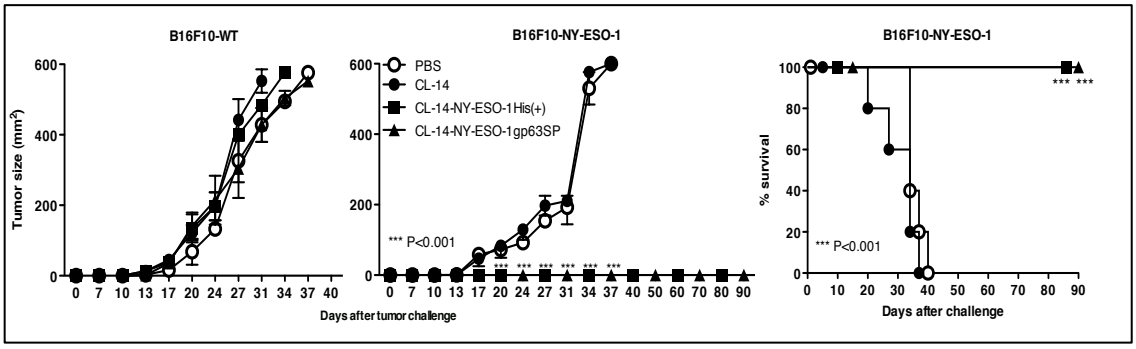

Figura 8. Acompanhamento do crescimento tumoral após vacinação com parasitos transgênicos. Animais imunizados com os parasitos transgênicos e seus controles foram desafiados com $5x10^4$ células de melanoma B16-F10, expressando ou não o antígeno tumoral NY-ESO-1. (A) O crescimento tumoral foi medido por 40 dias nos animais desafiados com as células B16F10-WT e por (B) 90 dias nos animais desafiados com as células tumorais que expressam o *cancer testis*. (C) Os animais que receberam melanoma B16-NY-ESO-1 foram monitorados também quanto à porcentagem de sobrevivência após o desafio.

Nessa tese, o parasito CL-14-NY-ESO-1 gp63SP foi utilizado em todos os nossos experimentos, devido ao fato do CTA ser processado e apresentado tanto pela via exógena quanto a via endógena de apresentação do antígeno (Junqueira, Santos *et al.*, 2011). Dessa forma, de agora em diante, o denominaremos apenas CL-14-NY-ESO-1.

1.1. Duas doses de parasito transgênico são necessárias para induzir imunidade protetora antitumoral

Primeiramente nós investigamos o número mínimo de doses do parasito transgênico necessárias para induzir a imunidade protetora em um protocolo de vacinação homóloga. Camundongos C57BL/6 foram divididos em 4 grupos para imunização: PBS, CL-14, CL-14-NY-ESO-1 e CL-14-NY-ESO-1 morto. O intervalo entre as doses foi de trinta dias e os subgrupos que receberam apenas a dose inicial foram denominados "prime", enquanto os que tiveram a dose de reforço foram denominados "prime/boost". Nós observamos que a imunização única com CL-14-NY-ESO-1 não foi capaz de proteger contra o subsequente desafio com o melanoma B16-NY-ESO-1. Por

outro lado, a aplicação de uma dose de reforço do parasito transgênico vivo foi suficiente para garantir a eficácia tanto para o controle tumoral quanto para a sobrevida dos animais (Figura 9). Previamente foi descrito que os parasitos CL-14 são incapazes de replicar e reinvadir as células do hospedeiro sistematicamente. Assim, nós hipotetizamos que uma dose do parasito atenuado é silenciosa e não é capaz de estimular o sistema imune de forma ampla contra o tumor, devido a insuficiente apresentação dos antígenos cancerígenos. Corroborando essa hipótese e a provável necessidade da infecção ativa das células do sistema imune, foi observado que, mesmo com a aplicação da segunda dose, os parasitos mortos são ineficazes como vacina antitumoral, o que nos levou a excluir esse grupo dos experimentos posteriores.

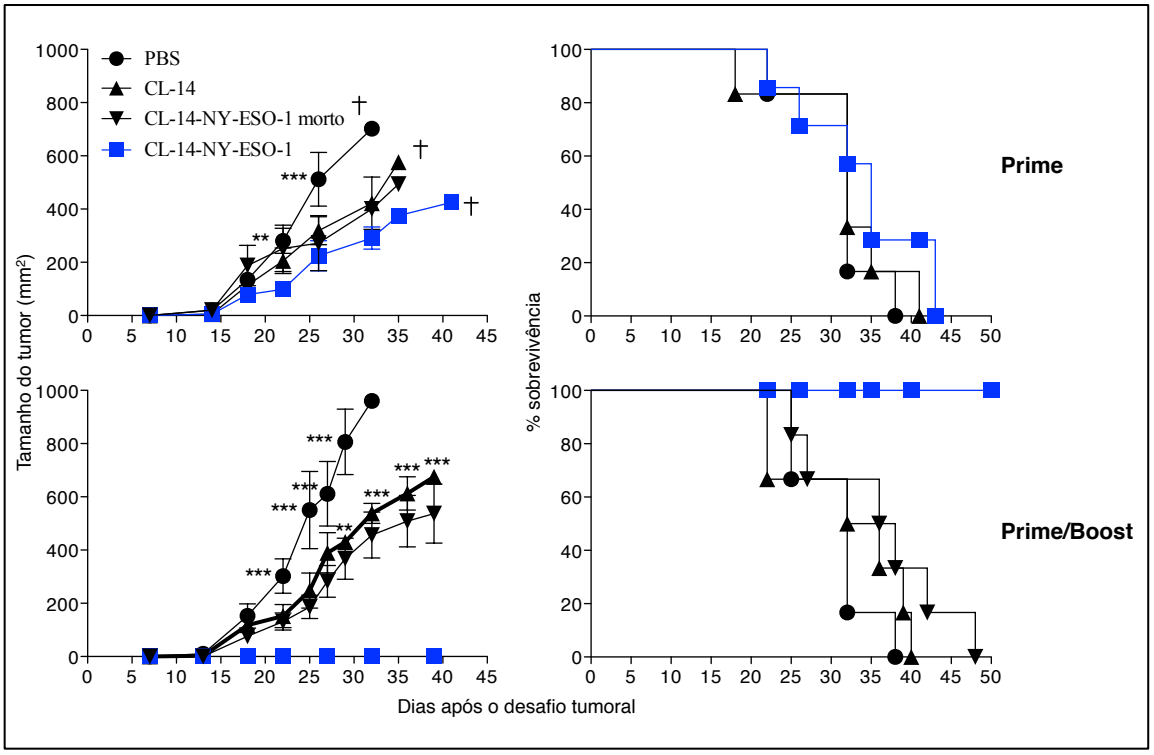

Figura 9. Acompanhamento do crescimento tumoral após vacinação com parasitos transgênicos. Camundongos C57BL/6 imunizados com controle PBS, uma dose (painel superior) ou duas doses homólogas (painel inferior) de parasitos transgênicos foram desafiados com $5x10^4$ células de melanoma B16-NY-ESO-1. A sobrevivência e o crescimento tumoral foram monitorados. $*P < 0.05$, $**P < 0.01$, $***P < 0.001$ por two-way ANOVA. Resultados similares foram encontrados em três experimentos independentes com seis animais em cada grupo.

Seguindo a avaliação da capacidade do CL-14-NY-ESO-1 em estimular o sistema imune, nós avaliamos quais os tipos de células foram infectadas após a inoculação intraperitoneal. Para isso, tripomastigotas metacíclicos foram marcados com CFSE, e inoculados em camundongos C57BL/6. Após os intervalos de 1 hora, 20 horas e 3 dias coletamos o lavado intraperitoneal, o linfonodo mesentérico e o baço dos animais. Procedemos a marcação de superfície com os anticorpos e avaliamos imediatamente por citometria de fluxo (Figura 10). Nossos dados demonstraram que na primeira hora os macrófagos, na região intraperitoneal, foram a fonte primária de células infectadas, seguido pelas células dendríticas. Nos tecidos linfoides secundários as células dendríticas foram a principal fonte de parasitos intracelulares uma hora (linfonodo mesentérico) e 20 horas (baço) após a inoculação do CL-14-NY-ESO-1. Assim, nós inferimos que depois da internalização do parasito transgênico, as células dendríticas migram para o tecido linfoide secundário iniciando a resposta imune.

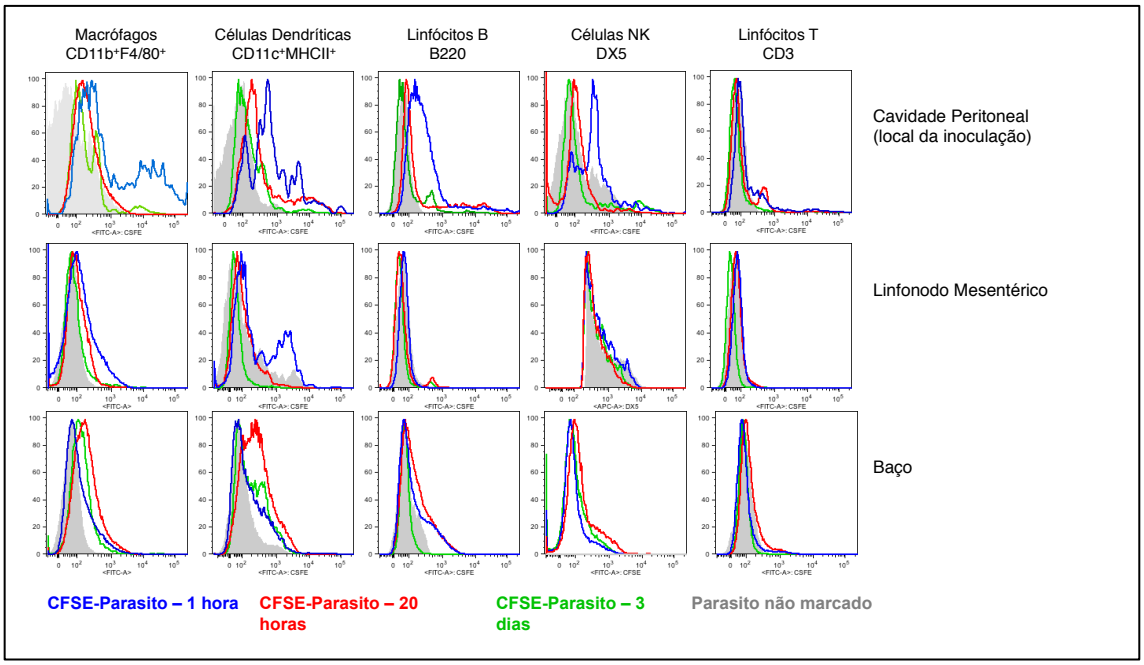

Figura 10. Células dendríticas são a principal fonte de parasitos intracelulares nos tecidos linfoides secundários. Dez milhões de parasitos da forma metacíclica do CL-14-NY-ESO-1 marcados ou não (controle) com CFSE foram injetados intraperitonealmente e a presença dos parasitos intracelulares foram avaliados 1 hora, 20 horas e 3 dias após infecção. Resultados similares foram encontrados em três experimentos independentes com quatro animais em cada grupo.

Comparamos então, a ativação das células T no linfonodo mesentérico proporcionada pela inoculação de uma dose do CL-14-NY-ESO-1 versus duas doses em um protocolo homólogo com intervalo de 30 dias. As avaliações ocorreram 1 hora, 1 dia e 3 dias após a injeção intraperitoneal. Corroborando os dados do controle antitumoral, nós demonstramos que em todos os tempos avaliados há um aumento das células T ativadas ($CD3^{+}CD44^{high}$) quando o camundongo recebeu a dose de reforço (Figura 11).

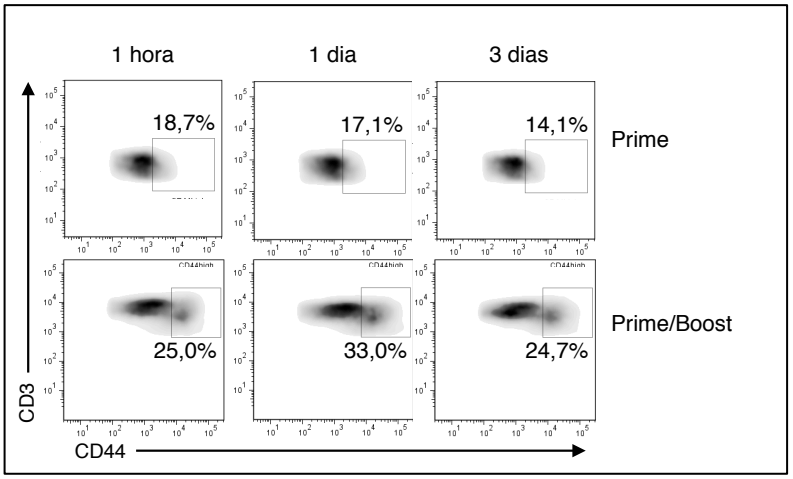

Figura 11. A dose de reforço estimula o aumento da porcentagem das células T ativadas no linfonodo mesentérico. Camundongos C57BL/6 receberam uma dose de dez milhões da forma metacíclica do CL-14-NY-ESO-1 intraperitonealmente (painel superior, prime) ou duas doses homólogas com intervalo de 30 dias (painel inferior, prime/boost). O linfonodo foi coletado 1 hora, 1 dia ou 3 dias e, após marcação das células com CD3 e CD44 foi realizado a análise por citometria de fluxo. Resultados similares foram encontrados em três experimentos independentes com quatro animais em cada grupo.

A fim de avaliar a indução de citocinas no local da infecção, foi realizado o lavado intraperitoneal com 5 mL de PBS e a dosagem de citocinas foi aferida por CBA. As avaliações ocorreram 1 hora, 1 dia e 3 dias após a injeção intraperitoneal. Os dados representados na Figura 12 sugerem a ativação de macrófagos do tipo M1, mais eficientemente após duas doses do parasito transgênico.

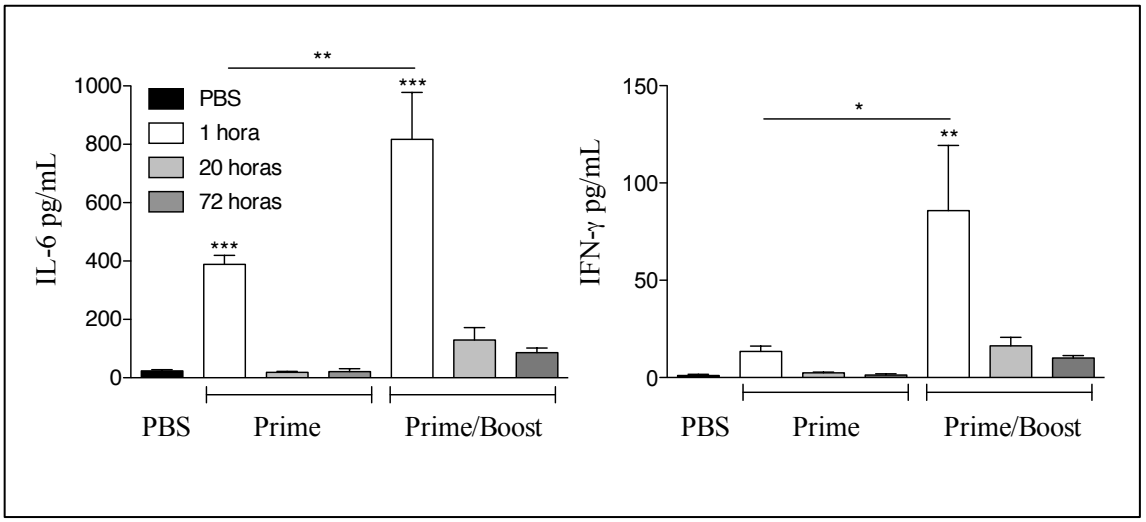

Figura 12. Dose de reforço induz maior produção de citocinas no sítio da infecção. Camundongos C57BL/6 receberam uma dose (Prime) de dez milhões da forma metacíclica do CL-14-NY-ESO-1 intraperitonealmente ou duas doses homólogas (Prime/Boost) com intervalo de 30 dias ou PBS (controle negativo). O lavado intraperitoneal foi coletado 1 hora, 1 dia ou 3 dias e as citocinas foram aferidas por CBA. Resultados similares foram encontrados em três experimentos independentes com quatro animais em cada grupo.

Para avaliação da resposta imune especifica contra NY-ESO-1, os esplenócitos dos camundongos vacinados foram coletados e estimulados com a proteína rNY-ESO-1 e/ou avaliados *ex vivo* por citometria de fluxo. Os níveis das principais citocinas relacionadas ao controle tumoral, IFN-γ e IL-2, foram medidos por ELISA após 72 horas de estimulação. IL-2 elucida efeitos antitumorais pela estimulação da proliferação das células do sistema imune, incluindo células T e NK, e pela atividade citolíticas (Tanaka, Saijo *et al.*, 2000). Em consonância com nossa teoria, uma única dose do parasito transgênico não induziu produção de IL-2 e nem a indução das células T $CD8^+$ tetrâmero específicas para NY-ESO-1 (Figura 13). Entretanto, com uma dose adicional dos parasitos transgênicos, os camundongos produziram IL-2 e IFN-γ além de altos níveis de células T $CD8^+$ NY-ESO-1-específicas.

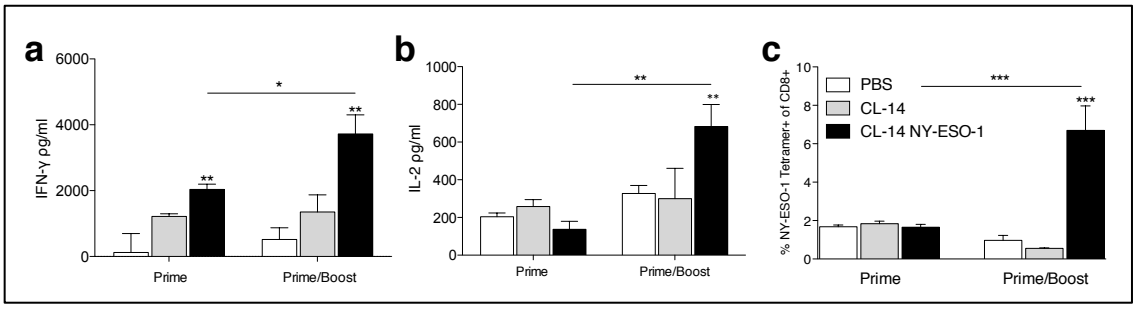

Figura 13. Duas doses do CL-14-NY-ESO-1 são suficientes para induzir resposta imune antitumoral. Esplenócitos dos camundongos que receberam uma (Prime) ou duas doses homólogas (Prime/Boost) do parasito ou PBS (controle negativo) foram avaliados 21 dias após a última dose. Para avaliação das citocinas IFN-γ **(a)** e IL-2 **(b)** produzidas, as células foram submetidas a estimulação com rNY-ESO-1. As células NY-ESO-1-tetramero^{+} foram avaliadas por citometria de fluxo *ex vivo* **(c)**. $*P < 0.05$, $**P < 0.01$, $***P < 0.001$ por teste T. Resultados similares foram encontrados em três experimentos independentes com quatro animais em cada grupo.

5.2 Vacinação com a cepa atenuada de *T. cruzi* é segura e fornece resposta imune eficiente

Então nós avaliamos se a resposta antitumoral induzida pelo parasito é sustentada. Para isso foi realizada a aplicação do protocolo prime-boost e após 21, 45 e 85 dias da dose de reforço os esplenócitos foram coletados, processados e submetidos ao procedimento desejado. Nós encontramos que a produção das citocinas e a frequência das células T CD8^{+} *T. cruzi*-específicas, que respondem ao peptídeo imunodominante do parasito TSKB20 (ANYKFTLV), manteve-se elevada até 45 dias após o boost. Essa resposta foi, entretanto, insignificante na avaliação após 85 dias (Figura 14*a*).

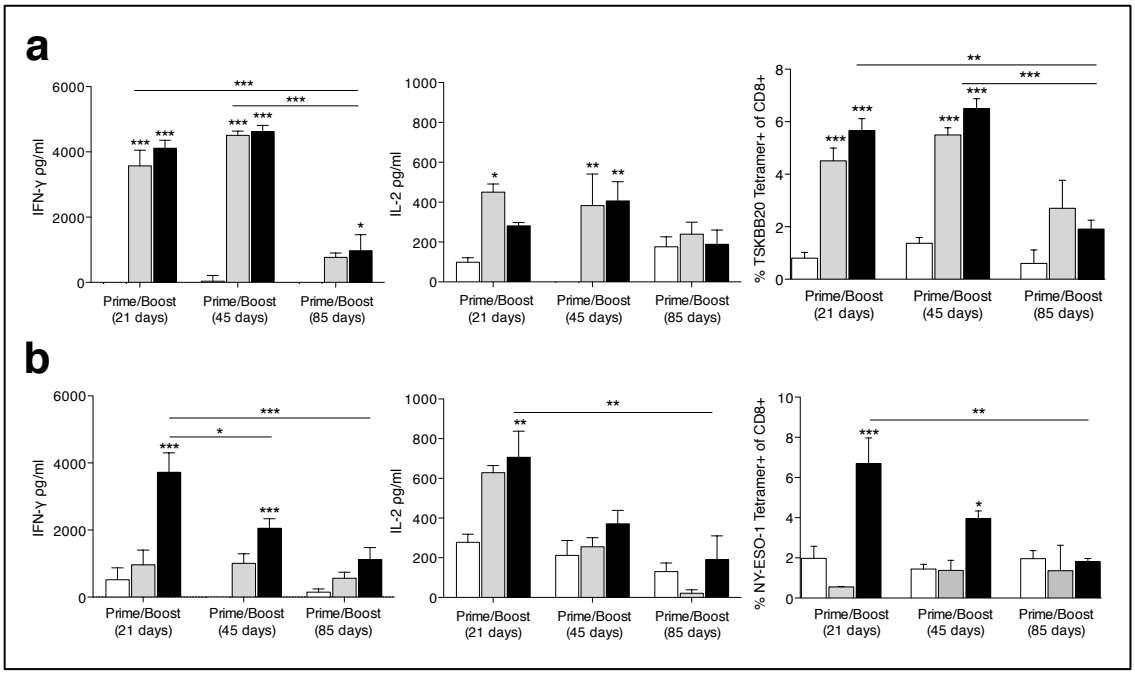

Figura 14. Indução da produção de citocinas foi maior 21 dias após a dose de reforço. Ativação da resposta imune antígeno-específica foi avaliada após protocolo prime/boost em três pontos: 21, 45 e 85 dias após o boost. A resposta específica ao parasito **(a)** ou ao tumor **(b)** foi representada no conjunto dos gráficos de barra superior e inferior, respectivamente. Os níveis de produção das citocinas IFN-γ e IL-2 foi medido após estimulação por 48 horas com peptídeo de *T. cruzi* TSKB20 (a), ou com rNY-ESO-1 (b). O sobrenadante da cultura foi avaliado por ELISA. As células específicas-tetrâmero$^+$ foram avaliadas por citometria de fluxo *ex vivo*. **P* < 0.05, ***P* < 0.01, ****P* < 0.001 por teste T. Resultados similares foram encontrados em três experimentos independentes com quatro animais em cada grupo.

O decaimento da resposta imune também foi observado quando verificamos a resposta frente ao CTA carreado pelo parasito transgênico. Embora tenha sido encontrada alta produção de IFN-γ após estimulação com a proteína rNY-ESO-1 mesmo com 45 dias após a imunização, o nível de IL-2 foi insignificante e a frequência das células T CD8$^+$ tumorais-específicas foi quase duas vezes menor, quando comparada com 21 dias, e desapareceu no tempo de 85 dias (Figura 14*b*). Esses dados sugerem que as células efetoras se transformaram em células de memória efetora, que não produzem IL-2 de forma eficiente quanto comparadas às células efetoras e às células de memória central.

A melhor resposta efetora foi encontrada na avaliação de 21 dias após o boost, para ambos os estímulos submetidos. A alta produção das citocinas e a frequência das células específicas tanto para o parasito quanto para o CTA, demonstram alta capacidade

sugestiva de combater eficientemente o tumor. Em adição, nós encontramos, nesse tempo, que cerca de 30% das células NY-ESO-1-tetramero^{+} são funcionais, ou seja, capazes de produzir IFN-γ quando submetidas ao estímulo com a proteína recombinante NY-ESO-1 (Figura 15).

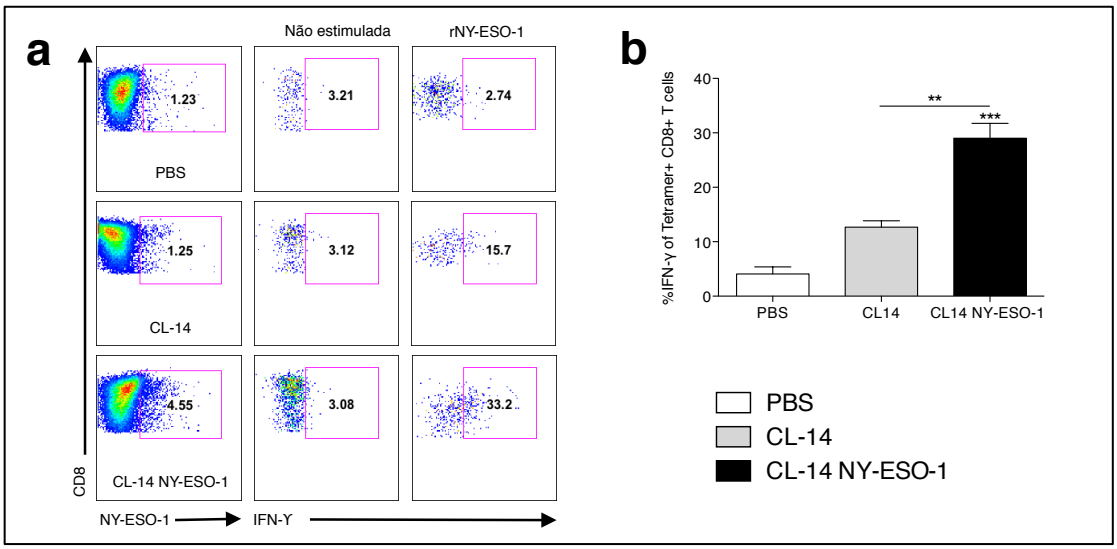

Figura 15. Produção de IFN-γ pelas células tetrâmero positivas NY-ESO-1. Células específicas ao CTA são capazes de produzir IFN-γ frente ao estímulo com a proteína rNY-ESO-1. O gráfico de barras é representativo do experimento com 4 camundongos por grupo. A estatística foi realizada com o teste 1way ANOVA/Bonferroni comparando com todos com o grupo PBS e entre o CL-14 e CL-14-NY-ESO-1. Resultados similares foram encontrados em três experimentos independentes com quatro animais em cada grupo.

5.3 Determinação do subtipo das células CD8 induzidas

O próximo passo foi analisar as características fenotípicas das células T CD8^{+} induzidas após a imunização com o parasito transgênico. Nossos dados mostraram que os parasitos transgênicos induziram a proliferação e diferenciação das células T para o fenótipo T_E quando avaliadas 21 dias após o boost com cerca de 60% das células T CD8^{+} ativadas, enquanto somente 36,4% desse subtipo foi encontrado no grupo controle imunizado com PBS. No dia 45 após o boost, entretanto, a frequência das células T_{EM}

foi aumentada. Nós encontramos 43% das T_{EM} nos animais vacinados com parasitos transgênicos, enquanto que a porcentagem de cerca de 30% foi mantida no grupo controle (Figura 16).

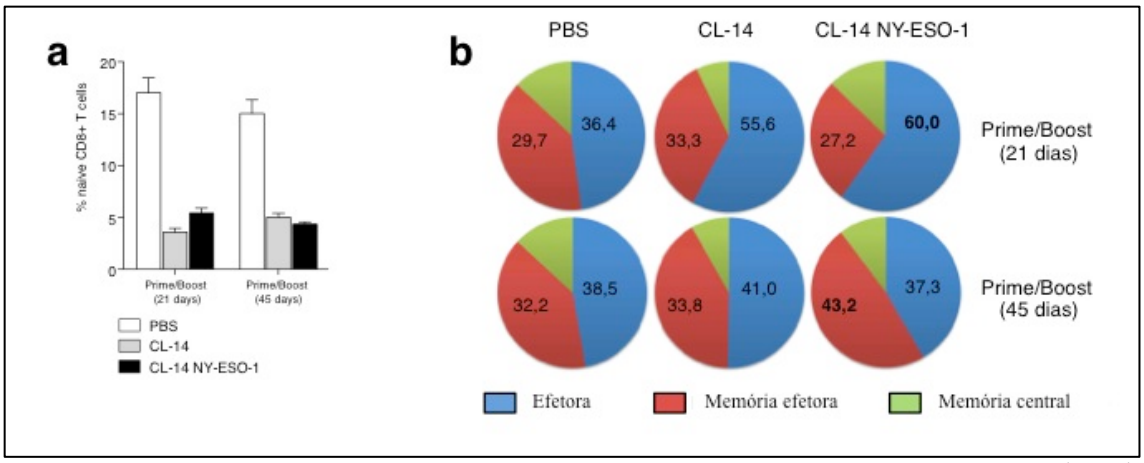

Figura 16. Subtipos das células T CD8 determinados por citometria de fluxo. As células $CD3^{+}CD8^{+}$ foram avaliadas quanto ao fenótipo dos seus subtipos: Naive (CD62LHighCD44Low), Efetora (CD62LLowCD127Low), Memória Efetora (CD62LLowCD127High) e Memória Central (CD62LHighCD127High). As células naive foram representadas no gráfico de barras (**a**) e após a determinação das células ativadas ($CD44^{high}$) foram determinados os demais subtipos representados nos gráficos de pizza (**b**). Resultados similares foram encontrados em quatro experimentos independentes com quatro animais em cada grupo.

A resposta imune efetiva contra qualquer patologia é diretamente relacionada à resposta específica gerada. Para isso fizemos a analise fenotípica dos subtipos das células T $CD3^{+}CD8^{+}$Tetrâmero^{+} e encontramos que ambas populações de células específicas, tanto para o parasito quanto para o NY-ESO-1, eram T_E no dia 21 enquanto com 45 dias eram T_{EM} após o boost. Assim, nossos achados indicaram que o parasito transgênico além de induzir uma alta frequência das células efetoras também é capaz de promover a geração de células de memória efetora contra o tumor (Figura 17).

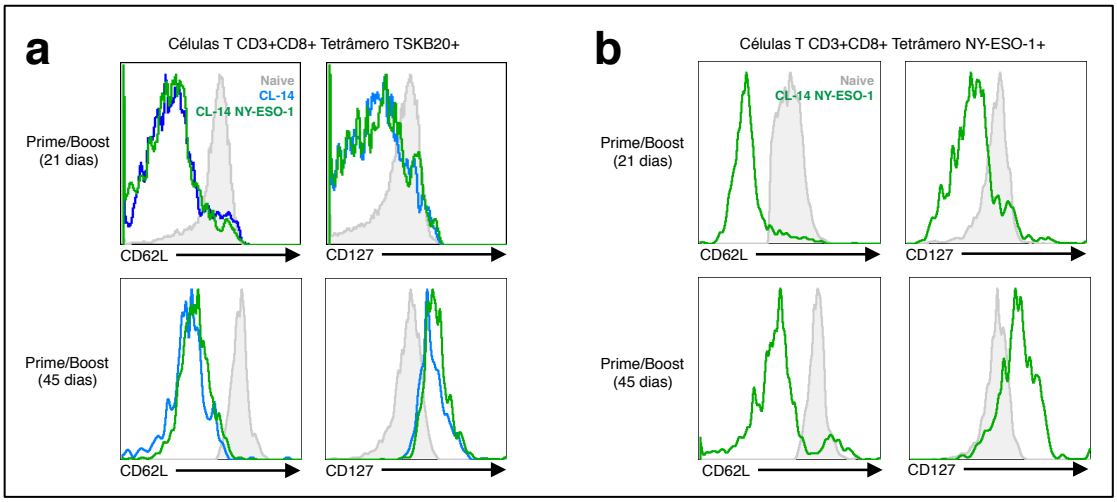

Figura 17. Caracterização do subtipo das células $CD8^{+}$Tetrâmero^{+}. Após determinação das populações de células T CD8 tetrâmero-específicas ao parasito (TSKB20) (a) e ao *cancer testis* (NY-ESO-1) (b), avaliamos o subtipo fenotípico dessas células. Os gráficos superiores são representativos de 21 dias após o boost e os gráficos inferiores demonstram o tempo de 45 dias após o boost. Resultados similares foram encontrados em quatro experimentos independentes com quatro animais em cada grupo.

5.4 Avaliação da geração de células CD8 citolíticas granzima B^{+}

Os linfócitos T citotóxicos (LTCs) são indispensáveis na defesa permanente do organismo contra a infecção viral e no controle do desenvolvimento do tumor. A linhagem de animais transgênicos gzmBCreER^{T2}/ROSA26EYFP foi usada nesses experimentos por permitirem a marcação *ex vivo* de células T $CD8^{+}$ com a proteína fluorescente amarela (EYFP), no momento que adquiriram a capacidade efetora com a expressão da gzmB. Nesse modelo a magnitude da expressão do granulo lítico correlaciona-se com a proporção de células $EYFP^{+}$ (Bannard, Kraman *et al.*, 2009) (Figura 18*a*).

Primeiramente observamos que as células $CD8^{+}gzmB^{+}$ estavam presentes nos camundongos imunizados com CL-14-NY-ESO-1 em ambos os tempos de 21 e 45 dias após o boost (Figura 18*b*). Ao avaliarmos os subtipos das células gzmB constatamos que as células evoluíram do perfil $CD8^{+}$ T_E no 21° dia para $CD8^{+}$ T_{EM} com 45 dias após

a última vacinação (Figura 18*c, d*). Previamente foi descrito que as células $CD8^+$ T_{EM} são as únicas células de memória capazes de expressar o granulo lítico perforina (Wherry, Teichgraber *et al.*, 2003). Apoiando esse potencial citolítico descrito das $CD8^+$ T_{EM} , aqui nós demonstramos a expressão da gzmB, outro granulo lítico considerado essencial no controle tumoral.

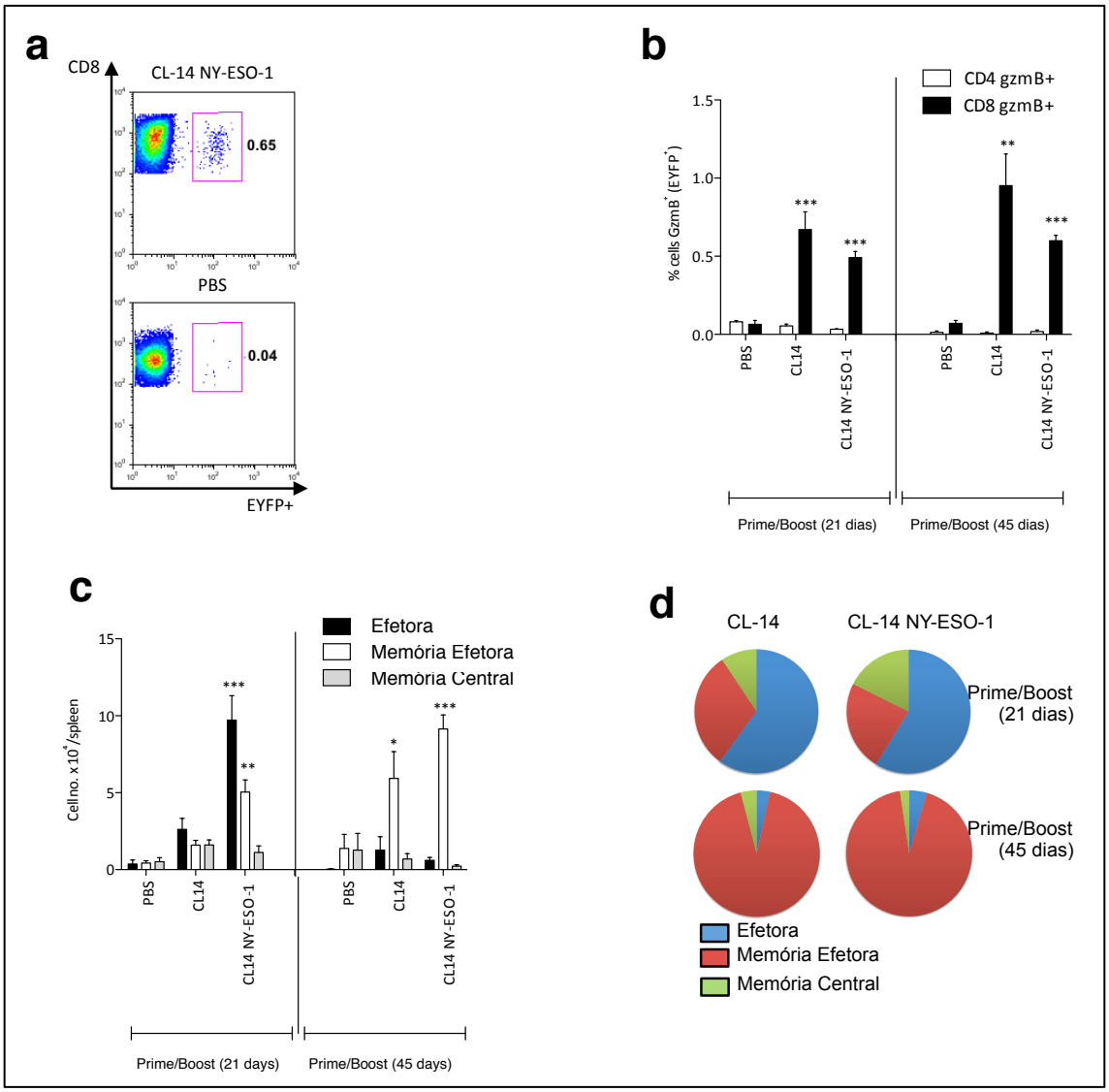

Figura 18. Expressão de gzmB em camundongos gzmBCreER^{T2}/ROSA26EYFP. Camundongos transgênicos foram vacinados com parasitos e PBS e avaliados quanto a presença de células $EYFP^+$ que concomitantemente expressam $gzmB^+$. O gráfico 'pseudo-color density plots' demonstra o gate realizado nas células $CD8^+EYFP^+$(**a**). O primeiro gráfico de barras corresponde a análise da frequência das células EYFP que são células T $CD3^+CD4^+$ ou $CD3^+CD8^+$(**b**). As células caracterizadas como $EYFP^+CD8^+$ foram fenotipadas quanto ao seu subtipo e foi representado no segundo gráfico de barras (**c**). A análise estatística intra-grupo foi feita por meio do teste T comparando com animais que receberam PBS. Resultados similares foram encontrados em quatro experimentos independentes com três animais em cada grupo.

A próxima questão levantada foi se haviam células específicas com capacidade tumoricida, expressando gzmB. Nessa vertente, observamos dentro da população das células EYFP$^+$ a presença de células específicas ao tumor. Nossos dados demonstram que mais de 30% das células T CD8$^+$gzmB$^+$ são NY-ESO-1-específicas, 21 dias após o protocolo vacinal prime/boost (Figura 19*a,b*). Assim, nós concluímos que a imunização com os parasitos transgênicos promovem a geração de células efetoras, potencialmente capazes de lisar as células tumorais através da atividade dos grânulos líticos.

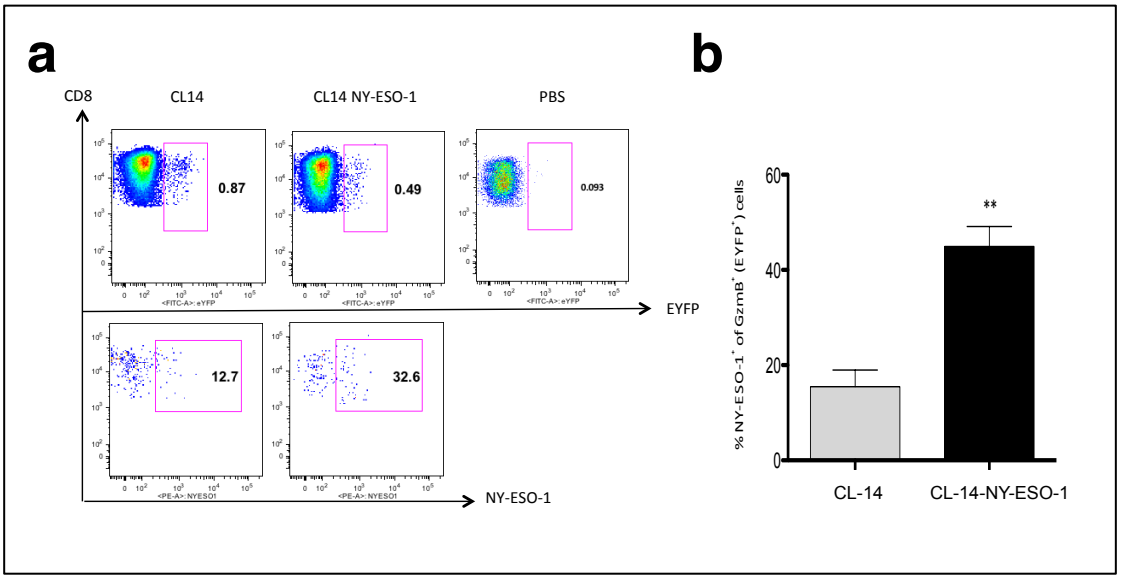

Figura 19. Células específicas antitumoral tem capacidade citolitica. Animais vacinados com duas doses de parasitos transgênicos e que tiveram o baço coletado após 22 dias da última dose foram avaliados quanto a presença de células gzmB$^+$tetrâmero-NY-ESO-1$^+$. Para isso, após determinarmos a população de células EYFP$^+$, avaliamos a presença de células específicas ao *cancer testis* NY-ESO-1, pela marcação com o tetrâmero (**a**). O gráfico de barras é representativo do experimento realizado (**b**). O PBS apesar de estar representado no 'pseudo-color density plots' não foi representado no gráfico de barras devido a quantidade reduzida de células, considerada negativa. A análise estatística foi realizada pelo teste T. Resultados similares foram encontrados em quatro experimentos independentes com quatro animais em cada grupo.

5.5 Alta frequência de células CD8 efetoras associada ao controle do tumor B16-NY-ESO-1 em animais vacinados

Após avaliação do perfil imune induzido pela vacinação com CL-14-NY-ESO-1 em diferentes tempos, checamos o impacto dessas respostas no controle do crescimento tumoral. Nós demonstramos que quando o desafio com o melanoma B16-NY-ESO-1 ocorre precocemente no período efetor, 21 dias após o boost, o controle do crescimento tumoral é completo nos camundongos vacinados, assim como sua sobrevida (100%). Entretanto, com um desafio tardio, 45 dias após a dose de reforço, foi constatado uma diminuição no controle do crescimento tumoral e na sobrevivência dos animais (60%). Em um prazo maior, 85 dias após a última dose, quando já constatamos que o parasito provavelmente foi eliminado pela avaliação da resposta imune, não há diferença entre os grupos vacinados e controle. Aliado aos nossos dados de caracterização da resposta imune, esses resultados nos permitem afirmar que o controle do crescimento tumoral está diretamente associado à presença de um potencial efetor completo, com as células efetoras. Dessa forma, sugerimos doses subsequentes da vacina para manter uma resposta adequada. O entendimento do perfil imune adequado para o controle tumoral induzido pelo CL-14-NY-ESO-1 nos conduziu a ingressar para um caminho mais inovador e urgente contra o câncer: a terapia.

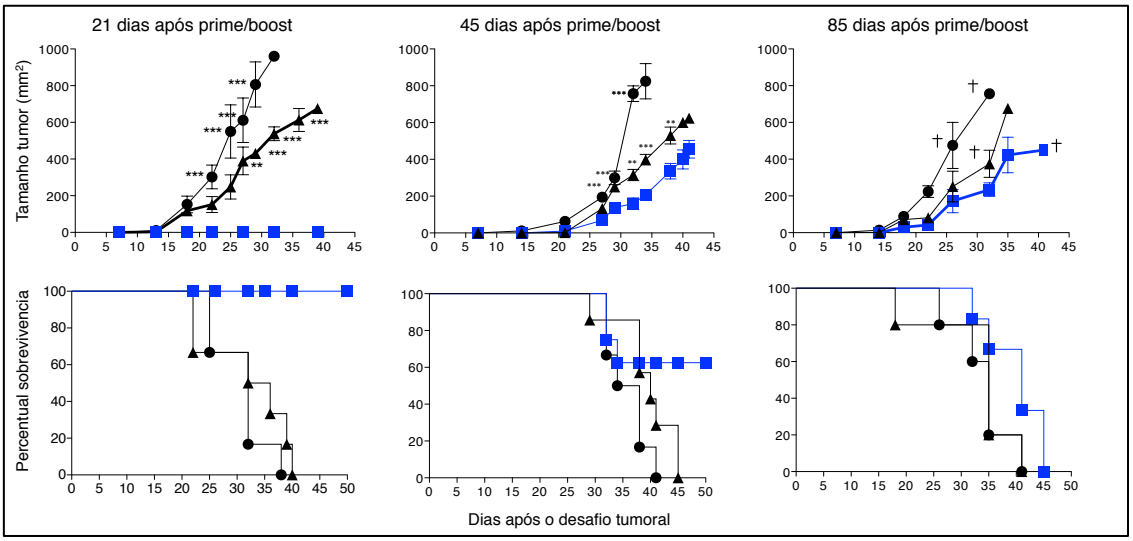

Figura 20. Protocolo profilático com duas doses do parasito transgênico e o controle do crescimento tumoral. Camundongos C57BL/6 foram vacinados com protocolo prime/boost do parasito CL-14-NY-ESO-1 e decorridos 21 dias (esquerda), 45 dias (meio) e 85 dias (direita) após a dose de reforço foram desafiados com células de melanoma B16-NY-ESO-1. O crescimento tumoral e a sobrevivência foram acompanhados por 45 e 50 dias, respectivamente. A análise estatística foi feita pelo teste Two-way ANOVA/Bonferroni comparando todos os grupos com o grupo dos animais vacinados com CL-14 NY-ESO-1. $*P < 0.05$, $**P < 0.01$, $***P < 0.001$. Resultados similares foram encontrados em três experimentos independentes com seis animais em cada grupo.

5.6 Protocolo Imunoterapêutico contra o melanoma

No primeiro protocolo, inserimos o anticorpo monoclonal anti-CD25 com o objetivo de depletar células regulatórias, que tem um impacto ainda controverso no controle tumoral (Mitsui, Nishikawa *et al.*, 2010; Nishikawa e Sakaguchi, 2010; Saha e Chatterjee, 2010) (Figura 21).

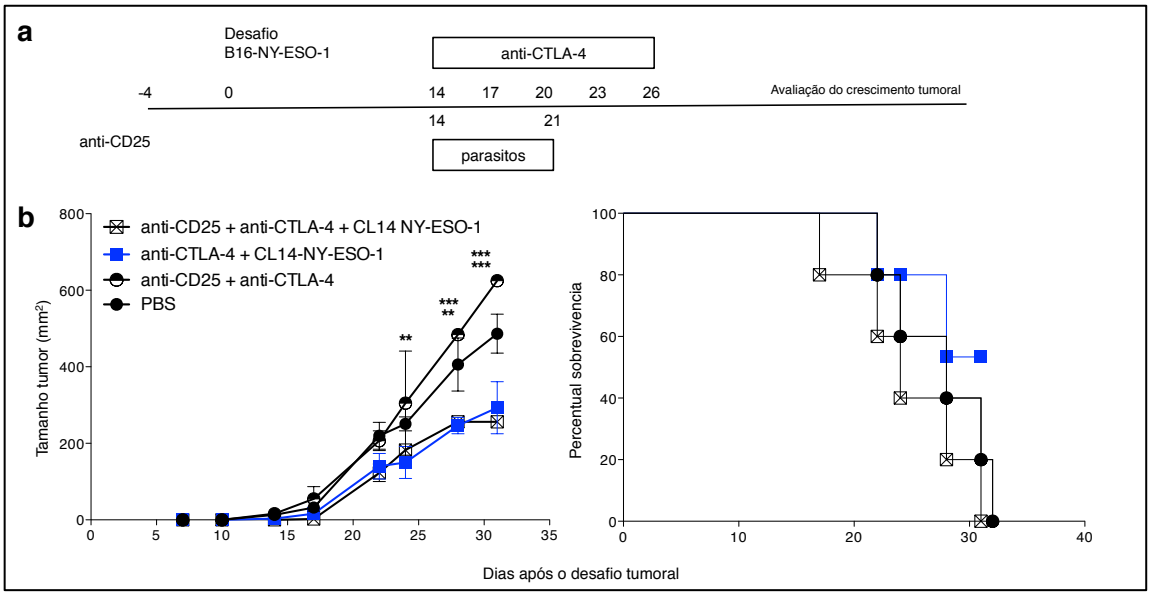

Figura 21. Tratamento combinado com parasito transgênico com anti-CTLA-4 retarda o crescimento tumoral. O primeiro protocolo terapêutico proposto para o melanoma B16-NY-ESO-1 foi representado na linha superior (a). Em animais C57BL/6 foram usadas combinações com os anticorpos anti-CTLA-4, anti-CD25 e parasitos transgênicos expressando a proteína *cancer testis*, visando controlar o crescimento tumoral do melanoma B16-NY-ESO-1. O crescimento tumoral e a sobrevivência foram acompanhados durante 35 e 40 dias, respectivamente. (**b**). A análise estatística foi feita pelo teste Two-way ANOVA/Bonferroni comparando todos os grupos com os animais tratados com anti-CTLA-4 + CL-14-NY-ESO-1. $*P < 0.05$, $**P < 0.01$, $***P < 0.001$. Resultados similares foram encontrados em três experimentos independentes com seis animais em cada grupo.

Acompanhamos no primeiro protocolo um controle no crescimento tumoral de maneira semelhante nos grupos tratados com anti-CTLA-4 em combinação com o parasito e no grupo em que foi acrescido anti-CD25 a esse tratamento. Na Figura 22*a* está representado o segundo protocolo de tratamento utilizado. Nós decidimos retirar o uso do anti-CD25 já que, além da sua combinação não ter alterado a resposta, a aplicação desse anticorpo deve ser realizada antes do desafio com as células tumorais e dessa forma, não mimetiza um tratamento real, que é iniciado após a detecção tumoral. O início do tratamento também foi alterado para o 11° dia. Essa modificação foi devida ao tamanho do tumor detectado com 14 dias nos camundongos ser representativo em humano de um tumor em estágio avançado. O controle do crescimento tumoral e a sobrevivência foram acompanhados por 35 e 40 dias, respectivamente (Figura 22*b*).

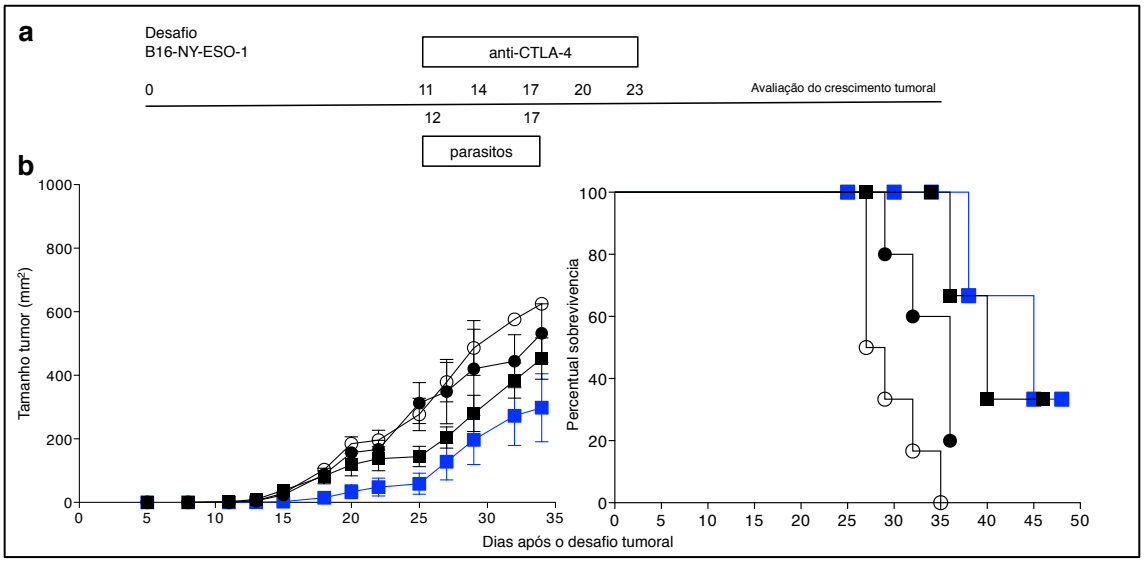

Figura 22. Tratamento iniciado com 11 dias retarda o crescimento tumoral. Tratamento do melanoma B16-NY-ESO-1 a partir do 11° dia de desafio (**a**). Animais C57BL/6 foram desafiado com tumor B16 expressando NY-ESO-1 e posteriormente tratados com combinações com o anticorpo anti-CTLA-4 mais parasitos transgênicos expressando a proteína *cancer testis*. O crescimento tumoral e a sobrevivência foram acompanhados durante 35 e 40 dias, respectivamente. (**b**). A análise estatística foi feita pelo teste Two-way ANOVA/Bonferroni comparando todos os grupos com os animais tratados com anti-CTLA-4 + CL-14-NY-ESO-1. *$P < 0.05$, **$P < 0.01$, ***$P < 0.001$. Resultados similares foram encontrados em três experimentos independentes com seis animais em cada grupo.

Apesar do controle da progressão tumoral ter sido observado no grupo tratado com o parasito transgênico associado ao bloqueio do CTLA-4, nós desejávamos uma resposta objetiva com melhor regressão tumoral. Visando atingir esse resultado e devido a agressividade do tumor, no protocolo seguinte proposto, iniciamos o tratamento mais precocemente, 3 dias após o desafio, representando assim o reconhecimento do tumor em sua fase inicial. O melanoma é detectado no paciente no estágio inicial, identificado como uma mancha escura e irregular na pele, dessa forma o novo protocolo precoce proposto por nosso grupo está mais apropriado para a realidade (Figura 23*a*). Os resultados demonstraram o controle efetivo da progressão tumoral, tendo crescido menos de duas vezes quando comparado ao parasito transgênico sozinho e cerca de quatro vezes ao comparar com o grupo controle PBS (Figura 23*b*). Além disso, a sobrevivência desses pacientes foi de 100%, enquanto os animais tratados somente com anti-CTLA-4 morreram no inicio do tratamento, provavelmente devido a uma desordem

linfoproliferativa.

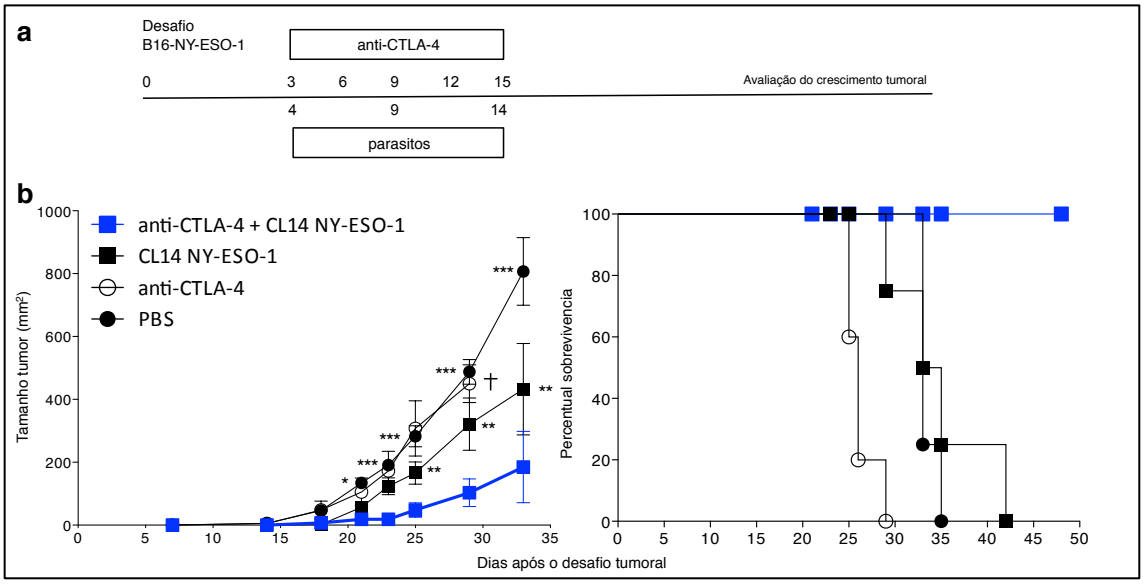

Figura 23. Tratamento combinado com parasito transgênico e anti-CTLA-4 é capaz de controlar efetivamente o crescimento tumoral. O tratamento do melanoma B16-NY-ESO-1 foi iniciado a partir do 3° dia de desafio. Animais C57BL/6 foram desafiado com tumor B16 expressando NY-ESO-1 e tratados com combinações com o anticorpo anti-CTLA-4 mais parasitos transgênicos expressando a proteína *cancer testis* (Fig 25 **a**). O crescimento tumoral e a sobrevivência foram acompanhados durante 35 e 40 dias, respectivamente. (**b**). A análise estatística foi feita pelo teste Two-way ANOVA/Bonferroni comparando todos os grupos com os animais tratados com anti-CTLA-4 + CL-14-NY-ESO-1. $*P < 0.05$, $**P < 0.01$, $***P < 0.001$. Resultados similares foram encontrados em três experimentos independentes com seis animais em cada grupo.

A fim de avaliar a importância das células T CD8 no controle tumoral proporcionado pela terapia proposta nós realizamos o mesmo protocolo terapêutico adotado anteriormente, e que apresentou resultados objetivos, (Figura 24) em animais β2-microglobulin$^{-/-}$. A deficiência em células T CD8 e em células NK1.1, presentes nesses animais, demonstrou ser fatal para a sobrevida dos camundongos e para o controle do crescimento tumoral, mesmo quando tratados com o melhor modelo proposto. Podemos, assim inferir que essas células auxiliam em conjunto no controle do crescimento tumoral, já que o tumor apresenta-se um pouco aumentado quando comparado aos animais C57BL/6.

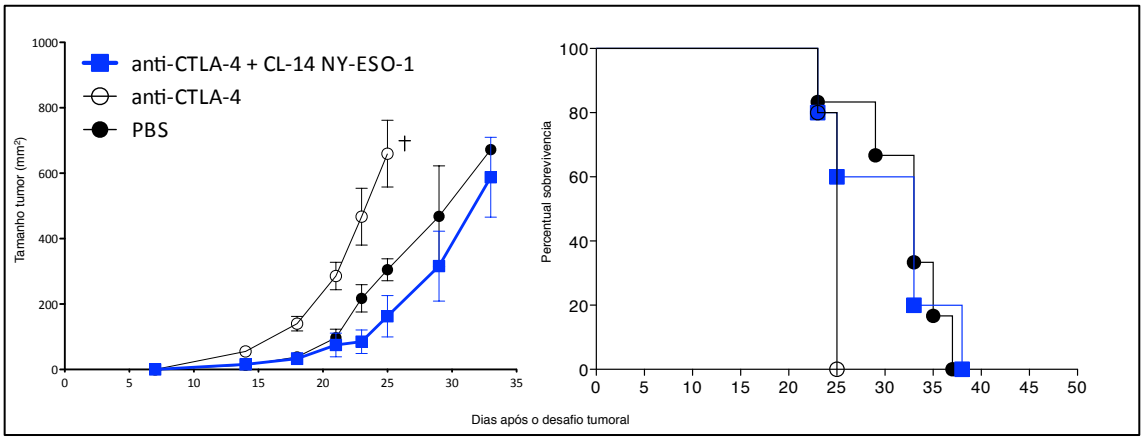

Figura 24. Tratamento do melanoma em camundongos CD8 nocautes. Animais CD8 nocautes foram desafiados com tumor B16 expressando NY-ESO-1 e tratados com combinações com o anticorpo anti-CTLA-4 mais parasitos transgênicos expressando a proteína *cancer testis*. Resultados similares foram encontrados em três experimentos independentes com cinco animais em cada grupo.

5.7 CL-14-NY-ESO-1 e anti-CTLA-4 aumentam a frequência das células NY-ESO-1-específicas e estimula a migração dos linfócitos T CD8+ para o infiltrado tumoral.

A fim de compreender melhor o mecanismo imunológico através do qual o tratamento com anti-CTLA-4 aumenta a eficácia da imunoterapia com CL-14-NY-ESO-1, foram caracterizados os fenótipos das células T $CD8^+$, aos 21 e 28 dias após o desafio com as células B16-NY-ESO-1. A porcentagem total das células efetoras encontrada no baço dos camundongos sugere que o tratamento com anti-CTLA-4 atua prolongando o tempo das células $CD8^+$ T_E induzidas pelos parasitos transgênicos (Figura 25*a*). Interessantemente, nós encontramos que o bloqueio do CTLA-4 promove ainda a expansão das células T NY-ESO-1-tetramero$^+$(Fig.27*b*).

A indução do *spreading* antigênico para outras proteínas do melanoma foi avaliada pelo uso do tetrâmero específico para a glicoproteína (gp) 100, que é altamente expressa nos melanócitos. O *spreading* antigênico acontece quando o sistema imune reconhece antígenos tumorais que não foram apresentados pela vacina utilizada. Nossa análise

mostrou um significante aumento na frequência dos linfócitos T gp100-tetramero^{+} nos camundongos tratados, quando comparados ao grupo controle (Figura 25*c*). Posteriormente nós avaliamos o estado funcional das células T CD8^{+} a partir da produção da citocina IFN-γ. Nós constatamos alta frequência de células produtoras de IFN-γ nos camundongos tratados com CL-14-NY-ESO-1/anti-CTLA-4, em resposta a estimulação *in vitro* com rNY-ESO-1 (Figura 25*d*) e ainda secreção dessa citocina no soro dos camundongos cerca de três vezes maior nos grupos com tratamento combinado ao comparar a terapia somente com o parasito (Figura 25*e*). Complementarmente, como previamente descrito (Mahmoud, Paish *et al.*, 2011; Nasman, Romanitan *et al.*, 2012), nossos experimentos indicaram a presença de células T CD8^{+} no infiltrado tumoral que correlaciona positivamente com melhor prognóstico dos camundongos desafiados com melanoma B16-NY-ESO-1. Nós observamos aproximadamente 1% das células T CD8^{+} no infiltrado tumoral dos camundongos tratados com CL-14-NY-ESO-1/anti-CTLA-4, e menos de 0.5% nos outros grupos (Figura 25*f*).

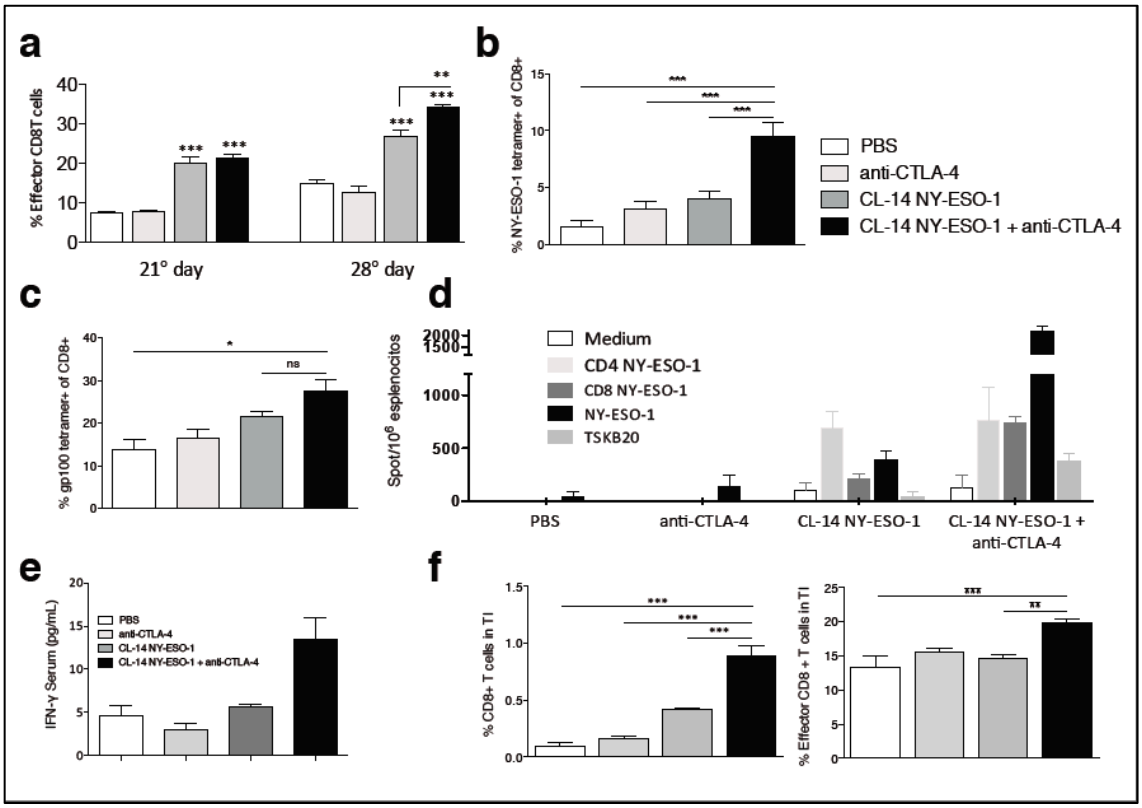

Figura 25. Longevidade das células efetoras específicas protegem o camundongo contra o desenvolvimento do tumor. Camundongos C57BL/6 foram desafiados com células B16-NY-ESO-1 e após 21 e 28 dias foram avaliadas a porcentagem de células efetoras no baço **(a)**. A frequência das células T $CD8^+$ tetrâmero-específicas foram determinadas por citometria de fluxo no dia 28 para o antígeno NY-ESO-1 **(b)** e o *spreading* antigênico foi avaliado pelo gp100 **(c)**. No mesmo dia, o número dos esplenócitos produtores de IFN-γ foram estimados por ELISPOT. Para isso, células dos camundongos foram estimuladas *in vitro* com peptídeos restritos para NY-ESO-1 (epítopo T $CD4^+$ FYLAMPFATPMEAEL assim como para o epítopo T $CD8^+$/ LLEFYLAM) ou proteína recombinante NY-ESO-1 ou um peptídeo *T. cruzi*-específico (TSKB20/ ANYDFTLV) **(d)**. A produção dessa citocina foi medida ainda no soro 48 horas após a última dose do tratamento **(e)**. Nós observamos por citometria de fluxo células T $CD8^+$ no infiltrado tumoral (esquerda) e o fenótipo efetor dessas células (direita) **(f)**. Dados estão representados como a média ± s.e.m. de três a cinco experimentos independentes realizados em triplicata. $*P < 0.05$, $**P < 0.01$, $***P < 0.001$ por one-way ANOVA e Bonferroni pós teste.

6. Discussão

O principal desafio no campo de desenvolvimento de uma vacina contra o câncer é a indução de uma resposta antitumoral efetiva com resposta do tipo 1 e com memória imunológica. Esses objetivos são semelhantes à construção de vacinas contra várias doenças infecciosas, em que a proteção imunológica bem sucedida é normalmente induzida com vacinas vivas (Bolhassani, Safaiyan *et al.*, 2011). Nesse sentido, ambos os vetores baseados em vírus e bactérias estão sendo estudados como potenciais veículos antigênicos para as células do sistema imunológico contra o tumor. Fowlpox vírus, cepas atenuadas de Salmonella e *Listeria monocytogenes* têm mostrado grande potencial como vetores vivos com amplas aplicações (Pan, Ikonomidis *et al.*, 1995; Wherry, Barber *et al.*, 2004; Moreno, Kramer *et al.*, 2010; Odunsi, Matsuzaki *et al.*, 2012). No entanto, apenas alguns ensaios clínicos foram realizados até agora, e apesar de terem mostrado de forma conclusiva a segurança de alguns desses sistemas, os resultados de imunogenicidade estão abaixo do ideal (Moreno, Kramer *et al.*, 2010).

Nosso grupo tem aplicado valiosos esforços no desenvolvimento de uma estratégia inovadora que usa um clone de *T. cruzi* altamente atenuado (CL-14) como um vetor vacinal, expressando o antígeno *cancer testis* NY-ESO-1, considerado o CTA mais imunogênico atualmente descrito. Usando estes parasitos transgênicos como uma vacina profilática, obtivemos 100% de proteção perante o desafio com uma linhagem celular de melanoma (Junqueira, Santos *et al.*, 2011). O CL-14 clone foi derivado da cepa CL, isolada no início de 1980 e é consistentemente avirulenta. Ambos parasitemia e parasitismo tecidual estão ausentes, mesmo em camundongos recém-nascidos ou imunodeficientes, conhecido por ser altamente suscetível à infecção pelo *T. cruzi* (Lima,

Lenzi *et al.*, 1995; Junqueira, Santos *et al.*, 2011). Entretanto, nós mostramos que apesar do fenótipo altamente atenuado, a infeção é suficiente para iniciar a resposta imune.

A chave para o desenvolvimento de uma resposta antitumoral eficaz é a quebra da tolerância imunológica e ativação de células T antígeno-específicos com função efetora robusta (Smyth, Godfrey *et al.*, 2001). Existe um consenso de que uma vacina eficaz contra o câncer deve induzir células T $CD8^+$ citotóxicas, e vigorosa produção de citocinas, tais como IFN-γ e IL-2, que medeiam várias funções efetoras (Schuler-Thurner, Schultz *et al.*, 2002).

Acreditamos que pelo menos dois atributos tornam o CL-14 um grande vetor vacinal. Para começar, a infecção com o *T. cruzi* continuamente estimula a resposta, pela expressão intrínseca de agonistas de TLR, tais como âncoras glicosylphosphatidyliositol, CpG não metilado e ssRNA (Bartholomeu, Ropert *et al.*, 2008; Caetano, Carmo *et al.*, 2011; Junqueira, Santos *et al.*, 2011). Isso resulta na polarização de linfócitos Th1 específicos de antígenos ideais para controlar o tumor. Em segundo lugar, em seu ambiente citoplasmático, o *T. cruzi* libera proteínas que são processadas para a apresentação por moléculas de MHC classe I. Cada ciclo de replicação intracelular dura até 5 dias, proporcionando assim um tempo considerável para a detecção dessas células infectadas por células T $CD8^+$ parasito-específicas (Padilla, Bustamante *et al.*, 2009). Em particular, o parasito transgênico CL-14 expressando o NY-ESO-1 é capaz de secretar o CTA para o citoplasma da célula hospedeira, conduzindo a uma apresentação direta MHC I (Junqueira, Santos *et al.*, 2011). Além disso, foi descrito que o parasito CL-14-NY-ESO-1 escolhido nessa tese é capaz de gerar resposta específica das células T CD4. Essas células são responsáveis, na resposta efetora contra o tumor, principalmente por estimular os LTCs. Em modelo

murino foi demonstrado que a depleção de células T CD4 resulta na inabilidade da rejeição completa de modelos tumorais exercendo assim um papel auxiliar fundamental na ativação dos linfócitos T CD8 (Hung, Hayashi *et al.*, 1998; Wang, 2001).

LTCs reconhecem e matam as células-alvo por duas vias principais: através da introdução de uma bateria de proteases chamadas granzimas, no citosol da célula-alvo, ou através da superfamília TNF. A morte da célula alvo de maneira granzima-dependente é rápida e eficiente, pois sua ação ocorre por meio de vias redundantes da morte celular (Cullen, Brunet *et al.*, 2010).

A granzima B (gzmB) é a mais abundante das granzimas e sua importância na execução oportuna de células infectadas ou tumorigênicas foi demonstrada em estudos onde observou-se que as células efetoras ausentes de gzmB tem a atividade citotóxica muito mais lenta do que aquelas células que as tem (Heusel, Wesselschmidt *et al.*, 1994; Pardo, Bosque *et al.*, 2004). A eficiência da gzmB é em grande parte devido à sua capacidade para ativar proteases da célula-alvo, as caspases, direta ou indiretamente (Cullen e Martin, 2008).

Nesse trabalho, nós demonstramos que as duas doses homólogas com o clone atenuado CL-14-NY-ESO-1 é capaz de promover a expansão das células T $CD8^+$ específicas contra o tumor expressando granzima B^+, e a produção de níveis elevados de IFN-γ e IL-2. Uma resposta típica das células $CD8^+$, no entanto consiste em três fases principais: a expansão do desenvolvimento e diferenciação celular efetora; contração das células efetoras, e a estabilização e a manutenção da população de células de memória (Kaech, Tan *et al.*, 2003). Os linfócitos T $CD8^+$ de memória são classificadas em células de memória central ($CD8^+T_{CM}$) ou células de memória efetora ($CD8^+T_{EM}$) (Bixby e

Tarleton, 2008; Vasconcelos, Dominguez *et al.*, 2012). Similar a outras infecções persistentes, tem sido mostrado que as células $CD8^+T_{EM}$ formadas durante a infecção com o protozoário *T. cruzi* são mantidas primariamente pela continua apresentação do antígeno (Padilla, Bustamante *et al.*, 2009). A frequência da subpopulação das células $CD8^+T_{CM}$ aumenta à medida que a infecção se torna mais crônica (Bixby e Tarleton, 2008).

No nosso modelo, o CL-14-NY-ESO-1 foi capaz de estimular a formação das células $CD8^+T_{EM}$ mas, provavelmente devido à eliminação do parasito, a frequência dessas células decaiu para os níveis basais e apenas algumas células $CD8^+T_{CM}$ foram geradas.

O *clearance* do parasito é sugerido ao analisarmos a longevidade da resposta específica. É extensivamente descrito que as células TSKB20-específicas expandem e contraem durante a infecção aguda causada pelo parasito, mas são mantidas durante a fase crônica (Martin, Weatherly *et al.*, 2006; Bixby e Tarleton, 2008). Ao usarmos o parasito atenuado na vacinação dos camundongos observamos a contração da resposta imune, conforme descrito anteriormente, mas os níveis posteriores são insignificantes. Os valores indetectáveis da resposta imune contra o protozoário sugerem que esses foram eliminados do organismo dos animais e apesar de não induzirem a resposta das células $CD8^+T_{CM,}$ garantem a biossegurança da vacina.

Alguns estudos também mostraram que a estimulação *in vitro* das células $CD8^+T_{CM}$ resultam na produção de IL-2, mas pouco IFN-γ, IL-4 ou IL-5 (Kaech e Ahmed, 2001). Em contraste, as células $CD8^+T_{EM}$ produzem citocinas efetoras rapidamente, mas produzem menos IL-2 (Wherry, Teichgraber *et al.*, 2003). Além disso, apenas na subpopulação das células $CD8^+T_{EM}$ foi encontrado perforina intracelular (Wherry,

Teichgraber *et al.*, 2003). Aqui, nós demonstramos que a produção da citocina efetora IFN-γ foi mantida por um longo período. Essa produção prolongada foi associada à presença das células $CD8^{+}T_{EM}$. A diminuição da IL-2 pode estar relacionada com a estimulação de poucas células $CD8^{+}T_{CM.}$ Além disso, as células expressando a molécula citotóxica granzima B, semanas após o boost, foram células $CD8^{+}T_{EM}$ como mostrado por outros estudos para a perforina intracelular. No entanto, previamente foi descrito que apesar das células efetoras de memória serem capazes de ter as suas funções efetoras ativadas, elas proliferam deficientemente em resposta ao antígeno (Stemberger, Huster et ai., 2007). De acordo com essas descrições e a necessidade de uma resposta robusta para controle do tumor, observou-se que a proteção integral da vacina requer a presença de células efetoras funcionais em sua plenitude.

Mais urgente do que a produção de uma vacina profilática eficaz contra o tumor é o estabelecimento de novas terapias antitumorais. A ativação dos linfócitos T requer o reconhecimento de antígenos específicos em conjunto com sinais coestimulatórios como o receptor constitutivo CD28. Uma vez ativadas, as células T aumentam a expressão transiente do receptor CTLA-4. Esse último concorre com o primeiro para a ligação dos mesmos ligantes, CD80 e CD86, expressos na superfície das células apresentadoras de antígenos (Scott, Wolchok *et al.*, 2012). Enquanto a ligação com o CD28 promove a ativação da célula T, o CTLA-4 funciona como um sinal de exaustão, inibindo a progressão do ciclo da célula imune e a produção de IL-2 (Scott, Wolchok *et al.*, 2012). Assim, a sinalização pelo CTLA-4 fornece o feedback negativo para as células T ativadas, atenuando assim a resposta imune. A deficiência da expressão do CTLA-4 leva a linfoproliferação fatal e autoimunidade, exemplificando a sua importância na

regulação negativa fisiológica das células T (Corse e Allison, 2012; Scott, Wolchok *et al.*, 2012).

Devido a sua eficácia, a droga Yervoy® (Ipilimumab, Bristol-Myers Squibb Company), um anticorpo que se liga ao CTLA-4, foi aprovada nos Estados Unidos da América e na Europa como uma alternativa para o tratamento antitumoral (Hodi, O'day *et al.*, 2010). O Ipilimumab bloqueia especificamente a ligação do CTLA-4 aos seus ligantes e assim proporciona a ativação e proliferação dos linfócitos T e consequentemente a regressão tumoral (Dillard, Yedinak *et al.*, 2010; Hodi, O'day *et al.*, 2010; Robert, Thomas *et al.*, 2011; Yuan, Ginsberg *et al.*, 2011; Fellner, 2012). Entretanto, a monoterapia com o Ipilimumab foi eficaz somente em 20-30% dos pacientes e diversos efeitos tóxicos foram reportados devido a modulação não específica do sistema imune (Dillard, Yedinak *et al.*, 2010; Heger, 2012). Além disso, o bloqueio do CTLA-4 não induziu a rejeição de tumores menos imunogênicos, tais como o melanoma B16 e o carcinoma mamário SM1 (Hurwitz, Yu *et al.*, 1998; Sotomayor, Borrello *et al.*, 1999; Curran, Montalvo *et al.*, 2010). Uma estratégia para minimizar os efeitos secundários e aumentar a eficiência da terapia com o anti-CTLA-4 seria a estimulação da resposta imune específica em uma terapia combinada com adjuvantes imunológicos ou uma vacina antitumoral (Quezada, Peggs *et al.*, 2006).

Diferentes estudos tem demostrado que a infecção com o *T. cruzi* promove o aumento da expressão do CTLA-4 e, embora não haja um consenso sobre o efeito nos linfócitos T $CD8^+$, foi descrito que o uso do anti-CTLA-4 aumenta a resistência do hospedeiro à infecção mesmo para as cepas mais virulentas do parasito (Martins, Tadokoro *et al.*, 2004). Nesse contexto, nós combinamos o parasito atenuado que expressa o CTA NY-ESO-1, como uma vacina, com o bloqueio do CTLA-4, objetivando o aumento da ação

do parasito pelo bloqueio dos mecanismos imunoregulatórios, assim como a diminuição dos efeitos adversos da administração do anti-CTLA-4.

A fim de controlar ainda mais a imunoregulação nós sugerimos, em um primeiro momento, a depleção das células regulatórias $CD4^{+}CD25^{+}FoxP3^{+}$ pelo uso do anticorpo monoclonal anti-CD25. Existe uma vasta literatura do papel dessas células na inibição da resposta antitumoral e a sua depleção tem sido utilizada visando aumentar a resposta efetora contra o câncer seja pelo uso apenas do anticorpo monoclonal ou em associação com outras ferramentas vacinais (Dannull, Su *et al.*, 2005; Saha e Chatterjee, 2010). No nosso modelo, nós não observamos diferença significativa na combinação anti-CD25/anti-CTLA-4/CL-14-NY-ESO-1 quando comparado com a terapia apenas com anti-CTLA-4/CL-14-NY-ESO-1. Devido a esse fato e por ser preconizado nos tratamentos antitumorais a depleção das células regulatórias antes do desafio com as células cancerígenas nós optamos por excluir essa ferramenta da nossa terapia.

Em conclusão, relatamos que a terapia com CL-14-NY-ESO-1 associada com o bloqueio do CTLA-4 é altamente eficaz em camundongos portadores do melanoma. A eficiência desse protocolo foi dependente da habilidade do anti-CTLA-4 em promover o desenvolvimento das células $CD8^{+}$ T_E NY-ESO-1-específicas induzidas pelo parasito transgênico. Adicionalmente, pela primeira vez, nós mostramos claramente a manutenção das células tumorais-específicas no tratamento com o anti-CTLA-4. Foi demonstrado também que a vacina terapêutica contribuiu para o *spreading* antigênico, favorecendo a expansão e desenvolvimento da resposta das células T aos antígenos relacionados ao tumor, como mostrado para o gp100. A expressão do gp100 é restrita à linhagem de células melanocíticas e tem sido usado com frequência em testes vacinais contra o tumor devido ao alvo potencial para linfócitos T citotóxicos (Benlalam,

Labarriere *et al.*, 2001). Esse *spreading* antigênico favorece o uso da nossa vacina terapêutica pois demonstra que outros antígenos associados ao tumor, diferentes do alvo da vacina, foram induzidos por esse processo. Finalmente, reportamos que como consequência da expansão das $CD8^+$ T_E nos camundongos tratados coma terapia combinada há uma migração das células T CD8 para o micro ambiente tumoral. A relevância clinica e o prognóstico favorável dessas células no infiltrado tumoral já foi relatado em vários estudos (Hadrup, Donia *et al.*, 2012), e assim parece ser um evento crítico na eficiência da imunoterapia com CL-14-NY-ESO-1/CTLA-4.

7. Sumário dos resultados

O parasito transgênico atenuado CL-14-NY-ESO-1 é internalizado pelas células dendríticas e macrófagos que migram para o linfonodo e baço iniciando a resposta imune.

Duas doses do CL-14-NY-ESO-1 são suficientes e necessárias para indução de uma resposta específica antitumoral capaz de controlar o crescimento do melanoma. No entanto, os dados de longevidade do crescimento tumoral sugerem doses subsequentes da vacina para manter o controle do tumor em um modelo vacinal.

O controle tumoral está diretamente relacionado com a maior frequência e atividade funcional, como a produção de citocinas pelas células CD8 efetoras, principalmente células específicas. Apesar das células de memória efetora serem capazes de controlar o crescimento do câncer elas não são suficientes para impedi-lo.

O bloqueio do CTLA-4 proporciona a manutenção da resposta efetora induzida pelo parasito transgênico e ainda aumenta a frequência das células específicas contra o tumor.

O prognóstico favorável do tratamento, diretamente relacionado com a presença de células CD8 no infiltrado tumoral, correlaciona com os dados obtidos em pacientes descritos na literatura e reforça o potencial terapêutico do uso do CL-14-NY-ESO-1/CTLA-4.

8. Conclusão

Os parasitos transgênicos CL-14-NY-ESO-1 em um modelo profilático induzem uma resposta efetora antitumoral eficiente de maneira antígeno-específica com a geração de células T CD8 efetoras e de memória efetora e produção de IFN-γ e IL-2, além de células NY-ESO-1-específicas com perfil citotóxico. No entanto, essa resposta não é de longa duração e doses subsequentes da vacina seriam necessárias. Frente a um protocolo terapêutico o parasito mostrou-se altamente eficaz associado com o anti-CTLA-4. Foi demonstrado o aumento de células tumor-específicas e o prolongamento da resposta efetora conseguindo assim o controle do melanoma em curso.

Referências

BANNARD, O. *et al.* Secondary replicative function of CD8+ T cells that had developed an effector phenotype. *Science* [S.I.], v. 323, n. 5913, p. 505-9, Jan 23 2009.

BIXBY, L. M.; TARLETON, R. L. Stable CD8+ T cell memory during persistent Trypanosoma cruzi infection. *J Immunol* [S.I.], v. 181, n. 4, p. 2644-50, Aug 15 2008.

CUI, W.; KAECH, S. M. Generation of effector CD8+ T cells and their conversion to memory T cells. *Immunol Rev* [S.I.], v. 236, p. 151-66, Jul 2010.

CULLEN, S. P. *et al.* Granzymes in cancer and immunity. *Cell Death Differ* [S.I.], v. 17, n. 4, p. 616-23, Apr 2010.

CULLEN, S. P.; MARTIN, S. J. Mechanisms of granule-dependent killing. *Cell Death Differ* [S.I.], v. 15, n. 2, p. 251-62, Feb 2008.

HEUSEL, J. W. *et al.* Cytotoxic lymphocytes require granzyme B for the rapid induction of DNA fragmentation and apoptosis in allogeneic target cells. *Cell* [S.I.], v. 76, n. 6, p. 977-87, Mar 25 1994.

HODI, F. S. *et al.* Improved survival with ipilimumab in patients with metastatic melanoma. *N Engl J Med* [S.I.], v. 363, n. 8, p. 711-23, Aug 19 2010.

JUNQUEIRA, C. *et al.* Trypanosoma cruzi as an effective cancer antigen delivery vector. *Proceedings of the National Academy of Sciences of the United States of America* [S.I.], v. 108, n. 49, p. 19695-700, Dec 6 2011.

KAECH, S. M. *et al.* Selective expression of the interleukin 7 receptor identifies effector CD8 T cells that give rise to long-lived memory cells. *Nature immunology* [S.I.], v. 4, n. 12, p. 1191-8, Dec 2003.

KLEIN, O. *et al.* Melanoma vaccines: developments over the past 10 years. *Expert Rev Vaccines* [S.I.], v. 10, n. 6, p. 853-73, Jun 2011.

MARTIN, D. L. *et al.* CD8+ T-Cell responses to Trypanosoma cruzi are highly focused on strain-variant trans-sialidase epitopes. *PLoS Pathog* [S.I.], v. 2, n. 8, p. e77, Aug 2006.

MITSUI, J. *et al.* Two distinct mechanisms of augmented antitumor activity by modulation of immunostimulatory/inhibitory signals. *Clin Cancer Res* [S.I.], v. 16, n. 10, p. 2781-91, May 15 2010.

NISHIKAWA, H.; SAKAGUCHI, S. Regulatory T cells in tumor immunity. *Int J Cancer* [S.I.], v. 127, n. 4, p. 759-67, Aug 15 2010.

PARDO, J. *et al.* Apoptotic pathways are selectively activated by granzyme A and/or granzyme B in CTL-mediated target cell lysis. *J Cell Biol* [S.I.], v. 167, n. 3, p. 457-68, Nov 8 2004.

SAHA, A.; CHATTERJEE, S. K. Combination of CTL-associated antigen-4 blockade and depletion of CD25 regulatory T cells enhance tumour immunity of dendritic cell-based vaccine in a mouse model of colon cancer. *Scand J Immunol* [S.I.], v. 71, n. 2, p. 70-82, Feb 2010.

SEDER, R. A. *et al.* T-cell quality in memory and protection: implications for vaccine design. *Nat Rev Immunol* [S.I.], v. 8, n. 4, p. 247-58, Apr 2008.

TANAKA, M. *et al.* Induction of antitumor immunity by combined immunogene therapy using IL-2 and IL-12 in low antigenic Lewis lung carcinoma. *Cancer Gene Ther* [S.I.], v. 7, n. 11, p. 1481-90, Nov 2000.

ACS, A. C. S. The history of cancer. *What is cancer?* v. 2013. n. 08/07: American Cancer Society, 2012.

AL-HAJJ, M. *et al.* Prospective identification of tumorigenic breast cancer cells. *Proceedings of the National Academy of Sciences of the United States of America* [S.I.], v. 100, n. 7, p. 3983-8, Apr 1 2003.

ANGELOSANTO, J. M.; WHERRY, E. J. Transcription factor regulation of CD8+ T-cell memory and exhaustion. *Immunol Rev* [S.I.], v. 236, p. 167-75, Jul 2010.

APOSTOLOPOULOS, V. Vaccines in clinical trials: cancer. *Expert Rev Vaccines* [S.I.], v. 10, n. 6, p. 711-2, Jun 2011.

ATAYDE, V. D. *et al.* Molecular basis of non-virulence of Trypanosoma cruzi clone CL-14. *Int J Parasitol* [S.I.], v. 34, n. 7, p. 851-60, Jun 2004.

BANNARD, O. *et al.* Secondary replicative function of CD8+ T cells that had developed an effector phenotype. *Science* [S.I.], v. 323, n. 5913, p. 505-9, Jan 23 2009.

BARTHOLOMEU, D. C. *et al.* Recruitment and endo-lysosomal activation of TLR9 in dendritic cells infected with Trypanosoma cruzi. *J Immunol* [S.I.], v. 181, n. 2, p. 1333-44, Jul 15 2008.

BATMONKH, Z. *et al.* In vivo anticancer activity of lysates from trypanosoma cruzi of different genetic groups. *Bull Exp Biol Med* [S.I.], v. 142, n. 4, p. 470-3, Oct 2006.

BELKIN, M.; HARDY, W. G. Effect of reserpine and chlorpromazine on sarcoma 37. *Science* [S.I.], v. 125, n. 3241, p. 233-4, Feb 8 1957.

BENLALAM, H. *et al.* Comprehensive analysis of the frequency of recognition of melanoma-associated antigen (MAA) by CD8 melanoma infiltrating lymphocytes (TIL): implications for immunotherapy. *Eur J Immunol* [S.I.], v. 31, n. 7, p. 2007-15, Jul 2001.

BEYER, M.; SCHULTZE, J. L. Regulatory T cells in cancer. *Blood* [S.I.], v. 108, n. 3, p. 804-11, Aug 1 2006.

BIXBY, L. M.; TARLETON, R. L. Stable CD8+ T cell memory during persistent Trypanosoma cruzi infection. *J Immunol* [S.I.], v. 181, n. 4, p. 2644-50, Aug 15 2008.

BOLHASSANI, A. *et al.* Improvement of different vaccine delivery systems for cancer therapy. *Mol Cancer* [S.I.], v. 10, p. 3, 2011.

BOSLY, A. *et al.* High-dose treatment with autologous stem cell transplantation versus sequential chemotherapy: the GELA experience. *Eur J Haematol Suppl* [S.I.], v. 64, p. 3-7, Jul 2001.

BUSTAMANTE, J. M. *et al.* Drug-induced cure drives conversion to a stable and protective CD8+ T central memory response in chronic Chagas disease. *Nat Med* [S.I.], v. 14, n. 5, p. 542-50, May 2008.

CAETANO, B. C. *et al.* Requirement of UNC93B1 reveals a critical role for TLR7 in host resistance to primary infection with Trypanosoma cruzi. *J Immunol* [S.I.], v. 187, n. 4, p. 1903-11, Aug 15 2011.

CHENG, Y. H. *et al.* Cancer/testis (CT) antigens, carcinogenesis and spermatogenesis. *Spermatogenesis* [S.I.], v. 1, n. 3, p. 209-220, Jul 2011.

COLEY, W. B. The treatment of malignant tumors by repeated inoculations of Erysipelas, with a report of ten original cases. *Am J Med Sci* [S.I.], v. 105, p. 487-511, 1893.

COLLINS, A. T. *et al.* Prospective identification of tumorigenic prostate cancer stem cells. *Cancer research* [S.I.], v. 65, n. 23, p. 10946-51, Dec 1 2005.

CORSE, E.; ALLISON, J. P. Cutting edge: CTLA-4 on effector T cells inhibits in trans. *J Immunol* [S.I.], v. 189, n. 3, p. 1123-7, Aug 1 2012.

CULLEN, S. P. *et al.* Granzymes in cancer and immunity. *Cell Death Differ* [S.I.], v. 17, n. 4, p. 616-23, Apr 2010.

CULLEN, S. P.; MARTIN, S. J. Mechanisms of granule-dependent killing. *Cell Death Differ* [S.I.], v. 15, n. 2, p. 251-62, Feb 2008.

CUNHA-NETO, E. *et al.* Autoimmunity in Chagas' disease. Identification of cardiac myosin-B13 Trypanosoma cruzi protein crossreactive T cell clones in heart lesions of a chronic Chagas' cardiomyopathy patient. *J Clin Invest* [S.I.], v. 98, n. 8, p. 1709-12, Oct 15 1996.

CUNHA-NETO, E. *et al.* Autoimmunity. *Adv Parasitol* [S.I.], v. 76, p. 129-52, 2011.

CURRAN, M. A. *et al.* PD-1 and CTLA-4 combination blockade expands infiltrating T cells and reduces regulatory T and myeloid cells within B16 melanoma tumors. *Proceedings of the National Academy of Sciences of the United States of America* [S.I.], v. 107, n. 9, p. 4275-80, Mar 2 2010.

DANNENMANN, S. R. *et al.* Tumor-associated macrophages subvert T-cell function and correlate with reduced survival in clear cell renal cell carcinoma. *Oncoimmunology* [S.I.], v. 2, n. 3, p. e23562, Mar 1 2013.

DANNULL, J. *et al.* Enhancement of vaccine-mediated antitumor immunity in cancer patients after depletion of regulatory T cells. *J Clin Invest* [S.I.], v. 115, n. 12, p. 3623-33, Dec 2005.

DEVITA, V. T., JR.; ROSENBERG, S. A. Two hundred years of cancer research. *N Engl J Med* [S.I.], v. 366, n. 23, p. 2207-14, Jun 7 2012.

DILLARD, T. *et al.* Anti-CTLA-4 antibody therapy associated autoimmune hypophysitis: serious immune related adverse events across a spectrum of cancer subtypes. *Pituitary* [S.I.], v. 13, n. 1, p. 29-38, 2010.

EDIN, S. *et al.* The distribution of macrophages with a M1 or M2 phenotype in relation to prognosis and the molecular characteristics of colorectal cancer. *PLoS One* [S.I.], v. 7, n. 10, p. e47045, 2012.

FELLNER, C. Ipilimumab (yervoy) prolongs survival in advanced melanoma: serious side effects and a hefty price tag may limit its use. *P T* [S.I.], v. 37, n. 9, p. 503-30, Sep 2012.

FRATTA, E. *et al.* The biology of cancer testis antigens: putative function, regulation and therapeutic potential. *Mol Oncol* [S.I.], v. 5, n. 2, p. 164-82, Apr 2011.

GALLUCCI, B. B. Selected concepts of cancer as a disease: from the Greeks to 1900. *Oncol Nurs Forum* [S.I.], v. 12, n. 4, p. 67-71, Jul-Aug 1985.

GARG, N. *et al.* Delivery by Trypanosoma cruzi of proteins into the MHC class I antigen processing and presentation pathway. *J Immunol* [S.I.], v. 158, n. 7, p. 3293-302, Apr 1 1997.

GOLGHER, D.; GAZZINELLI, R. T. Innate and acquired immunity in the pathogenesis of Chagas disease. *Autoimmunity* [S.I.], v. 37, n. 5, p. 399-409, Aug 2004.

GREAVES, M.; MALEY, C. C. Clonal evolution in cancer. *Nature* [S.I.], v. 481, n. 7381, p. 306-13, Jan 19 2012.

HAAS, M. *et al.* Stromal regulatory T-cells are associated with a favourable prognosis in gastric cancer of the cardia. *BMC Gastroenterol* [S.I.], v. 9, p. 65, 2009.

HADRUP, S. *et al.* Effector CD4 and CD8 T Cells and Their Role in the Tumor Microenvironment. *Cancer Microenviron* [S.I.], Dec 16 2012.

HAJDU, S. I. A note from history: landmarks in history of cancer, part 1. *Cancer* [S.I.], v. 117, n. 5, p. 1097-102, Mar 1 2011a.

HAJDU, S. I. A note from history: landmarks in history of cancer, part 2. *Cancer* [S.I.], v. 117, n. 12, p. 2811-20, Jun 15 2011b.

HAJDU, S. I. A note from history: landmarks in history of cancer, part 3. *Cancer* [S.I.], v. 118, n. 4, p. 1155-68, Feb 15 2012.

HAUSCHKA, T. S.; GOODWIN, M. B. Trypanosoma cruzi Endotoxin (KR) in the Treatment of Malignant Mouse Tumors. *Science* [S.I.], v. 107, n. 2788, p. 600-2, Jun 4 1948.

HEGER, M. Cancer immunotherapy shows promise in multiple tumor types. *Nat Med* [S.I.], v. 18, n. 7, p. 993, Jul 2012.

HEUSEL, J. W. *et al.* Cytotoxic lymphocytes require granzyme B for the rapid induction of DNA fragmentation and apoptosis in allogeneic target cells. *Cell* [S.I.], v. 76, n. 6, p. 977-87, Mar 25 1994.

HODI, F. S. *et al.* Improved survival with ipilimumab in patients with metastatic melanoma. *N Engl J Med* [S.I.], v. 363, n. 8, p. 711-23, Aug 19 2010.

HUNG, K. *et al.* The central role of CD4(+) T cells in the antitumor immune response. *J Exp Med* [S.I.], v. 188, n. 12, p. 2357-68, Dec 21 1998.

HURWITZ, A. A. *et al.* CTLA-4 blockade synergizes with tumor-derived granulocyte-macrophage colony-stimulating factor for treatment of an experimental mammary carcinoma. *Proceedings of the National Academy of Sciences of the United States of America* [S.I.], v. 95, n. 17, p. 10067-71, Aug 18 1998.

HUSTER, K. M. *et al.* Selective expression of IL-7 receptor on memory T cells identifies early CD40L-dependent generation of distinct CD8+ memory T cell subsets. *Proceedings of the National Academy of Sciences of the United States of America* [S.I.], v. 101, n. 15, p. 5610-5, Apr 13 2004.

INTERNATIONAL AGENCY FOR RESEARCH ON CANCER, I. *IARC Monographs on the Evaluation of Carcinogenic Risks to Humans.* Lyon: 2011. Disponível em:<http://monographs.iarc.fr/ENG/Classification/index.php%3E. Acesso em: 07.11.2011.

INTERNATIONAL AGENCY FOR RESEARCH ON CANCER, I. IARC monographs on the evaluation of carcinogenic risks to humans. v. 100B, 2012 2012.

JENSEN, T. O. *et al.* Macrophage markers in serum and tumor have prognostic impact in American Joint Committee on Cancer stage I/II melanoma. *J Clin Oncol* [S.I.], v. 27, n. 20, p. 3330-7, Jul 10 2009.

JUNGBLUTH, A. A. *et al.* Immunohistochemical analysis of NY-ESO-1 antigen expression in normal and malignant human tissues. *Int J Cancer* [S.I.], v. 92, n. 6, p. 856-60, Jun 15 2001.

JUNQUEIRA, C. *et al.* Trypanosoma cruzi adjuvants potentiate T cell-mediated immunity induced by a NY-ESO-1 based antitumor vaccine. *PLoS One* [S.I.], v. 7, n. 5, p. e36245, 2012.

JUNQUEIRA, C. *et al.* Trypanosoma cruzi as an effective cancer antigen delivery vector. *Proceedings of the National Academy of Sciences of the United States of America* [S.I.], v. 108, n. 49, p. 19695-700, Dec 6 2011.

JUNQUEIRA, C. F. *Clone não patogênico de Trypanosoma cruzi expressando antígeno tumoral como vetor vacinal contra o câncer*. (2011). (Doutorado) - Departamento de Bioquimica e Imunologia, Universidade Federal de Minas Gerais, Belo Horizonte, 2011.

KAECH, S. M.; AHMED, R. Memory CD8+ T cell differentiation: initial antigen encounter triggers a developmental program in naive cells. *Nature immunology* [S.I.], v. 2, n. 5, p. 415-22, May 2001.

KAECH, S. M. *et al.* Selective expression of the interleukin 7 receptor identifies effector CD8 T cells that give rise to long-lived memory cells. *Nature immunology* [S.I.], v. 4, n. 12, p. 1191-8, Dec 2003.

KALIL, J.; CUNHA-NETO, E. Autoimmunity in chagas disease cardiomyopathy: Fulfilling the criteria at last? *Parasitol Today* [S.I.], v. 12, n. 10, p. 396-9, Oct 1996.

KALLINIKOVA, V. D. *et al.* [Immunization against Trypanosoma cruzi and tumor growth in mice]. *Med Parazitol (Mosk)* [S.I.], n. 4, p. 9-12, Oct-Dec 2006.

KASHANI-SABET, M. *et al.* A multimarker prognostic assay for primary cutaneous melanoma. *Clin Cancer Res* [S.I.], v. 15, n. 22, p. 6987-92, Nov 15 2009.

KLEBANOFF, C. A. *et al.* CD8+ T-cell memory in tumor immunology and immunotherapy. *Immunol Rev* [S.I.], v. 211, p. 214-24, Jun 2006.

KLYUEVA, N. G. Paths of cancer biotherapy. *Am Rev Sov Med* [S.I.], v. 4, n. 5, p. 408-14, Jun 1947.

KLYUEVA, N. G.; ROSKIN, G. Cancerolytic substance of Schizotrypanum cruzi. *Am Rev Sov Med* [S.I.], v. 4, n. 2, p. 127-9, Dec 1946.

KO, K. *et al.* Treatment of advanced tumors with agonistic anti-GITR mAb and its effects on tumor-infiltrating Foxp3+CD25+CD4+ regulatory T cells. *J Exp Med* [S.I.], v. 202, n. 7, p. 885-91, Oct 3 2005.

KRONTIRIS, T. G.; COOPER, G. M. Transforming activity of human tumor DNAs. *Proceedings of the National Academy of Sciences of the United States of America* [S.I.], v. 78, n. 2, p. 1181-4, Feb 1981.

LEACH, D. R. *et al.* Enhancement of antitumor immunity by CTLA-4 blockade. *Science* [S.I.], v. 271, n. 5256, p. 1734-6, Mar 22 1996.

LEON, J. S.; ENGMAN, D. M. The significance of autoimmunity in the pathogenesis of Chagas heart disease. *Front Biosci* [S.I.], v. 8, p. e315-22, May 1 2003.

LEVY, E. M. *et al.* Natural killer cells in human cancer: from biological functions to clinical applications. *J Biomed Biotechnol* [S.I.], v. 2011, p. 676198, 2011.

LI, C. *et al.* Identification of pancreatic cancer stem cells. *Cancer research* [S.I.], v. 67, n. 3, p. 1030-7, Feb 1 2007.

LIMA, M. T. *et al.* Negative tissue parasitism in mice injected with a noninfective clone of Trypanosoma cruzi. *Parasitol Res* [S.I.], v. 81, n. 1, p. 6-12, 1995.

LYFORD-PIKE, S. *et al.* Evidence for a role of the PD-1:PD-L1 pathway in immune resistance of HPV-associated head and neck squamous cell carcinoma. *Cancer research* [S.I.], v. 73, n. 6, p. 1733-41, Mar 15 2013.

MAHMOUD, S. M. *et al.* Tumor-infiltrating CD8+ lymphocytes predict clinical outcome in breast cancer. *J Clin Oncol* [S.I.], v. 29, n. 15, p. 1949-55, May 20 2011.

MALISOFF, W. M. The Action of the Endotoxin of Trypanosoma cruzi (KR) on Malignant Mouse Tumors. *Science* [S.I.], v. 106, n. 2763, p. 591-4, Dec 12 1947.

MANGSBO, S. M. *et al.* Enhanced tumor eradication by combining CTLA-4 or PD-1 blockade with CpG therapy. *J Immunother* [S.I.], v. 33, n. 3, p. 225-35, Apr 2010.

MANTOVANI, A. *et al.* Macrophage polarization: tumor-associated macrophages as a paradigm for polarized M2 mononuclear phagocytes. *Trends Immunol* [S.I.], v. 23, n. 11, p. 549-55, Nov 2002.

MARTIN, D. L. *et al.* CD8+ T-Cell responses to Trypanosoma cruzi are highly focused on strain-variant trans-sialidase epitopes. *PLoS Pathog* [S.I.], v. 2, n. 8, p. e77, Aug 2006.

MARTINS, G. A. *et al.* CTLA-4 blockage increases resistance to infection with the intracellular protozoan Trypanosoma cruzi. *J Immunol* [S.I.], v. 172, n. 8, p. 4893-901, Apr 15 2004.

MASSARI, L. P. *et al.* Epidermal malignant tumors: pathogenesis, influence of UV light and apoptosis. *Coll Antropol* [S.I.], v. 31 Suppl 1, p. 83-5, Jan 2007.

MITSUI, J. *et al.* Two distinct mechanisms of augmented antitumor activity by modulation of immunostimulatory/inhibitory signals. *Clin Cancer Res* [S.I.], v. 16, n. 10, p. 2781-91, May 15 2010.

MORENO, M. *et al.* Salmonella as live trojan horse for vaccine development and cancer gene therapy. *Curr Gene Ther* [S.I.], v. 10, n. 1, p. 56-76, Feb 2010.

MULHOLLAND, D. J. *et al.* Lin-Sca-1+CD49fhigh stem/progenitors are tumor-initiating cells in the Pten-null prostate cancer model. *Cancer research* [S.I.], v. 69, n. 22, p. 8555-62, Nov 15 2009.

MURAOKA, D. *et al.* Peptide vaccine induces enhanced tumor growth associated with apoptosis induction in CD8+ T cells. *J Immunol* [S.I.], v. 185, n. 6, p. 3768-76, Sep 15 2010.

MURRAY, M. J. *et al.* Three different human tumor cell lines contain different oncogenes. *Cell* [S.I.], v. 25, n. 2, p. 355-61, Aug 1981.

NAITO, Y. *et al.* CD8+ T cells infiltrated within cancer cell nests as a prognostic factor in human colorectal cancer. *Cancer research* [S.I.], v. 58, n. 16, p. 3491-4, Aug 15 1998.

NASMAN, A. *et al.* Tumor infiltrating CD8+ and Foxp3+ lymphocytes correlate to clinical outcome and human papillomavirus (HPV) status in tonsillar cancer. *PLoS One* [S.I.], v. 7, n. 6, p. e38711, 2012.

NATIONAL CANCER INSTITUTE, N. I. O. H., NIH. General Information About Melanoma. *National Institutes of Health*2013.

NAUTS, H. C.; MCLAREN, J. R. Coley toxins--the first century. *Adv Exp Med Biol* [S.I.], v. 267, p. 483-500, 1990.

NICHOLAOU, T. *et al.* Immunoediting and persistence of antigen-specific immunity in patients who have previously been vaccinated with NY-ESO-1 protein formulated in ISCOMATRIX. *Cancer Immunol Immunother* [S.I.], Jun 23 2011.

NISHIKAWA, H.; SAKAGUCHI, S. Regulatory T cells in tumor immunity. *Int J Cancer* [S.I.], v. 127, n. 4, p. 759-67, Aug 15 2010.

ODUNSI, K. *et al.* Efficacy of vaccination with recombinant vaccinia and fowlpox vectors expressing NY-ESO-1 antigen in ovarian cancer and melanoma patients. *Proceedings of the National Academy of Sciences of the United States of America* [S.I.], v. 109, n. 15, p. 5797-802, Apr 10 2012.

OLD, L. J. *et al.* Effect of Bacillus Calmette-Guerin infection on transplanted tumours in the mouse. *Nature* [S.I.], v. 184(Suppl 5), p. 291-2, Jul 25 1959.

PADILLA, A. M. *et al.* CD8+ T cells in Trypanosoma cruzi infection. *Curr Opin Immunol* [S.I.], v. 21, n. 4, p. 385-90, Aug 2009.

PAIVA, C. N. *et al.* Trypanosoma cruzi: lack of T cell abnormalities in mice vaccinated with live trypomastigotes. *Parasitol Res* [S.I.], v. 85, n. 12, p. 1012-7, Dec 1999.

PAN, Z. K. *et al.* A recombinant Listeria monocytogenes vaccine expressing a model tumour antigen protects mice against lethal tumour cell challenge and causes regression of established tumours. *Nat Med* [S.I.], v. 1, n. 5, p. 471-7, May 1995.

PARDO, J. *et al.* Apoptotic pathways are selectively activated by granzyme A and/or granzyme B in CTL-mediated target cell lysis. *J Cell Biol* [S.I.], v. 167, n. 3, p. 457-68, Nov 8 2004.

PRINCE, M. E. *et al.* Identification of a subpopulation of cells with cancer stem cell properties in head and neck squamous cell carcinoma. *Proceedings of the National Academy of Sciences of the United States of America* [S.I.], v. 104, n. 3, p. 973-8, Jan 16 2007.

QUEZADA, S. A. *et al.* CTLA4 blockade and GM-CSF combination immunotherapy alters the intratumor balance of effector and regulatory T cells. *J Clin Invest* [S.I.], v. 116, n. 7, p. 1935-45, Jul 2006.

ROBERT, C. *et al.* Ipilimumab plus dacarbazine for previously untreated metastatic melanoma. *N Engl J Med* [S.I.], v. 364, n. 26, p. 2517-26, Jun 30 2011.

ROGERS, T. L.; HOLEN, I. Tumour macrophages as potential targets of bisphosphonates. *J Transl Med* [S.I.], v. 9, n. 1, p. 177, Oct 17 2011.

ROSENBERG, S. A. *et al.* Durable complete responses in heavily pretreated patients with metastatic melanoma using T-cell transfer immunotherapy. *Clin Cancer Res* [S.I.], v. 17, n. 13, p. 4550-7, Jul 1 2011.

ROSKIN, G. Toxin therapy of experimental cancer; the influence of protozoan infections upon transplanted cancer. *Cancer research* [S.I.], v. 6, p. 363-5, Jul 1946.

SAHA, A.; CHATTERJEE, S. K. Combination of CTL-associated antigen-4 blockade and depletion of CD25 regulatory T cells enhance tumour immunity of dendritic cell-based vaccine in a mouse model of colon cancer. *Scand J Immunol* [S.I.], v. 71, n. 2, p. 70-82, Feb 2010.

SATO, E. *et al.* Intraepithelial CD8+ tumor-infiltrating lymphocytes and a high CD8+/regulatory T cell ratio are associated with favorable prognosis in ovarian cancer. *Proceedings of the National Academy of Sciences of the United States of America* [S.I.], v. 102, n. 51, p. 18538-43, Dec 20 2005.

SCANLAN, M. J. *et al.* Cancer/testis antigens: an expanding family of targets for cancer immunotherapy. *Immunol Rev* [S.I.], v. 188, p. 22-32, Oct 2002.

SCANLAN, M. J. *et al.* The cancer/testis genes: review, standardization, and commentary. *Cancer Immun* [S.I.], v. 4, p. 1, Jan 23 2004.

SCHULER-THURNER, B. *et al.* Rapid induction of tumor-specific type 1 T helper cells in metastatic melanoma patients by vaccination with mature, cryopreserved, peptide-loaded monocyte-derived dendritic cells. *J Exp Med* [S.I.], v. 195, n. 10, p. 1279-88, May 20 2002.

SCOTT, A. M. *et al.* Monoclonal antibodies in cancer therapy. *Cancer Immun* [S.I.], v. 12, p. 14, 2012.

SCOTT, A. M. *et al.* Antibody therapy of cancer. *Nat Rev Cancer* [S.I.], v. 12, n. 4, p. 278-87, Apr 2012.

SEDER, R. A. *et al.* T-cell quality in memory and protection: implications for vaccine design. *Nat Rev Immunol* [S.I.], v. 8, n. 4, p. 247-58, Apr 2008.

SICA, A. *et al.* Macrophage polarization in tumour progression. *Semin Cancer Biol* [S.I.], v. 18, n. 5, p. 349-55, Oct 2008.

SIMPSON, A. J. *et al.* Cancer/testis antigens, gametogenesis and cancer. *Nat Rev Cancer* [S.I.], v. 5, n. 8, p. 615-25, Aug 2005.

SMYTH, M. J. *et al.* A fresh look at tumor immunosurveillance and immunotherapy. *Nature immunology* [S.I.], v. 2, n. 4, p. 293-9, Apr 2001.

SONNENSCHEIN, C.; SOTO, A. M. Theories of carcinogenesis: an emerging perspective. *Semin Cancer Biol* [S.I.], v. 18, n. 5, p. 372-7, Oct 2008.

SOTOMAYOR, E. M. *et al.* In vivo blockade of CTLA-4 enhances the priming of responsive T cells but fails to prevent the induction of tumor antigen-specific tolerance. *Proceedings of the National Academy of Sciences of the United States of America* [S.I.], v. 96, n. 20, p. 11476-81, Sep 28 1999.

SOUZA, P. E. *et al.* Monocytes from patients with indeterminate and cardiac forms of Chagas' disease display distinct phenotypic and functional characteristics associated with morbidity. *Infect Immun* [S.I.], v. 72, n. 9, p. 5283-91, Sep 2004.

STRATTON, M. R. *et al.* The cancer genome. *Nature* [S.I.], v. 458, n. 7239, p. 719-24, Apr 9 2009.

TANAKA, M. *et al.* Induction of antitumor immunity by combined immunogene therapy using IL-2 and IL-12 in low antigenic Lewis lung carcinoma. *Cancer Gene Ther* [S.I.], v. 7, n. 11, p. 1481-90, Nov 2000.

TARLETON, R. L. Chagas disease: a role for autoimmunity? *Trends Parasitol* [S.I.], v. 19, n. 10, p. 447-51, Oct 2003.

TARLETON, R. L.; ZHANG, L. Chagas disease etiology: autoimmunity or parasite persistence? *Parasitol Today* [S.I.], v. 15, n. 3, p. 94-9, Mar 1999.

TOPALIAN, S. L. *et al.* Safety, activity, and immune correlates of anti-PD-1 antibody in cancer. *N Engl J Med* [S.I.], v. 366, n. 26, p. 2443-54, Jun 28 2012.

TSUTSUI, S. *et al.* Macrophage infiltration and its prognostic implications in breast cancer: the relationship with VEGF expression and microvessel density. *Oncol Rep* [S.I.], v. 14, n. 2, p. 425-31, Aug 2005.

VAN RHEE, F. *et al.* NY-ESO-1 is highly expressed in poor-prognosis multiple myeloma and induces spontaneous humoral and cellular immune responses. *Blood* [S.I.], v. 105, n. 10, p. 3939-44, May 15 2005.

VASCONCELOS, J. R. *et al.* Relevance of long-lived CD8(+) T effector memory cells for protective immunity elicited by heterologous prime-boost vaccination. *Front Immunol* [S.I.], v. 3, p. 358, 2012.

VEGLIA, F. *et al.* Occupational exposures, environmental tobacco smoke, and lung cancer. *Epidemiology* [S.I.], v. 18, n. 6, p. 769-75, Nov 2007.

WANG, R. F. The role of MHC class II-restricted tumor antigens and CD4+ T cells in antitumor immunity. *Trends Immunol* [S.I.], v. 22, n. 5, p. 269-76, May 2001.

WHERRY, E. J. T cell exhaustion. *Nature immunology* [S.I.], v. 12, n. 6, p. 492-9, Jun 2011.

WHERRY, E. J. *et al.* Antigen-independent memory CD8 T cells do not develop during chronic viral infection. *Proceedings of the National Academy of Sciences of the United States of America* [S.I.], v. 101, n. 45, p. 16004-9, Nov 9 2004.

WHERRY, E. J. *et al.* Lineage relationship and protective immunity of memory CD8 T cell subsets. *Nature immunology* [S.I.], v. 4, n. 3, p. 225-34, Mar 2003.

WHO, W. H. O.-. Cancer. *WHO, Fact sheet*. v. 2972013.

WONG, J. L. *et al.* IL-18-primed helper NK cells collaborate with dendritic cells to promote recruitment of effector CD8+ T cells to the tumor microenvironment. *Cancer research* [S.I.], Jun 12 2013.

YAMAZAKI, T. *et al.* Expression of programmed death 1 ligands by murine T cells and APC. *J Immunol* [S.I.], v. 169, n. 10, p. 5538-45, Nov 15 2002.

YUAN, J. *et al.* Integrated NY-ESO-1 antibody and CD8+ T-cell responses correlate with clinical benefit in advanced melanoma patients treated with ipilimumab. *Proceedings of the National Academy of Sciences of the United States of America* [S.I.], v. 108, n. 40, p. 16723-8, Oct 4 2011.

YUAN, J. *et al.* CTLA-4 blockade increases antigen-specific CD8(+) T cells in prevaccinated patients with melanoma: three cases. *Cancer Immunol Immunother* [S.I.], v. 60, n. 8, p. 1137-46, Aug 2011.

ZITVOGEL, L. *et al.* Cancer despite immunosurveillance: immunoselection and immunosubversion. *Nat Rev Immunol* [S.I.], v. 6, n. 10, p. 715-27, Oct 2006.

Anexo A

Consentimento do Comitê de Ética em Experimentação Animal (CETEA)

UNIVERSIDADE FEDERAL DE MINAS GERAIS
COMITÊ DE ÉTICA EM EXPERIMENTAÇÃO ANIMAL
- C E T E A -

CERTIFICADO

Certificamos que o **Protocolo nº 19/2008,** relativo ao projeto intitulado "***Adjuvantes derivados de parasitas para vacina contra o câncer***", que tem como responsável(is) **Ricardo Tostes Gazzinelli** , está(ão) de acordo com os Princípios Éticos da Experimentação Animal, adotados pelo ***Comitê de Ética em Experimentação Animal*** **(CETEA/UFMG),** tendo sido aprovado na reunião de **9/ 04/2008.**

Este certificado expira-se em **9/ 04/ 2013.**

CERTIFICATE

We hereby certify that the **Protocol nº 19/2008,** related to the project entitled "***Parasite derived adjuvants for cancer vaccines***", under the supervisiors of **Ricardo Tostes Gazzinelli,** is in agreement with the Ethical Principles in Animal Experimentation, adopted by the ***Ethics Committee in Animal Experimentation*** **(CETEA/UFMG),** and was approved in **April 9, 2008.**

This certificate expires in **April 9, 2013.**

Belo Horizonte, 14 de Abril de 2008.

Prof. Humberto Pereira Oliveira
Coordenador do CETEA/UFMG

Universidade Federal de Minas Gerais
Avenida Antônio Carlos, 6627 – Campus Pampulha
Unidade Administrativa II – 2° Andar, Sala 2005
31270-901 - Belo Horizonte, MG - Brasil
Telefone: (31) 3499-4516 – Fax: (31) 3499-4592
www.ufmg.br/bioetica/cetea - cetea@prpq.ufmg.br

(Mod.Cert. v1.0)

Artigos

Junqueira, C. ; **SANTOS, L. I.** ; Galvao-Filho, B. ; TEIXEIRA, S. M. ; RODRIGUES, F. G. ; DAROCHA, W. D. ; Chiari, E. ; Jungbluth, A. A. ; Ritter, G. ; Gnjatic, S. ; Old, L. J. ; Gazzinelli, R. T. ***Trypanosoma cruzi* as an effective cancer antigen delivery vector.** Proceedings of the National Academy of Sciences of the United States of America, v. 108, n. 49, p. 19695-700, Dec 6 2011.

Luara Isabela dos Santos, Bruno Galvão-Filho, Paula C. B. de Faria, Caroline Junqueira, Miriam S. Dutra, Santuza R. Teixeira, Maurício M. Rodrigues, Gerd Ritter, Douglas T. Fearon, Lis R. Antonelli, Ricardo T. Gazzinelli. **Blockade of CTLA-4 promotes development of effector CD8+ T lymphocytes and the therapeutic effect of vaccination with an attenuated protozoan expressing NY-ESO-1.** SUBMETIDO a Cancer Research.

Rafael Polidoro Alves Barbosa; Bruno Galvão Filho; **Luara Isabela dos Santos**; Policarpo Sales Junior; Oscar Bruña-Romero; Maurício Martins Rodrigues; Ricardo Tostes Gazzinelli; Alexandre Vieira Machado. **Vaccination using recombinants Influenza and Adenoviruses encoding amastigote surface protein-2 are highly effective on protection against *Trypanosoma cruzi* infection**. Plos One, v. 8, p. e61795, 2013.

Paula Cristina Batista de Faria, **Luara Isabela dos Santos**, João Paulo Coelho, Sara Daniela da Costa, Marcos Assunção Pimenta, Luiz Orlando Ladeira, Dawidson Assis Gomes, Clascídia Aparecida Furtado, Ricardo Tostes Gazzinelli. **Carbon nanotubes-based vaccine induces superior $CD8^+$ T cell response and immunoprotective effect for cancer.** SUBMETIDO a Nature Nanotechnology.

Trypanosoma cruzi as an effective cancer antigen delivery vector

Caroline Junqueira[a,b], Luara I. Santos[a,b], Bruno Galvão-Filho[a,b], Santuza M. Teixeira[a], Flávia G. Rodrigues[b], Wanderson D. DaRocha[c], Egler Chiari[a], Achim A. Jungbluth[d], Gerd Ritter[d], Sacha Gnjatic[d], Lloyd J. Old[d], and Ricardo T. Gazzinelli[a,b,e,1]

[a]Departamento de Bioquímica e Imunologia and Departamento de Parasitologia, Instituto de Ciências Biológicas, Universidade Federal de Minas Gerais, 31270-901, Belo Horizonte, Minas Gerais, Brazil; [b]Laboratório de Imunopatologia, Centro de Pesquisas René Rachou, Fundação Oswaldo Cruz, 30190-000, Belo Horizonte, Minas Gerais, Brazil; [c]Departamento de Bioquímica e Biologia Molecular, Setor de Ciências Biológicas, Centro Politécnico, Universidade Federal do Paraná, 81531-980, Curitiba, Paraná, Brazil; [d]Ludwig Institute for Cancer Research, New York Branch at Memorial Sloan-Kettering Cancer Center, New York, NY 10065-6007; and [e]Division of Infectious Disease and Immunology, University of Massachusetts Medical School, Worcester, MA 01605

Edited by Robert D. Schreiber, Washington University School of Medicine in St. Louis, St. Louis, MO, and accepted by the Editorial Board October 29, 2011 (received for review June 25, 2011)

One of the main challenges in cancer research is the development of vaccines that induce effective and long-lived protective immunity against tumors. Significant progress has been made in identifying members of the cancer testis antigen family as potential vaccine candidates. However, an ideal form for antigen delivery that induces robust and sustainable antigen-specific T-cell responses, and in particular of $CD8^+$ T lymphocytes, remains to be developed. Here we report the use of a recombinant nonpathogenic clone of *Trypanosoma cruzi* as a vaccine vector to induce vigorous and long-term T cell-mediated immunity. The rationale for using the highly attenuated *T. cruzi* clone was (*i*) the ability of the parasite to persist in host tissues and therefore to induce a long-term antigen-specific immune response; (*ii*) the existence of intrinsic parasite agonists for Toll-like receptors and consequent induction of highly polarized T helper cell type 1 responses; and (*iii*) the parasite replication in the host cell cytoplasm, leading to direct antigen presentation through the endogenous pathway and consequent induction of antigen-specific $CD8^+$ T cells. Importantly, we found that parasites expressing a cancer testis antigen (NY-ESO-1) were able to elicit human antigen-specific T-cell responses in vitro and solid protection against melanoma in a mouse model. Furthermore, in a therapeutic protocol, the parasites expressing NY-ESO-1 delayed the rate of tumor development in mice. We conclude that the *T. cruzi* vector is highly efficient in inducing T cell-mediated immunity and protection against cancer cells. More broadly, this strategy could be used to elicit a long-term T cell-mediated immunity and used for prophylaxis or therapy of chronic infectious diseases.

cytokine | prophylaxis | protozoa | innate immunity | *Trypanosoma cruzi* CL-14

The NY-ESO-1 antigen, a member of the cancer testis antigen (CTA) family, has been extensively characterized in terms of its distribution in tumor cells and immunological properties in humans (1). It induces integrated responses involving both the cellular and humoral arms of the immune system and is currently being tested in different clinical trials of antitumor vaccines (2). However, a major challenge for the development of an effective anticancer vaccine is the process and context of antigen delivery.

In addition to antigen retention and slow release, an inflammatory milieu is necessary for development of T cell-mediated immunity with the characteristics required to control tumor cells. The discovery of Toll-like receptors (TLRs), which recognize microbial molecular patterns, has led to significant progress in the field of immunological adjuvants, necessary to initiate adaptive immune responses and T cell-mediated immunity in vaccine protocols (3, 4). Although able to induce potent B- and T-cell responses, the frequency of antigen-specific T lymphocytes induced by TLR agonists rapidly decays. Furthermore, the conventional delivery of antigens associated to adjuvants favors antigen processing and presentation by MHC class II and results in relatively weak responses of $CD8^+$ T cells, which are critical for immunological control of different types of tumors (5).

The development of nonreplicative viral vectors partially resolved this question and brought advancement to the field (6). However, clinical trials with existing vectors have yielded poor results. Here, we propose that the intracellular protozoan *Trypanosoma cruzi* would be a highly effective vaccine vector to induce antitumor protective immunity mediated by T lymphocytes. The rationale for using *T. cruzi* as a tumor vaccine vector is based on earlier immunological studies demonstrating the capacity of this parasite to elicit a strong and persistent T cell-mediated immunity (7, 8). The critical immunostimulatory characteristics of this parasite are (*i*) the existence of intrinsic agonists for TLRs (9–13), which favor induction of highly polarized T helper cell type 1 (Th1) response; (*ii*) the ability to persist in host tissues and keep boosting the immune response; and (*iii*) the ability to replicate in the host cell cytoplasm, resulting in direct antigen presentation to $CD8^+$ T-cell response (14).

To test our hypothesis, we have chosen to use the highly attenuated CL-14 clone of *T. cruzi* (15). Through the use of the CL-14 clone we generated three different *T. cruzi* lineages expressing NY-ESO-1. The transgenic parasites were shown to induce strong NY-ESO-1–specific immune responses, both in human cells in vitro and in the mouse model in vivo. The development of NY-ESO-1–specific immunity, including $CD8^+$ T-cell responses, and antitumor activity were dependent on both IL-12 and MyD88 pathway. Furthermore, immunization with CL-14 stably expressing NY-ESO-1 resulted in prevention and delay of tumor development in prophylactic and therapeutic protocols, respectively. Hence, we demonstrated that *T. cruzi* is an effective antigen delivery vector for induction of T cell-mediated immunity and should be further explored as a potential vaccine vector for anticancer vaccines.

Results

Stable Transgenic *T. cruzi-NY-ESO-1* Are Able to Express the Exogenous Protein. We engineered the CL-14 to express NY-ESO-1, a well-defined and highly immunogenic CTA, which is currently being tested as a vaccine candidate against cancer in different clinical trials (16–19). For homologous recombination, we used

Author contributions: C.J., S.M.R.T., F.G.R., W.D.D., S.G., L.J.O., and R.T.G. designed research; C.J., L.I.S., B.G.-F., F.G.R., and A.A.J. performed research; W.D.D., E.C., and G.R. contributed new reagents/analytic tools; C.J., S.G., and R.T.G. analyzed data; and C.J. and R.T.G. wrote the paper.

The authors declare no conflict of interest.

This article is a PNAS Direct Submission. R.D.S. is a guest editor invited by the Editorial Board.

[1]To whom correspondence should be addressed. E-mail: ritoga@cpqrr.fiocruz.br.

This article contains supporting information online at www.pnas.org/lookup/suppl/doi:10.1073/pnas.1110030108/-/DCSupplemental.

the **pROCKNeo** plasmid (20) that promotes insertion of the transgene in one of the many copies of the *β-tubulin* gene in the *T. cruzi* genome (Fig. S1*A*). Parasites were stably transfected with three different constructs of *NY-ESO-1*. Two plasmids encoded the *NY-ESO-1* gene, with or without a 6x histidine (His) tag, were used to promote NY-ESO-1 expression in the parasite cytoplasm (Fig. S1 *B* and *C*). The third plasmid encoded the *NY-ESO-1* gene along with a signal peptide (SP) from a *T. cruzi* metalloprotease, named glycoprotein 63 (gp63) (21), and used to favor NY-ESO-1 secretion by the parasite (Fig. S1*D*). Fig. S1*E* shows an agarose gel confirming the plasmid constructs. As shown in Fig. 1*A*, each of the constructs containing *NY-ESO-1* gene were efficiently inserted into the genomic DNA from transgenic parasites. After digestion of parasite genomic DNA with BamHI and SacI, only one major band hybridized with the *NY-ESO-1* probe. Thus, we assume that *NY-ESO-1* gene was inserted in the *β-tubulin* locus. Fig. 1*A*, *Right*, shows control hybridization with the *T. cruzi* gene named *amastin*, which was present in the genome from all WT (22) and transgenic parasites. Recombinant NY-ESO-1 (rNY-ESO-1) was recovered in the pellet of parasites transfected with the coding region of the gene for NY-ESO-1 protein with 6x-His tag [CL-14-NY-ESO-1His (+)] or without the tag [CL-14-NY-ESO-1His(-)], being consistent with the localization in the cytoplasm. In contrast, the rNY-ESO-1 was found primarily in the supernatants of cultures with parasites transfected with *NY-ESO-1* gene, which included the gp63 SP (CL-14-NY-ESO-1gp63SP) (Fig. 1*B*). Immunofluorescence analyses indicate that rNY-ESO-1 is expressed by all different stages of the parasite (Fig. 1*C*), including the trypomastigote metacyclic form, which was used to vaccinate mice and infect human cells in all experiments described below.

The amastigote forms are the replicative intracellular stage of *T. cruzi* and persist in the host tissues for life. This is thought to be critical for eliciting long-lasting $CD8^+$ T lymphocytes during *T. cruzi* infection. We carefully examined the expression of rNY-ESO-1 by intracellular amastigotes in two human cell lines, SK-MEL-149 and SK-MEL-52, which were selected on the basis of their ability to constitutively express NY-ESO-1. SK-MEL-52 that expresses NY-ESO-1 was used as a positive control (Fig. 2*A*, *Upper*). As negative control, the SK-MEL-149 cell line, which does not express NY-ESO-1, was used uninfected or infected with WT parasite (Fig. 2*A*, *Lower*). The immunocytochemistry results clearly show the presence of NY-ESO-1 only in the SK-MEL-149 cell line infected with either CL-14-NY-ESO-1His(+) or CL-14-NY-ESO-1gp63SP. NY-ESO-1 was localized in the intracellular amastigotes expressing NY-ESO-1His(+) protein. Consistent with protein secretion, the recombinant CTA was homogeneously diffused in the cytoplasm of cells infected with CL-14-NY-ESO-1gp63SP (Fig. 2*A*, *Lower*).

Human T-Cell Immunity Induced by Transgenic Parasites. We also assessed the ability of CL-14-NY-ESO-1His(+) or CL-14-NY-ESO-1gp63SP to stimulate in vitro $CD4^+$ T and $CD8^+$ T cells purified from peripheral blood mononuclear cells (PBMCs) from unprimed healthy donors. Autologous antigen-presenting cells (APCs, $CD4^-/CD8^-$) were infected with WT (negative control) or transfected parasites and used for in vitro sensitization followed by evaluation of both $CD4^+$ T and $CD8^+$ T-cell responses specific for NY-ESO-1. To detect the T-cell response elicited by transgenic parasites, presensitized cells were washed and cocultured with target APCs (EBV-transformed B lymphocytes) from the same donor, infected with *T. cruzi*, fowlpox expressing or not NY-ESO-1, or APCs primed with a pool of immunostimulatory peptides derived from NY-ESO-1 amino acid sequence. Our results with two donors (NC235 and NC236) presented in Fig. 2 *B* and *C* demonstrate the ability of transgenic parasites to elicit NY-ESO-1–specific $CD4^+$ T as well as $CD8^+$ T lymphocytes. The latter results were confirmed by the increased frequency of $CD8^+$ T lymphocytes, which reacted with a tetramer construct containing HLA*0201 compatible to the donors used in the study, and the NY-ESO-$1_{157–165}$ peptide (Fig. 2*C*). Thus, we concluded that CL-14 clone expressing NY-ESO-1 was a potent inducer of both $CD4^+$ T as well as $CD8^+$ T-cell responses in humans.

***T. cruzi-NY-ESO-1* Parasites Induce Antigen-Specific Immune Response and Tumor Inhibition in Mice.** We next tested the ability of transgenic CL-14 (CL-14-NY-ESO-1) to elicit NY-ESO-1–specific humoral and cellular responses in mice. We first performed an experiment to define the protocol of immunization. One hour and 20 h after i.p. injection of 1×10^7 carboxyfluorescein succinimidyl ester-labeled CL-14-NY-ESO-1 metacyclics, a significant proportion of the dendritic cells in the lymph nodes (≈39%) and spleens (≈67%), respectively, contained intracellular parasites. Thus, we decided to use this dose and route of parasite inoculation. Furthermore, we tested a single vs. a homologous prime and boost protocol. As shown in Fig. S2 the prime-boost protocol, using CL-14-NY-ESO-1gp63, induced a stronger T-cell response to NY-ESO-1 peptides than a single-dose immunization. Thereafter, we used in all experiments described in this study two immunization doses 30 d apart. The results shown in Fig. 3 were obtained in vivo and demonstrated that all stably transfected parasites elicited high levels of antibodies specific for rNY-ESO-1 (Fig. 3*A*). In particular, we observed the induction of the isotype IgG2c, which is normally induced by IFN-γ produced by $CD4^+$ Th1 lymphocytes. Consistently, we demonstrated a strong IFN-γ response by splenocytes from vaccinated mice, stimulated in vitro with NY-ESO-1–derived peptides that encode epitopes recognized by either $CD4^+$ T or $CD8^+$ T lymphocytes (Fig. 3*B*). As control, we used the $CD8^+$ T cell-specific epitope

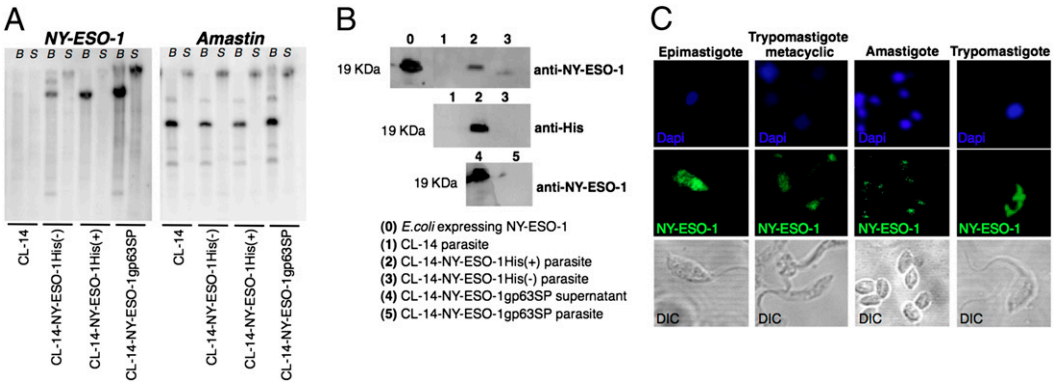

Fig. 1. Expression of recombinant NY-ESO-1 by stably transfected *T. cruzi* parasites. (*A*) Genomic DNA from WT and transgenic parasites was digested with BamHI (B) or SacI (S), submitted to Southern blot, and hybridized with *NY-ESO-1* or *amastin* probes. (*B*) Western blot analysis was used to detect NY-ESO-1 expression, in metacyclic lysates (lanes 1–3 and 5) or supernatants (lane 4) of parasite cultures, using anti-NY-ESO-1 or anti-His tag mAbs. (*C*) NY-ESO-1 expression by the four different stages of the CL-14-NY-ESO-1His(+) was analyzed by immunofluorescence. Parasites stained with anti-NY-ESO-1 mAb (green), or DAPI for DNA, were visualized by differential interference contrast (DIC).

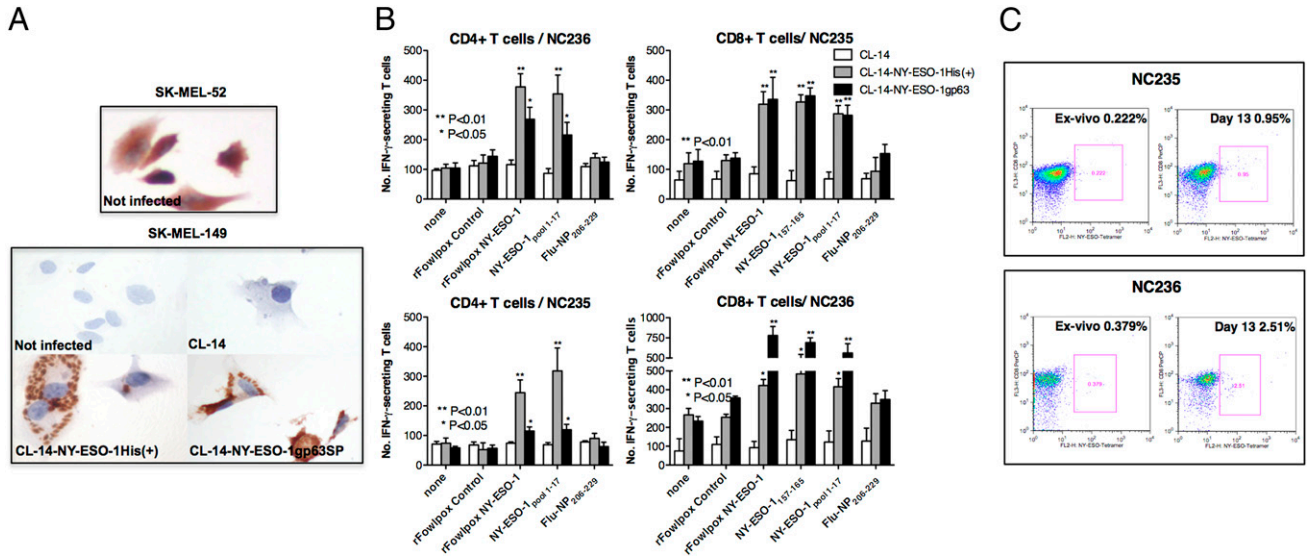

Fig. 2. Priming with transgenic parasites elicits IFN-γ–producing T cells specific for NY-ESO-1. (*A*) A melanoma cell line (SK-MEL-149) that does not express NY-ESO-1 was infected with either WT or transgenic parasites and expression of rNY-ESO-1 detected by immunohistochemistry. SK-MEL-52 cells were used as positive control. (*B*) $CD8^+$ T as well as $CD4^+$ T cells from healthy donors (NC235 and NC236) were cocultured with autologous APCs infected with WT or transgenic parasites expressing different forms of rNY-ESO-1. Induction of antigen-specific T cells was analyzed by quantifying the number of IFN-γ–producing cells by ELISPOT after restimulation with autologous EBV-B cells pulsed with peptides or infected with rFowlpox virus, as indicated. (*C*) The frequency of NY-ESO-1–specific $CD8^+$ T cells was determined by flow cytometry. Percentages indicate the frequency of $CD8^+$ T cells stained with NY-ESO-1 tetramer.

derived from transialidase, a surface antigen from *T. cruzi*. Both WT and transgenic parasites primed $CD8^+$ T cells to produce high levels of IFN-γ in response to this epitope. We also observed that the induction of NY-ESO-1–specific IgG2c, the levels of IFN-γ, and the frequency of IFN-γ–producing $CD4^+$ T as well as $CD8^+$ T lymphocytes correlated with protection, which was significantly higher in mice vaccinated with transgenic parasites than with recombinant NY-ESO-1 protein associated to TLR agonists (Fig. S3 *A* and *B*).

Importantly, vaccination with transgenic parasites expressing NY-ESO-1gp63SP as well as NY-ESO-1His(+) induced complete protection and prevented mortality in mice challenged with a syngeneic transgenic melanoma, the B16F10 cell line expressing NY-ESO-1 (23) (Fig. 3 *C* and *D*). In contrast, the formulations using rNY-ESO-1 protein and TLRs agonists were only able to delay tumor development and mortality (Fig. S3 *C* and *D*). We also tested the ability of transgenic parasites in a therapeutic protocol to reverse/delay B16-NY-ESO-1 growth in C57BL/6 mice (Fig. S4 *A* and *B*) or in BALB/c mice challenged with fibrosarcoma (CMS5a) (24) or colon adenoma (CT26) (25) cell lines. The results shown in Fig. 4 also demonstrate that repeated injections with trypomastigote metacyclics expressing NY-ESO-1 were able to delay tumor growth and prolong survival for both tumor cell lines CMS5a-NY-ESO-1 (Fig. 4 *A* and *B*) and CT26-NY-ESO-1 (Fig. S4 *C* and *D*). It is noteworthy that no parasitemia/parasitism or any sign of *T. cruzi* infection was observed, even after 90 d of immunization with CL-14-NY-ESO-1 (Fig. 3*D* and Fig. S3*D*).

***T. cruzi-NY-ESO-1* Leads to IL-12 and MyD88 Dependent Pathway.** To investigate the mechanism by which CL-14-NY-ESO-1gp63SP induces protective immunity against the B16-NY-ESO-1 cell line, we used the *MyD88*$^{-/-}$, *IL-12p40*$^{-/-}$, *iNOS*$^{-/-}$, and *β2-microglobulin*$^{-/-}$ ($CD8^-$ T cell-deficient) mice. None of these knockout mice that are otherwise highly susceptible to *T. cruzi* (11, 14, 26, 27) showed any sign of disease when vaccinated with the live transgenic parasites or the WT CL-14 (Fig. S5). Importantly, our results show that upon in vitro stimulation with either rNY-ESO-1, NY-ESO-1, or *T. cruzi*–derived peptide (TSKB20), the IFN-γ production by $CD4^+$ T and $CD8^+$ T lymphocytes was severely impaired in both *MyD88*$^{-/-}$ and *IL-12p40*$^{-/-}$ mice vaccinated with CL-14-NY-ESO-1gp63SP (Fig. 5*A*). Similar results were obtained when we immunized knockout mice with either Alum/CpG/NY-ESO-1 or Alum/MPL/NY-ESO-1 (Fig. S6). On the other hand, we found no significant decrease in the frequency of $CD8^+$ T lymphocytes specific for NY-ESO-1 epitope in the various knockout (KO) mice vaccinated with the transgenic parasites (Fig. 5*B*).

We also challenged the different KO mice with B16-NY-ESO-1 (Fig. 5*C*). We observed that protective immunity elicited by vaccination was not effective in either *MyD88*$^{-/-}$ or *IL-12p40*$^{-/-}$ mice, suggesting the critical role of TLRs in inducing IL-12 and consequently IFN-γ production and protection elicited by the CL-14-NY-ESO-1gp63SP. We also observed that vaccinated *β2-microglobulin*$^{-/-}$ mice ($CD8^{-/-}$), which lack $CD8^+$ T lymphocytes, were unable to control tumor growth, suggesting a critical role of this T-cell subset in host resistance to B16-NY-ESO-1. In contrast, mice deficient in inducible nitric oxide synthase controlled tumor growth when vaccinated with CL-14-NY-ESO-1 (Fig. 5*C*). Together, these results indicate that the adjuvant activity of CL-14 clone is highly dependent on MyD88 and IL-12, whereas $CD4^+$ T as well as $CD8^+$ T lymphocytes are the main cellular sources of IFN-γ.

Discussion

Both attenuated viruses and bacteria have been largely explored as vaccine vectors to elicit T cell mediated immunity and in particular $CD8^+$ T-cell responses (6, 24). Although effective, some of these vectors induce strong but not persistent immunity. A possible explanation for the decay of the antigen-specific T-cell response is related to the fact that these attenuated viruses or bacteria are often not replicative, and infection is rapidly eliminated by the immune system. One possible alternative is to vaccinate with vectors that persist in the host, ensuring long-term immunity. In this regard, like other parasites, *T. cruzi* coevolved with their hosts, to maintain a long-lived infection (8). As a consequence, the parasite induces a strong immunity that

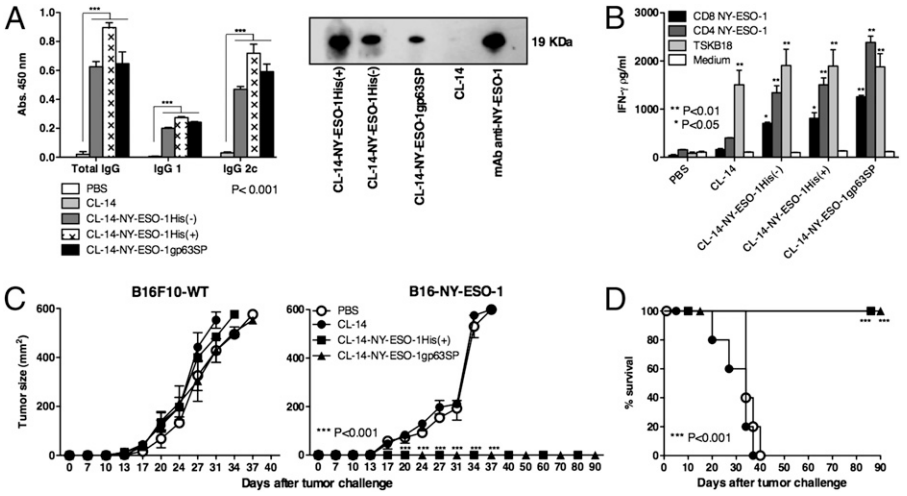

Fig. 3. Antigen-specific humoral and cellular responses and complete protection induced by immunization with transgenic parasites expressing NY-ESO-1. (*A*) ELISA plates coated with rNY-ESO-1 were used to quantify the levels of NY-ESO-1–specific total IgG, IgG1, and IgG2c isotypes present in sera of control and immunized mice; Western blot membranes containing rNY-ESO-1 were individually incubated with sera of mice immunized with each of the three transgenic or WT parasites, or the anti-NY-ESO-1 mAb. (*B*) Splenocytes from control or immunized mice were cultured in the presence or absence of NY-ESO-1 peptides encoding epitopes specific for $CD4^+$ T or $CD8^+$ T cells. As positive control we used a *T. cruzi*–derived immunodominant epitope named TSKB18. IFN-γ production was measured at 72 h after stimulation by a sandwich ELISA. Control and immunized mice were challenged with 5×10^4 B16F10 melanoma cells expressing or not NY-ESO-1 ($n = 4$). Tumor growth (*C*) and survival (*D*) were measured for 90 d ($n = 6$).

persists throughout the infection, which prevents reemergence of intense parasitism and secondary infection with *T. cruzi*.

Different studies associate the presence of local tissue parasitism with the development of chronic cardiac and digestive pathology, both in humans and mice (28–30). Hence, we used CL-14, a highly attenuated clone of *T. cruzi* that was derived from the CL strain (15, 31) in the early 1980s and kept attenuated, even after continuous passages in liquid cultures. The CL-14 clone is consistently avirulent, and both parasitemia and tissue parasitism are absent or very scarce, even when infecting newborn mice that are highly susceptible to *T. cruzi* infection (31). In addition, our results show that various KO mice, which are otherwise very susceptible to *T. cruzi* infection (11, 14, 26, 27), did not show signs of parasitemia or lethality upon vaccination with the live CL-14 clone or the CL-14 clone expressing NY-ESO-1. As a consequence, the systemic aberrant activation of the immune system and pathogenesis are not observed even in highly susceptible strains of mice, as one would predict from studies with virulent strains of *T. cruzi* (32). Importantly, vaccination with live CL-14 was repeatedly shown to induce a potent and long-lasting parasite-specific antibody and T cell-mediated immunity, characterized by high levels of IgG2, IFN-γ, and $CD8^+$ T-cell responses, as well as solid protection against highly virulent strains of *T. cruzi* (33). Thus, we assume that the immunological adjuvant properties of CL-14 are still effective. *T. cruzi* parasites have intrinsic TLR agonists, such as glycosylphosphatidylinositol anchors (9, 10), unmethylated CpG motifs found on its nuclear DNA (11, 12) and RNA (13) that ensure the continuous stimulation of polarized antigen-specific Th1 lymphocytes. In addition, long-lived intracellular parasitism is likely to be another important characteristic of CL-14-NY-ESO-1 for the prolonged stimulation of $CD8^+$ T cells by MHC class I from parasitized host cells (34) and persistent immunity.

Inspired by the "malariotherapy," which used infection with *Plasmodium* to treat neurosyphilis (35), Roskin and colleagues thought that parasitic infections that cause serious diseases produced a "toxin" that could act on and kill tumor cells (36–38). Almost 10 y after he started his studies, Roskin published an article demonstrating tumor regression after infection with *T. cruzi* in mice (37). Later, he published an article demonstrating tumor regression in human patients infected with *T. cruzi* (38). A growing interest in using *T. cruzi* to treat cancer was pursued by different research groups (39, 40), and *T. cruzi* preparations for cancer therapy were launched by French and Russian pharmaceutical companies (36). Although similar results were found, the ambiguity of the findings obtained by various investigators regarding efficacy against experimental tumors (41) led to the discontinuation of this line of investigation and commercial distribution of this anticancer compound. We assume that, at least in part, the antitumor activity of *T. cruzi* infection was due to the strong activation of the innate immune system. The immunostimulatory effect of *T. cruzi* infection results in the production of high levels of proinflammatory cytokines, such as TNF-α (42), which leads to activation of effector mechanisms that efficiently destroy tumor cells (43).

Importantly, either CL-14-NY-ESO-1-His(+) or CL-14-NY-ESO-1gp63 induced in vitro, both human $CD4^+$ T as well as $CD8^+$ T lymphocytes to produce IFN-γ after restimulation with either fowlpox expressing NY-ESO-1 or NY-ESO-1 peptides. Our results also show that in a prophylactic protocol, CL-14-NY-ESO-1 was highly effective in inducing immunity to tumor development, compared with vaccination with recombinant NY-

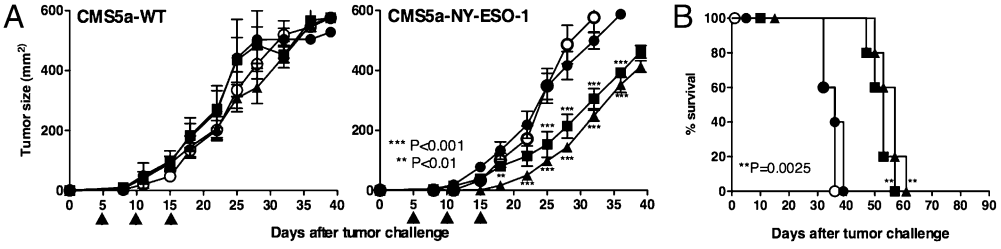

Fig. 4. Therapeutic protocols using transgenic parasites delay the growth of tumor cells expressing NY-ESO-1. 1×10^6 cells of the fibrosarcoma CMS5a (*A* and *B*) expressing or not rNY-ESO-1 were used to challenge BALB/c mice ($n = 6$). Mice were treated with three doses of 10^7 metacyclic forms of WT (CL-14) or transgenic parasites given 5 d apart (arrows), starting at day 5 after challenge. Tumor growth (*A*) and survival (*B*) were monitored for 40 and 90 d, respectively.

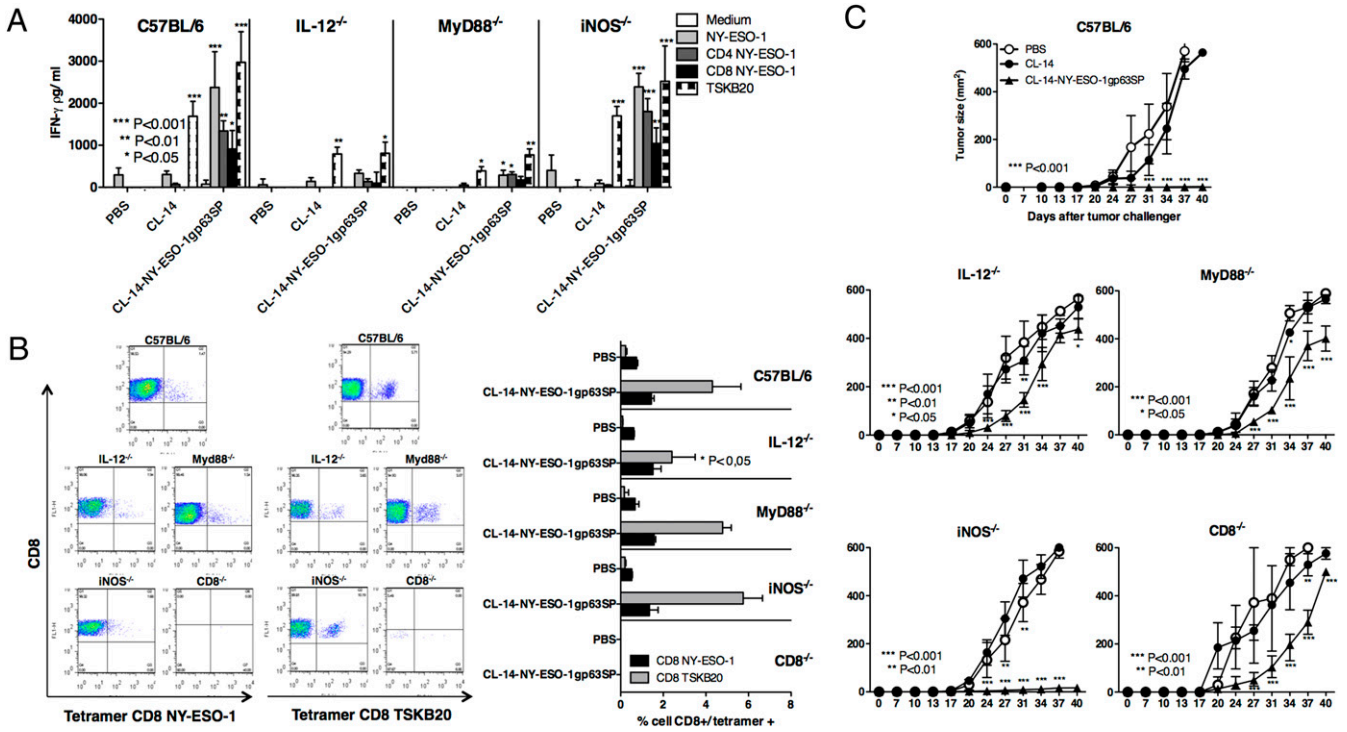

Fig. 5. MyD88- and IL-12–dependent induction of IFN-γ–producing T cells and protective immunity elicited by immunization with CL-14 expressing NY-ESO-1. (*A*) Splenocytes from vaccinated WT (C57BL/6) and KO mice (*MyD88*$^{-/-}$, *IL-12*$^{-/-}$, *iNOs*$^{-/-}$, and *CD8*$^{-/-}$) were restimulated with T CD4^{+}- or T CD8^{+}-specific peptides or with rNY-ESO-1 protein (n = 4). IFN-γ production was measured by ELISA at 72 h after stimulation. (*B*) Before restimulation, the splenocytes were stained with anti-CD3, anti-CD8, and NY-ESO-1 or TSKB20 tetramers and analyzed by flow cytometry. Representative dot blots and a graph summarizing the percentage of double-positive cells are shown at *Left* and *Right*, respectively. (*C*) Immunized C57BL/6 and KO mice were challenged with 5 × 10^{4} of the B16F10 melanoma cells expressing the NY-ESO-1 and monitored 40 d for tumor growth (n = 6).

ESO-1 associated with classic TLR agonists. Furthermore, we show that the levels of IFN-γ responses and frequency of IFN-γ–producing T cells nicely correlate with protective immunity and were dependent of MyD88, IL-12, and CD8^{+} T lymphocytes. In contrast, the effect of therapeutic vaccination with CL-14-NY-ESO-1 was only partial. We believe that this might be explained in part by the ability of tumors to elicit immunoregulatory mechanisms, such as regulatory T cells, expression of CTLA-4, IL-10, and TGF-β (44–47), that prevent establishment of an optimal immune response and complete reversion of tumor growth. This is an important question, which is currently being investigated in our laboratory.

It is noteworthy that the technology we developed for stable transfection targets the *β-tubulin* gene, which has multiple copies (≈40 copies) in the *T. cruzi* genome (48). Although CL-14 is highly susceptible to the existing drug (benznidazole) used to treat Chagas disease (49), we also have engineered *T. cruzi* to simultaneously express both NY-ESO-1 and the herpes virus thymidine kinase. Thus, an additional safety mechanism for eliminating persistent parasites could be the use of acyclovir therapy. Another attractive idea that has already been tested in the laboratory is the generation of CL-14 expressing different tumor antigens, which could be used as polyvalent antitumor vaccine. One important question that is currently being addressed in our laboratory concerns the molecular basis of the attenuated phenotype of the CL-14 clone. CL-14 has been kept stable for 3 decades, and this strategy could lead us to develop genetically engineered parasites with lower risk of reversion of the attenuated phenotype.

In conclusion, on the basis of the ability of *T. cruzi* parasites to strongly activate both innate and acquired immunity, we explored genetically engineered attenuated parasites to express tumor antigens as a strategy to develop an anticancer vaccine. Our initial hypothesis was that by triggering innate immunity and production of proinflammatory cytokines, in particular IL-12, *T. cruzi* parasites stimulate strong and long-lasting antigen-specific CD4^{+} Th1 as well as CD8^{+} T-cell responses. As a consequence, vaccination with *T. cruzi* infection would lead to activation of immunological effector mechanisms, including the production of TNF-α, that are highly effective in killing or controlling the growth of tumor cells. We envisage ethical barriers of using *T. cruzi* parasites to prevent or treat cancer. Nevertheless, this study highlights a new strategy to induce a highly and long-lasting T cell-mediated immune response, which is often poorly achieved in vaccine protocols against different types of tumors. Hence, the experiments presented here indicate that use of *T. cruzi* parasites as a live vector for an anticancer vaccine should be further explored.

Materials and Methods

Parasite Construction and Characterization. Transgenic parasites were obtained by cloning the *NY-ESO-1* Open reading frame (ORF), fused to His tag or to the gp63 SP sequences into the pROCKNeo plasmid. *T. cruzi* epimastigotes were transfected and maintained as previously described (20). The integration of the exogenous gene into the parasite genome was confirmed by Southern blot analysis of genomic DNA digested with BamHI and SacI and hybridized with *NY-ESO-1* and *amastin* probes labeled with ^{32}P. Expression of rNY-ESO-1 was detected by Western blot and fluorescence microscopy using the anti-NY-ESO-1 or anti-His tag mAbs.

Immunohistochemistry and Human T-Cell Immune Response. For immunohistochemistry, the SK-MEL-149 melanoma cell line infected or not with WT or transgenic parasites and the SK-MEL-52 cell line that constitutively expresses NY-ESO-1 (positive control) were stained with anti-NY-ESO-1 mAb (PowerVison Kit; Leica Microsystems). For human T-cell responses we used PBMC-derived irradiated APCs (CD4^{-}CD8^{-}) infected with 30 parasites per cell and cocultured with purified autologous CD8^{+} T or CD4^{+} T cells (50). The cellular immune

response was evaluated by an IFN-γ enzyme-linked immunosorbent spot assay (ELISPOT), 72 h after restimulation with autologous EBV-B cells pulsed with peptides or infected with recombinant Fowlpox (rFowlpox) virus. For flow cytometry analysis, $CD8^+$ T cells were stained with anti-CD8 mAb and NY-ESO-1 tetramer using the HLA-A*0201 and $NY\text{-}ESO_{157–165}$ peptide.

Mouse Immune Response and Tumor Challenge. WT and KO mice received two i.p. doses, 30 d apart, of 10^7 metacyclic forms of *T. cruzi*. At 21 d after the boost, sera was collected to measure the levels of anti-NY-ESO-1 IgG isotypes by ELISA or Western blot; and spleen cells were cultured with or without 10 μM of either CD4-NY-ESO-1, CD8-NY-ESO-1, or TSKB18 peptides. IFN-γ was quantified in tissue culture supernatants by ELISA (R&D Systems). For flow cytometry analysis, splenocytes were stained with anti-CD3, anti-CD8 (BD Pharmingen), and NY-ESO-1 or TSKB18 tetramers. Alternatively, mice were challenged s.c. with 5×10^4 B16 melanoma cell lines expressing or not NY-ESO-1. For immunotherapy, mice were challenged s.c. with either 5×10^4 B16 melanoma, 1×10^6 CT26 colon adenoma, or CMS5a fibrosarcoma cell lines expressing or not NY-ESO-1 and treated with three doses of live parasites, 5 d apart, starting at day 5 after challenge.

ACKNOWLEDGMENTS. We thank Andrew Simpson, Jonathan Skipper from the Ludwig Institute for Cancer Research (LICR), and Denise Golgher for incentive, scientific discussions, and suggestions during the development of this work; the New York branch of the LICR for providing the anti-NY-ESO-1 mAb and a plasmid containing the *NY-ESO-1* coding region; the LICR Tetramer Facility for tetramers synthesis; the LICR–Cornell University for the recombinant NY-ESO-1 protein; Dr. Jonathan Cebon from LICR–Melbourne for the B16F10 and B16-NY-ESO-1 cell lines; and Dr. Hiroyoshi Nishikawa from Mie University Medical School for the CT26, CT26-NY-ESO-1, CMS5a, and CMS5a-NY-ESO-1 cell lines. This study was funded by the Atlantic Philanthropies/Program of Clinical Discoveries from the LICR, Fundação de Amparo a Pesquisa de Minas Gerais (FAPEMIG), Fundação Oswaldo Cruz, and the National Institute of Science and Technology for Vaccines/Conselho Nacional de Desenvolvimento Científico e Tecnológico (CNPq). R.T.G. and C.J. are recipients of CNPq fellowships; B.G.-F. and L.I.S. are fellows from FAPEMIG; and C.J. is a fellow from Coordenação de Aperfeiçoamento de Pessoal de Ensino Superior.

1. Gnjatic S, et al. (2006) NY-ESO-1: Review of an immunogenic tumor antigen. *Adv Cancer Res* 95:1–30.
2. Caballero OL, Chen YT (2009) Cancer/testis (CT) antigens: Potential targets for immunotherapy. *Cancer Sci* 100:2014–2021.
3. Coffman RL, Sher A, Seder RA (2010) Vaccine adjuvants: Putting innate immunity to work. *Immunity* 33:492–503.
4. Takeuchi O, Akira S (2010) Pattern recognition receptors and inflammation. *Cell* 140: 805–820.
5. Crotzer VL, Blum JS (2009) Autophagy and its role in MHC-mediated antigen presentation. *J Immunol* 182:3335–3341.
6. Liu MA (2010) Immunologic basis of vaccine vectors. *Immunity* 33:504–515.
7. Gazzinelli RT, Denkers EY (2006) Protozoan encounters with Toll-like receptor signalling pathways: Implications for host parasitism. *Nat Rev Immunol* 6:895–906.
8. Junqueira C, et al. (2010) The endless race between *Trypanosoma cruzi* and host immunity: Lessons for and beyond Chagas disease. *Expert Rev Mol Med* 12:e29.
9. Campos MA, et al. (2001) Activation of Toll-like receptor-2 by glycosylphosphatidylinositol anchors from a protozoan parasite. *J Immunol* 167:416–423.
10. Oliveira AC, et al. (2004) Expression of functional TLR4 confers proinflammatory responsiveness to *Trypanosoma cruzi* glycoinositolphospholipids and higher resistance to infection with *T. cruzi*. *J Immunol* 173:5688–5696.
11. Bafica A, et al. (2006) Cutting edge: TLR9 and TLR2 signaling together account for MyD88-dependent control of parasitemia in *Trypanosoma cruzi* infection. *J Immunol* 177:3515–3519.
12. Bartholomeu DC, et al. (2008) Recruitment and endo-lysosomal activation of TLR9 in dendritic cells infected with *Trypanosoma cruzi*. *J Immunol* 181:1333–1344.
13. Caetano BC, et al. (2011) Requirement of UNC93B1 reveals a critical role for TLR7 in host resistance to primary infection with *Trypanosoma cruzi*. *J Immunol* 187:1903–1911.
14. Tarleton RL, Koller BH, Latour A, Postan M (1992) Susceptibility of beta 2-microglobulin-deficient mice to *Trypanosoma cruzi* infection. *Nature* 356:338–340.
15. Lima MT, Jansen AM, Rondinelli E, Gattass CR (1991) *Trypanosoma cruzi*: Properties of a clone isolated from CL strain. *Parasitol Res* 77:77–81.
16. Davis ID, et al. (2004) Recombinant NY-ESO-1 protein with ISCOMATRIX adjuvant induces broad integrated antibody and CD4(+) and CD8(+) T cell responses in humans. *Proc Natl Acad Sci USA* 101:10697–10702.
17. Aoki M, et al. (2009) Antibody responses against NY-ESO-1 and HER2 antigens in patients vaccinated with combinations of cholesteryl pullulan (CHP)-NY-ESO-1 and CHP-HER2 with OK-432. *Vaccine* 27:6854–6861.
18. Bioley G, et al. (2009) Vaccination with recombinant NY-ESO-1 protein elicits immunodominant HLA-DR52b-restricted CD4+ T cell responses with a conserved T cell receptor repertoire. *Clin Cancer Res* 15:4467–4474.
19. Bioley G, et al. (2009) Vaccination with a recombinant protein encoding the tumor-specific antigen NY-ESO-1 elicits an A2/157-165-specific CTL repertoire structurally distinct and of reduced tumor reactivity than that elicited by spontaneous immune responses to NY-ESO-1-expressing Tumors. *J Immunother* 32:161–168.
20. DaRocha WD, et al. (2004) Expression of exogenous genes in *Trypanosoma cruzi*: improving vectors and electroporation protocols. *Parasitol Res* 92:113–120.
21. Grandgenett PM, Coughlin BC, Kirchhoff LV, Donelson JE (2000) Differential expression of GP63 genes in *Trypanosoma cruzi*. *Mol Biochem Parasitol* 110:409–415.
22. Teixeira SM, Russell DG, Kirchhoff LV, Donelson JE (1994) A differentially expressed gene family encoding "amastin," a surface protein of *Trypanosoma cruzi* amastigotes. *J Biol Chem* 269:20509–20516.
23. Maraskovsky E, et al. (2004) NY-ESO-1 protein formulated in ISCOMATRIX adjuvant is a potent anticancer vaccine inducing both humoral and CD8+ t-cell-mediated immunity and protection against NY-ESO-1+ tumors. *Clin Cancer Res* 10:2879–2890.
24. Nishikawa H, et al. (2006) In vivo antigen delivery by a *Salmonella typhimurium* type III secretion system for therapeutic cancer vaccines. *J Clin Invest* 116:1946–1954.
25. Mitsui J, et al. (2010) Two distinct mechanisms of augmented antitumor activity by modulation of immunostimulatory/inhibitory signals. *Clin Cancer Res* 16:2781–2791.
26. Campos MA, et al. (2004) Impaired production of proinflammatory cytokines and host resistance to acute infection with *Trypanosoma cruzi* in mice lacking functional myeloid differentiation factor 88. *J Immunol* 172:1711–1718.
27. Michailowsky V, et al. (2001) Pivotal role of interleukin-12 and interferon-gamma axis in controlling tissue parasitism and inflammation in the heart and central nervous system during *Trypanosoma cruzi* infection. *Am J Pathol* 159:1723–1733.
28. Vago AR, Macedo AM, Adad SJ, Reis DD, Corrêa-Oliveira R (1996) PCR detection of *Trypanosoma cruzi* DNA in oesophageal tissues of patients with chronic digestive Chagas' disease. *Lancet* 348:891–892.
29. Higuchi MLBT, et al. (1993) Correlation between *Trypanosoma cruzi* parasitism and myocardial inflammatory infiltrate in human chronic chagasic myocarditis: Light microscopy and immunohistochemical findings. *Cardiovasc Pathol* 2:101–106.
30. Zhang L, Tarleton RL (1999) Parasite persistence correlates with disease severity and localization in chronic Chagas' disease. *J Infect Dis* 180:480–486.
31. Lima MT, Lenzi HL, Gattass CR (1995) Negative tissue parasitism in mice injected with a noninfective clone of *Trypanosoma cruzi*. *Parasitol Res* 81:6–12.
32. Paiva CN, Castelo-Branco MT, Lannes-Vieira J, Gattass CR (1999) *Trypanosoma cruzi*: Protective response of vaccinated mice is mediated by CD8+ cells, prevents signs of polyclonal T lymphocyte activation, and allows restoration of a resting immune state after challenge. *Exp Parasitol* 91:7–19.
33. Paiva CN, Castelo-Branco MT, Rocha JA, Lannes-Vieira J, Gattass CR (1999) *Trypanosoma cruzi*: Lack of T cell abnormalities in mice vaccinated with live trypomastigotes. *Parasitol Res* 85:1012–1017.
34. Tzelepis F, et al. (2008) Infection with *Trypanosoma cruzi* restricts the repertoire of parasite-specific CD8+ T cells leading to immunodominance. *J Immunol* 180:1737–1748.
35. Whitrow M (1990) Wagner-Jauregg and fever therapy. *Med Hist* 34:294–310.
36. Krementsov N (2009) *Trypanosoma cruzi*, cancer and the Cold War. *Hist Cienc Saude Manguinhos* 16(Suppl 1):75–94.
37. Roskin G (1946) Toxin therapy of experimental cancer; the influence of protozoan infections upon transplanted cancer. *Cancer Res* 6:363–365.
38. Klyueva NG, Roskin G (1946) Cancerolytic substance of *Schizotrypanum cruzi*. *Am Rev Sov Med* 4:127–129.
39. Malisoff WM (1947) The action of the endotoxin of *Trypanosoma cruzi* (KR) on malignant mouse tumors. *Science* 106:591–594.
40. Hauschka TS, Goodwin MB (1948) *Trypanosoma cruzi* endotoxin (KR) in the treatment of malignant mouse tumors. *Science* 107:600–602.
41. Belkin M, Hardy WG (1957) Effect of reserpine and chlorpromazine on sarcoma 37. *Science* 125:233–234.
42. Silva JS, Vespa GN, Cardoso MA, Aliberti JC, Cunha FQ (1995) Tumor necrosis factor alpha mediates resistance to *Trypanosoma cruzi* infection in mice by inducing nitric oxide production in infected gamma interferon-activated macrophages. *Infect Immun* 63:4862–4867.
43. Rubin BY, et al. (1988) Tumor necrosis factor and IFN induce a common set of proteins. *J Immunol* 141:1180–1184.
44. Golgher D, Jones E, Powrie F, Elliott T, Gallimore A (2002) Depletion of CD25+ regulatory cells uncovers immune responses to shared murine tumor rejection antigens. *Eur J Immunol* 32:3267–3275.
45. Leach DR, Krummel MF, Allison JP (1996) Enhancement of antitumor immunity by CTLA-4 blockade. *Science* 271:1734–1736.
46. Ikushima H, Miyazono K (2010) TGFbeta signalling: A complex web in cancer progression. *Nat Rev Cancer* 10:415–424.
47. Steinbrink K, et al. (1999) Interleukin-10-treated human dendritic cells induce a melanoma-antigen-specific anergy in CD8(+) T cells resulting in a failure to lyse tumor cells. *Blood* 93:1634–1642.
48. El-Sayed NM, et al. (2005) The genome sequence of *Trypanosoma cruzi*, etiologic agent of Chagas disease. *Science* 309:409–415.
49. Murta SM, Gazzinelli RT, Brener Z, Romanha AJ (1998) Molecular characterization of susceptible and naturally resistant strains of *Trypanosoma cruzi* to benznidazole and nifurtimox. *Mol Biochem Parasitol* 93:203–214.
50. Dutoit V, et al. (2002) Multiepitope CD8(+) T cell response to a NY-ESO-1 peptide vaccine results in imprecise tumor targeting. *J Clin Invest* 110:1813–1822.

Blockade of CTLA-4 promotes development of effector CD8+ T lymphocytes and the therapeutic effect of vaccination with an attenuated protozoan expressing NY-ESO-1

Luara Isabela dos Santos[1,2], Bruno Galvão-Filho[1,2], Paula C. B. de Faria[2,3], Caroline Junqueira[1,2], Miriam S. Dutra[1,2], Santuza R. Teixeira[2], Maurício M. Rodrigues[4], Gerd Ritter[5], Douglas T. Fearon[6], Lis R. Antonelli[1], Ricardo T. Gazzinelli[1,2,7]

Authors' Affiliations: [1]Centro de Pesquisas René Rachou, CPqRR – Fundação Oswaldo Cruz, FIOCRUZ, Avenida Augusto de Lima 1517, Belo Horizonte 30190-002, Minas Gerais, Brazil; [2]Instituto de Ciências Biológicas, Universidade Federal de Minas Gerais, Avenida Antônio Carlos 6627, Belo Horizonte, 31270-901 Minas Gerais, Brazil; [3]Instituto de Genética e Bioquímica, Universidade Federal de Uberlândia, Avenida Amazonas, Uberlândia, 38400-902, [4]Universidade Federal de São Paulo, Departamento de Microbiologia Imunologia e Parasitologia, São Paulo, SP, Brazil; [5]Ludwig Institute for Cancer Research, New York Branch at Memorial Sloan-Kettering Cancer Center, New York, NY 10065-6007; [6]Department of Medicine, University of Cambridge School of Clinical Medicine, Cambridge CB2 2QH, United Kingdom; [7]University of Massachusetts Medical School, 01605-2324 Worcester, Massachusetts, USA.

Running title: Trypanosoma cruzi expressing NY-ESO-1 as a cancer vaccine

Keywords: Cancer, Immunotherapy, NY-ESO-1, anti-CTLA-4, *Trypanosoma cruzi*

Financial support: Atlantic Philanthropies/Program of Clinical Discoveries from the Ludwig Institute of Cancer Research, Fundação de Amparo a Pesquisa de Minas Gerais (FAPEMIG), Fundação Oswaldo Cruz and the National Institute of Science and Technology for Vaccines/Conselho Nacional de Desenvolvimento Científico e Tecnológico (CNPq). R.T.G., B.G-F, C.J. and M.S.D. are recipients of CNPq fellowships; P.C.B.F and C.J. are fellows from Coordenação de Aperfeiçoamento de Pessoal de Ensino Superior; and L.I.S. is a fellow from FAPEMIG.

Corresponding Author: Ricardo T. Gazzinelli, Department of Medicine, Division of Infectious diseases and Immunology. 364 Plantation Street, Worcester, MA 01605-02324. Phone: 1-508-856-2400, E-mail: ricardo.gazzinelli@umassmed.edu

Competing financial interests. The authors declare no competing financial interests.

Abstract

The development of immunotherapy for cancer has long been a challenge. Here we report that a prophylactic vaccination with a highly attenuated *Trypanosoma cruzi* strain expressing NY-ESO-1 (CL-14-NY-ESO-1) induces both memory effector and effector $CD8^+$ T lymphocytes that efficiently prevent tumor development. However, the therapeutic effect of such vaccine is rather limited. We also demonstrate that blockade of the Cytotoxic T Lymphocyte Antigen 4 (CTLA-4) during vaccination enhances the frequency of NY-ESO-1-specific effector $CD8^+$ T cells producing IFN-□, and promotes lymphocyte migration to the tumor infiltrate. As a result, therapy with CL-14-NY-ESO-1 associated with anti-CTLA-4 is highly effective in controlling the development of an ongoing melanoma.

Introduction

Cancer incidence rates have increased in the last 30 years(1). Nevertheless, a significant improvement of cancer therapy has been achieved over the years, and immunotherapy has emerged as an important alternative to the classic methods. While many clinical trials of immunotherapy protocols have resulted in the development of measurable immune responses, only a minority of the treated patients experienced tumor regression(2, 3). Thus, the field of cancer immunotherapy still faces major challenges, such as selection of appropriate target antigens and effective antigen delivery systems to stimulate robust and durable immune responses(4).

To achieve positive clinical results, cancer vaccines should combine immunogenic tumor-specific proteins associated to effective delivery systems and immunological adjuvants(5). Currently, various vaccine formulations against experimental tumors have been employed to induce strong T cell-mediated immunity in particular $CD8^+$ T cells specific for tumor antigens(6). Due to restricted expression in normal tissues, cancer testis antigens (CTA) are of particular interest as candidates for cancer vaccines(7, 8). NY-ESO-1 is a CTA expressed in a variety of human cancer cells including melanoma, breast, lung and prostate tumors(9, 10). It has been shown that NY-ESO-1 induces both cellular and humoral immunity in different vaccination protocols. Additionally, a number of strategies aimed at improving both magnitude and quality of anti-NY-ESO-1 responses have been proposed (11-13).

Recently, we have used the highly attenuated CL-14 clone of *Trypanosoma cruzi*, engineered to express NY-ESO-1 (CL14-NY-ESO-1), as

a cancer antigen delivery vector(14). The use of *T. cruzi* as a live vaccine-delivery system is based on its capacity to elicit a strong $CD8^+$ T cell mediated immunity, which are the main arm of the immune system involved in tumor elimination(15, 16). This transgenic parasite was shown effective in prophylactic vaccine inducing complete protection against NY-ESO-1 expressing cancer cells. However, this vector was shown to be inefficient in therapeutic protocols(14).

The cytotoxic T-lymphocyte antigen 4 (CTLA-4) has been widely used in preclinical and clinical trials for solid tumors. Blockade of CTLA-4 with an antibody, used as a means to potentiate T cell activation and initiate responses to target tumor cells, provided a step forward in the development of various treatments against cancer(17-19). Here we report the highly significant therapeutic effect of CL14-NY-ESO-1 in combination with anti-CTLA-4. The immunological mechanism involved in inhibition of tumor growth was associated with high frequency of both effector and memory effector $CD8^+$ T cells. The tumor-specific effector $CD8^+$ T cells were cytolytic and produced high levels of IFN-γ and IL-2 upon stimulation with recombinant NY-ESO-1 (rNY-ESO-1). Furthermore, we found a substantial increase in the frequency of tumor infiltrating effector $CD8^+$ T cells in animals treated with transgenic parasites allied with anti-CTLA-4. The multiple effects resulting from this combined strategy undoubtedly represent a novel tool for a therapeutic anticancer vaccine.

Materials and Methods

Mice: Female (8–12 weeks old) C57BL/6 mice were obtained from CEBIO (Federal University of Minas Gerais, Brazil) and CD8 KO mice from René Rachou Research Institute's (CPqRR) animal facility center (Fiocruz, Belo Horizonte, Brazil). GzmBCreER^{T2}/ROSA26EYFP mice were provided from Dr. Douglas T. Fearon (Cambridge, UK). GzmBCreER^{T2}/ROSA26EYFP mice received 1mg tamoxifen daily in 10% EtoH/90% sunflower seed oil (Sigma Aldrich) via intraperitoneal injection (i.p.), for five consecutive days, a week before harvesting spleens. Experiments for this study were approved by the Ethical Commission on Animals' Use (CETEA) at Federal University of Minas Gerais and performed following Institutional Guide for the Care and Use of Laboratory Animals.

Cells and parasites: B16-NY-ESO-1 melanoma cells were grown at 37°C under 5% CO_2 in complete RPMI 1640 (Sigma) with 100 U/ml penicillin and 100 µg/ml streptomycin and supplemented with 10% heat inactivated fetal calf serum (FCS; GIBCO). The selection was performed with G418 (250 µg/ml) as recommended(14, 20, 21). To establish subcutaneous tumors, 5×10^4 B16-NY-ESO-1 cells in 100 µl PBS were subcutaneously injected into the right flank of mice. Trypomastigotes from *T. cruzi* CL-14 strain were maintained as previously described(14, 20, 21) Immunizations were performed by inoculating the mice with 10^7 trypomastigotes by i.p. route with one or two doses, 30 days apart. Monoclonal antibody anti-CTLA-4 (clone 9D9) was produced from hybridoma and purified in protein G columns.

Determination of cytokine levels: Spleen cells of immunized mice were treated with ACK buffer for erythrocytes lysis and washed twice in RPMI containing 5% FCS before diluting in cell culture medium RPMI 1640 (pH 7.4) supplemented with 10 mM HEPES, 0.2% sodium bicarbonate, 59 mg of penicillin/liter, 133 mg of streptomycin/liter, and 10% fetal bovine serum (GIBCO) containing recombinant IL-2 (RD402). Spleen cells number were adjusted to 5 x 10^6 cells per well in cell culture medium and cultured with or without 10 µM of each rNY-ESO-1 (LICR - Cornel University) or peptide TSKB20 (Genscript, Piscataway, NJ) at 37°C for 48 h. The cell free supernatants were tested by specific ELISA for IL-2 or IFN-γ (R&D Systems). To determine the IL-6, TNF and IFN-γ levels the BD Cytometric Bead Array Mouse Inflammation Kit was used according to manufacturer's instructions.

T-cell immunophenotyping and intracellular cytokine measurement: A total of 1 x 10^6 splenocytes per well were stained for MHC tetramers presenting specific epitope NY-ESO-1 (87-94) (H-2K^b LLEFYLAM), TSKB20 or (H2K^b ANYKFTLV) or gp100 (25-33) (H-2D^b EGSRNQDWL) (all from LICR Tetramer Facility), for 30 minutes at room temperature. Cells were then washed and stained for surface molecules for 30 minutes at room temperature. The cells were washed and fixed in PBS with 2% paraformaldehyde. For intracellular staining of IFN-γ, cells were pre-stimulated or not with rNY-ESO-1 for 12 hours in a medium containing Brefeldin-A (GolgiPlug Protein Transport Inhibiton, BD Biosciences). After incubation, cells were washed, permeabilized (Cytofix/Cytoperm, BD

Biosciences), stained intracellular molecules for 30 minutes at 4°C and then fixed in 200µl of PBS with 2% paraformaldehyde. At least 200,000-gated events were acquired for analysis using LSR II with Diva (BD Biosciences). The antibodies used for staining were anti-CD3-APC-Cy7, anti-CD4-AlexaFlour700, anti-CD8-PE, anti-CD44- PerCP-Cy5.5, anti-CD62L-APC, anti-CD127-PE-Cy7, anti-CD11b-PerCP-Cy5.5, anti-F4/80-PE-Cy7, anti-CD11c-AlexaFluor700 and anti-MHCII-APC, all from eBioscience. FlowJo (v8.8.6) and GraphPad Prism (v5.0b) were used for data analysis and graphic presentation.

B16-NY-ESO-1 Melanoma Treatment Experiments: C57BL/6 and CD8KO mice were challenged at day 0 with B16-NY-ESO-1 cells. Treatment initiated on day 3 or 11 depending on the adopted protocol. Doses of anti-CTLA-4 (100 µg) were administrated every 3 days, in a total of 5 doses. The parasites (10^7 metacyclic forms) were inoculated every 5 days, in a total of two or three doses. ELISPOT assay was performed essentially as previously described(22). The splenocytes were stimulated with peptides CD4-NY-ESO-1, CD8-NY-ESO-1, TSKB20 and rNY-ESO-1 for 18h. The spots were counted on a S5 Core ELISPOT Analyser (CTL). To collect tumor-infiltrating T cells, tumors were minced and treated with 1 mg/mL of collagenase IA (Sigma) in HBSS for 90 minutes at room temperature (23), followed by passage a 0.45 µm filter. Cells were stained for flow cytometry analysis, according to previously described.

Migration of parasites: A total of 2 x 10^7 metacyclic forms of *T.cruzi* were

incubated with 5 μM CFSE for 10 min at 37°C, under 5% CO_2. Labeled parasites were washed three times and inoculated i.p. After 1 hour, 20 hours and 3 days, the mice were subjected to intraperitoneal lavage. Additionally the mesenteric lymph nodes and spleen were harvested. The cells were processed and stained for surface markers as described previously.

Statistical analyses: Statistic significance for ELISA, ELISPOT, cytokine staining assays and **immunophenotyping** were evaluated using One-Way ANOVA and non-parametric test followed by Bonferroni post-test. Statistic significance for tumor growth was evaluated by 2-way ANOVA with Bonferroni post-test.

Results

A homologous prime-boost protocol with CL14-NY-ESO-1 is required for protecting mice against challenge with the syngeneic B16F10 melanoma cell line expressing NY-ESO-1.

As described previously, the highly attenuated CL-14 strain of *T. cruzi* is partially impaired in invading host cells(24). We observed that after internalization of CL-14-NY-ESO-1, dendritic cells, but not macrophages, migrate to the secondary lymphoid tissue and initiate the immune response (Fig 1*a*). Thus, we first investigated the number of doses of the transgenic *T. cruzi* required to induce protective immunity in a prophylactic vaccination protocol. The increase of cytokines at the site of infection and the stimulation of T cells in the mesenteric lymph nodes after the second dose of the parasite is clearly observed at the expense of mice that received only one dose (Fig 1b, c). In agreement, a single dose of CL-14-NY-ESO-1 did not induce high production of IFN-γ and IL-2 nor activated NY-ESO-1 specific $CD8^+$ T cells (Fig.1*d*). Meanwhile an additional dose of transgenic parasite, mice produced IL-2 and IFN-γ, high levels of NY-ESO-1 specific $CD8^+$ T cells, controlled tumor growth and survived up to 50 days after challenge (Fig. 1*e*). Hence, two doses with CL-14-NY-ESO-1 were necessary and sufficient to induce a robust T-cell mediated immune response capable of preventing tumor growth.

The homologous prime-boost protocol with CL14-NY-ESO-1 induces Type 1 cytokine responses by NY-ESO-1-specific T lymphocytes.

The population of $CD8^+$ T lymphocytes responsive to the parasite-specific immunodominant peptide TSKB20 (ANYKFTLV) expands and contracts during acute infection but is, nevertheless, maintained during the chronic phase of infection with *T. cruzi* (15, 25). We next evaluated the longevity of the specific CL14-NY-ESO-1 $CD8^+$ T cell population. After the prime-boost protocol, we found that both the production of cytokines and the frequency TSKB20–specific $CD8^+$ T cells remained high up to 45 days after boost. This response was significantly lower at 85 days (Fig. 2*a*). The contraction of the $CD8^+$ T cell population was also observed in the specific response to NY-ESO-1 carried by the transgenic parasite. Upon stimulation with the rNY-ESO-1, we detected the production of high levels of IFN-γ and IL-2 as well as a high frequency of NY-ESO-1-specific $CD8^+$ T cells at 21 days after the last immunization (Fig.2*b*). In addition, we found that, at day 21, about 30% of the NY-ESO-1-tetramer$^+$ cells were functional and capable of producing IFN-γ under stimulation with the rNY-ESO-1 (Fig.2*c,d*). Although lower, the NY-ESO-1 specific T cell population was maintained by day 45, and became undetectable by day 85 post-immunization (Fig.2*b*).

Immunization with CL14-NY-ESO-1 induces a high frequency of $CD8^+$ T effector ($CD8^+T_E$) as well as memory effector cells ($CD8^+T_{EM}$).

The next step was to analyze the phenotypic characteristics of $CD8^+$ T cells induced after immunization with transgenic parasite (Fig.3). Upon initial priming, naive $CD8^+$ T cells can acquire a variety of effector functions, including cytotoxicity and cytokine production. In mice, short-living $CD8^+T_E$ express low amounts of the IL-7 receptor alpha-chain (CD127) and down-

regulate L-selectin (CD62L)(26). Only few primed cells are maintained as long-term memory cells, a heterogeneous population comprising at least two distinct subtypes: central memory ($CD8^+T_{CM}$) and $CD8^+T_{EM}$. The long-living T cells are characterized by their constitutive expression of CD127. CD62L expression is used to further discriminate $CD8^+T_{CM}$ ($CD62L^{high}$) from $CD8^+T_{EM}$ ($CD62L^{low}$). Our data showed that the transgenic parasite induced five times the proliferation and differentiation of effector cells (5.65 ± 0.25 x 10^6 cells/spleen) when compared to the absolute numbers found for the PBS group (0.72 ± 0.19 x 10^6 cells/spleen) (Supplementary Fig 1). In fact, when assessed at 21 days after the boost, about 60% of activated $CD8^+$ T cells ($CD44^{high}$) were $CD8^+T_E$ as compared to 36.4% in the control group immunized with PBS. At 45 days, however, the frequency of $CD8^+T_{EM}$ was enhanced to 43% in animals vaccinated with transgenic parasites, which was unchanged (30%) in mice from the control group (Fig. 3*a,b*). For the antigen-specific (tetramer-positive) $CD8^+$ T cells we showed that the majority of TSKB20 and NY-ESO-1 specific-cells were $CD8^+T_E$ at 21 days and became $CD8^+T_{EM}$ at 45 days after boost (Fig. 3*c,d*). Interestingly, our findings indicated that transgenic parasites besides inducing a high frequency of effector cells also promote the generation of memory effector cells against the tumor.

Immunization with CL14-NY-ESO-1 induces high frequency of NY-ESO-1-specific $CD8^+T_E$ expressing granzyme B.

In functional terms, it has been shown that in addition to effector, memory effector cells also exhibit constitutive levels of lytic activity(27, 28). The release of cytolytic granules protein granzyme B (gzmB) by cytotoxic

lymphocytes is an important effector function to exterminate tumor cells. To verify the *in vivo* expression of this protein in both cell subtypes, we used a transgenic mouse line, gzmBCreER^{T2}/ROSA26EYFP that allowed the identification of cells transcribing the *gzmB* gene, by the co-expression of EYFP(29). We first observed that gzmB cells were present in mice immunized with CL-14-NY-ESO-1 (Fig. 4*a*) either 21 or 45 days after boost (Fig. 4*b*). However, these cells evolved from T_E CD8$^+$ T at 21 days to T_{EM} CD8$^+$ T cells at 45 days after challenge (Fig. 4*c,d*). In agreement with the higher effector function observed at day 21, we found that more than 30% of gzmB$^+$ CD8$^+$ T cells were NY-ESO-1-specific at 21 days after the prime/boost protocol (Fig. 4*e*). Thus, we conclude that immunization with transgenic parasites promotes the generation of effector CD8$^+$ T cells that are potentially capable of lysing the tumor cells by the lytic granules.

High frequency of CD8$^+$ effector cells correlates with the ability of vaccinated mice to control of B16-NY-ESO-1 tumors

After evaluating the immune profile induced by vaccination with CL-14-NY-ESO-1 at different time points we checked the impact of these responses on the control of tumor growth. We demonstrated that upon an early challenge, 21 days after boost with the melanoma B16 cell line expressing NY-ESO-1, vaccinated mice could efficiently control tumor growth and survived (100%) (Fig. 5*a*). However, upon late challenge at 45 days after boost, we observed a decrease in tumor growth control and survival (60%). Altogether the characterization of CD8$^+$ T cells and protection in vaccinated mice suggest that the effector CD8$^+$ T cells induced by the CL-14-NY-ESO-1

are responsible for controlling the tumor growth. However, when used in an immunotherapeutic protocol the ability of CL14-NY-ESO-1 to control ongoing tumor was rather limited (Fig.*5a*). So, we were encouraged to use the blockade of CTLA-4 combined with the transgenic parasite to achieve the immune response required to control tumor growth. Therefore, mice were challenged with B16-NY-ESO-1 melanoma and treated with anti-CTLA-4 associated or not with transgenic parasites (Fig.5*b*). As in other observations for B16F10 model(30, 31), we noted no curative effect of the antibody treatment alone. However, when combined with the transgenic parasite, CTLA-4 blockade conferred 100% of survival (Fig.5*c*). Additionally, tumor growth was reduced four fold when compared with the untreated group and twice compared to the group treated with the parasite alone. Corroborating our initial hypothesis, we observed that β2-microglobulin$^{-/-}$ (deficient in CD8^{+} T cells) mice subjected to the same therapeutic protocol were unable to control tumor growth (Fig.5*c,* right panel).

CL14-NY-ESO-1 and anti-CTLA-4 increase the frequency of NY-ESO-1-specific cells and stimulate the migration of CD8^{+} T cells to tumor infiltrates.

In order to better understand the immunological mechanism by which treatment with anti-CTLA-4 enhances the efficacy of immunotherapy with CL14-NY-ESO-1, we characterized the phenotypes of CD8^{+} T cells in mice that received immunotherapy, at 21 and 28 days after challenge with B16F10 cells expressing NY-ESO-1. The overall percentage of effector cells in the spleen suggests that the treatment with anti-CTLA-4 acts promoting the

induction of $CD8^+$ T_E cells by the transgenic parasites (Fig.6*a*). Importantly, we found that blockade of CTLA-4 promoted the expansion of NY-ESO-1-tetramer$^+$ T cells (Fig.6*b*). The induction of antigen spreading to other melanoma proteins was evaluated by using a tetramer specific for the glycoprotein (gp) 100, which is highly expressed in melanocytic cells. Our analysis also showed a significant increased in the frequency of gp100 tetramer$^+$ T cells in treated mice, as compared to the control group (Fig.6*c*). Next, we evaluated the functional state of $CD8^+$ T cells by measuring the production of IFN-γ, a main cytokine involved in control of tumor growth. We observed that in mice treated with CL-14-NY-ESO-1/anti-CTLA-4, a high frequency of IFN-γ producing cells in response to *in vitro* stimulation with rNY-ESO-1 (Fig.6*d* and 6*e*). Interestingly, as previously reported(32, 33), our experiments indicated that the presence of infiltrating $CD8^+$ T cells within tumors was positively correlated with better prognosis of the mice challenged with the B16F10 melanoma cell lines expressing NY-ESO-1. We observed approximately 1% of $CD8^+$ T cells in the tumor infiltrates from mice treated with the CL-14-NY-ESO-1/anti-CTLA-4, and less than 0.5% in the other groups (Fig. 6*f*).

Discussion

The major challenge in the cancer vaccine field is to induce an effective anti-tumor immune response with efficient type 1 response and long-term immunological memory. These goals are similar as in many infectious diseases, where successful immune protection is ideally induced with live vaccines(5). In this sense both virus and bacteria-based vectors are being studied as potential vehicles for antigen and therapeutic gene delivery to immune and tumor cells. Fowlpox virus, attenuated *Salmonella* strains and *Listeria monocytogenes* have shown great potential as live vectors with broad applications(12, 34-36). However, only few clinical trials have been conducted so far, and although they have conclusively shown the safety of some of these systems, the results on immunogenicity are less than optimal(36).

The tumoricidal effect of *T. cruzi* was found in early experiments where tumor-bearing mice were infected with the parasite. At that time, it was suggested that tumor control would be due to toxins produced by the protozoan(27, 37, 38). Several clinical studies were conducted later aiming to describe the tumoricidal effect of *T. cruzi*, but they yield unsatisfactory results and tumorigenic action remained unclear(39-41). Our group has applied valiant efforts in developing an innovative strategy that uses a highly attenuated *T. cruzi* clone (CL-14) as a vaccine vector for NY-ESO-1 expression, the more immunogenic cancer testis antigen currently described. Using these transgenic parasites as a prophylactic vaccine, we achieved 100% protection against a syngeneic melanoma cell line(14). The CL-14 clone was derived from CL strain, isolated in the early 1980s and is

consistently avirulent. Both parasitemia and tissue parasitism are absent, even in newborn or immunodeficient mice, known to be highly susceptible to *T. cruzi* infection(14, 42). We have shown, however, that despite its highly attenuated phenotype, the short-term infection is sufficient to initiate the immune response.

The key to developing an effective antitumor response is the breakdown of the immunological tolerance and activation of antigen-specific T cells with robust effector functions(43). There is consensus that an effective cancer vaccine shall induce $CD8^+$ T cytotoxic cells, and robust production cytokines such as IFN-γ and IL-2 that mediate various effector functions(44). We believe that at least two attributes make CL-14 a great vaccine vector. To begin with, infection with *T. cruzi* continuously stimulates the response, by the intrinsic expression of TLR agonists, such as glicosylphosphatidyliositol anchors, unmethylated CpG and ssRNA(14, 45, 46). This results in the polarization of antigen-specific Th1 lymphocytes ideal to control the tumor. Secondly, in its cytoplasmic environment, *T. cruzi* releases proteins that are processed for presentation by class I MHC molecules. Each intracellular round of replication likely last up to 5 days, thus providing substantial time for detection of these infected cells by parasite-specific $CD8^+$ T cells(16). Furthermore, the transgenic CL-14 expressing NY-ESO-1 is able to secret the CTA into the host cell cytoplasm, leading to a direct class I MHC presentation(14).

Here, we demonstrate that two homologous doses of the attenuated parasite CL-14 expressing NY-ESO-1 are able to promote both expansion of NY-ESO-specific $CD8^+$ T cytotoxic cells expressing granzyme B^+, and

production of high levels of IFN-γ and IL-2. A typical $CD8^+$ T cell response, however consists of three main developmental stages: effector cell expansion and differentiation; effector cell contraction; and stabilization and maintenance of the memory cell population(47). $CD8^+$ memory cells have been broadly classified into T central memory ($CD8^+T_{CM}$) and T effector memory ($CD8^+T_{EM}$) subsets(25, 48). Similar to other persistent infections(34, 49) it has been shown that the $CD8^+T_{EM}$ cells developed during *T. cruzi* infection are maintained primarily by the continual antigen presentation(16). The frequency of the $CD8^+T_{CM}$ cells subpopulation increases as the infection becomes more chronic(25).

In our model, the attenuated parasite was able to stimulate the formation of $CD8^+T_{EM}$ cells but, probably due to its elimination, these cells decay to basal levels and only few $CD8^+T_{CM}$ cells were generated. Some studies have also shown that *in vitro* stimulation of $CD8^+T_{CM}$ resulted in the production of IL-2, but little IFN-γ, IL-4 or IL-5(50). By contrast, $CD8^+T_{EM}$ cells rapidly produced these effector cytokines, but produced less IL-2(51). Further, only the subpopulation of $CD8^+T_{EM}$ cells was found to contain intracellular perforin(51). Here, we demonstrated that the production of the effector cytokines IFN-γ was maintained for long-time correlated with the presence of $CD8^+T_{EM}$ cells. The decreased of IL-2 could be related to the stimulation of few $CD8^+T_{CM.}$ Moreover, cells expressing cytotoxic molecule granzyme B, weeks after the boost, were $CD8^+T_{EM}$ cells as shown by others to intracellular perforin. Nevertheless it has been previously described that although effector memory cells are able to have their effector functions activated they proliferate poorly in response to antigen(52). In agreement with these

355 descriptions and the need for a robust response to tumor control, we observed that the full protection of the vaccine requires the presence of functional effector cells in its fullness.

More urgent than the production of an effective vaccine is the establishment of new therapies against cancer. Activation of T cells requires
360 recognition of specific antigens in concert with costimulatory signals from the constitutive CD28 receptor on T cells. Once activated, T cells transiently upregulate the expression of CTLA-4 receptor. The latter competes with the former for the binding of the same ligands, CD80 and CD86, expressed in the surface of antigen presenting cells(53). While CD28 engagement promotes T
365 cell activation, CTLA-4 serves as an immune checkpoint, inhibiting cell cycle progression and IL-2 production(53). Thus, CTLA-4 signaling provides negative feedback to activated T cells, thereby dampening an immune response. CTLA-4 deficiency leads to fatal lymphoproliferation and autoimmunity, exemplifying its importance in the physiological negative
370 regulation of T cells(53, 54). Due to its efficacy, the drug Yervoy® (Ipilimumab, Bristol-Myers Squibb Company), an antibody that binds to CTLA-4, was approved in the U.S. and Europe as an alternative for anti-tumor treatment[(55)]. Ipilimumab specifically blocks the binding of CTLA-4 to its ligands and thereby augments T-cell activation and proliferation and tumor regression(55-59).
375 However, Ipilimumab works only 20-30% of patients who take it and severe toxic effects have been reported in monotherapy with this antibody due non-specific modulation of the immune system(56, 60). Furthermore CTLA-4 blockade failed to induce rejection of less immunogenic tumors such as the B16 melanoma and SM1 mammary carcinoma(31, 61, 62). One strategy to

minimize the secondary effects and increase the efficiency of the anti-CTLA-4 therapy would be the stimulation of specific immune response in a combined therapy with immunological adjuvants or a tumor-specific vaccine(63). Different studies have demonstrated that infection with *T. cruzi* provides increased expression of CTLA-4 and, although there is no consensus about the effect on CD8 + T cells, it was described that the use of anti-CTLA-4 enhances host resistance to infection even more virulent strains(64). In this regard, we combined the attenuated transgenic parasite stably expressing NY-ESO-1, as a vaccine, with the blockade of CTLA-4, aiming to enhance the parasite action by blocking immunoregulation mechanisms, as well as decreasing the several side effects of anti-CTLA-4 administration.

In conclusion, we report that the therapy combining CL14-NY-ESO-1 with anti-CTLA-4 is highly effective in melanoma-bearing mice. The efficiency of this protocol was dependent on the ability of anti-CTLA-4 antibodies to further promote the development of NY-ESO-1-specific $CD8^+$ T_E cells induced by the transgenic parasite. Additionally, for the first time, we were able to show clearly the preservation of tumor-specific $CD8^+$ T cells in anti-CTLA-4 treatment. It was also demonstrated that the therapeutic vaccine also contributed to antigen spreading, favoring expansion and development of T cell response to related tumor antigens, as shown for the gp100. Finally, we show that a consequence of the expansion of $CD8^+$ T_E in mice treated with CL14-NY-ESO-1 associated to CTLA-4 blockade is the enhanced migration of $CD8^+$ T cells to the tumor microenvironment. As various studies indicate the clinical relevance and better prognosis in patients presenting $CD8^+$ T cells in

tumor infiltrates(65), this seems to be a critical event in the effectiveness of the CL14-NY-ESO-1/CTLA-4 immunotherapy.

Acknowledgments. We thank the LICR Tetramer Facility for tetramers synthesis; the LICR–Cornell University for the recombinant NY-ESO-1 protein; Dr. James P. Allison from Memorial Sloan-Kettering Cancer Center for anti-CTLA-4 monoclonal antibody (9D9 hybridoma), Dr. Jonathan Cebon from LICR–Melbourne for the B16-NY-ESO-1 cell lines; and Dr. Luiz R. Travassos from São Paulo University for the B16F10 cell line, incentive, scientific discussions, and suggestions during the development of this work.

Author contributions. L.I.S., B.G.-F., P.C.B.F., C.J., M.S.D., L.R.A., M.M.R. and R.T.G. designed and performed experiments. L.I.S., L.R.A. and R.T.G. analyzed the data. S.R.T. contributed to optimization of transgenic parasite. D.T.F. generated and provided GzmBCreER^{T2}/ROSA26EYFP mice. G.R. provided recombinant protein NY-ESO-1 and M.M.R. provided peptides. L.I.S, M.S.D., P.C.B.F and R.T.G. wrote the manuscript.

References

1. Siegel R, Naishadham D, Jemal A. Cancer statistics, 2012. CA Cancer J Clin. 2012;62:10-29.
2. Rosenberg SA, Yang JC, Restifo NP. Cancer immunotherapy: moving beyond current vaccines. Nat Med. 2004;10:909-15.
3. Muraoka D, Kato T, Wang L, Maeda Y, Noguchi T, Harada N, et al. Peptide vaccine induces enhanced tumor growth associated with apoptosis induction in CD8+ T cells. J Immunol. 2010;185:3768-76.
4. Chen J, Zhang L, Wen W, Hao J, Zeng P, Qian X, et al. Induction of HCA587-specific antitumor immunity with HCA587 protein formulated with CpG and ISCOM in mice. PLoS One. 2012;7:e47219.
5. Bolhassani A, Safaiyan S, Rafati S. Improvement of different vaccine delivery systems for cancer therapy. Mol Cancer. 2011;10:3.
6. Junqueira C, Guerrero AT, Galvao-Filho B, Andrade WA, Salgado AP, Cunha TM, et al. Trypanosoma cruzi adjuvants potentiate T cell-mediated immunity induced by a NY-ESO-1 based antitumor vaccine. PLoS One. 2012;7:e36245.
7. Schreiber RD, Old LJ, Smyth MJ. Cancer immunoediting: integrating immunity's roles in cancer suppression and promotion. Science. 2011;331:1565-70.
8. Chen YT, Scanlan MJ, Sahin U, Tureci O, Gure AO, Tsang S, et al. A testicular antigen aberrantly expressed in human cancers detected by autologous antibody screening. Proc Natl Acad Sci U S A. 1997;94:1914-8.
9. Jungbluth AA, Chen YT, Stockert E, Busam KJ, Kolb D, Iversen K, et al. Immunohistochemical analysis of NY-ESO-1 antigen expression in normal and malignant human tissues. Int J Cancer. 2001;92:856-60.
10. Chen YT, Ross DS, Chiu R, Zhou XK, Chen YY, Lee P, et al. Multiple cancer/testis antigens are preferentially expressed in hormone-receptor negative and high-grade breast cancers. PLoS One. 2011;6:e17876.
11. Nicholaou T, Ebert L, Davis ID, Robson N, Klein O, Maraskovsky E, et al. Directions in the immune targeting of cancer: lessons learned from the cancer-testis Ag NY-ESO-1. Immunol Cell Biol. 2006;84:303-17.
12. Odunsi K, Matsuzaki J, Karbach J, Neumann A, Mhawech-Fauceglia P, Miller A, et al. Efficacy of vaccination with recombinant vaccinia and fowlpox vectors expressing NY-ESO-1 antigen in ovarian cancer and melanoma patients. Proc Natl Acad Sci U S A. 2012;109:5797-802.
13. Nicholaou T, Chen W, Davis ID, Jackson HM, Dimopoulos N, Barrow C, et al. Immunoediting and persistence of antigen-specific immunity in patients who have previously been vaccinated with NY-ESO-1 protein formulated in ISCOMATRIX. Cancer Immunol Immunother. 2011;60:1625-37.
14. Junqueira C, Santos LI, Galvao-Filho B, Teixeira SM, Rodrigues FG, DaRocha WD, et al. Trypanosoma cruzi as an effective cancer antigen delivery vector. Proc Natl Acad Sci U S A. 2011;108:19695-700.
15. Martin DL, Weatherly DB, Laucella SA, Cabinian MA, Crim MT, Sullivan S, et al. CD8+ T-Cell responses to Trypanosoma cruzi are highly focused on strain-variant trans-sialidase epitopes. PLoS Pathog. 2006;2:e77.
16. Padilla AM, Bustamante JM, Tarleton RL. CD8+ T cells in Trypanosoma cruzi infection. Curr Opin Immunol. 2009;21:385-90.

17. Leach DR, Krummel MF, Allison JP. Enhancement of antitumor immunity by CTLA-4 blockade. Science. 1996;271:1734-6.
18. Scott AM, Allison JP, Wolchok JD. Monoclonal antibodies in cancer therapy. Cancer Immun. 2012;12:14.
19. Kwek SS, Dao V, Roy R, Hou Y, Alajajian D, Simko JP, et al. Diversity of antigen-specific responses induced in vivo with CTLA-4 blockade in prostate cancer patients. J Immunol. 2012;189:3759-66.
20. DaRocha WD, Silva RA, Bartholomeu DC, Pires SF, Freitas JM, Macedo AM, et al. Expression of exogenous genes in Trypanosoma cruzi: improving vectors and electroporation protocols. Parasitol Res. 2004;92:113-20.
21. Maraskovsky E, Sjolander S, Drane DP, Schnurr M, Le TT, Mateo L, et al. NY-ESO-1 protein formulated in ISCOMATRIX adjuvant is a potent anticancer vaccine inducing both humoral and CD8+ t-cell-mediated immunity and protection against NY-ESO-1+ tumors. Clin Cancer Res. 2004;10:2879-90.
22. Streeck H, Frahm N, Walker BD. The role of IFN-gamma Elispot assay in HIV vaccine research. Nat Protoc. 2009;4:461-9.
23. Mitsui J, Nishikawa H, Muraoka D, Wang L, Noguchi T, Sato E, et al. Two distinct mechanisms of augmented antitumor activity by modulation of immunostimulatory/inhibitory signals. Clin Cancer Res. 2010;16:2781-91.
24. Atayde VD, Neira I, Cortez M, Ferreira D, Freymuller E, Yoshida N. Molecular basis of non-virulence of Trypanosoma cruzi clone CL-14. Int J Parasitol. 2004;34:851-60.
25. Bixby LM, Tarleton RL. Stable CD8+ T cell memory during persistent Trypanosoma cruzi infection. J Immunol. 2008;181:2644-50.
26. Huster KM, Busch V, Schiemann M, Linkemann K, Kerksiek KM, Wagner H, et al. Selective expression of IL-7 receptor on memory T cells identifies early CD40L-dependent generation of distinct CD8+ memory T cell subsets. Proc Natl Acad Sci U S A. 2004;101:5610-5.
27. Roskin G. Toxin therapy of experimental cancer; the influence of protozoan infections upon transplanted cancer. Cancer Res. 1946;6:363-5.
28. Kaech SM, Cui W. Transcriptional control of effector and memory CD8+ T cell differentiation. Nat Rev Immunol. 2012;12:749-61.
29. Bannard O, Kraman M, Fearon DT. Secondary replicative function of CD8+ T cells that had developed an effector phenotype. Science. 2009;323:505-9.
30. Curran MA, Kim M, Montalvo W, Al-Shamkhani A, Allison JP. Combination CTLA-4 blockade and 4-1BB activation enhances tumor rejection by increasing T-cell infiltration, proliferation, and cytokine production. PLoS One. 2011;6:e19499.
31. Curran MA, Montalvo W, Yagita H, Allison JP. PD-1 and CTLA-4 combination blockade expands infiltrating T cells and reduces regulatory T and myeloid cells within B16 melanoma tumors. Proc Natl Acad Sci U S A. 2010;107:4275-80.
32. Nasman A, Romanitan M, Nordfors C, Grun N, Johansson H, Hammarstedt L, et al. Tumor infiltrating CD8+ and Foxp3+ lymphocytes correlate to clinical outcome and human papillomavirus (HPV) status in tonsillar cancer. PLoS One. 2012;7:e38711.

33. Mahmoud SM, Paish EC, Powe DG, Macmillan RD, Grainge MJ, Lee AH, et al. Tumor-infiltrating CD8+ lymphocytes predict clinical outcome in breast cancer. J Clin Oncol. 2011;29:1949-55.
34. Wherry EJ, Barber DL, Kaech SM, Blattman JN, Ahmed R. Antigen-independent memory CD8 T cells do not develop during chronic viral infection. Proc Natl Acad Sci U S A. 2004;101:16004-9.
35. Pan ZK, Ikonomidis G, Lazenby A, Pardoll D, Paterson Y. A recombinant Listeria monocytogenes vaccine expressing a model tumour antigen protects mice against lethal tumour cell challenge and causes regression of established tumours. Nat Med. 1995;1:471-7.
36. Moreno M, Kramer MG, Yim L, Chabalgoity JA. Salmonella as live trojan horse for vaccine development and cancer gene therapy. Curr Gene Ther. 2010;10:56-76.
37. Klyueva NG. Paths of cancer biotherapy. Am Rev Sov Med. 1947;4:408-14.
38. Klyueva NG, Roskin G. Cancerolytic substance of Schizotrypanum cruzi. Am Rev Sov Med. 1946;4:127-9.
39. Malisoff WM. The Action of the Endotoxin of Trypanosoma cruzi (KR) on Malignant Mouse Tumors. Science. 1947;106:591-4.
40. Hauschka TS, Goodwin MB. Trypanosoma cruzi Endotoxin (KR) in the Treatment of Malignant Mouse Tumors. Science. 1948;107:600-2.
41. Belkin M, Hardy WG. Effect of reserpine and chlorpromazine on sarcoma 37. Science. 1957;125:233-4.
42. Lima MT, Lenzi HL, Gattass CR. Negative tissue parasitism in mice injected with a noninfective clone of Trypanosoma cruzi. Parasitol Res. 1995;81:6-12.
43. Smyth MJ, Godfrey DI, Trapani JA. A fresh look at tumor immunosurveillance and immunotherapy. Nat Immunol. 2001;2:293-9.
44. Schuler-Thurner B, Schultz ES, Berger TG, Weinlich G, Ebner S, Woerl P, et al. Rapid induction of tumor-specific type 1 T helper cells in metastatic melanoma patients by vaccination with mature, cryopreserved, peptide-loaded monocyte-derived dendritic cells. J Exp Med. 2002;195:1279-88.
45. Bartholomeu DC, Ropert C, Melo MB, Parroche P, Junqueira CF, Teixeira SM, et al. Recruitment and endo-lysosomal activation of TLR9 in dendritic cells infected with Trypanosoma cruzi. J Immunol. 2008;181:1333-44.
46. Caetano BC, Carmo BB, Melo MB, Cerny A, dos Santos SL, Bartholomeu DC, et al. Requirement of UNC93B1 reveals a critical role for TLR7 in host resistance to primary infection with Trypanosoma cruzi. J Immunol. 2011;187:1903-11.
47. Kaech SM, Tan JT, Wherry EJ, Konieczny BT, Surh CD, Ahmed R. Selective expression of the interleukin 7 receptor identifies effector CD8 T cells that give rise to long-lived memory cells. Nat Immunol. 2003;4:1191-8.
48. Vasconcelos JR, Dominguez MR, Araujo AF, Ersching J, Tararam CA, Bruna-Romero O, et al. Relevance of long-lived CD8(+) T effector memory cells for protective immunity elicited by heterologous prime-boost vaccination. Front Immunol. 2012;3:358.
49. Shin H, Blackburn SD, Blattman JN, Wherry EJ. Viral antigen and extensive division maintain virus-specific CD8 T cells during chronic infection. J Exp Med. 2007;204:941-9.

50. Kaech SM, Ahmed R. Memory CD8+ T cell differentiation: initial antigen encounter triggers a developmental program in naive cells. Nat Immunol. 2001;2:415-22.
51. Wherry EJ, Teichgraber V, Becker TC, Masopust D, Kaech SM, Antia R, et al. Lineage relationship and protective immunity of memory CD8 T cell subsets. Nat Immunol. 2003;4:225-34.
52. Stemberger C, Huster KM, Koffler M, Anderl F, Schiemann M, Wagner H, et al. A single naive CD8+ T cell precursor can develop into diverse effector and memory subsets. Immunity. 2007;27:985-97.
53. Scott AM, Wolchok JD, Old LJ. Antibody therapy of cancer. Nat Rev Cancer. 2012;12:278-87.
54. Corse E, Allison JP. Cutting edge: CTLA-4 on effector T cells inhibits in trans. J Immunol. 2012;189:1123-7.
55. Hodi FS, O'Day SJ, McDermott DF, Weber RW, Sosman JA, Haanen JB, et al. Improved survival with ipilimumab in patients with metastatic melanoma. N Engl J Med. 2010;363:711-23.
56. Dillard T, Yedinak CG, Alumkal J, Fleseriu M. Anti-CTLA-4 antibody therapy associated autoimmune hypophysitis: serious immune related adverse events across a spectrum of cancer subtypes. Pituitary. 2010;13:29-38.
57. Fellner C. Ipilimumab (yervoy) prolongs survival in advanced melanoma: serious side effects and a hefty price tag may limit its use. P T. 2012;37:503-30.
58. Robert C, Thomas L, Bondarenko I, O'Day S, M DJ, Garbe C, et al. Ipilimumab plus dacarbazine for previously untreated metastatic melanoma. N Engl J Med. 2011;364:2517-26.
59. Yuan J, Ginsberg B, Page D, Li Y, Rasalan T, Gallardo HF, et al. CTLA-4 blockade increases antigen-specific CD8(+) T cells in prevaccinated patients with melanoma: three cases. Cancer Immunol Immunother. 2011;60:1137-46.
60. Heger M. Cancer immunotherapy shows promise in multiple tumor types. Nat Med. 2012;18:993.
61. Sotomayor EM, Borrello I, Tubb E, Allison JP, Levitsky HI. In vivo blockade of CTLA-4 enhances the priming of responsive T cells but fails to prevent the induction of tumor antigen-specific tolerance. Proc Natl Acad Sci U S A. 1999;96:11476-81.
62. Hurwitz AA, Yu TF, Leach DR, Allison JP. CTLA-4 blockade synergizes with tumor-derived granulocyte-macrophage colony-stimulating factor for treatment of an experimental mammary carcinoma. Proc Natl Acad Sci U S A. 1998;95:10067-71.
63. Quezada SA, Peggs KS, Curran MA, Allison JP. CTLA4 blockade and GM-CSF combination immunotherapy alters the intratumor balance of effector and regulatory T cells. J Clin Invest. 2006;116:1935-45.
64. Martins GA, Tadokoro CE, Silva RB, Silva JS, Rizzo LV. CTLA-4 blockage increases resistance to infection with the intracellular protozoan Trypanosoma cruzi. J Immunol. 2004;172:4893-901.
65. Hadrup S, Donia M, Thor Straten P. Effector CD4 and CD8 T Cells and Their Role in the Tumor Microenvironment. Cancer Microenviron. 2012.

620

Figure 1. Two doses of CL-14-NY-ESO-1 are sufficient to ensure antitumor protection. **(a)** Ten million metacyclic forms of CL-14-NY-ESO-1 labeled or not (control) with CFSE were injected intraperitoneally in C57BL/6 mice and the presence of intracellular parasites evaluated at 1 hour, 20 hours and 3 days post-infection. The presence of intracellular parasites in macrophages ($CD11b^{+}F4/80^{+}$) and dendritic cells ($CD11c^{+}MHCII^{High}$) was evaluated by FACS. **(b)** The peritoneal fluid (site of infection) was collected 1, 20 or 72 hours after the infection with one or two doses of transgenic parasite or PBS (control) and the cytokine production was measured by cytometric bead array assay. **(c)** The lymph nodes were collected one hour, 1 or 3 days after infection and the frequency of T cells stimulated was analyzed by flow cytometry. **(d)** The profile of NY-ESO-1 specific $CD8^{+}$ T cells of spleen was assessed on gate $CD3^{+}CD8^{+}$ T lymphocytes 21 days post-infection. To evaluate the level of IFN-γ and IL-2 produced, splenocytes of vaccinated animals were collected and subjected to stimulation with recombinant NY-ESO-1 protein. (**e**) Tumor growth (left panels) and survival rate (right panels) were evaluated after vaccination and challenge of C57BL/6 mice immunized with one (upper panels) or two doses (lower panels) of PBS or *T. cruzi* strain CL-14 expressing or not NY-ESO-1. $^{*}P < 0.05$, $^{**}P < 0.01$, $^{***}P < 0.001$ by two-way or one-way ANOVA and Bonferroni post test. Similar results were found in three independent experiments with four animals in each group.

Figure 2. Induction of cytokine production was greater at 21 days after boost. (a,b) Activation of antigen-specific immune response was evaluated after prime/boost protocol in three time points: 21, 45 and 85 days after boost. The production of cytokines IFN-γ and IL-2 was measured after stimulating splenocytes for 48 hours with either (**a**) *T. cruzi* peptide TSKB20, or (**b**) rNY-ESO-1. The culture supernatants were evaluated by ELISA. (**c**) Representative pseudo-color plots show NY-ESO-1-specific CD8+ T cells collected 21 days after boost, re-stimulated with rNY-ESO-1 and then evaluated for their ability to produce IFN-γ. (**d**) The percentage of double-positive cells was summarized in the bar graph. $^{*}P < 0.05$, $^{**}P < 0.01$, $^{***}P < 0.001$. Within each time interval the groups were compared with the control group. Statistical analyses were performed using one-way ANOVA with Bonferroni post-test. Data are the mean ±s.e.m. of three to four independent experiments performed in triplicate.

Figure 3. Effector and memory effector $CD8^{+}$ T cells were generated with immunization. Splenocytes were harvested 21 and 45 days after boost vaccination. The expression of the surface markers CD44, CD62L and CD127 were used to define subpopulations within $CD3^{+}CD8^{+}$ T cells. (**a**) The bar graph shows the percentage of naïve cells ($CD44^{low}CD62L^{high}$) in mice vaccinated with parasites at both time points assessed. (**b-d**) To evaluate the profile of activated cells $CD44^{high}$ was considered in the gates (**b**) The subpopulations of $CD8^{+}$ T cells were depicted with different color patterns: effector ($CD62L^{low}CD127^{low}$) as blue, memory effector ($CD62L^{low}CD127^{high}$) in red and central memory ($CD62L^{high}CD127^{high}$) as green. (**c,d**) The profile of specific cells to the parasite and tumor were evaluated after gate on (**c**) TSKB20-tetramers^{+} and (**d**) NY-ESO-1-tetramer^{+}, respectively. The groups that were not vaccinated (naïve) or immunized with CL-14 or CL-14-NY-ESO-

1 are represented in each histogram. Similar results were found in three independent experiments with four animals in each group.

Figure 4. Transgenic parasites were able to induce granzyme B tumor-specific CD8$^+$ T cells. gzmBCreERT2/ROSA26EYFP mice were vaccinated with two doses of PBS, or *T. cruzi* strain CL-14 expressing or not NY-ESO-1. Treatment with tamoxifen was performed during five days as described in methods and the splenocytes were collected 21 and 45 days after boost vaccination. (**a**) The expression of EYFP, that is restricted to cells expressing granzyme B (gzmB), was gated. (**b**) Frequencies of EYFP$^+$CD3$^+$CD4$^+$ and EYFP$^+$CD3$^+$CD8$^+$ cells were determined. (**c, d**) The different subtypes of CD8$^+$/gzm$^+$ lymphocytes were defined from the markers CD44, CD62L and CD127 and the (**c**) number of cells and (**d**) percentage were plotted. (**e**) Representative pseudo-color plots shows within gate of CD8$^+$/gzm$^+$ cells (upper panels) collected 21 days after boost, the assess of NY-ESO-1-tetramer$^+$ (lower panels). The numbers represents the percentage found and the bar graph on the right summarizes data obtained in three independent experiments performed. *P < 0.05, **P < 0.01, ***P < 0.001. Within each time interval the groups were compared with the control group. Statistical analyses were performed using one-way ANOVA with Bonferroni post-test. Data are the mean ± s.e.m. of three to four independent experiments performed in triplicate.

Figure 5. Transgenic parasite controls tumor growth. (a) Prophylactic vaccination efficiency was evaluated in C57BL/6 mice that received a prime/boost protocol at the same time. The challenged with B16 cells expressing NY-ESO-1 happened 21 (left panel) or 45 days (right panels) after the last dose. Than the tumor growth was measured during 45 days and the rate of survival was observed for 50 days. (**b, c**) For the therapeutic vaccination mice were subjected to two different protocols (**b**) and the tumor growth and survival were monitored for 35 and 50 days, respectively. The best result was applied in CD8KO (**c**). Tumor growth was compared with the group that received the entire treatment. *P < 0.05, **P < 0.01, ***P < 0.001 by two-way ANOVA and Bonferroni post test. Similar results were found in three independent experiments with five animals in each group

Figure 6. Longevity of specific effector cells protects against tumor development. (a) C57BL/6 mice were challenged with B16-NY-ESO-1 cells and after 21 and 28 days we evaluated the percentage of effector CD8$^+$ T cells in the spleen. (**b,c**) Frequency of tetramer-specific CD8$^+$ T cells was determined by flow cytometry on day 28 for (**b**) antigen NY-ESO-1 and the (**c**) specificity to melanocytic cells using gp100. (**d**) On the same day, numbers of IFN-γ-producing spleen cells were estimated by the ELISPOT assay. Cells of individual mice were stimulated *in vitro* with restricted peptides from NY-ESO-1 (CD4$^+$ T cell epitopes/ FYLAMPFATPMEAEL as well as CD8$^+$ T cell epitopes/ LLEFYLAM) or NY-ESO-1 recombinant protein or a *T. cruzi*-specific peptide (TSKB20/ ANYDFTLV). (**e**) The production of this cytokine was measured at serum 48 hours after the last dose of treatment. (**f**) We observed by flow cytometry CD8$^+$ T cells in tumor infiltrate (left) and the effector phenotype of these cells (right). Data are the mean ±s.e.m. of three to five

720 independent experiments performed in triplicate. *P < 0.05, **P < 0.01,□***P < 0.001 by one-way ANOVA and Bonferroni post test.

Santos *et al.* Figure 1

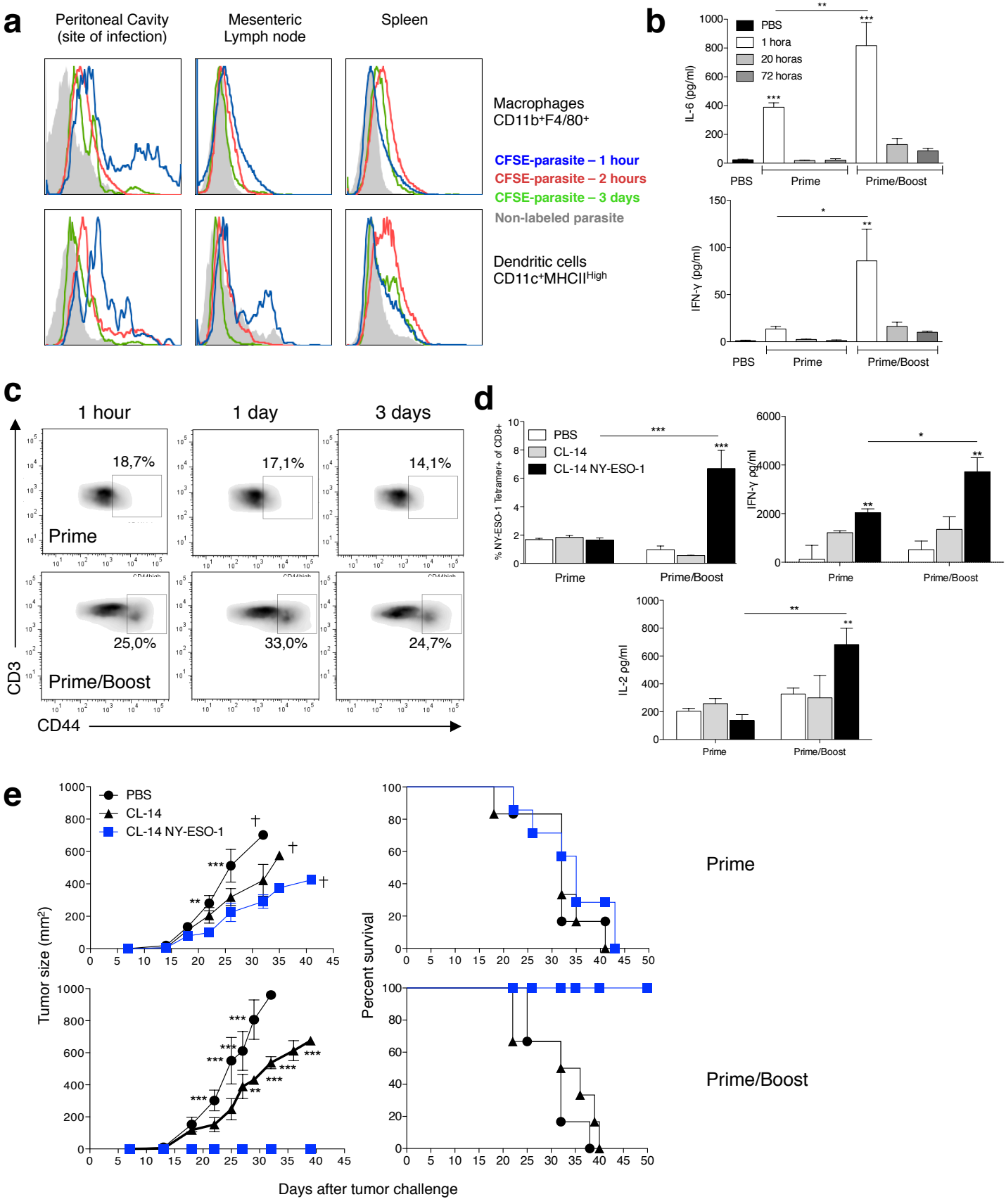

Santos *et al.* Figure 2

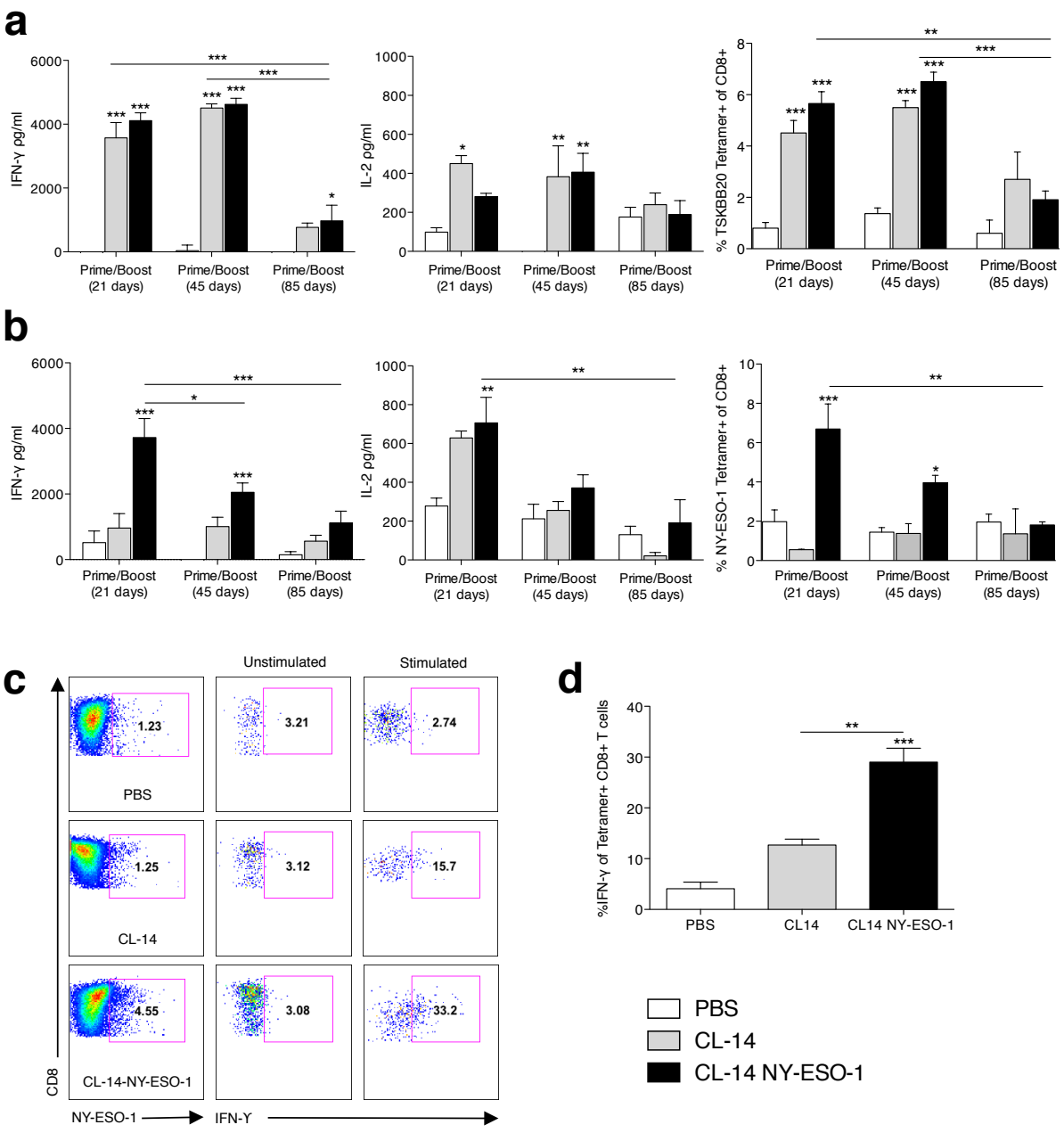

Santos *et al.* Figure 3

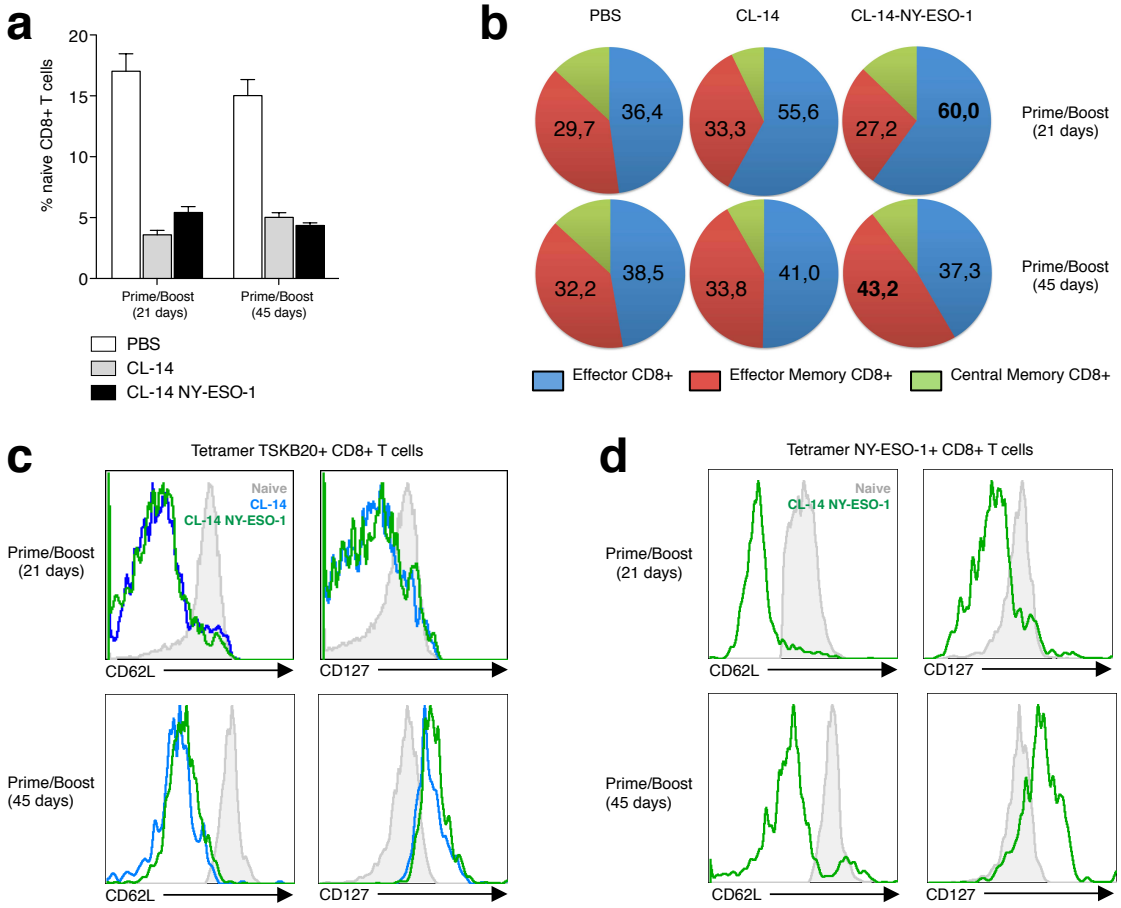

Santos *et al.* Figure 4

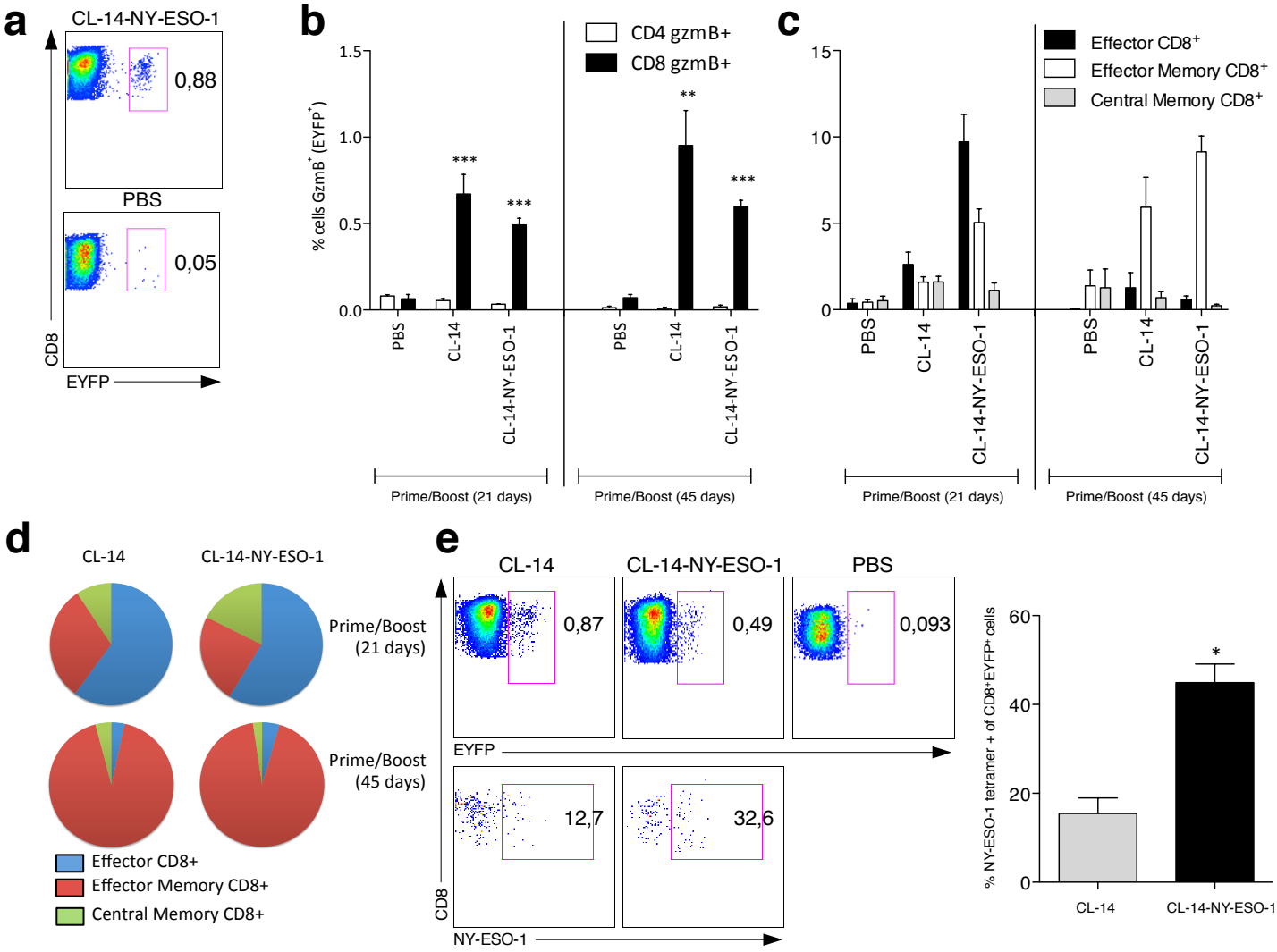

Santos *et al.* Figure 5

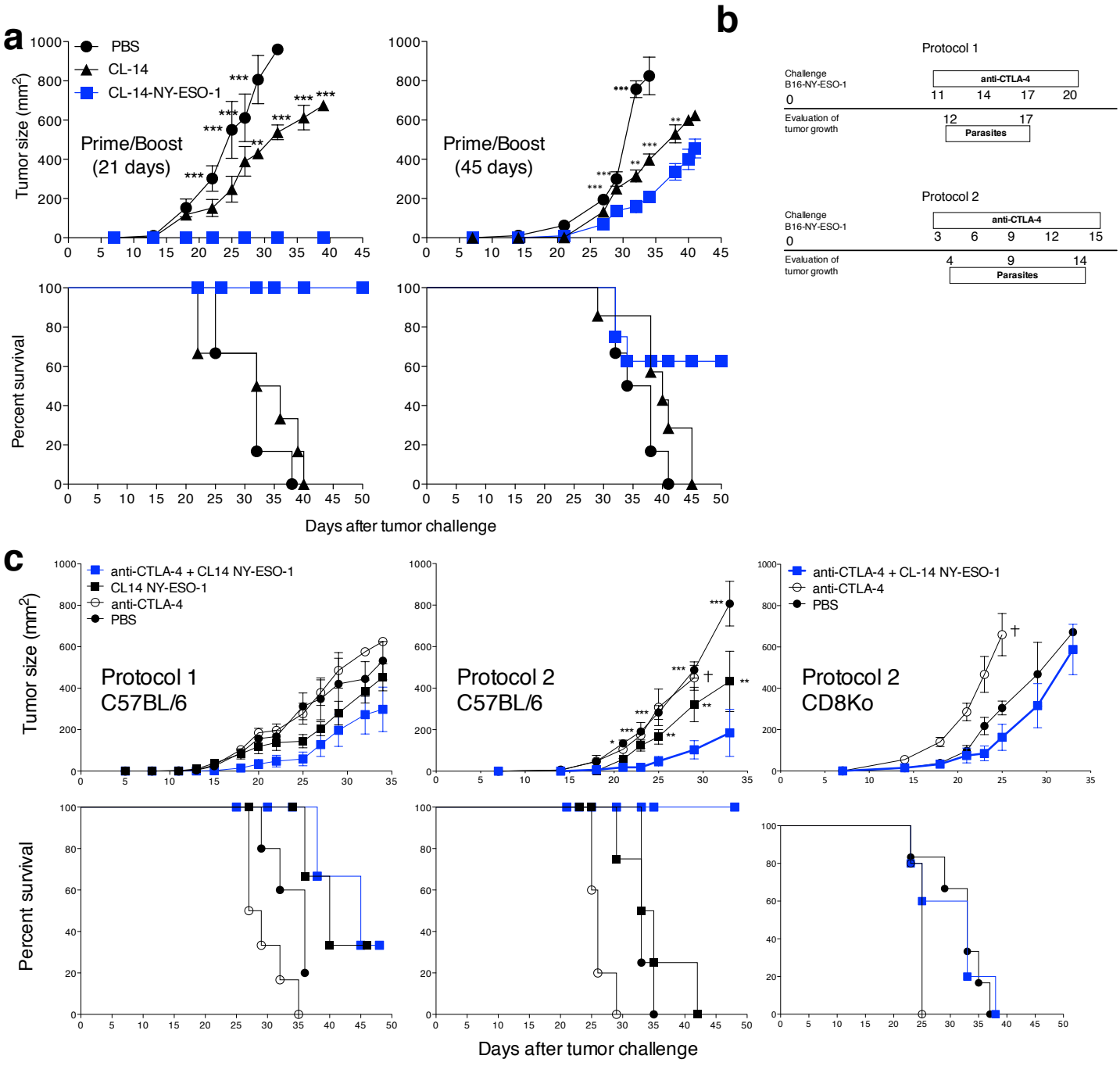

Santos *et al.* Figure 6

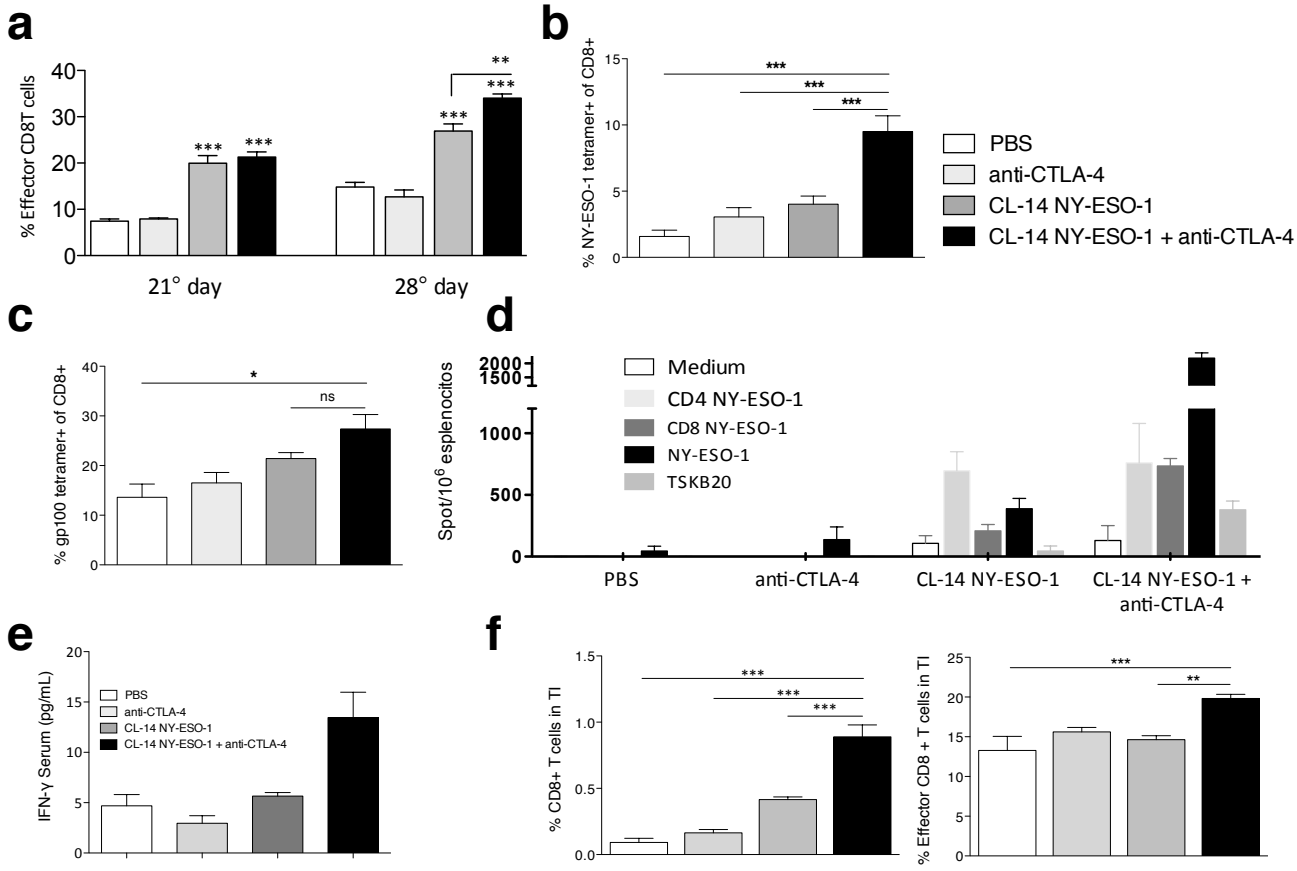

OPEN ACCESS Freely available online

PLOS ONE

Vaccination Using Recombinants Influenza and Adenoviruses Encoding Amastigote Surface Protein-2 Are Highly Effective on Protection against *Trypanosoma cruzi* Infection

Rafael Polidoro Alves Barbosa[1], Bruno Galvão Filho[1], Luara Isabela dos Santos[1], Policarpo Ademar Sales Junior[4], Pedro Elias Marques[3], Rafaela Vaz Sousa Pereira[3], Denise Carmona Cara[3], Oscar Bruña-Romero[2], Maurício Martins Rodrigues[5], Ricardo Tostes Gazzinelli[1,4,6], Alexandre Vieira Machado[4]*

1 Departamento de Bioquímica e Imunologia, Instituto de Ciências Biológicas, Universidade Federal de Minas Gerais, Belo Horizonte, Minas Gerais, Brasil, **2** Departamento de Microbiologia, Instituto de Ciências Biológicas, Universidade Federal de Minas Gerais, Belo Horizonte, Minas Gerais, Brasil, **3** Departamento de Morfologia, Instituto de Ciências Biológicas, Universidade Federal de Minas Gerais, Belo Horizonte, Minas Gerais, Brasil, **4** Centro de Pesquisas René Rachou, FIOCRUZ, Belo Horizonte, Minas Gerais, Brasil, **5** Centro de Terapia Celular e Molecular (CTCMol), Universidade Federal de São Paulo, Escola Paulista de Medicina, São Paulo, Brasil, **6** Division of Infectious Diseases and Immunology, Department of Medicine, University of Massachusetts Medical School, Worcester, Massachusetts, United States of America

Abstract

In the present study we evaluated the protection raised by immunization with recombinant influenza viruses carrying sequences coding for polypeptides corresponding to medial and carboxi-terminal moieties of *Trypanosoma cruzi*s amastigote surface protein 2 (ASP2). Those viruses were used in sequential immunization with recombinant adenovirus (heterologous prime-boost immunization protocol) encoding the complete sequence of ASP2 (Ad-ASP2) in two mouse strains (C57BL/6 and C3H/He). The CD8 effector response elicited by this protocol was comparable to that observed in mice immunized twice with Ad-ASP2 and more robust than that observed in mice that were immunized once with Ad-ASP2. Whereas a single immunization with Ad-ASP2 sufficed to completely protect C57BL/6 mice, a higher survival rate was observed in C3H/He mice that were primed with recombinant influenza virus and boosted with Ad-ASP2 after being challenged with *T. cruzi*. Analyzing the phenotype of CD8+ T cells obtained from spleen of vaccinated C3H/He mice we observed that heterologous prime-boost immunization protocol elicited more CD8+ T cells specific for the immunodominant epitope as well as a higher number of CD8+ T cells producing TNF-α and IFN-γ and a higher mobilization of surface marker CD107a. Taken together, our results suggest that immunodominant subpopulations of CD8+ T elicited after immunization could be directly related to degree of protection achieved by different immunization protocols using different viral vectors. Overall, these results demonstrated the usefulness of recombinant influenza viruses in immunization protocols against Chagas Disease.

Citation: Barbosa RPA, Filho BG, Santos LId, Junior PAS, Marques PE, et al. (2013) Vaccination Using Recombinants Influenza and Adenoviruses Encoding Amastigote Surface Protein-2 Are Highly Effective on Protection against *Trypanosoma cruzi* Infection. PLoS ONE 8(4): e61795. doi:10.1371/journal.pone.0061795

Editor: Dario S. Zamboni, University of São Paulo, Brazil

Received October 8, 2012; **Accepted** March 13, 2013; **Published** April 24, 2013

Funding: This work was supported by grants from FIOCRUZ/PDTIS-Vacinas, and National Institute for Vaccine Development and Technology (CNPq/FAPEMIG N° 015/2008; http://www.cpqrr.fiocruz.br/inctv/), CNPq/MAPA/SDA N° 064/2008, and Universal FAPEMIG (http://www.fapemig.br). Fellowships were provided by CNPq (http://www.cnpq.br/) to all authors. The funders had no role in study design, data collection and analysis, decision to publish, or preparation of the manuscript.

Competing Interests: The authors declare that Dr. Maurício Martins Rodrigues is a PLOS ONE Editorial Board member, and this does not alter their adherence to all the PLOS ONE policies on sharing data and materials.

* E-mail: amarok@cpqrr.fiocruz.br

Introduction

Over a hundred years after its first description, Chagas Disease remains as an important public health problem, mostly in Latin America. Nonetheless, the infection rate is increasing in other continents, mostly by blood transfusion [1,2]. Accordingly to WHO, there are currently over 10 million people infected in Latin America and more than 100 million people live at risk areas in endemic countries. Moreover, this disease kills approximately 13 thousand people every year, due to the clinical complications and to the poor efficacy of the pharmacological treatment which is highly toxic and effective mostly during the acute phase of disease [3,4]. In addition, the resistance of parasites to chemotherapy is another major drawback to the pharmacological treatment [5,6,7]. Thus, the development of vaccines is an important approach to be used in therapy and prophylaxis of Chagas disease [3,8].

Many vaccination studies against Chagas' disease already provided evidence that $CD8^+$ T cells play pivotal role on the development of protective immunity [9,10,11,12]. Mechanisms used by these cells to eliminate the parasite include directly killing of infected cell or secretion of cytokines such as IFN-γ [13,14]. Among the antigens that have been studied as potential candidates for vaccine development, the surface amastigote protein 2 (ASP2) has been found as one of the most promising [15,16]. In addition, different strategies have already been tested to deliver this antigen in mice, including the use of recombinant protein, plasmid DNA

and recombinant viruses [17,18,19,20]. For instance, our group demonstrated that two sequential immunizations with recombinant HuA5 adenovirus encoding ASP2 were able to significantly reduce the parasitemia and improve the survival of vaccinated mice, when they were challenged with Y strain of *T. cruzi* [18]. However, in spite of these very promising results, a drawback in use the same viral vector in sequential immunizations rely on the risk that anti-vector antibodies generated after the priming could neutralize the vector when it is used in further immunizations and, consequently, hurdle the boost of heterospecific immune response [21,22]. The limitation of anti-vector response elicited by homologous prime-boost immunization could be surpassed by different strategies, such as the use of two different recombinant viruses on prime and boost immunizations [23,24].

Live recombinant influenza viruses have some features that make them attractive to be used in vaccination protocols against protozoan infections, as we can mention: They are well known inductors of Cytotoxic T Lymphocytes (CTLs) by direct infection of immature dendritic cells (DCs) and monocytes, facilitating antigen (Ag) presentation both local and systemically [25,26,27]; It is feasible to generate recombinant influenza viruses by reverse genetics techniques [28]; There are different influenza A strains and subtypes, which could be used in sequential immunizations to overcome previous immune responses directed to the vector [29].

Therefore, in the present study we exploited the use of recombinant influenza viruses carrying truncated sequences of ASP2 in sequential immunization with adenovirus encoding ASP2. This immunization protocol elicited potent anti-ASP2 cellular immune response, reduced the parasite burden and improved the survival of vaccinated mice when they were challenged with *T. cruzi*.

Materials and Methods

Mice and Ethics

Male of eight- to ten-weeks-old C57BL/6 and C3H/He mice were obtained from René Rachou Research Institute's (CPqRR) animal facility center (Fiocruz, Belo Horizonte, Brazil) and housed according to institutional standard guidelines. All animal studies were approved by the Ethical Commission on Animals' Use (CEUA) at Oswaldo Cruz Foundation (Fiocruz), license LW-9-09, and performed following institutional Guide for the Care and Use of Laboratory Animals.

Cells and Parasites

MDCK and 293T cells (obtained from Pasteur Institut, FR) were grown at 37°C under 5% CO_2 in complete Dulbeccos modified Eagle Medium (DMEM; SIGMA) with 1 mM sodium pyruvate, 4.5 mg/ml L-glucose, 100 U/ml penicillin and 100 µg/ml streptomycin (herein called complete DMEM medium) and respectively supplemented with 5% or 10% heat inactivated fetal calf serum (FCS; CULTILAB) [30]. Trypomastigotes from *T. cruzi* Y Strain were maintained as previously described [17] and challenge infections were performed by inoculating the mice with 1000 (C57BL/6) or 500 (C3H/He) bloodstream trypomastigotes by intraperitoneal route. Mice survival was monitored daily and parasite development was monitored by counting the number of bloodstream trypomastigotes in 5 µl of fresh blood collected from the tail vein [31].

Plasmids for Influenza Reverse Genetics

Wild type (pPRNA) and dicistronic (pPRNA38) plasmids from neuraminidase (NA) segments of A/WSN/33 virus (H1N1) were constructed as previously described [30,32,33]. Due the size constraints, we constructed plasmids encoding 660 nucleotides corresponding respectively to medial (M-ASP2) and carboxi-terminal (C-ASP2) segments of ASP2 (figure 1A). These sequences were obtained by PCR using the plasmid pAdCMV-ASP2 as template [18] and specific primers for each ASP2 portion. The amplicons were cloned into *Kpn*I and *Nhe*I digested pIgSP plasmid in frame to the sequence coding for κ chain of mice immunoglobulin that allows the secretion of the foreign sequence [17]. Those constructs were used as PCR templates to generate IgSP-M or C-ASP2 segments which were site directed cloned into *Xho*I and *Nhe*I digested pPRNA38 vector (Figure 1B). All primers sequences are available under request and the respective presenting haplotype were referenced within the correspondent portion (Figure 1A) [34,35]. The generated plasmids (pPRNA38-M-ASP2 and pPRNA38-C-ASP2) were analyzed using Dynamic ET Dye Terminator Cycle Sequencing KIT® (AMERSHAM) and a Megabace 1000 automatic sequencer (AMERSHAM).

Influenza segments transfer plasmids pPOLI-HA, M, NS, PB2, PB1, PA and NP and the expression plasmids pcDNA-PA, NP, PB1 and PB2 were kindly provided by Dr George Brownlee (Sir William Dunn School of Pathology, University of Oxford, Oxford, United Kingdom) [36].

Generation of Recombinant Viruses

Recombinant adenovirus harboring the entire ASP2 coding region (Ad-ASP2), recombinant adenovirus (Ad-CT) and influenza (Flu-CT) virus, which encode unrelated sequences were generated as previously described [18,30,37]. Recombinant influenza viruses carrying dicistronic NA38-ASP2 segments were generated by the twelve plasmid-driven genetic reverse technique, as described by Fodor and co-workers with modifications [30,36]. Briefly, co-cultures of HEK 293T and MDCK cells were simultaneously transfected with plasmid coding the dicistronic NA segment (pPRNA38-M-ASP2 or pPRNA38-C-ASP2; 0.5 µg), the expression plasmids (pcDNA-PB1, pcDNA-PB2, pcDNA-NP and pcDNA-PA; 0.5 µg of each plasmid) and the other seven transfer plasmids of influenza A/WSN/33 segments (0.5 µg of each plasmid) using Fugene 6 Reagent® (ROCHE). Three days after incubation, infectious viral particles of recombinant vNA38-M-ASP2, vNA38-C-ASP2 (herein named respectively Flu-M-ASP2, Flu-C-ASP2) were recovered, amplified, plaque purified and titrated on MDCK as previously described [30].

Viral RNA Extraction, RT-PCR Analysis

Viral RNA (vRNA) extraction from cell-free supernatants of infected MDCK cultures and RT-PCR analysis were performed as previously described [33]. Amplicons were analyzed on 1% agarose gel and visualized by ethidium bromide staining. RT-PCR products were purified and presence of mutations was determined by sequencing using Dynamic ET Dye Terminator Cycle Sequencing KIT® (AMERSHAM) and a Megabace 1000 automatic sequencer (AMERSHAM).

Peptides

Peptides VNHRFTLV and TEWETGQI were purchased from Genscript (Piscataway, NJ). Peptide purity was in higher than 90%. Their identities were confirmed by Q-TOF Micro equipped with an electrospray ionization source (Micromass, United Kingdom).

ELISPOT and Intracellular Cytokine Staining

ELISPOT assay was performed essentially as previously described [37]. Spleens cells of immunized mice were obtained

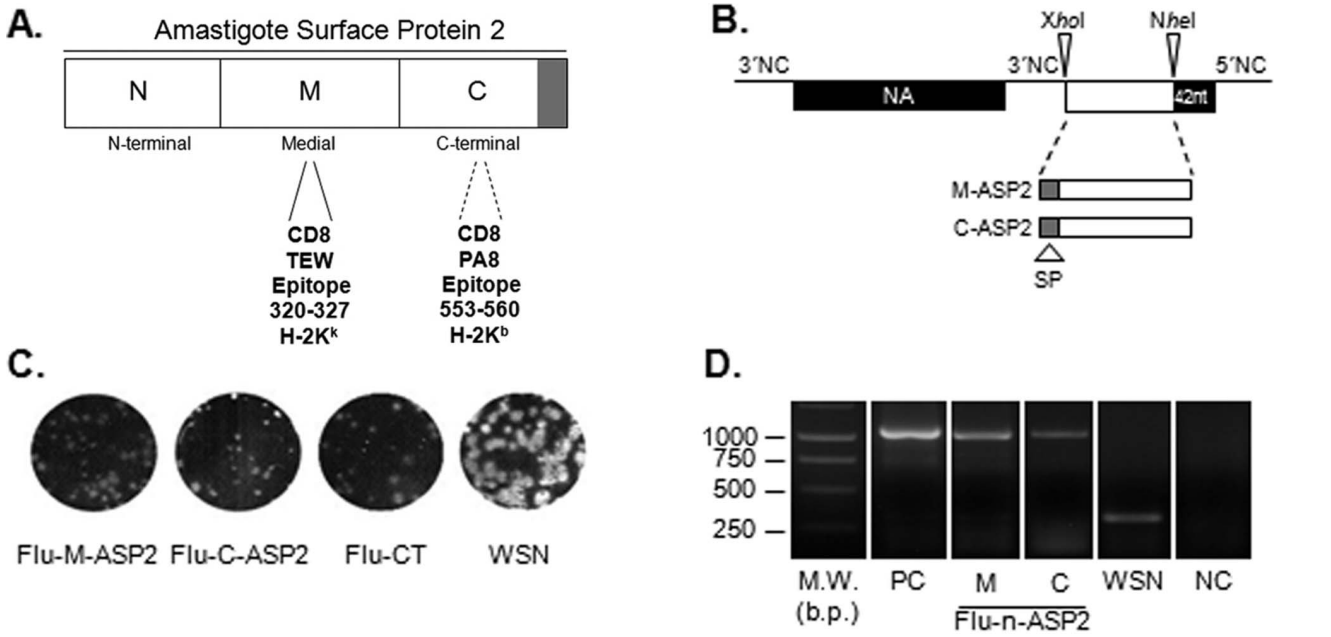

Figure 1. Construction and characterization of recombinant influenza viruses. Schematic representation of primary sequence of Amastigote Surface Protein 2 and its corresponding moieties, highlighting the mapped CD8 T cells epitopes (A). Schematic representation of the neuraminidase dicistronic segment. NA38 segment contains an A/WSN/33 (WSN) derived recombinant neuraminidase (NA) segment followed by a duplicated 3′non coding (NC) sequence, *Xho*I and *Nhe*I cloning sites, a duplication of the last 42 nucleotides of NA (dark box) and the original 5′NC sequence (28 nucleotides). The foreign sequences (open boxes) were cloned between *Xho*I and *Nhe*I cloning sites (B).The plaque phenotype of the wild type WSN and recombinant influenza viruses were assessed by standard agarose plaque assay in MDCK cells after 3 days of incubation at 35°C and 5% CO_2 (C).The NA segments of recombinant influenza viruses were analyzed by RT-PCR, using a set of primers that allows the amplification of the region containing the inserted foreign sequence. Corresponding plasmids DNAs were amplified in parallel as positive control. The amplified products were analyzes on a 1% agarose and visualized by ethidium bromide staining. The values depicted at the weight marker lane ar (D). W.M: weight marker; M: medial moiety of ASP2, C: carboxi-terminal moiety of ASP2; b.p.: base pairs.
doi:10.1371/journal.pone.0061795.g001

three weeks after boost immunization. They were treated with ACK buffer for erythrocytes lysis and washed twice in RPMI containing 5% FBS before to be resuspended in cell culture medium consisting of RPMI 1640 medium (pH 7.4) supplemented with 10 mM HEPES, 0.2% sodium bicarbonate, 59 mg of penicillin/liter, 133 mg of streptomycin/liter, and 10% fetal bovine serum (CULTILAB) containing recombinant IL-2 (100 U/ml). The viability of the cells was evaluated by using 0.2% trypan blue exclusion dye to discriminate between live and dead cells. The number of spleen cells was adjusted to 1×10^6 cells per well in cell culture medium and stimulated with specific peptides at final concentration of 10 µg/ml of VNHRFTLV (aa 553–560; for C57BL/6 splenocytes) or TEWETGQI (aa 320–327; for C3H/He splenocytes). The spots were counted on a S5 Core ELISPOT Analyser (CTL).

For Intracellular Cytokine Staining, the cell concentration was adjusted to 1×10^6 cells per well in cell culture medium containing GolgiStop ™ and GolgiPlug™ (according to manufacturer instructions; BD Pharmingen) and -phycoerythrin (PE) anti-CD107a (BD Pharmigen). In half of the cultures, a final concentration of 10 µg/ml of VNHRFTLV (for C57BL/6 splenocytes) or TEWETGQI (for C3H/He splenocytes) peptide was added. The cells were cultivated in U-bottom 96-well plates (Corning) in a final volume of 200 µl at 37°C in a 5% CO_2 humid atmosphere. After 12 hour-incubation, cells were stained for surface markers fluorescein isothiocyanate (FITC)-labeled dextramer TEWETGQI (Immudex), after 10 minutes incubation, cells were also stained with peridinin chlorophyll protein complex (PerCP) anti-CD8, avidin-phycoerythrin (PeCy7) anti-CD8, or FITC-labeled anti-CD3 (in samples without dextramer) antibodies (BD Pharmigen). The cells were fixed and permeabilized using Cytofix/Cytoperm kit (BD, Biosciences) according to manufacturer's recommendations. Cells were then stained for intracellular markers allophycocyanin (APC) anti-IFN-γ, APC-Cy7 anti-TNF-α, or PE Cy7 anti-TNF-α (BD Pharmigen). Finally, the cells were fixed in 2% PBS-paraformaldehyde and at least 100,000 cells were acquired on a FacsCanto, LSRFortessa or FacsAria II (BD, Biosciences) flow cytometers and then analyzed with FlowJo software (ThreeStar). The ancestry gates are represented in Figure S1.

ELISA and Western Blot

Recombinant ASP2 (rASP2) protein was produced in *Escherichia coli* as previously described [17]. The presence of sera specific anti-ASP2 antibodies were assessed by enzyme-linked immunosorbent assay (ELISA) on immunized mice sera obtained fourteen days after the boost immunization. Briefly, plates (Maxisorb, NUNC) were coated with 4 µg/mL (His65KDa, rASP2) and incubated at 4°C overnight. Mice sera were diluted 1:100 in blocking buffer and incubated for 2 hours at 37°C. Plates were incubated with peroxidase-conjugated goat anti-mouse IgG (SIGMA) one hour at room temperature, and reactions were developed with 3,3′5,5′-tetrametylbenzidine (TMB) reagent (SIGMA) and read at 450 nm.

Alternatively, 0.5 µg of His65KDa, rASP2 were loaded on 12% polyacrylamide gels and transferred to nitrocellulose membranes. Membranes were then blocked and incubated with individual sera of mice immunized with recombinant viruses. After extensive washes, membranes were incubated with peroxidase-conjugated

goat anti-mouse IgG (SIGMA) and detection was performed by membrane exposure to X-ray films after a standard chemoluminiscent reaction (ECL Detection System, Amersham Biosciences).

To measure IFN-γ production, spleen cells were obtained as described above and incubated for 72 hours at 37°C, 5% CO_2. The IFN-γ concentration was determined in cell culture supernatant with DuoSet ELISA Development System mouse IFN-γ kit (R&D Systems) according to manufacturer's recommendations.

Immunizations

Heterologous prime-boost immunizations were performed as previously described [30]. Briefly, the animals were lightly anesthetized with a mixture of ketamine and xylazine and inoculated by intranasal route (IN) with 10^3 plaque-forming unit (pfu) of recombinant influenza viruses (Flu-CT or Flu-nASP2) diluted in 25 µl of PBS. Four weeks later, the animals were boosted with 5×10^7 pfu of recombinant Ad-ASP2 or Ad-CT in 100 µl of PBS by subcutaneous route (SC). Alternatively, some animals received two immunizations with 5×10^7 pfu of recombinant Ad-ASP2 or AdCT by SC route four weeks apart (homologous prime-boost immunization protocol). Finally some mice received only one immunization with 5×10^7 pfu of recombinant Ad-ASP2 by SC route.

Statistical Analysis

Data are expressed as ± SEM and analyzed using GraphPad Prism ver.5 Software. Statistic significance for ELISA, ELISPOT and cytokine staining assays were evaluated using One-Way ANOVA and non-parametric test followed by Bonferroni post-test. Statistical significance for parasitemia was evaluated by 2-way ANOVA with Bonferroni post-test. The Gehan-Breslow-Wilcoxon test was performed to compare mouse survival curves.

Results

Generation and Characterization of Recombinant Influenza Viruses

Recombinant influenza viruses harboring the medial or the carboxi-terminal sequence of ASP-2 protein were recovered using the 12 plasmid driven reverse genetics as previously described [30]. These recombinant viruses, which were respectively named Flu-M-ASP2 and Flu-C-ASP2, displayed lysis plaques in MDCK cells similar in size than those found in cells infected with the recombinant Flu-CT. In contrast, those viruses displayed lysis plaques that were slightly smaller than those of the wild type WSN virus (Figure 1C). In addition, their infectious titers (1.4×10^6 pfu/ml Flu-M-ASP2 and 2.8×10^6 pfu/ml Flu-C-ASP2) were significantly lower than those of WSN virus(1×10^8 pfu/ml).

As shown in figure 1D, amplifications products of expected size (~1000 bp) were found for each recombinant influenza virus assayed. Moreover, when these amplicons were analyzed by sequencing, we found no mutations, demonstrating that those recombinant influenza viruses were genetically stable in cell culture (data not shown).

Evaluation of Humoral Immune Response

Immunization protocols were carried out according to the schedule depicted at figure 2A. Two weeks after the boost immunization, specific anti-ASP2 IgG serum antibodies were measured by ELISA and western blot, using the recombinant ASP2 (His65KDa) protein as capture antigen. Western blot results showed that specific anti-ASP2 IgG antibodies could be found in sera of all C57BL/6 mice primed with Flu-C-ASP2 and boosted with Ad-ASP2 (figure 2B), whereas only one animal that received a single immunization with Ad-ASP2 displayed detectable levels of specific anti-ASP2 antibodies. In addition, we detected higher levels of specific anti-ASP2 antibodies in the sera of mice primed with recombinant influenza than those found in animals that received only one immunization with Ad-ASP2 (Figure 2C). Interesting, neither by Western blot (data not shown) nor ELISA (figure 2D), we were able to detect specific anti-ASP2 antibodies in sera of C3H/He mice immunized with recombinant viruses, irrespective the immunization protocol used in vaccination. It is noteworthy that previous studies demonstrated that B epitopes are located in C-terminal moiety of ASP-2 protein and humoral immune response against intra-cellular amastigote proteins is not essential for protection [34,38].

Specific Cellular Immune Response Against Protective Epitopes

The activation of specific anti-ASP2 CD8+ T cell response was evaluated in spleen of immunized mice by stimulating their splenocytes with VNHRFTLV (H-2K^b-restricted, C57BL/6) or TEWETGQI (H-2K^k restricted, C3H) peptides, three weeks after the boost immunization. As depicted in figure 3, specific IFN-γ producing CD8+ T cells could be found in spleen cells of mice primed with Flu-C-ASP2 or Flu-M-ASP2 and boosted with Ad-ASP2 (figure 3A and C). In addition, high amounts of IFN-γ could be measured in spleen cell culture supernatants stimulated *ex-vivo* with their respective peptides (Figure 3B and D). Interesting, in both cases, there was a clear improvement in the prime-boost immunization, as we could find a significant increase in IFN-γ production on prime-boosted groups compared to single Ad-ASP2 immunized mice (Figure 3).

Protection Against Experimental Infection

The protection afforded by the vaccination protocols was evaluated by challenging the vaccinated mice with 500 (C3H/He) or 1000 (C57BL/6) bloodstream Y strain trypomastigotes. Regarding the resistant mice strain, C57BL/6, a single immunization with Ad-ASP2 sufficed to reduce the parasitemia and to completely protect the animals comparing to control immunized groups (Figure 4A, $p<0.05$; and 4B, $p<0.001$).

Regarding the C3H/He mice, which display remarkable susceptibility to *T. cruzi*, infection groups that received at least a single immunization with recombinant adenovirus-ASP2 were able to reduce the peak of parasitemia (Figure 4C, $p<0.001$), control tissue pathology (Figure S2) and prolong survival compared to the groups immunized with control recombinant viruses (Figure 4D $p<0.0005$). Remarkably, a higher survival rate was found in mice that were primed with Flu-M-ASP2 and boosted with Ad-ASP2 as close to 80% of vaccinated mice survived, comparing to mice that were primed with Flu-C-ASP2 and boosted with Ad-ASP2 ($p = 0.0019$). They also showed significant improvement of survival when compared to single or prime-boosted Ad-ASP2 immunized mice ($p = 0.05$, single and 0.08 homologous groups; Figure 4D).

In order to verify if the improvement of survival rate induced by the Flu-Ad protocol could be due to recombinant influenza properties, we tested the usefulness of a homologous intranasal prime subcutaneous-boost immunization using Flu-M-ASP2 virus in C3H/He mice strain. As demonstrated in Figure S3, we could not observe the production of specific immune response under stimulation neither by ELISPOT (Figure S3) nor intracellular staining for IFN-γ and TNF-α (data not shown) in splenocytes derived from homologous immunized mice. This could be expected since a single immunization with recombinant influenza

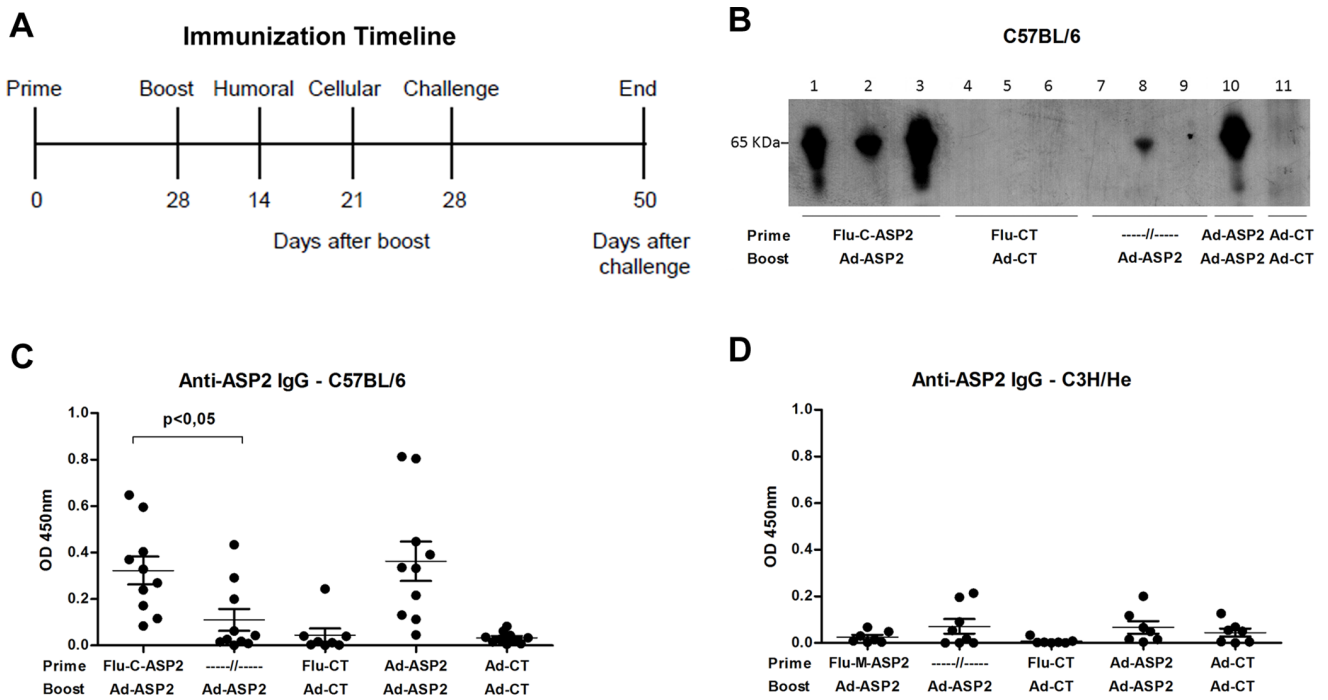

Figure 2. Immunization Schedule and Induction of specific anti-ASP2 humoral immune response in mice vaccinated with recombinant viruses. Timeline representation of immunization schedule and experimental procedures (A). C57BL/6 mice were immunized as described in Material and Methods. Two weeks after the boost immunization, the animals were bled and the presence of specific anti-ASP2 total IgG antibodies in mice sera was evaluated by western by incubating individual (lanes 1–9) or pooled (lanes 10 and 11) sera of C57BL/6 mice with nitrocellulose membranes loaded with recombinant ASP2 protein (His65KDa) as capture antigen blot (B). Alternatively, the antibodies levels were measured by ELISA using individual sera of C5BL/6 (C) or C3H/He (D) mice sera diluted 1:100 and recombinant ASP2 protein as capture antigen. Optical Density (OD) was measured at 450 nm.
doi:10.1371/journal.pone.0061795.g002

is known to elicit neutralizing antibodies that can prevent a proper boost against the heterologous M-ASP2 polypeptide [30,32].

Cellular Immune Response Profile Elicited by Different Immunization Protocols

The survival results found in C3H/He mice prompted us to study more deeply the cellular immune profile elicited by the immunization protocols. To this aim, C3H/He mice were immunized as previously described and three weeks after the boost immunization, spleen CD8+ T cells were evaluated for intracellular staining of IFN-γ and TNF-α cytokines and for the surface mobilization of CD107a upon *ex vivo* stimulation with peptide TEWETGQI, as described in Material and Methods section. As depicted in figure 5A, the percentage of CD8+T cells positive for at least one of the parameters evaluated were similar in mice that received two immunizations with recombinant viruses, irrespective the immunization strategy employed.

Regarding the phenotype of subpopulations of CD8+ T cells found in vaccinated mice, triple (IFN-γ, TNF-α, CD107a) and double (IFN-γ+CD107a+, and IFN-γ+TNF-α) positive cells are the major populations that were found after immunization with recombinant viruses encoding ASP2 (Figure 5B). Interestingly, mice immunized with recombinant viruses encoding ASP2 displayed similar percentage of CD8+ T cell subpopulations, irrespective if they were immunized according to heterologous or homologous immunization protocols, and similar to IFN-γ production seen by ELISPOT and ELISA, there was a clear impact of boost immunization in the frequency of specific effector CD8+ T cells comparing prime-boosted groups with Ad-ASP2 single immunized group (Figure 5A and 5B).

In order to perform a more accurate analysis on CD8+ T cells elicited by immunization, we used a specific H-2K^d/TEWETGQI dextramer. Mice were immunized as previously described and the phenotype of specific CD8+ T cells was assessed in TEWETGQI stimulated pooled spleen cells of vaccinated mice three weeks after the last immunization. As depicted in figure 5C, mice vaccinated with Flu-ASP2/Ad-ASP2 displayed the highest number of total dextramer positive CD8+ T cells. The main subpopulation of dextramer positive CD8+ T cells that were found in mice immunized irrespective the tested protocols were triple positives (IFN-γ, TNF-α, CD107), followed by single (CD107+) positives CD8+ T cells (Figure 5D). On the other hand, we could observe a higher frequency of single IFN-γ+TEWETGQI+ CD8+ T cells (CD107a- TNF-α-) in heterologous (19%) and Ad-ASP2 single (12.5%) immunized groups compared to Ad-ASP2/Ad-ASP2 group (2,9%).

Accordingly, Table 1 shows that besides heterologous Flu-Ad immunization elicited higher numbers of CD8+TEWETGQI+ T cells, also the frequency of CD8+TEWETGQI+ CD107a and/or IFN-γ and/or TNF-α positive cells increase above two fold compared to homologous or single immunized groups. We could also find a significant increase of perforin production under stimulation only in the heterologous vaccinated group (Figure S4). This results suggest the importance of those effector factors on protection and could also indicate that the improvement of survival by heterologous could be due to a higher number of effector specific CD8+ T cells.

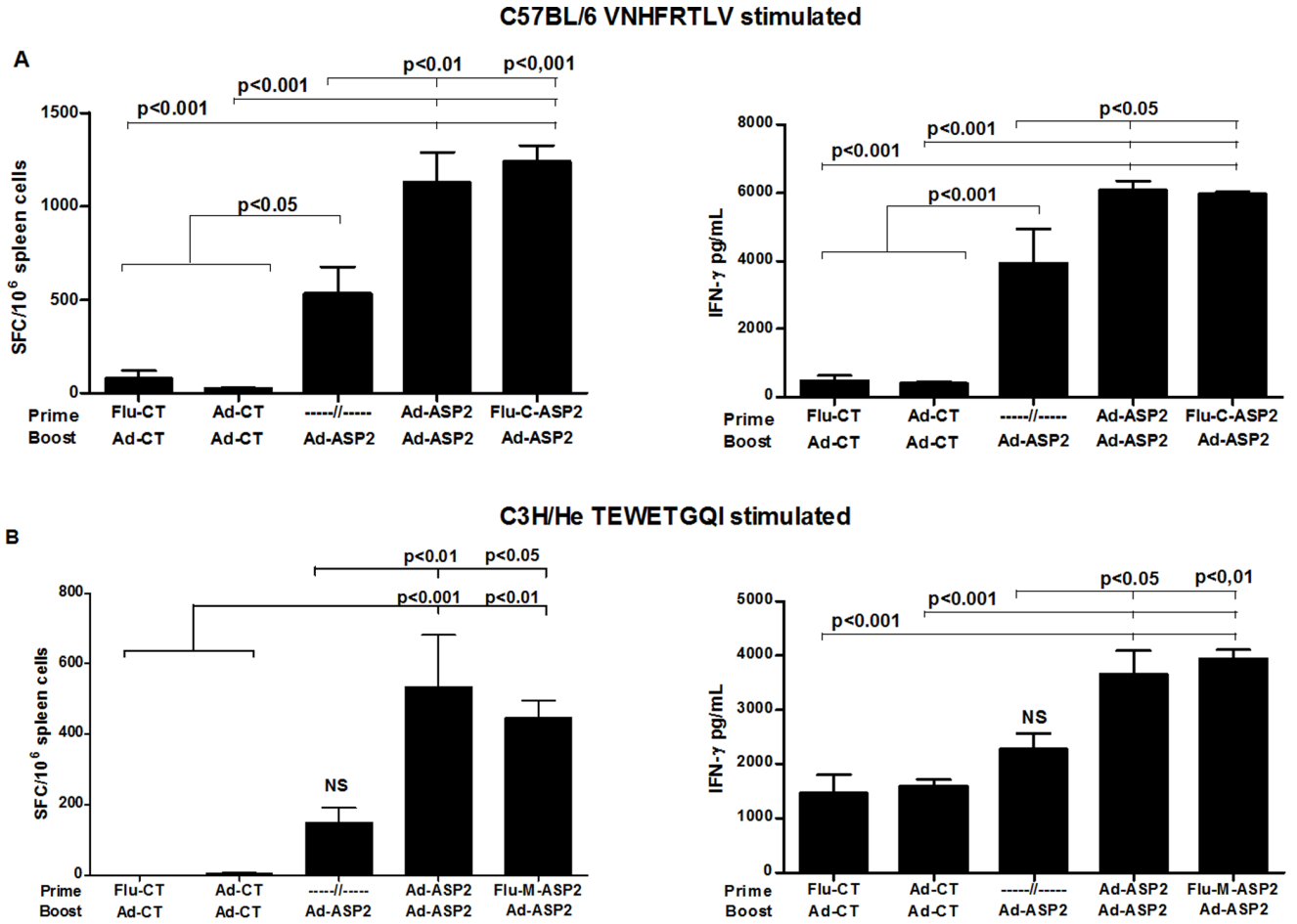

Figure 3. Cellular responses to immunodominant epitopes from ASP2 in mice immunized with recombinant viruses. C57BL/6 and C3H/He mice were immunized as described in Material and Methods. Three weeks after the boost immunization, the presence of ASP-2 specific IFN-γ producing T cells in spleen cells of C57BL/6 (A) or C3H/He (B) mice were assessed by ELISPOT and culture supernatant ELISA (n = 8). To this aim, the spleen cells of individual mice were stimulated 18 hours (ELISPOT) or 72 hours (ELISA) *ex vivo* with VNHRFTLV (aa 553–560; for C57BL/6) or TEWETGQI (aa 320–327; for C3H/He) specific ASP2 peptides. Optical Density (OD) was measured at 450 nm.
doi:10.1371/journal.pone.0061795.g003

Discussion

Recombinant viruses carrying foreign sequences have been proven to be useful tools as vaccines against many pathogens, including those which require the induction of potent type I T cell immune responses, such as *Leishmania s.p.*, *Toxoplasma gondii* and *Trypanosoma cruzi* [39]. Studies carried out by our group demonstrated that two immunizations with recombinant adenovirus carrying *T. gondii* or *T. cruzi* antigens were able to elicit specific humoral and cellular immune response and to protect different mouse lineages after challenge with those protozoan parasites [18,37]. In spite of these very promising results, two immunizations with recombinant adenovirus (homologous immunization protocol) raises some concerns, mostly due to the elicited anti-vector immune response, which could hurdle the immune response directed against the foreign sequence in subsequent vaccinations. This problem could be surpassed by using two different vectors for each immunization [24]. Therefore, we evaluated the use of recombinant influenza viruses encoding ASP2 derived polypeptides as a tool for priming the specific anti-ASP2 immune response, followed by sequential immunization with a recombinant adenovirus encoding ASP2. Regarding the naturally resistant C57BL/6 mice, the prime with recombinant influenza virus encoding the carboxi-terminal portion of ASP2 was as useful as recombinant adenovirus in priming specific anti-ASP2 immune response. Indeed, antibodies levels and the number IFN-γ producers CD8+ T cells specific for ASP2 were similar in mice primed with recombinant influenza or adenovirus. Interesting, regarding C57BL/6 mice strain, a single immunization with recombinant adenovirus suffice to control parasitemia and to completely protect the animals after challenge. Similar findings were obtained by Duan and collaborators using recombinant Sendai virus encoding ASP2, which was able to significantly reduce the parasitemia and to completely protect C57BL/6 mice after the challenge with Tulahuen strain [19].

Regarding the susceptible strain C3H/He, all immunizations protocols employing Ad-ASP2 in our study were able to significantly reduce the parasitemia, control at certain extent tissue pathology and prolong survival of challenged animals. Considering Y strain of *Trypanosoma cruzi*, there is a variable correlation between blood parasitemia and survival rate, as demonstrated in different mice strains [40,41]. However, we could observe a correlation of parasitemia control with prolonged survival in our model. Notwithstanding, an improvement on the survival rate was observed in mice primed with

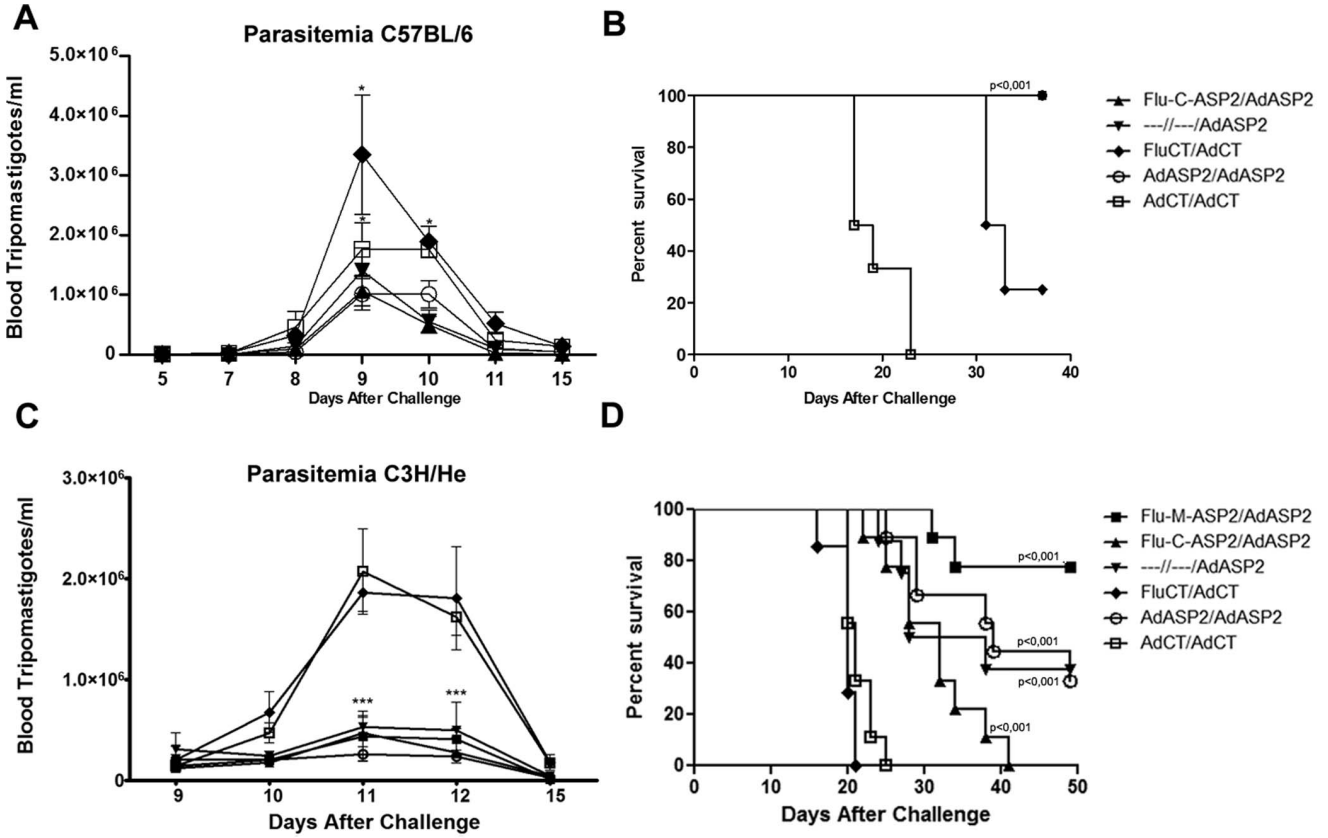

Figure 4. Parasitemia and survival curves of immunized mice challenged with *T. cruzi*. B6 and C3H/He mice were immunized as described in Material and Methods. Four weeks after boost immunization, they were challenged intraperitoneally with 1000 and 500, respectively, *T. cruzi* Y strain bloodstream trypomastigotes. Parasitemia was monitored on blood and depicted as the number of bloodstream trypomastigotes per milliliter of blood (A, n = 4; C, n = 8). The survival of vaccinated C57BL/6 (B, n = 7) and C3H/He (D, n = 7–9) mice was followed during 50 days and showed as Kaplan-Meier curves. * $p<0.05$, *** $p<0.001$.
doi:10.1371/journal.pone.0061795.g004

recombinant influenza-M-ASP2 and boosted with recombinant adenovirus even when compared to the survival of the animals that were immunized once or twice with recombinant adenovirus, or primed using Flu-C-ASP2 which does not contain an immunodominant epitope to C3H/He MHC-I haplotype. These results seemed quite surprising because the specific anti-ASP2 cellular immune response, measured by the number of specific CD8+ T as well as by production of IFN-γ was similar in mice that were submitted either to the homologous or heterologous prime and boost immunization protocols.

Phenotype analyses performed on total CD8+ T cells obtained from vaccinated C3H/He showed that most effector CD8+ T cells were polyfunctional and mostly triple (IFN-γ, TNF-α and CD107a) and double (IFN-γ, CD107a) positives. These results were similar to those obtained previously in C57BL/6 mice that were immunized with naked DNA and adenovirus encoding ASP2 [42]. Our results also showed that mice that received one immunization with Ad-ASP2 displayed similar CD8+ T cells phenotype than those observed in mice that received two immunizations with recombinant viruses encoding ASP2, suggesting that just one immunization with Ad-ASP2 suffice for shaping the CD8+ T cells phenotype. Thus, our observations indicate that a single immunization using Ad-ASP2 suffice to stimulate a significant production of effector cytokines IFN-γ, TNF-α and mobilize CD107a, elicit an immunodominant effector population which can control parasitemia, reduce tissue pathology and prolong survival when compared to control immunized mice even in a susceptible model. This is particularly important because often, studies using different recombinant viruses or other vaccine vectors, mice models and *Trypanosoma cruzi* strains without the single immunized group could be overestimating their protection using prime-boost protocols.

Remarkably, C3H/He mice that were primed with Flu-M-ASP2 displayed higher number of dextramer positives CD8+ T cells than mice that were immunized with Ad-ASP2. Moreover, our results showed that a boost immunization with Ad-ASP2 did not augment the number of TEWETGQI dextramer positive CD8+ T cells in mice primed with Ad-ASP2. To discuss the reason by which the heterologous prime-boost protocol could improve protection and enhance the frequency of TEWETGQI CD8+ T cells we hypothesized that immunization with Flu-M-ASP2, which encodes only the medial moiety of ASP2, primed the immunodominant CD8+ response towards TEWETGQI epitope resulting in the expansion of this population after boosting with Ad-ASP2. In contrast, priming with Ad-ASP2, which carries the entire sequence of ASP2, could possibly elicit immune response also against subdominant epitopes of ASP2, resulting in a lower secondary response against TEWETGQI immunodominant epitope after boost [34,38,42,43,44]. Accordingly, previous results of our group suggest that immunization with plasmids or adenovirus encoding

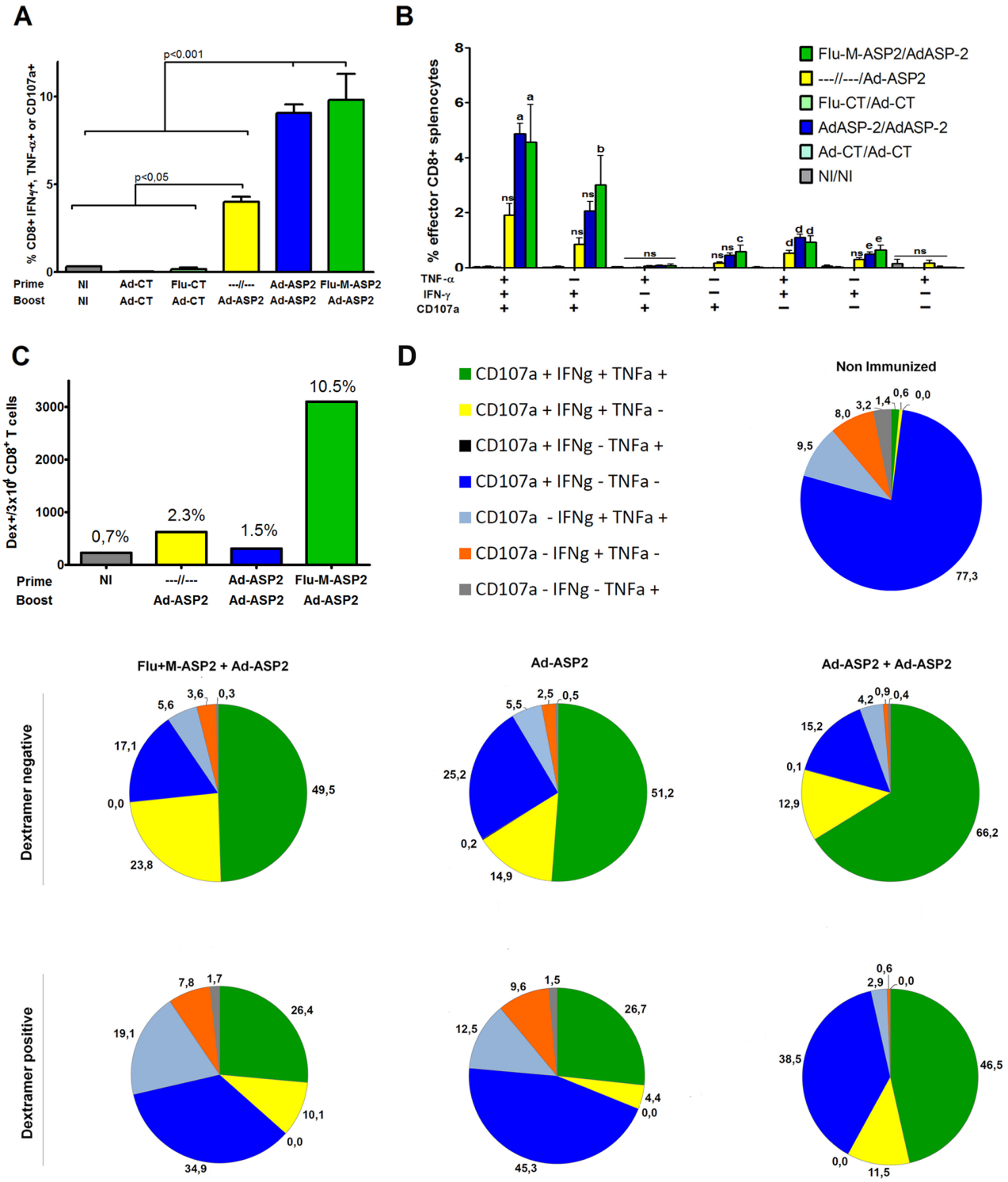

Figure 5. Phenotype of anti-ASP2 specific CD8+ T cells elicited by vaccination with recombinant viruses. C3H/He mice were immunized with recombinant viruses as described in Material and Methods. Two weeks after the last immunization, the spleen cells were harvested and cultivated *ex vivo* with specific TEWETGQI CD8+ T peptide and incubated with anti-CD3, anti-CD8, permeabilized and fixed and stained with anti-CD107a, anti-IFN-γ and anti-TNF-α antibodies and assessed by flow cytometry. Percentage of effector CD8+ T cells reacting to the presence of TEWETGQI peptide obtained from spleen cells of mice immunized with recombinant viruses (A). Percentage of CD8 T cells which produces IFN-γ or/and TNF-α or/and mobilizes the degranulation marker CD107a after stimulation with TEWETGQI (B), the statistics depicted are compared to groups of mice immunized with control recombinant viruses. The number and frequency of dextramer positive CD8+ T found in 3×10^4 CD8+ T (C). Functional profile of CD8+ T cells subpopulations obtained from mice immunized with recombinant viruses (D). Response were depicted with different color patterns according to the number of assessed functions (IFN-γ, TNF-α and CD107a) displayed by each dextramer negative or dextramer positive CD8+ T cells subpopulations.

doi:10.1371/journal.pone.0061795.g005

Table 1. Percentage of effector CD8+ T cells in splenocytes of immunized mice.

% of effector CD8+ T cells in mice immunized with recombinant viruses								
	%Total	% CD8+ T cell Dex. Neg.			%Total	% CD8+ T cell Dex. Pos.		
Immun. Protocol	CD8+ T cell Dex. Neg.	CD107+	IFNγ	TNFα	CD8+ T cell Dex. Pos.	CD107+	IFNγ	TNFα
Flu-ASP2+ Ad-ASP2	89.5	9.9	9.0	6.1	10.5	2.1	1.8	1.3
-----+Ad-ASP2	97.7	5.1	4.1	3.2	2.3	0.5	0.4	0.3
Ad-ASP2+ Ad-ASP2	98.5	11.5	10.3	8.7	1.5	0.6	0.4	0.3
Non infected	99.3	1.1	0.3	0.2	0.7	0.2	0.0	0.0

doi:10.1371/journal.pone.0061795.t001

ASP2 subdominants epitopes afforded lower degree of protection when compared to that observed in animals immunized with vectors encoding the immunodominant epitope [42]. A reinforcement to this hypothesis could be found in the low number of proteins encoded by influenza when compared to adenovirus, which potentially reduces the number of viral antigens that could compete with the heterologous antigen for presentation by antigen-presenting cells [45,46]. The correlation between TEWETGQI (present in medial portion of ASP2, M-ASP2) immunodominant frequency and protection is reinforced by the result of C3H/He mice that were immunized using recombinant influenza encoding the C-terminus portion of ASP2 as prime and Ad-ASP2 as boost presented a survival curve similar to single immunized or homologous prime-boost using Ad-ASP2 after infection ($p = 0.46$).

Another finding of our study was that the number of dextramer stained CD8+ T cells producing IFN-γ, TNF-α or the surface marker CD107a found in animals primed with Flu-M-ASP2 were approximately three times higher than those observed in other vaccinated groups. However, while the role of different T cell subpopulation to control the infection with some viruses, bacteria and Plasmodium was already well documented [47,48,49,50], the biological relevance of CD8+ T cells subpopulations phenotypes to control the infection with *T. cruzi* remains elusive [51]. The IFN-γ production itself is known to be important for protection against *Trypanosoma cruzi* infection in many previous work of our and other groups [14,52,53,54,55]. On the other hand, other factors as the effector phenotype of specific CD8+ T cells, the production of perforin, the re-circulation of those cells out of spleen [56], their presence in the heart [57,58], apoptosis of specific immunodominant anti-ASP2 CD8+ T cells [59], and the type of memory cells involved are important to be considered [51]. Recently a group has elegantly shown that multiple redundant effector CD8+ T cells factors deriving from transferred Tc1 and Tc17 populations are capable of protecting mice against viral infection [60], and as CD8+ T cells have a major role in protection against *Trypanosoma cruzi* infection, this statement is an interesting subject of research. Thus, if the improvement of protection observed in mice primed with recombinant influenza-M-ASP2 virus was only due to the higher number of CD8+T specific for the immunodominant epitope or could also be due to other factors remains to be solved.

In summary, we demonstrated that recombinant influenza viruses encoding an ASP2 derived polypeptide would be useful in heterologous prime-boost studies aiming the development of vaccines against Chagas Disease. The priming with recombinant influenza virus followed by boost with recombinant adenovirus could properly augment the number of effector CD8+ T cells specific for ASP2 immunodominant epitope, whose displayed unique phenotype and resulted in increased survival of vaccinated C3H/He mice challenged with *T. cruzi*.

Supporting Information

Figure S1 Representative of ancestry gates for flow cytometry experiments. Correspondent ancestry gates for the figure 5 analysis.
(TIF)

Figure S2 Histopathological analyses of liver, spleen and heart derived from infected mice. Male C3H/He mice were primed and boosted according different immunization protocols and infected with 500 bloodstream trypomastigotes of Y strain of *T. cruzi*. Fifteen days after the infection, mice were euthanized and spleen, liver and heart were harvested, fixed and processed for histopathology. The organ sections were stained using hematoxilin-eosin and the degree of tissue inflammation was evaluated (scale bar - 100 μm).
(TIF)

Figure S3 Cellular responses to immunodominant epitope from ASP2 in mice immunized twice using Flu-M-ASP2. ELISPOT of stimulated splenocytes taken from C3H/He mice immunized with the depicted protocols. The prime-boost was performed within an interval of 28 days and the experiment was performed 21 days post boost. The splenocytes were incubated 18 h in the presence of 10 μg of TEWETGQI peptide ($n = 5$ for all groups except non-immunized group NI/NI, $n = 3$).
(TIF)

Figure S4 Perforin production in splenocytes derived from C3H/He immunized mice. Splenocytes derived from immunized C3H/He mice were *ex vivo* stimulated or not in the presence of Brefeldin A and Monesin A and the immunodominant peptide TEWETGQI for 12 hours, prepared, labeled and submitted to flow cytometry ($n = 4$). N.I. Non-immunized/Non-infected. Their staining profiles were analyzed using FlowJo and statistical analysis performed was 2-Way ANOVA with Bonferroni post-test using GraphPad Prism 5.0 Software.
(TIF)

Acknowledgments

We thanks to Dr George Brownlee,Sir William Dunn School of Pathology, University of Oxford, Oxford, United Kingdom who kindly provided most of plasmids use in reverse genetics experiments; We thanks to Msc Thais Boccia, from University of São Paulo who kindly made spell checks and other recommendations.

Author Contributions

Conceived and designed the experiments: RPAB DCC OBR MMR RTG AVM. Performed the experiments: RPAB BGF LIS PASJ RVSP PEM AVM. Analyzed the data: RPAB BGF LIS PEM DCC MMR RTG AVM. Contributed reagents/materials/analysis tools: DCC MMR OBR RTG AVM. Wrote the paper: RPAB AVM.

References

1. Gascon J, Bern C, Pinazo MJ (2012) Chagas disease in Spain, the United States and other non-endemic countries. Acta Trop 115: 22–27.
2. Bern C, Kjos S, Yabsley MJ, Montgomery SP (2011) Trypanosoma cruzi and Chagas' Disease in the United States. Clin Microbiol Rev 24: 655–681.
3. Vazquez-Chagoyan JC, Gupta S, Garg NJ (2011) Vaccine development against Trypanosoma cruzi and Chagas disease. Adv Parasitol 75: 121–146.
4. Rassi A, Jr., Rassi A, Marin-Neto JA (2010) Chagas disease. Lancet 375: 1388–1402.
5. Camandaroba EL, Reis EA, Goncalves MS, Reis MG, Andrade SG (2003) Trypanosoma cruzi: susceptibility to chemotherapy with benznidazole of clones isolated from the highly resistant Colombian strain. Rev Soc Bras Med Trop 36: 201–209.
6. Le Loup G, Pialoux G, Lescure FX (2011) Update in treatment of Chagas disease. Curr Opin Infect Dis 24: 428–434.
7. Urbina JA (2001) Specific treatment of Chagas disease: current status and new developments. Curr Opin Infect Dis 14: 733–741.
8. Bethony JM, Cole RN, Guo X, Kamhawi S, Lightowlers MW, et al. (2011) Vaccines to combat the neglected tropical diseases. Immunol Rev 239: 237–270.
9. Rodrigues MM, Boscardin SB, Vasconcelos JR, Hiyane MI, Salay G, et al. (2003) Importance of CD8 T cell-mediated immune response during intracellular parasitic infections and its implications for the development of effective vaccines. An Acad Bras Cienc 75: 443–468.
10. Parodi C, Padilla AM, Basombrio MA (2009) Protective immunity against Trypanosoma cruzi. Mem Inst Oswaldo Cruz 104 Suppl 1: 288–294.
11. Miyahira Y (2008) Trypanosoma cruzi infection from the view of CD8+ T cell immunity–an infection model for developing T cell vaccine. Parasitol Int 57: 38–48.
12. Junqueira C, Caetano B, Bartholomeu DC, Melo MB, Ropert C, et al. (2010) The endless race between Trypanosoma cruzi and host immunity: lessons for and beyond Chagas disease. Expert Rev Mol Med 12: e29.
13. Muller U, Sobek V, Balkow S, Holscher C, Mullbacher A, et al. (2003) Concerted action of perforin and granzymes is critical for the elimination of Trypanosoma cruzi from mouse tissues, but prevention of early host death is in addition dependent on the FasL/Fas pathway. Eur J Immunol 33: 70–78.
14. de Alencar BC, Persechini PM, Haolla FA, de Oliveira G, Silverio JC, et al. (2009) Perforin and gamma interferon expression are required for CD4+ and CD8+ T-cell-dependent protective immunity against a human parasite, Trypanosoma cruzi, elicited by heterologous plasmid DNA prime-recombinant adenovirus 5 boost vaccination. Infect Immun 77: 4383–4395.
15. Wizel B, Palmieri M, Mendoza C, Arana B, Sidney J, et al. (1998) Human infection with Trypanosoma cruzi induces parasite antigen-specific cytotoxic T lymphocyte responses. J Clin Invest 102: 1062–1071.
16. Garg N, Tarleton RL (2002) Genetic immunization elicits antigen-specific protective immune responses and decreases disease severity in Trypanosoma cruzi infection. Infect Immun 70: 5547–5555.
17. Boscardin SB, Kinoshita SS, Fujimura AE, Rodrigues MM (2003) Immunization with cDNA expressed by amastigotes of Trypanosoma cruzi elicits protective immune response against experimental infection. Infect Immun 71: 2744–2757.
18. Machado AV, Cardoso JE, Claser C, Rodrigues MM, Gazzinelli RT, et al. (2006) Long-term protective immunity induced against Trypanosoma cruzi infection after vaccination with recombinant adenoviruses encoding amastigote surface protein-2 and trans-sialidase. Hum Gene Ther 17: 898–908.
19. Duan X, Yonemitsu Y, Chou B, Yoshida K, Tanaka S, et al. (2009) Efficient protective immunity against Trypanosoma cruzi infection after nasal vaccination with recombinant Sendai virus vector expressing amastigote surface protein-2. Vaccine 27: 6154–6159.
20. Nogueira RT, Nogueira AR, Pereira MC, Rodrigues MM, Galler R, et al. (2011) Biological and immunological characterization of recombinant Yellow Fever 17D viruses expressing a Trypanosoma cruzi Amastigote Surface Protein-2 CD8+ T cell epitope at two distinct regions of the genome. Virol J 8: 127.
21. Schneider J, Gilbert SC, Hannan CM, Degano P, Prieur E, et al. (1999) Induction of CD8+ T cells using heterologous prime-boost immunisation strategies. Immunol Rev 170: 29–38.
22. Ramshaw IA, Ramsay AJ (2000) The prime-boost strategy: exciting prospects for improved vaccination. Immunol Today 21: 163–165.
23. Lu S (2009) Heterologous prime-boost vaccination. Curr Opin Immunol 21: 346–351.
24. Radosevic K, Rodriguez A, Lemckert A, Goudsmit J (2009) Heterologous prime-boost vaccinations for poverty-related diseases: advantages and future prospects. Expert Rev Vaccines 8: 577–592.
25. Manicassamy B, Manicassamy S, Belicha-Villanueva A, Pisanelli G, Pulendran B, et al (2010). Analysis of in vivo dynamics of influenza virus infection in mice using a GFP reporter virus. Proc Natl Acad Sci U S A 107: 11531–11536.
26. Kreijtz JH, Fouchier RA, Rimmelzwaan GF (2011) Immune responses to influenza virus infection. Virus Res 162: 19–30.
27. Johnson S, Zhan Y, Sutherland RM, Mount AM, Bedoui S, et al. (2009) Selected Toll-like receptor ligands and viruses promote helper-independent cytotoxic T cell priming by upregulating CD40L on dendritic cells. Immunity 30: 218–227.
28. Horimoto T, Kawaoka Y (2009) Designing vaccines for pandemic influenza. Curr Top Microbiol Immunol 333: 165–176.
29. Ferko B, Stasakova J, Sereinig S, Romanova J, Katinger D, et al. (2001) Hyperattenuated recombinant influenza A virus nonstructural-protein-encoding vectors induce human immunodeficiency virus type 1 Nef-specific systemic and mucosal immune responses in mice. J Virol 75: 8899–8908.
30. Machado AV, Caetano BC, Barbosa RP, Salgado AP, Rabelo RH, et al. (2010) Prime and boost immunization with influenza and adenovirus encoding the Toxoplasma gondii surface antigen 2 (SAG2) induces strong protective immunity. Vaccine 28: 3247–3256.
31. Krettli AU, Brener Z (1976) Protective effects of specific antibodies in Trypanosoma cruzi infections. J Immunol 116: 755–760.
32. Vieira Machado A, Naffakh N, Gerbaud S, van der Werf S, Escriou N (2006) Recombinant influenza A viruses harboring optimized dicistronic NA segment with an extended native 5′ terminal sequence: induction of heterospecific B and T cell responses in mice. Virology 345: 73–87.
33. Machado AV, Naffakh N, van der Werf S, Escriou N (2003) Expression of a foreign gene by stable recombinant influenza viruses harboring a dicistronic genomic segment with an internal promoter. Virology 313: 235–249.
34. Araujo AF, de Alencar BC, Vasconcelos JR, Hiyane MI, Marinho CR, et al. (2005) CD8+-T-cell-dependent control of Trypanosoma cruzi infection in a highly susceptible mouse strain after immunization with recombinant proteins based on amastigote surface protein 2. Infect Immun 73: 6017–6025.
35. Low HP, Santos MA, Wizel B, Tarleton RL (1998) Amastigote surface proteins of Trypanosoma cruzi are targets for CD8+ CTL. J Immunol 160: 1817–1823.
36. Fodor E, Devenish L, Engelhardt OG, Palese P, Brownlee GG, et al. (1999) Rescue of influenza A virus from recombinant DNA. J Virol 73: 9679–9682.
37. Caetano BC, Bruna-Romero O, Fux B, Mendes EA, Penido ML, et al. (2006) Vaccination with replication-deficient recombinant adenoviruses encoding the main surface antigens of toxoplasma gondii induces immune response and protection against infection in mice. Hum Gene Ther 17: 415–426.
38. Tzelepis F, de Alencar BC, Penido ML, Gazzinelli RT, Persechini PM, et al. (2006) Distinct kinetics of effector CD8+ cytotoxic T cells after infection with Trypanosoma cruzi in naive or vaccinated mice. Infect Immun 74: 2477–2481.
39. Liniger M, Zuniga A, Naim HY (2007) Use of viral vectors for the development of vaccines. Expert Rev Vaccines 6: 255–266.
40. Roffe E, Rothfuchs AG, Santiago HC, Marino AP, Ribeiro-Gomes FL, et al. (2012) IL-10 limits parasite burden and protects against fatal myocarditis in a mouse model of Trypanosoma cruzi infection. J Immunol 188: 649–660.
41. Goncalves da Costa SC, Calabrese KS, Zaverucha do Valle T, Lagrange PH (2002) Trypanosoma cruzi: infection patterns in intact and athymic mice of susceptible and resistant genotypes. Histol Histopathol 17: 837–844.
42. Dominguez MR, Silveira EL, de Vasconcelos JR, de Alencar BC, Machado AV, et al. (2011) Subdominant/cryptic CD8 T cell epitopes contribute to resistance against experimental infection with a human protozoan parasite. PLoS One 6: e22011.
43. Rosenberg CS, Martin DL, Tarleton RL (2010) CD8+ T cells specific for immunodominant trans-sialidase epitopes contribute to control of Trypanosoma cruzi infection but are not required for resistance. J Immunol 185: 560–568.
44. Schirmbeck R, Reimann J, Kochanek S, Kreppel F (2008) The immunogenicity of adenovirus vectors limits the multispecificity of CD8 T-cell responses to vector-encoded transgenic antigens. Mol Ther 16: 1609–1616.
45. Kastenmuller W, Gasteiger G, Gronau JH, Baier R, Ljapoci R, et al. (2007) Cross-competition of CD8+ T cells shapes the immunodominance hierarchy during boost vaccination. J Exp Med 204: 2187–2198.
46. Yewdell JW, Bennink JR (1999) Immunodominance in major histocompatibility complex class I-restricted T lymphocyte responses. Annu Rev Immunol 17: 51–88.
47. Gomez CE, Najera JL, Perdiguero B, Garcia-Arriaza J, Sorzano CO, et al. (2011) The HIV/AIDS vaccine candidate MVA-B administered as a single immunogen in humans triggers robust, polyfunctional, and selective effector memory T cell responses to HIV-1 antigens. J Virol 85: 11468–11478.
48. Tan AC, Eriksson EM, Kedzierska K, Deliyannis G, Valkenburg SA, et al. (2012) Polyfunctional CD8(+) T cells are associated with the vaccination-induced control of a novel recombinant influenza virus expressing an HCV epitope. Antiviral Res 94: 168–178.
49. Rodriguez D, Gonzalez-Aseguinolaza G, Rodriguez JR, Vijayan A, Gherardi M, et al. (2012) Vaccine efficacy against malaria by the combination of porcine parvovirus-like particles and vaccinia virus vectors expressing CS of Plasmodium. PLoS One 7: e34445.
50. Elvang T, Christensen JP, Billeskov R, Thi Kim Thanh Hoang T, Holst P, et al. (2009) CD4 and CD8 T cell responses to the M. tuberculosis Ag85B-TB10.4

promoted by adjuvanted subunit, adenovector or heterologous prime boost vaccination. PLoS One 4: e5139.

51. Vasconcelos JR, Dominguez MR, Araujo AF, Ersching J, Tararam CA, et al. (2012) Relevance of long-lived CD8(+) T effector memory cells for protective immunity elicited by heterologous prime-boost vaccination. Front Immunol 3: 358.
52. Michailowsky V, Silva NM, Rocha CD, Vieira LQ, Lannes-Vieira J, et al. (2001) Pivotal role of interleukin-12 and interferon-gamma axis in controlling tissue parasitism and inflammation in the heart and central nervous system during Trypanosoma cruzi infection. Am J Pathol 159: 1723–1733.
53. Rodrigues AA, Saosa JS, da Silva GK, Martins FA, da Silva AA, et al. (2012) IFN-gamma plays a unique role in protection against low virulent Trypanosoma cruzi strain. PLoS Negl Trop Dis 6: e1598.
54. Takayama E, Ono T, Carnero E, Umemoto S, Yamaguchi Y, et al. (2010) Quantitative and qualitative features of heterologous virus-vector-induced antigen-specific CD8+ T cells against Trypanosoma cruzi infection. Int J Parasitol 40: 1549–1561.
55. Marinho CR, Nunez-Apaza LN, Martins-Santos R, Bastos KR, Bombeiro AL, et al. (2007) IFN-gamma, but not nitric oxide or specific IgG, is essential for the in vivo control of low-virulence Sylvio X10/4 Trypanosoma cruzi parasites. Scand J Immunol 66: 297–308.
56. Dominguez MR, Ersching J, Lemos R, Machado AV, Bruna-Romero O, et al. (2012) Re-circulation of lymphocytes mediated by sphingosine-1-phosphate receptor-1 contributes to resistance against experimental infection with the protozoan parasite Trypanosoma cruzi. Vaccine 30: 2882–2891.
57. Silverio JC, Pereira IR, Cipitelli Mda C, Vinagre NF, Rodrigues MM, et al. (2012) CD8+ T-cells expressing interferon gamma or perforin play antagonistic roles in heart injury in experimental Trypanosoma cruzi-elicited cardiomyopathy. PLoS Pathog 8: e1002645.
58. Silverio JC, de-Oliveira-Pinto LM, da Silva AA, de Oliveira GM, Lannes-Vieira J (2009) Perforin-expressing cytotoxic cells contribute to chronic cardiomyopathy in Trypanosoma cruzi infection. Int J Exp Pathol 91: 72–86.
59. Vasconcelos JR, Bruna-Romero O, Araujo AF, Dominguez MR, Ersching J, et al. (2012) Pathogen-induced proapoptotic phenotype and high CD95 (Fas) expression accompany a suboptimal CD8+ T-cell response: reversal by adenoviral vaccine. PLoS Pathog 8: e1002699.
60. Hamada H, Bassity E, Flies A, Strutt TM, Garcia-Hernandez Mde L, et al. (2013) Multiple redundant effector mechanisms of CD8+ T cells protect against influenza infection. J Immunol 190: 296–306.

Carbon nanotubes-based vaccine induces superior $CD8^+$ T cell response and immunoprotective effect for cancer

Paula Cristina Batista de Faria[1,2], Luara Isabela dos Santos[1,3], João Paulo Coelho[4], Sara Daniela da Costa[5], Marcos Assunção Pimenta[5], Luiz Orlando Ladeira[5], Dawidson Assis Gomes[3], Clascídia Aparecida Furtado[4], Ricardo Tostes Gazzinelli[1,3,6*].

1 - Instituto René Rachou, Fundação Oswaldo Cruz, 30190-002 Belo Horizonte, MG, Brazil; 2 - Instituto de Genética e Bioquímica, Universidade Federal d Uberlândia, 38400-902 Uberlândia, MG, Brazil; 3 - Departamento de Bioquímica e Imunologia, Universidade Federal de Minas Gerais, 31270-001 Belo Horizonte, MG, Brazil; 4 - Centro de Desenvolvimento da Tecnologia Nuclear, CDTN/CNEN, 31270-001 Belo Horizonte, MG, Brazil, 5 - Departamento de Física, Universidade Federal de Minas Gerais, 31270-001 Belo Horizonte, MG, Brazil; 6 - Division of Infectious Diseases and Immunology, University of Massachusetts Medical School, Worcester 01605, MA, USA.

Corresponding author

* Correspondence to: Ricardo Tostes Gazzinelli. Instituto René Rachou, Fundação Oswaldo Cruz, Av. Augusto de Lima, 1715, 30190-002 Belo Horizonte, MG, Brazil. Tel: (0055) (31) 3349-7774 Fax: (0055) (31)3295-3115. e-mail: ritoga@cpqrr.fiocruz.br

Abstract

Properties like high interfacial area with cellular membranes, unique ability to incorporate multiple functionalization as well as compatibility and transport in biological fluids make carbon nanotubes (CNTs) useful for a variety of therapeutic and drug-delivery applications. Here we used a totally synthetic hybrid supramolecule as an anti-cancer vaccine. This complex structure comprises CNTs as delivery system for the Cancer Testis Antigen named NY-ESO-1, allied to a synthetic Toll-Like Receptor agonist. The CNT constructs were rapidly internalized into dendritic cells, both *in vitro* and *in vivo*, and served as an intracellular antigen depot. This property favored the induction of a strong $CD4^+$ T as well as $CD8^+$ T cell-mediated immune responses against the NY-ESO-1. Importantly, the vaccination significantly delayed the tumor

development and prolonged the mice survival, highlighting the potential application of CNTs as a vaccine delivery system to provide superior immunogenicity and strong protection against cancer.

Introduction

The peculiar sizes and shapes of nanoparticles endow them with properties that can be very useful in biomedical applications. Nanomedicine has been explored, to overcome some limitations of the approaches currently used, in order to optimize the delivery of antigens and increase the efficacy of vaccines towards a more selective and effective way[1,2].

Carbon nanotubes (CNTs) are of particular interest for vaccine development, as they are not immunogenic and as delivery vector should induce strong and long-lasting antigen-specific humoral and cellular immune responses[3,4]. Among their intrinsic properties these nanosized particles have the ability to interact to or cross biological membranes and deliver biomolecules into the cytoplasm[1]. In addition, the characteristic of extremely high surface area to volume ratio confers to CNTs the capacity to provide multiple attachment sites for various bioactive molecules such as peptides[3-5], proteins[6-7], nucleic acids[8-11] and drugs[12-14], and therefore to generate hybrid supramolecules of high specificity and selective biological function. Moreover, CNTs can protect the attached molecules against enzymatic degradation[15] resulting in a superior intracellular biostability and providing a depot effect[3,16], allowing enough time for migration and boost lymphocytes and consequently to induce a long-lasting immune response.

Optimally designed cancer vaccines should combine the best tumor antigens with the most effective immunotherapy agents and/or delivery strategies to achieve positive clinical results[17]. Currently, vaccine formulations against experimental tumors and other diseases have already been tested, combining protein antigens with Toll-Like Receptor (TLR) agonists, which act as immunological adjuvants. This strategy enhances the ability to activate dendritic cells (DCs), favoring antigen cross-presentation and then the development of a strong CD8+ T cells and Th1 lymphocyte-mediated immunity[18,19]. Due to restricted expression in normal tissues, cancer testis (CT) antigens represent particularly interesting candidates for immunotherapy of cancer[20]. NY-ESO-1 is a CT antigen that is expressed in a variety of human cancers including melanoma, breast, lung, prostate tumors, and others[21-23] being highly immunogenic and able to induce T-cell mediated immunity [24,25]. Consistently, immunotherapy has shown promise in

several early-phase clinical trials involving NY-ESO-1-expressing tumors in humans[26-28].

Here we report that both prophylactic and therapeutic strategies are highly effective when employing CNTs as delivery system for an anti-cancer vaccine. This anti-tumor vaccine was composed of NY-ESO-1 as antigen, and CpG oligonucleotides (CpG-ODNs), a TLR9 agonist, as immunological adjuvants, both attached non-covalently to oxidized multi-walled CNTs (MWCNTs). Our findings showed that the MWCNT constructs were rapidly internalized into DCs within and were highly efficient in inducing both humoral as well as $CD4^+$ T and $CD8^+$ T cell responses that effectively controlled melanoma growth in antigen-specific manner.

Noncovalent immobilization of biomolecules on the CNT surface

The surface chemistry and size of carbon nanotubes play critical roles in enhancing their compatibility with the biological medium, changing their toxicity and regulating their interactions with cells and biological molecules. Oxidation in nitric acid is known to produce shortened CNTs containing oxygenated groups along the sidewalls and extremities of the tubes[29-31]. These functional groups provide hydrophilicity to the tubes allowing the preparation of stable dispersions in water, buffer solutions and culture media. As shown in Fig. 1a, this was the first step of our approach to link immunogenic proteins and the TLR9 agonist to MWCTNs surface. Purified MWCNTs (purity of 95 wt%) were oxidized by acid treatment and dispersed in water by tip sonication at a concentration of 0.25 $mg.mL^{-1}$. After the oxidation/dispersion process, we obtained a stable aqueous dispersion of shortened MWCNTs functionalized with similar amount of carboxylic acids and phenols distributed at the ends and walls of the tubes. The nanotube lengths up to 1 μm were statistically measured in transmission electron microscopy (TEM) images. This finding was in good correlation with sizes calculated from dynamic light scattering measurements. The purity, morphology and good structural quality of the oxidized MWCNTs are illustrated in Supplementary Fig. S1.

The simple mixing of oxidized CNTs with protein solutions has led to nonspecific binding of proteins to CNTs[7]. Here, the protein antigens and CpG-ODNs were solubilized in the oxidized MWCNT dispersion, forming a MWCNT-antigen-CpG complex highly soluble and stable in aqueous solution. Interestingly, Fig. 1b shows however that the biological molecules seem to not compete for the same binding sites

on the nanotube surface. TEM analysis of oxidized MWCNT dispersions containing only the model protein antigen, ovalbumin (OVA) (Fig. 1b – left panel), or CpG-ODNs (Fig. 1b – right panel) illustrate that the protein interacts preferentially with the nanotube ends and the CpG-ODNs attach rather to the nanotube wall. While the entanglement and size of OVA and NY-ESO-1 macromolecules favor an electrostatic interaction between positively charged domains on proteins and the edges with high density of acid oxygenated groups, the finite size of the single-strand CpG-ODNs also facilitate π-stacking interaction with the nanotube surface not fully oxidized[32]. This non-competition encouraged us to perform the attachments simultaneously, which significantly simplified the process.

The maintenance of the structural integrity of the biological molecules after interaction with MWCNTs was evidenced by Raman spectroscopy. This technique is a fundamental tool to understand the electronic, optical and vibrational properties of carbon nanotubes[33], and also comprehend the secondary structure of proteins[34]. Figure 1c and 1d show the Raman spectra for MWCNT (left), OVA (middle), MWCNT-OVA (right), and MWCNT (left), CpG (middle) and MWCNT-CpG (right), respectively. The spectra in Fig. 1c were obtained using an excitation wavelength of 441.6 nm (2.81 eV). The characteristic D (1364 cm^{-1}), G (1581 cm^{-1}) and D' (1613 cm^{-1}) bands were observed for the oxidized MWCNT[33]. The rich spectrum of OVA protein shows the following bands: amide III for β-turn (1246, 1293 cm^{-1}) and α-helix (1340 cm^{-1}), amide S (C_α-H) (1392 cm^{-1}), C-H bending (1451 cm^{-1}), -NCH_3 bending (1471 cm^{-1}), amide II (1555 cm^{-1}), aromatic ring stretching (1606 cm^{-1}) and amide I for α-helix (1648 cm^{-1}), β-turn (1659 cm^{-1}) and β-sheet (1674 cm^{-1})[35]. Even though the higher intensity of the nanotube bands excited at 441.6 nm dominates the spectrum of MWCNT-OVA sample, we could further observe bands of the biomolecule, C-H bending (1455 cm^{-1}), amide II (1555 cm^{-1}) and aromatic ring stretching (1598 cm^{-1}), indicating the structural integrity of the protein after interaction with MWCNT. The Raman spectra in Fig. 1d were obtained using an excitation wavelength of 632.8 nm (1.96 eV). D, G and D' bands of the oxidized MWCNT were observed at 1336, 1589 and 1623 cm^{-1}, respectively. CpG shows also a very rich Raman spectrum where the bands are related to the backbone structure and vibrational modes of cytosine (C), guanine (G) and thymine (T) bases: rings deformation and breathing are observed below 750 cm^{-1}; 750-900 cm^{-1} range shows O-P-O stretching; bands in the 1200-1300 cm^{-1} range are sensitive to cytidine, guanosine and thymidine conformation; 1300-1400 cm^{-1} range shows namely ribose-

ring puckering state; and N-H and C-H bending and C-N, C=C and C=O stretching modes are observed between 1400 and 1650 cm^{-1} [36]. These bands are maintained in the MWCNT-CpG spectrum in addition to the oxidized nanotube bands.

Only a slightly displacement in frequency of 2 cm^{-1} was observed for G band in the MWCNT-OVA and MWCNT-CpG spectra, showing that there is no significant charge transfer between the nanotubes and the biomolecules. This result suggests that the noncovalent attachment of the molecules to the oxidized MWCNTs occurs mainly between the hydrophilic groups of the proteins and the functional groups on the nanotube surface, in agreement with previous observations[7]. This behavior was somehow expected, since proteins and DNA segments usually hide hydrophobic groups and exposes hydrophilic groups aiming at solubility in water. Most importantly, our observations indicate that the noncovalent attachment ensured the integrity of nanoparticles as well as biological molecules structures and hence intrinsic physicochemical properties that are primordial to biomedical applications[2].

Delivery of MWCNT-peptide complex into DCs

We examined cellular uptake of oxidized MWCNT alone and conjugated with FITC-labeled OVA-derived K^b-SIINFEKL 257-264 peptide (OTI). Fig. 2a shows confocal fluorescence microscopy images of phagocytic DCs after treatment with 20 $\mu g.mL^{-1}$ of MWCNT or MWCNT- OTI-FITC conjugates, for 24 h at 37 °C. The presence of MWCNT in the cytoplasm, mainly distributed in the perinuclear region of DCs, shows the phagocytic ability and the functional viability of these cells, as previously reported for same sized single-walled CNTs[3]. We could observe evident co-localization between the nanotubes and the fluorescent peptides, confirming the efficacy of the attachment. Moreover, we observed a significant enhancement of the fluorescence inside the cells loaded with MWCNT-OTI complex, when compared to those with the peptide alone (Supplementary Fig. S2a).

Although the mechanism for the internalization of CNTs into cells has not been fully established (endocytic or needle like penetration), it is generally recognized that CNTs are able to enter various biological membrane barriers[1], but largely depends on their length and surface chemistry[37,38]. Live-cell confocal microscopic images showed that the majority of FITC fluorescence is co-localized with the endo-lysosomal compartment marker, indicating that antigen-nanoparticle complexes were internalized through endocytosis (Fig. 2a). This is consistent with reported observations that confirm

that well-dispersed carbon nanotubes transporting proteins or oligonucleotides are internalized into living cells via energy-dependent endocytosis[7,38]. These findings strengthen the idea that the attachment of antigens onto carbon nanotubes surface greatly enhances the delivery of antigens to a degradative perinuclear region into the cytosol, leading to improved antigen presentation in competent cross-presenting cells[3,39].

Flow cytometry analyses on treated live cells are consistent with the confocal microscopic observations. Internalization could be observed through an increase in side-scatter intensity with MWCNT-OTI-FITC complex confirming that peptide was taken up by DCs much more efficiently when attached to the nanotubes (Fig. 2b). We also observed that in the secondary lymphoid tissues, dendritic cells were the main source of intracellular MWCNTs constructs at one hour (inguinal lymph nodes) and 3 days (spleen) post subcutaneous injection (Fig. 2c). Thus, we conclude that after uptake of MWCNT-antigen complex, dendritic cells followed by macrophages (but not NK, B- or T-cells) drained into secondary lymphoid tissue[40] permitting premature antigen presentation[41] and then activating resting T cells (Supplementary Fig. S3).

To assess the DCs viability exposed to functionalized MWCNTs, MTT assay was performed, to evaluate the metabolization of MTT tetrazolium salt by mitochondrial enzymes[42]. Each group was cultured in triplicates and then DCs were incubated with different amounts of oxidized MWCNTs (5, 10, 20 and 50 $\mu g.mL^{-1}$) and we observed no significant changes in viability up to 20 $\mu g.mL^{-1}$ (Supplementary Fig. S2b). Therefore, we adopt this concentration for all subsequent assays. This minimal toxic effect observed with the treated nanotubes was not unexpected since acid treatment removes the metal catalyst, which should substantially reduce the potential cytotoxic effect of the CNTs[39,43]. The reduced length and high solubility of MWCNTs in aqueous solution acquired after functionalization process also could play a relevant role in enhancing cytocompatibility[14]. Furthermore, we used a standardized protocol for sample preparation, which allowed the manufacturing of CNTs with a high purity grade. The capacity to induce acute toxicity or oxidative stress of high concentrations of impurities like metals or amorphous carbon is well-known[44].

B- and T-cell-mediated immunity induced by CNT constructs

Having shown that MWCNTs constructs could be internalized by dendritic cells without affecting cellular viability, we next examined the capability of DCs loaded with

MWCNTs complexes to stimulate OVA-specific T cells *in vitro*. Fig. 3a shows the CFSE profiles of CFSE-labeled ovalbumin (OVA)-specific $CD4^+$ and $CD8^+$ T-cells after 4 days culture with dendritic cells loaded with MWCNTs, OVA or MWCNT-OVA conjugated. As controls, T cells cultured with no stimulation shows the CFSE intensity of non-divided cells. We detected a robust proliferative response for both $CD4^+$ and $CD8^+$ in MWCNTs-OVA stimulated cultures compared with the controls, as determined by protein uptake and efficient *in vitro* cross-presentation of OVA facilitated by MWCNT-based antigen delivery. In the nanotubes-antigen treated cultures, populations of CFSE-low $CD3^+$ lymphocytes emerged, which represented 32.5 and 29.7% for $CD4^+$ and $CD8^+$ of the cells in culture, respectively. The results showed that even if the DCs function was preserved, as demonstrated by cytotoxicity assay, the specific T-cell proliferation was minimal in the cells loaded with only MWCNT (7.68% for $CD4^+$ and 5.87% for $CD8^+$ T-cells) or OVA (11.9% for $CD4^+$ and 9.03% for $CD8^+$ T-cells) alone (Fig. 3a). Consistent with our *in vitro* results, MWCNT complexes were also capable of enhancing $CD4^+$ and $CD8^+$ T-cell proliferation in the peripheral circulation and splenic tissue of immunized mice[45]. These findings indicated that our nanoparticle-based formulation becomes particularly suitable for a vaccination purpose by providing a multiple signals necessary for both $CD4^+$ T as well as $CD8^+$ T-cell expansion through APC activation[46].

We further tested the extent to which the internalized MWCNTs conjugated with ovalbumin could induce an antigen-specific immune response *in vivo* (Fig. 3b,c). BALB/c mice were submitted to a protocol of three equivalent immunizations, within an interval of 15 days. These immunizations were performed by the administration of 100 μL of the vaccine formulation, subcutaneously. For each dose, 10 μg of the immunogenic protein with addition or not of 18 μg of CpG oligonucleotides (B-class-297 TCCTCGTTTTGACGTG)[47] were added to 20 μg of oxidized MWCNT in aqueous dispersion. The kinetics for both protein binding and synthetic adjuvant hybridization was accelerated by continuous sonication for 30 min[48].

To characterize T-cell responses from immunized mice we examined their production of IFN-γ, a central cytokine that orchestrates T-cell mediated immunity against tumor cells. Splenocytes were stimulated *in vitro* with OVA-derived peptides that encode epitopes recognized by either $CD4^+$ or $CD8^+$ T lymphocytes. Our data demonstrated that immunization of mice with the model antigen (ovalbumin) adsorbed onto MWCNTs causes priming of T cell activation to a greater extent than

immunization with OVA adsorbed onto alum, which is widely used as an adjuvant (Fig. 3c). As control, the protein alone did not show such response, indicating the good carrier ability of MWCNTs *in vivo*. As expected, we noted that the antigen immunogenicity was greatly enhanced when allied to the combined delivery of synthetic CpG oligonucleotide. The group immunized with MWCNT-OVA-CpG complexes was more effective at generating OVA specific, IFN-γ-producing $CD4^+$ and $CD8^+$ T-cells (Fig. 3c). It is well known that TLR9, a potent inducer of both innate and adaptive immune responses, is located intracellularly[49]. Thereby, we assume that MWCNTs play a pivotal role in improving the immunostimulatory signal of CpG molecules by enhancing CpG oligonucleotides internalization by APCs[8,50].

To determine whether the nanoparticles complexes could also induce specific anti-OVA antibody production, we measured antibody titers in serum 21 days after the last immunization. We found that the immunization with the complete formulation containing OVA and CpG molecules, both adsorbed onto MWCNTs surfaces, substantially enhanced OVA-specific IgG antibody titers (Fig. 3b). Taking together, our findings suggest that the larger amount of MWCNT-delivered CpG, was able to trigger an strong intracellular signaling leading to the activation of the dendritic cells and B cells, and the production of cytokines, chemokines, and immunoglobulins. Subsequently, cytokines produced by DCs, such as IL-12 (Supplementary Fig. 4), induced the differentiation of naive T cells into T helper 1 (Th1), as seen by the higher INF-γ secretion, as well as $CD8^+$ T-cells.

MWCNT-NY-ESO-1 conjugates induce antigen-specific immunity and tumor inhibition in mice

After confirming the potential activity of the MWCNTs-based formulation *in vivo*, they were tested in another system, aiming at their use as an antitumor vaccine. C57BL/6 mice were immunized with the new formulation, containing the same proportions of nanoparticle, antigen and adjuvant as in immunizations with OVA. We used in this experiment two immunization doses 21 days apart. Our results demonstrate that formulations containing MWCNTs were more effective in stimulating the host immune system to mount an integrated humoral and cellular responses to NY-ESO-1 antigen (Fig. 4a,b). We could also confirm the effective antigen specificity on the response of the $CD8^+$ T lymphocytes to the tumor cells by evaluating the double positive CD8 and NY-ESO-1 tetramer T-cells (Fig. 4c). The increase in T-cell

responses resulted in a greater protection and prolonged survival of mice challenged with a syngeneic transgenic melanoma, the B16F10 cell line expressing NY-ESO-1, as compared with the formulations using the recombinant protein and CpG oligonucleotides adsorbed onto alum (Fig. 4d,e).

We also tested the ability of all nanoformulations in a therapeutic protocol to reverse/delay tumor growth in B16-NY-ESO-1-bearing mice. Mice were challenged with melanoma cell line, and 3 and 10 days later injected subcutaneously with MWCNT-based formulations. Nanotube-complexes vaccination induced both $CD4^+$ T as well as $CD8^+$ T lymphocytes to produce IFN-γ after restimulation with recombinant NY-ESO-1 or NY-ESO-1 specific peptides (Fig. 5a). The latter results were confirmed by the increased frequency of $CD8^+$ T lymphocytes, which reacted with the NY-ESO-1 tetramer. Furthermore, we found that the nanotubes-based treatment was capable of induce spreading to other melanoma antigens beyond NY-ESO-1, as can be seen by the frequency of gp100 $tetramer^+$ cytolytic T-cells (Fig. 5b). We also report a delay in tumor growth and survival rate in mice treated with MWCNTs-NY-ESO-1-CpG formulation (Fig. 5c and 5d).

We found very similar results with CT26, a colon carcinoma cell line expressing NY-ESO-1. Our formulation containing MWCNTs, both inhibited and delayed tumor growth in prophylactic and therapeutic protocols, respectively (Supplementary Fig. S5).

Conclusions

In this study, we report the effectiveness of a fully synthetic supramolecule that allied the advantage of the MWCNTs, as a vector in biology systems associated with a recombinant antigen and synthetic adjuvant, to efficiently target APCs and to induce strong $CD8^+$ T cell mediated immunity. Facing the difficulties of finding an effective way to counterattack different cancer cells, our nanocomplex represents an important tool for *in vivo* intracellular dispensation and activation, even for more than one antigen simultaneously. This strategy could be applied in diverse cross-presentation pathway-related protocols that need both humoral- and cell-mediated immune responses. The relative simplicity and low coast of fabrication of MWCNTs can indeed offer a highly attractive and promising alternative for prophylactic and therapeutic vaccines for cancer and infectious diseases.

Methods

Synthesis and oxidation of multi-walled carbon nanotubes

MWCNT was grown by chemical vapor deposition (CVD) at a growth temperature of 700 to 900ºC, using ethylene as carbon precursor gas, and argon as carrying gas. The pyrolysis process was catalyzed by cobalt and iron oxide nanoparticles anchored to a magnesium oxide matrix. Residual amorphous carbon, metallic nanoparticles and ceramic matrix were initially removed by thermal oxidation and thereafter digestion in hydrochloric acid. An additional oxidative treatment was performed in sulfuric and nitric acid, under microwave-assisted reflux, aiming at the functionalization of the tube extremities and walls with acidic oxygenated groups. The oxidized MWCNT sample was exhaustively base washed with a pH 11 NaOH solution to remove carboxylated carbon (CC) impurities that might have adsorbed onto the nanotube surface during the oxidation process. Then, it was dispersed in MiliQ water at a concentration of 0.25 $mg.mL^{-1}$, after 60 min of direct tip sonication. At the end of this process, an aqueous dispersion of multi-walled carbon nanotubes functionalized with similar amount of carboxylic acids and phenols (by acid base potentiometric titration), mostly up to 1 μm in length and with average diameter of 10-40 nm (by TEM) and approximate purity of 95% in mass (by thermogravimetry) was obtained.

Raman spectroscopy and transmission electron microscopy

Micro-Raman measurements were performed under ambient conditions using a back-scattering geometry. The spectra were recorded on a Horiba T64000 triple monochromator spectrometer, using laser excitation energy of 2.81 eV (λ = 441.6 nm, He/Cd laser) for MWCNT, OVA and MWCNT-OVA samples; and a Horiba Jobin Yvon iHR 550 Raman spectrometer, using laser excitation energy of 1.96 eV (λ = 632.8 nm, He/Ne laser) for MWCNT, CpG and MWCNT-CpG samples. The samples were focused with a 50x objective and the laser power was kept at around 2.0 mW. TEM images were obtained in Tecnai G2-12-SpiritBiotwin-120 KV and Tecnai G2-20-SpiritBiotwin-200 KV equipments. The samples were dropped on copper grids covered with holey carbon film, and dried at room temperature for 24 h.

Animals and immunizations

C57BL/6 and BALB/c mice were obtained from CEBIO (Federal University of Minas Gerais, Brazil). Six- to eight-week-old females, weight-matched, were used in the different experimental groups. Immunizations were performed by inoculating 100 μL of the vaccine formulation into the right flank of mice, subcutaneously. For each dose, 10 μg of the immunogenic protein (OVA or NY-ESO-1) with addition or not of 18 μg of CpG oligonucleotides (Alpha DNA) were added to 20 μg of oxidized MWCNT in aqueous dispersion. Positive controls were prepared with 10 μg of the immunogenic protein and 18 μg of CpG co-adsorbed in 30% (v/v) of alum Rehydragel L.V. solution (Reheis) for 1 hour at room temperature in a tube rotator. After incubation, saline solution was added to each sample to the final volume. Experiments for this study were approved by the Ethical Commission on Animals' Use (CETEA) at Federal University of Minas Gerais and performed following Institutional Guide for the Care and Use of Laboratory Animals.

Measurement of antibody and T cell responses

Vaccinated and control mice were bled from the retro-orbital plexus under ether anesthesia. Antigen-specific antibodies were measured in sera from immunized mice by enzyme-linked immunosorbent assay (ELISA). Secondary Ab, peroxidase-conjugated goat antimouse total Immunoglobulin G (IgG), IgG1, and IgG2a (BALB/c) or IgG2c (C57BL/6) (SouthernBiotech) were used and the reactions were detected with 3,39,5,59-tetramethylbenzidine reagent (Sigma-Aldrich). For IFN-γ production assays, splenocytes from vaccinated mice were prepared in complete RPMI supplemented with 100 $U.mL^{-1}$ rIL-2 (R&D Systems), plated at $5x10^6$ $cells.mL^{-1}$ and incubated at 37 ^0C and 5% CO_2 for 72 h in the presence or absence of epitopes derived from OVA or NY-ESO-1 proteins. IFN-γ concentrations were determined in cell culture supernatants with DuoSet ELISA (R&D Systems). For flow cytometry analysis, $CD8^+$ T cells were stained with anti-CD8mAb and MHC tetramers presenting specific epitope NY-ESO-1 or gp100 (LICR Tetramer Facility).

Flow cytometry analysis

Cells were processed and stained for surface molecules for 30 minutes at room temperature. The cells were washed and fixed in PBS with 2% paraformaldehyde. After incubation, cells were washed, permeabilized (Cytofix/Cytoperm, BD Biosciences), stained intracellular molecules for 30 minutes at 4 ^{0}C and then fixed in 200 μL of PBS with 2% paraformaldehyde. At least 200,000-gated events were acquired for analysis using LSR II with Diva (BD Biosciences). The antibodies used for staining were anti-CD3-APC-Cy7, anti-CD4-AlexaFlour700, anti-CD8-PE-Cy7, anti-CD3-APC-Cy7, anti-CD11c-AlexaFluor700, anti-MHCII-APC, anti-B220- PerCP-Cy5.5, anti-CD11b- PE-Cy7, anti- GR-PerCP-Cy5.5 and anti-DX5-APC (eBioscience). FlowJo (v8.8.6) and GraphPad Prism (v5.0b) were used for data analysis and graphic presentation.

Tumor challenge

B16-NY-ESO-1 melanoma and CT26-NY-ESO-1 colon carcinoma cell lines were grown at 37°C under 5% CO_2 in complete RPMI 1640 (Sigma) with 100 U.mL^{-1} penicillin and 100 μg.mL^{-1} streptomycin and supplemented with 10% heat inactivated fetal calf serum (FCS; GIBCO). The selection was performed with G418 (800 μg.mL^{-1}). To establish subcutaneous tumors, control and immunized mice were challenged with 5 × 10^4 B16-NY-ESO-1 or 10^6 CT26-NY-ESO-1 cells in 100 μL PBS subcutaneously injected into the right flank. Mice were followed up to 30 days for evaluation of tumor growth and survival was measured for 90 days.

Immunotherapy

C57BL/6 were challenged by subcutaneous injection with 5 × 10^4 NY-ESO-1–expressing B16F10 melanoma tumor cells, and BALB/c mice were challenged with 10^6 of CT26-NY-ESO-1. Mice were treated with two doses of each MWCNT-based formulations, the same used in prophylactic protocols given 7 days apart, starting at day 3 after challenge. The percentages of survival were measured for 90 days and tumor size was scored by measuring perpendicular diameters for 30 days.

Generation of dendritic cells (DCs).

Bone marrow was collected from tibias and femurs of female BALB/c mice, passed through a nylon mesh to remove small pieces of bone and debris, resuspended in complete medium (RPMI-1640 medium containing 10% fetal bovine serum, L-glutamine, penicillin/streptomycin and 20 ng.mL^{-1} mouse GM-CSF) and cultured in cell

culture dishes at an initial density of 2×10^6 cells in 20 mL/plate. On days 3 and 6 of incubation, fresh medium with GM-CSF was either added or replaced half of the culture medium. On day 9 of culture, most of the non adherent cells had acquired typical dendritic morphology, and these cells were used as the source of DC in subsequent experiments. For cellular viability assay, MWCNT-peptide uptake experiments and microscopy, immature DCs were seeded into multiwell plates or coverglass bottom microscopy dishes and assayed as described. To determine the cytokine profile of CpG-loaded DCs, immature differentiated cell cultures were incubated at 37 ^{0}C and 5% CO_2 for 24 h, with 18 μg.mL^{-1} of CpG ODNs coupled or not to different concentrations (10 or 20 μg.mL^{-1}) of MWCNT. LPS was used as positive control. IL-12 and IL-10 concentrations were determined in cell culture supernatants with DuoSet ELISA (R&D Systems).

Cell viability determination

The viability of DCs was measured by using MTT assay. Briefly, cells were seeded at a concentration of 5×10^5 cells in 24-well culture plate. After 24 h culture with different concentrations of MWCNT (0, 5, 10, 20 and 50 μg.mL^{-1}), 3-[4,5-dimethylthiazol-2-yl]-2,5-diphenyltetrazolium bromide (MTT, Sigma) was added at a concentration of 0.5 mg.mL^{-1}and incubated at 37°C in CO_2 incubator for 2 h. Viable DCs generate insoluble crystal, but DCs are floating and loosely attached on the surface of culture plates. So, 100 μL/well 10% SDS solution containing 0.01 N HCl was directly added into wells to avoid the potential loss of and dissolve the insoluble crystal generated by DCs. After 24 h, the absorbance of sample was measured at 570 nm by using microplate reader.

Confocal microscopy

Immature bone marrow-derived (day 9) dendritic cells were loaded for 18 h with the constructs (MWCNT alone, FITC-labeled OVA peptide only and with MWCNT-peptide complexes). For assessment of co-localization studies in live cells, ER-Tracker Blue-White DPX (100 nM, Life Technologies), LysoTracker Red (100 nM, Life Technologies), and AF633-Cholera toxin B (10 μg.ml^{-1}, Life Technologies) was added

for 30 min at 37°C. After incubation, the cells were rinsed off with a gentle PBS wash, the incubation buffer replaced, and observed using a Zeiss 5 Live confocal microscope equipped with 405nm laser diode, 488nm laser diode, diode-pumped solid-state laser 532nm and laser diode 635nm for confocal fluorescence microscopy using a 63X, 1.4 NA objective lens at 1–5 frames/s.

Migration of MWCNT-peptide complexes

A total of 10 μg of FITC-labeled OVA peptide adsorbed to 20 μg MWCNT were inoculated subcutaneously. After 1 hour, 20 hours and 3 days, the inguinal lymph nodes and spleen were harvested. The cells were processed and stained for the surface markers as described above. The presence of FITC-labeled constructs in macrophages ($CD11b^+$ $GR1^-$), dendritic cells ($CD11c^+$ $MHCII^{high}$), B lymphocytes ($B220^+$), NK cells ($DX5^+$)and T lymphocytes ($CD3^+$) was evaluated by flow cytometry.

Lymphocyte proliferation assay

In vitro cross-presentation of OVA was measured by a dye dilution assay of CFSE-labelled T cells. For splenic DC isolation, splenocytes from mice previous immunized with OVA were processed and the DC population enriched using EasySep CD11c positive selection (StemCell Technologies) according to the manufacturer's instructions. MWCNT (20 $\mu g.mL^{-1}$), OVA (10 $\mu g.mL^{-1}$) or MWCNT-OVA were incubated with 5×10^4 $CD11c^+$ cells for 24 h. $CD8^+$ T and $CD4^+$ T cells were isolated from total splenocytes using Dynabeads (Invitrogen Dynal, Oslo, Norway), and stained with 1.25 μM CFSE at $1x10^7$ cells/mL for 8 minutes. After incubation, DCs were washed three times, and co-incubated at 37˚C, 5% CO_2. After 5 days of culture, the cells were stained with the following antibodies: anti-CD3-APC-Cy7, anti-CD4-FITC, anti-CD8-PE-Cy7, anti-MHCII-APC, anti-CD11c-Alexa 700, as described above.

Statistics

Statistic significance for ELISA and cytokine staining assays were evaluated using One-Way ANOVA and non-parametric test followed by Bonferroni post-test. Statistic significance for tumor growth was evaluated by 2-way ANOVA with Bonferroni post-test.

References

1. Fabbro, C. *et al.* Targeting carbon nanotubes against cancer. *Chem. Commun.* **48,** 3911-3926 (2012).

2. Desai, N. Challenges in development of nanoparticle-based therapeutics. *AAPS J.* **14,** 282-95 (2012).

3. Villa, C. H. *et al.* Single-Walled Carbon Nanotubes Deliver Peptide Antigen into Dendritic Cells and Enhance IgG Responses to Tumor-Associated Antigens. *ACS Nano.* **5,** 5300-5311 (2011).

4. Pantarotto D. *et al.* Immunization with Peptide-Functionalized Carbon Nanotubes Enhances Virus-Specific Neutralizing Antibody Responses. *Chem. Biol.* **10,** 961-966 (2003).

5. Pantarotto, D. Briand, J. P. Prato & M. Bianco, A. Translocation of bioactive peptides across cell membranes by carbon nanotubes. *Chem Commun.* **7,** 16-17 (2004).

6. Han, Z. J. Ostrikov, K. K. Tan, C. M. Tay, B. K. & Peel, S. A. Effect of hydrophilicity of carbon nanotube arrays on the release rate and activity of recombinant human bone morphogenetic protein-2. *Nanotechnology*. **22,** 295712 (2011).

7. Kam, N. W. S. & Dai, H. Carbon nanotubes as intracellular protein transporters: generality and biological functionality. *J. Am. Chem. Soc.* **127,** 6021-6026 (2005).

8. Zhao, D. *et al.* Carbon nanotubes enhance CpG uptake and potentiate antiglioma immunity. *Clin. Cancer Res.* **17,** 771-782 (2011).

9. Pantarotto, D. *et al*. Functionalized carbon nanotubes for plasmid DNA gene delivery. *Angew. Chem. Int. Ed. Engl.* **43,** 5242–5246 (2004).

10. Santosh, M. Panigrahi, S. Bhattacharyya, D. Sood, A. K. & Maiti, P. K. Unzipping and binding of small interfering RNA with single walled carbon nanotube : a platform forsmall interfering RNA delivery. *J. Chem. Phys.* **136,** 065106 (2012).

11. Ladeira, M. S. *et al.* Highly efficient siRNA delivery system into human and murine cells using single-wall carbon nanotubes. *Nanotechnology*. **2,** 385101 (2010).

12. Liu, Z. *et al.* Drug delivery with carbon nanotubes for *in vivo* cancer treatment. *Cancer Res.* **68,** 6652-6660 (2008).

13. Wu, W. *et al.* Targeted delivery of amphotericin B to cells by using functionalized carbon nanotubes. *Angew. Chem. Int. Ed. Engl*. **44,** 6358-6362 (2005).

14. Bianco, A. Kostarelos, K. & Prato, M. Applications of carbon nanotubes in drug delivery. *Curr. Opin. Chem. Biol*. **9,** 674-679 (2005).

15. Wu, Y. Phillips, J. A. Liu, H. Yang, R. & Tan, W. Carbon nanotubes protect DNA strands during cellular delivery. *ACS Nano*. **2,** 2023-2028 (2008).

16. Zhao, D. *et al.* Carbon Nanotubes Enhance CpG Uptake and Potentiate Antiglioma Immunity. *Clin. Cancer Res.* **17,** 771-782 (2011).

17. Bolhassani, A. Safaiyan, S. & Rafati, S. Improvement of different vaccine delivery systems for cancer therapy. *Mol. Cancer.* **7,** 3 (2011).

18. Huleatt, J. W. *et al*. Vaccination with recombinant fusion proteins incorporating Toll-like receptor ligands induces rapid cellular and humoral immunity. *Vaccine*. **25,** 763–775 (2007).

19. Wille-Reece, U. *et al.* HIV Gag protein conjugated to a Toll-like receptor 7/8 agonist improves the magnitude and quality of Th1 and CD8+ T cell responses in nonhuman primates. *Proc. Natl. Acad. Sci. USA.* **102,** 5190-15194 (2005).

20. Chen, Y. T. *et al.* Multiple cancer/testis antigens are preferentially expressed in hormone-receptor negative and high-grade breast cancers. *PLoS One.* **6,** e17876 (2011).

21. Almeida, L. G. *et al.* CT database: a knowledge-base of high-throughput and curated data on cancer-testis antigens. *Nucleic Acids Res.* **37,** D816-819 (2009).

22. Jungbluth, A. A. *et al*. Immunohistochemical analysis of NY-ESO-1 antigen expression in normal and malignant human tissues. *Int. J. Cancer.* **92,** 856-860 (2001).

23. Chen, Y. T. *et al*. A testicular antigen aberrantly expressed in human cancers detected by autologous antibody screening. *Proc. Natl. Acad. Sci USA.* **94,** 1914-1918 (1997).

24. Hemminger, J. A. *et al*. The cancer-testis antigen NY-ESO-1 is highly expressed in myxoid and round cell subset of liposarcomas. *Mod. Pathol.* http://dx.doi.org/10.1038/modpathol.2012.133 (2012).

25. Jager, E. *et al*. Simultaneous humoral and cellular immune response against cancer-testis antigen NY-ESO-1: definition of human histocompatibility leukocyte antigen (HLA)-A2-binding peptide epitopes. *J. Exp. Med.* **187,** 265–270 (1998).

26. Kakimi, K. *et al*. A phase I study of vaccination with NY-ESO-1f peptide mixed with Picibanil OK-432 and Montanide ISA-51 in patients with cancers expressing the NY-ESO-1 antigen. *Int. J. Cancer*. **129,** 2836-2846 (2011).

27. Nicholaou, T. *et al*. Immunoediting and persistence of antigen-specific immunity in patients who have previously been vaccinated with NY-ESO-1 protein formulated in ISCOMATRIX. *Cancer Immunol. Immunother.* **60,** 1625-1637(2011).

28. Gnjatic, S. *et al*. NY-ESO-1 DNA vaccine induces T-cell responses that are suppressed by regulatory T cells. *Clin. Cancer Res.* **15,** 2130-2139 (2009).

29. Liu, J. *et al.* Fullerene pipes. *Science*. **280,** 1253-1256 (1998).

30. Hu, H. Zhao, B. Itkis, M. E.. & Haddon, R. C Nitric acid purification of single-walled carbon nanotubes. *J. Phys. Chem. B*. **107,**13838-13842 (2003).

31. Kim U. J. *et al.* Raman and IR spectroscopy of chemically processed single-walled carbon nanotubes *J. Am. Chem. Soc.* **127** 15437-15445.

32. Tu, X. & Zheng, M. A DNA-Based Approach to the Carbon Nanotube Sorting Problem. *Nano Res.* **1,** 185-194 (2008).

33. Baisuk, V. A. and Baisuk, E. V. Chemistry of carbon nanotubes cap 8 – Spectroscopy Characterization of Carbon Nanotubes (Califórnia / American Scientific Publishers), 141-174 (2008).

34. Spiro, T. G. & Gaber, B. P. Laser Raman scattering as a probe of protein structure. *Annu. Rev. Biochem*. **46,** 553-572 (1977).

35. Huang, C. Y. Balakrishnan, G. & Spiro, T. G. Protein secondary structure from deep-UV resonance Raman spectroscopy, *J. Raman Spectrosc.* **37,** 277-282 (2006).

36. Nishimura, Y. Tsuboi, M. Sato, T. & Aoki, K. Conformation-sensitiveRamanlines of mononucleotides and their use in a structure analysis of polynucleotides: guanine and cytosinenucleotides. *J. Mol. Struct.* **146,** 123-153 (1986).

37. Jain, S. Singh, S. R. & Pillai, S. Toxicity Issues Related to Biomedical Applications of Carbon Nanotubes. *J. Nanomed. Nanotechol*. **3,** 140 (2012).

38. Kam, N. W. Liu, Z. & Dai, H. Carbon nanotubes as intracellular transporters for proteins and DNA: an investigation of the uptake mechanism and pathway. *Angew. Chem. Int. Ed. Engl.* **45,** 577-581 (2006).

39. Porter, A. E. *et al.* Uptake of noncytotoxic acid-treated single-walled carbon nanotubes into the cytoplasm of human macrophage cells. *ACS Nano.* **3,** 1485-1492 (2009).

40. Randolph, G. J. Angeli, V. & Swartz, M. A. Dendritic-cell trafficking to lymph nodes through lymphatic vessels. *Nat. Rev. Immunol.* **5,** 617–628 (2005).

41. Pack, D. W. Timing is everything. *Nat. Mater.* **3,** 133-134 (2004).

42. Mosmann, T. Rapid colorimetric assay for cellular growth and survival: application to proliferation and cytotoxicity assays. *J. Immunol. Methods.* **65,** 55-63 (1983).

43. Dumortier, H. Functionalized carbon nanotubes are non-cytotoxic and preserve the functionality of primary immune cells. *Nano Lett.* **6,** 1522-1528 (2006).

44. Wörle-Knirsch, J. M. Pulskamp, K. & Krug, H. F. Oops they did it again! Carbon nanotubes hoax scientists in viability assays. *Nano Lett.* **6,** 1261-1268 (2006).

45. Mocan, T. & Iancu, C. Effective colon cancer prophylaxis in mice using embryonic stem cells and carbon nanotubes. *Int. J. Nanomedicine*. **6,** 1945–1954 (2011).

46. Reddy, S. T. *et al.* Exploiting lymphatic transport and complement activation in nanoparticle vaccines. *Nat. Biotechnol.* **25,** 1159-1164 (2007).

47. Junqueira, C. *et al*. Trypanosoma cruzi adjuvants potentiate T cell-mediated immunity induced by a NY-ESO-1 based antitumor vaccine. *PloS One*. **7,** e36245 (2012).

48. Yang, R. *et al.* Noncovalent assembly of carbon nanotubes and single-stranded DNA: an effective sensing platform for probing biomolecular interactions. *Anal. Chem.* **80,** 7408-7413 (2008).

49. McCluskie, M. J. Weeratna, R. D. & Davis, H. L. The potential of oligodeoxynucleotides as mucosal and parenteral adjuvants. *Vaccine.* **19,** 2657-2660 (2001).

50. Bianco, A. *et al*. Cationic carbon nanotubes bind to CpG oligodeoxynucleotides and enhance their immunostimulatory properties. *J. Am. Chem. Soc.* **127,** 58-59 (2005).

Acknowledgements

We thank Adelina Pinheiro Santos from Centro de Desenvolvimento da Tecnologia Nuclear and Cristiano Fantini from Federal University of Minas Gerais for scientific discussions and suggestions during the development of this work; Bruno Galvão Filho from Federal University of Minas Gerais for help with animal experiments; the LICR Tetramer Facility for tetramers synthesis; the LICR–Cornell University for the recombinant NY-ESO-1 protein; Dr. Jonathan Cebon from LICR–Melbourne for the B16-NY-ESO-1 cell line; and Dr. Hiroyoshi Nishikawa from Mie University Medical School for the CT26-NY-ESO-1cell line. This study was funded by Fundação de Amparo a Pesquisa de Minas Gerais (FAPEMIG), Fundação Oswaldo Cruz, the National Institute of Science and Technology for Vaccines/Conselho Nacional de Desenvolvimento Científico e Tecnológico (CNPq), the National Institute of Science and Technology for Carbon Nanomaterials/CNPq, and the Nanotoxicology Network (CNPq process number 552131/2011-3).

Author Contributions

P.C.B.F., M.A.P., L.O.L., C.A.F. and R.T.G. designed research; P.C.B.F., L.I.S., J.P.C., S.D.C. and D.A.G. performed research; L.O.L. and M.A.P. contributed new reagents/analytic tools; P.C.B.F., L.I.S., D.A.G and C.A.F. analyzed data; and P.C.B.F., C.A.F. and R.T.G. wrote the paper. All authors discussed the results and implications and commented on the manuscript.

Competing Financial Interests statement

The authors declare no competing financial interests.

Figure Legends

Figure 1 | Noncovalent immobilization of the biological entities on the oxidized multi-walled carbon nanotubes (MWCNTs). **a,** Schematic diagram showing the strategy for preparation of MWCNT-based delivery systems. **b**, transmission eletronic microscopy images evidencing the interaction between MWCNT and OVA (left) mainly in the edges of CNTs, and CpG molecules (right) along the walls of the nanotubes. Both images are representative of the whole sample. **c**, Raman spectra (1200 – 1800 cm^{-1}, λ = 441.6 nm) of oxidized MWCNT (left), OVA (middle) and MWCNT-OVA samples. **d**, Raman spectra (500 – 1750 cm^{-1}, λ = 632.8 nm) of oxidized MWCNT (left), CpG (middle) and MWCNT-CpG samples. The band at 970 cm^{-1} refers to the silicon substrate.

Figure 2 | Intracellular delivery of the multi-walled carbon nanotubes (MWCNTs) constructs into DCs. **a,** Live-cell confocal fluorescence microscopy images of untreated dendritic cells (DCs) (top), or loaded with FITC-labeled OVA peptide only (middle) and with MWCNT-peptide complexes (bottom). Intracelullar peptide (green), plasmatic membrane (pink), lysossomes (red) and endoplasmatic reticulum (blue) were stained. **b**, Optical intensities of randomly selected cells from each sample in **a**. Flow cytometric analysis of the internalization into DCs. DCs without antigen (shadow), and DCs pulsed with MWCNT only (black), peptide-FITC only (red) or MWCNT-peptide-FITC complexes. Error bars, standard errors of the mean. **c**, MWCNT-peptide-FITC were injected subcutaneously and the presence of intracellular constructs in dendritic cells at 1h (green), 20h (red) and 3 days (blue) post-injection were evaluated by flow cytometry.

Figure 3 | Carbon nanotubes increased the efficiency of cross-presentation of OVA *in vitro* and induced a specific immune response *in vivo*. **a,** *In vitro* mouse lymphocyte proliferation measured using CFSE labeling and flow cytometric analysis. (Left) CFSE-labeled pattern of control non-proliferating cells in culture without any stimulus. (Right) Both $CD4^+$ and $CD8^+$ T-cells proliferation and consequently cross-presentation of OVA was increased by conjugation with carbon nanotubes. Numbers presented in the two determined gates represent the percentage of cells in relation to the

total cell number. **b,c,** BALB/c mice were immunized with formulations containing OVA antigen and/or CpG oligonucleotides attached to carbon nanotubes or adsorbed onto alum. **b,** ELISA plates coated with OVA were used to quantify the levels of OVA-specific total IgG, IgG1, and IgG2a isotypes present in sera of control and immunized mice. **c,** Splenocytes from vaccinated were stimulated with T $CD4^+$- or T $CD8^+$-specific peptides or with OVA protein. IFN-g production was measured by ELISA at 72 h after stimulation. Error bars show standard error of the mean. Statistical analyses were performed using one-way ANOVA with Bonferroni post-test.

Figure 4 | Carbon nanotubes-based antitumor formulation induced strong humoral and cellular specific immune response and protected mice against tumor development. a,b, C57BL/6 mice were immunized with formulations containing the tumor-associated antigen NY-ESO-1 and/or CpG oligonucleotides non-covalently adsorbed to multi-walled carbon nanotubes or adsorbed onto alum. The specific antibody in sera of control and immunized mice (**a**) and IFN-γ production by splenocytes after stimulation with T $CD4^+$- or T $CD8^+$-specific peptides or with rNY-ESO-1 protein (**b**) was evaluated by ELISA. Vaccination with the antigen alone or mixed with alum did not induce such response. **c,** Splenocytes from immunized mice were stained with anti-CD3, anti-CD8 and NY-ESO-1 tetramers and analyzed by flow cytometry. Representative dot plots and a graph summarizing the percentage of double-positive cells are shown at right and left, respectively. **d,e,** Mice that received immunization with NY-ESO-1 were challenged with B16F10 transgenic melanoma expressing NY-ESO-1. Tumor growth (**d**) and survival (**e**) were monitored for 35 and 90 days, respectively. Error bars show standard errors of the mean.

Figure 5 | Therapeutic protocol using multi-walled carbon nanotubes (MWCNTs) delayed tumor growth expressing NY-ESO-1 and prolonged the survival in treated mouse. B16F10 -NY-ESO-1-bearing mice were treated with two doses of formulations containing or not CNTs given 7 days apart, starting at day 3 post-challenge. **a,** The cellular immune response induced by the therapeutic protocol was assessed 21 days after the last dose and the IFN-γ production by splenocytes was measured by ELISA at 72 h after re-stimulation. **b,** Before stimulation, the splenocytes were stained with anti-CD3, anti-CD8, and NY-ESO-1 or gp100 tetramers and analyzed by flow cytometry.

Representative dot blots and a graph summarizing the percentage of double-positive cells are shown at left and right, respectively. Tumor growth (**c**) and survival (**d**) were monitored for 30 and 90 days, respectively.

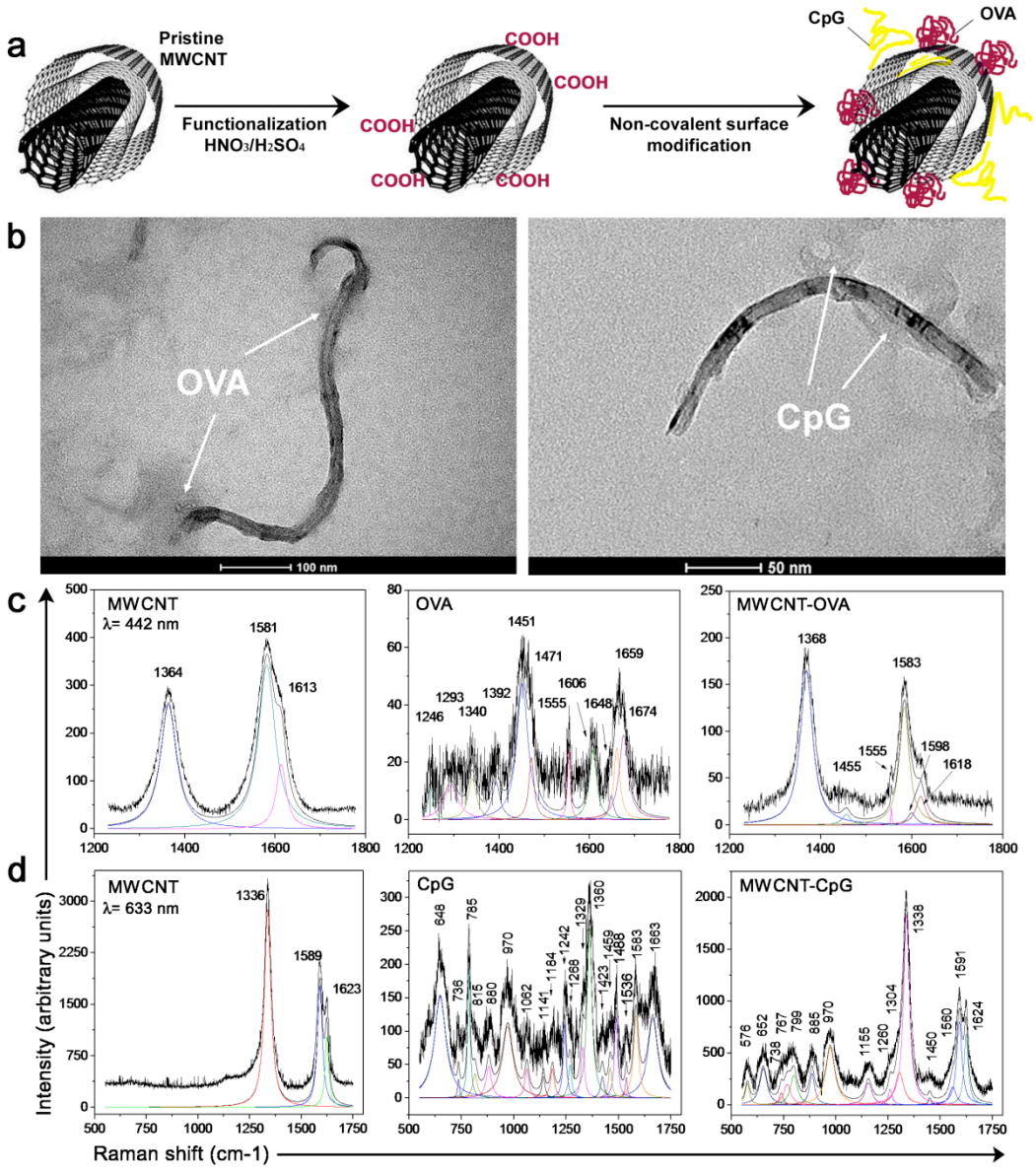
a
Pristine MWCNT
Functionalization HNO3/H2SO4
COOH
Non-covalent surface modification
CpG
OVA
b
OVA
100 nm
CpG
50 nm
c
MWCNT
λ= 442 nm
1364
1581
1613
OVA
1451
1471
1659
1606
1555
1648
1674
1293
1392
1246
1340
MWCNT-OVA
1368
1583
1555
1455
1598
1618
d
MWCNT
λ= 633 nm
1336
1589
1623
CpG
MWCNT-CpG
Intensity (arbitrary units)
Raman shift (cm-1)

Figure 1

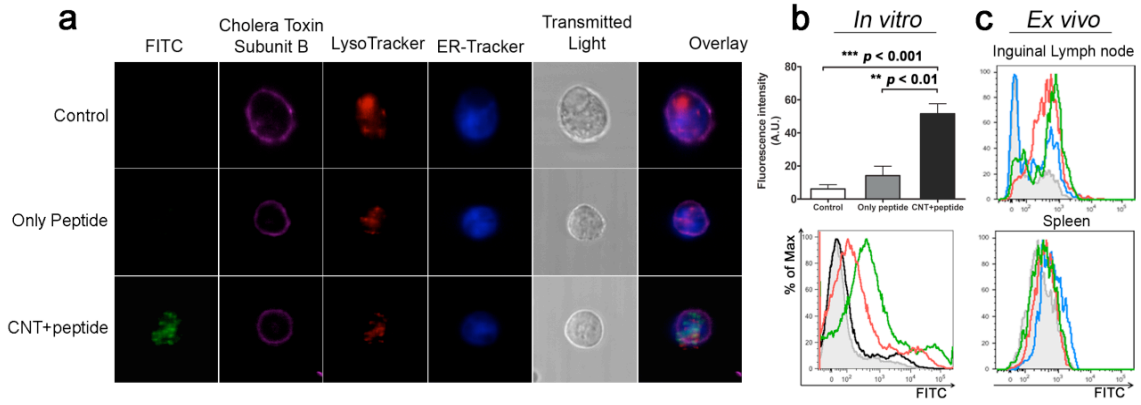

Figure 2

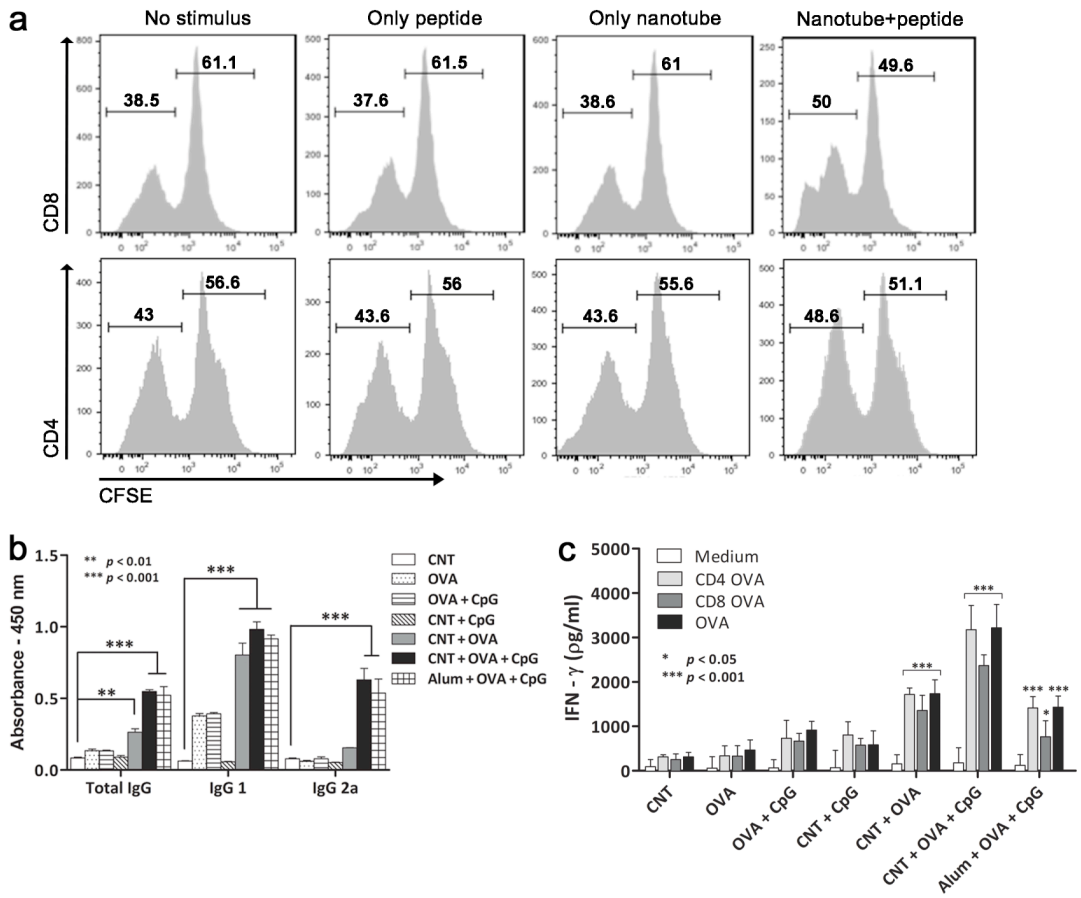

Figure 3

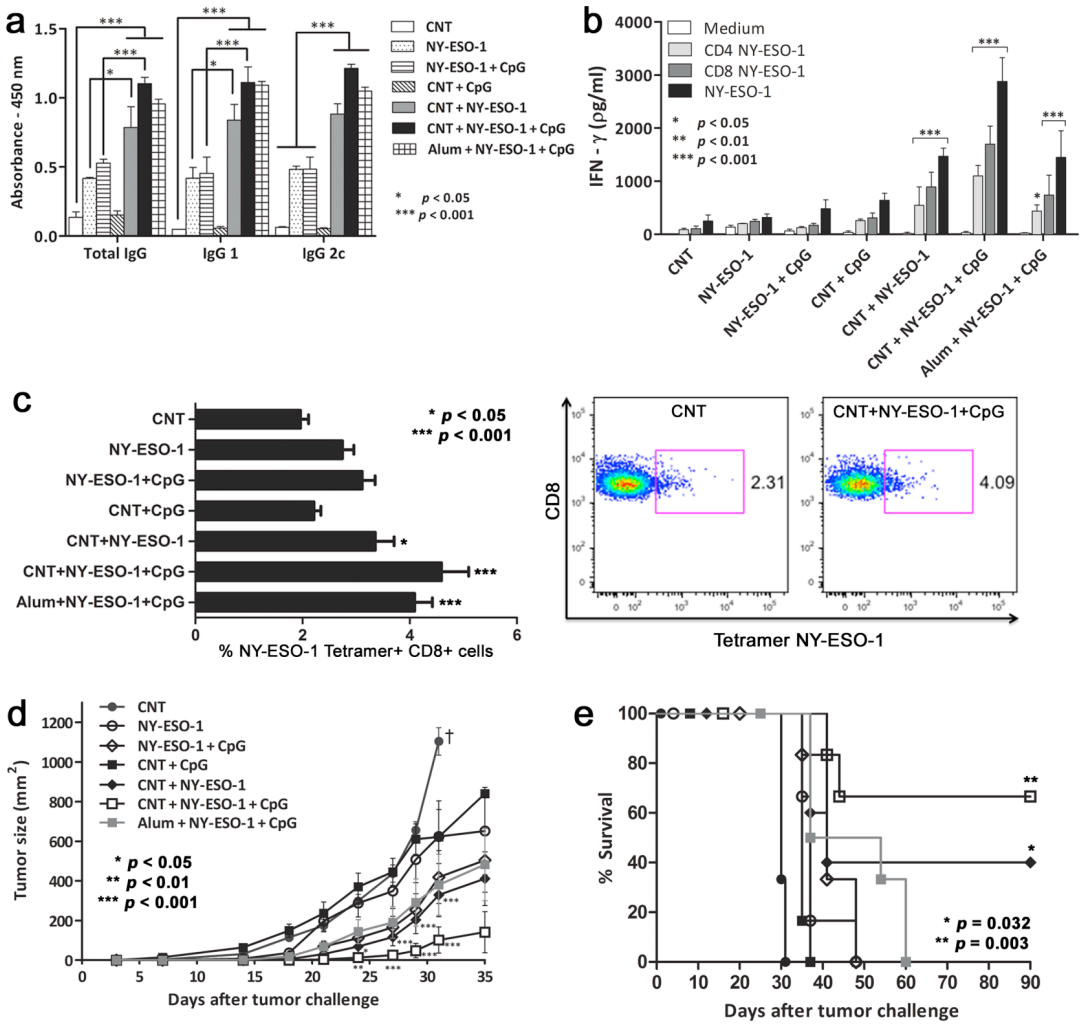
a
Absorbance - 450 nm
Total IgG
IgG 1
IgG 2c
CNT
NY-ESO-1
NY-ESO-1 + CpG
CNT + CpG
CNT + NY-ESO-1
CNT + NY-ESO-1 + CpG
Alum + NY-ESO-1 + CpG
* p < 0.05
*** p < 0.001
b
IFN - γ (pg/ml)
Medium
CD4 NY-ESO-1
CD8 NY-ESO-1
NY-ESO-1
* p < 0.05
** p < 0.01
*** p < 0.001
c
CNT
NY-ESO-1
NY-ESO-1+CpG
CNT+CpG
CNT+NY-ESO-1
CNT+NY-ESO-1+CpG
Alum+NY-ESO-1+CpG
* p < 0.05
*** p < 0.001
% NY-ESO-1 Tetramer+ CD8+ cells
CD8
Tetramer NY-ESO-1
2.31
4.09
d
Tumor size (mm²)
Days after tumor challenge
* p < 0.05
** p < 0.01
*** p < 0.001
e
% Survival
Days after tumor challenge
* p = 0.032
** p = 0.003

Figure 4

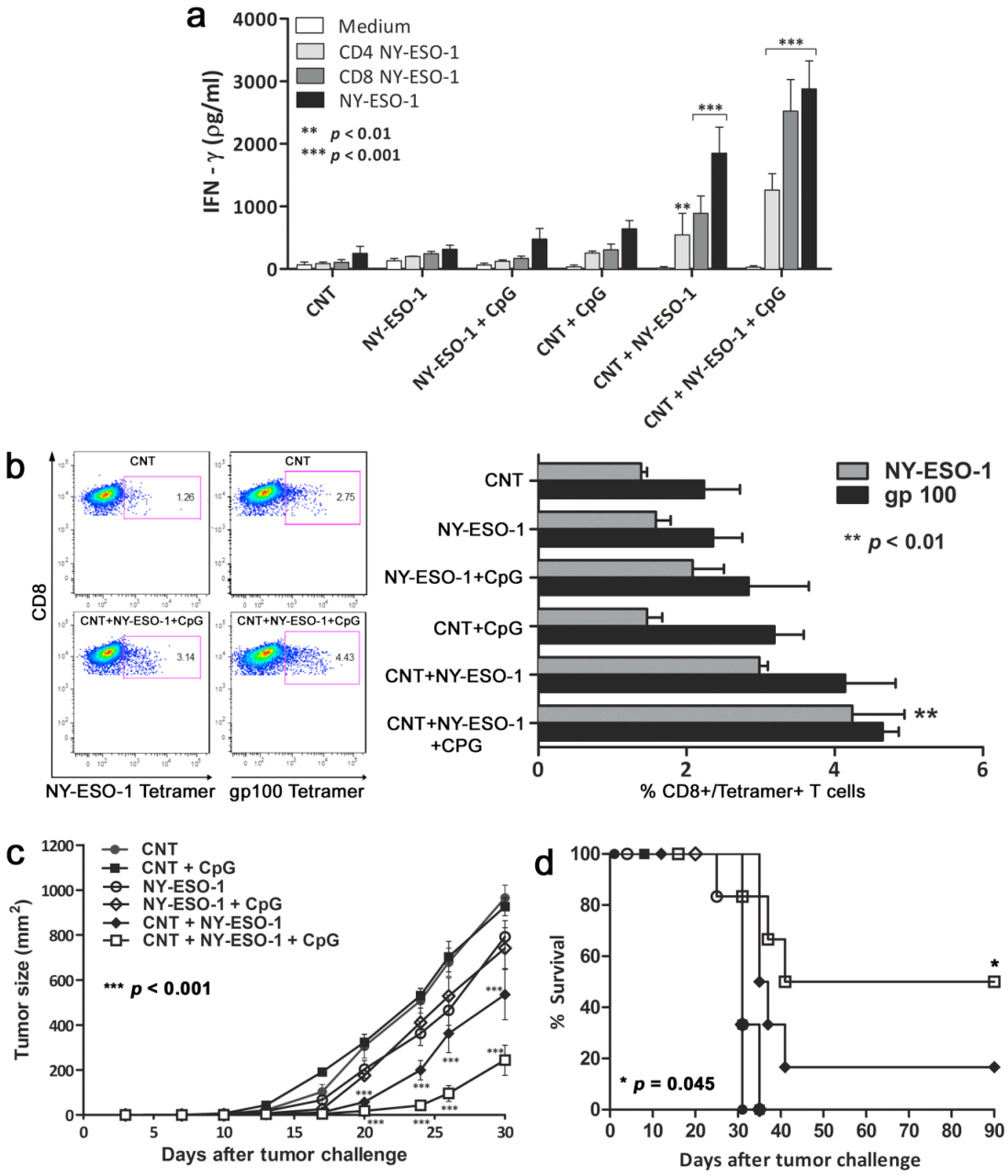
a
IFN - γ (ρg/ml)
Medium
CD4 NY-ESO-1
CD8 NY-ESO-1
NY-ESO-1
** p < 0.01
*** p < 0.001
CNT
NY-ESO-1
NY-ESO-1 + CpG
CNT + CpG
CNT + NY-ESO-1
CNT + NY-ESO-1 + CpG
b
CD8
NY-ESO-1 Tetramer
gp100 Tetramer
1.26
2.75
3.14
4.43
NY-ESO-1
gp 100
** p < 0.01
CNT+CpG
CNT+NY-ESO-1
CNT+NY-ESO-1 +CPG
% CD8+/Tetramer+ T cells
c
Tumor size (mm2)
CNT + NY-ESO-1
CNT + NY-ESO-1 + CpG
*** p < 0.001
Days after tumor challenge
d
% Survival
* p = 0.045
Days after tumor challenge

Figure 5

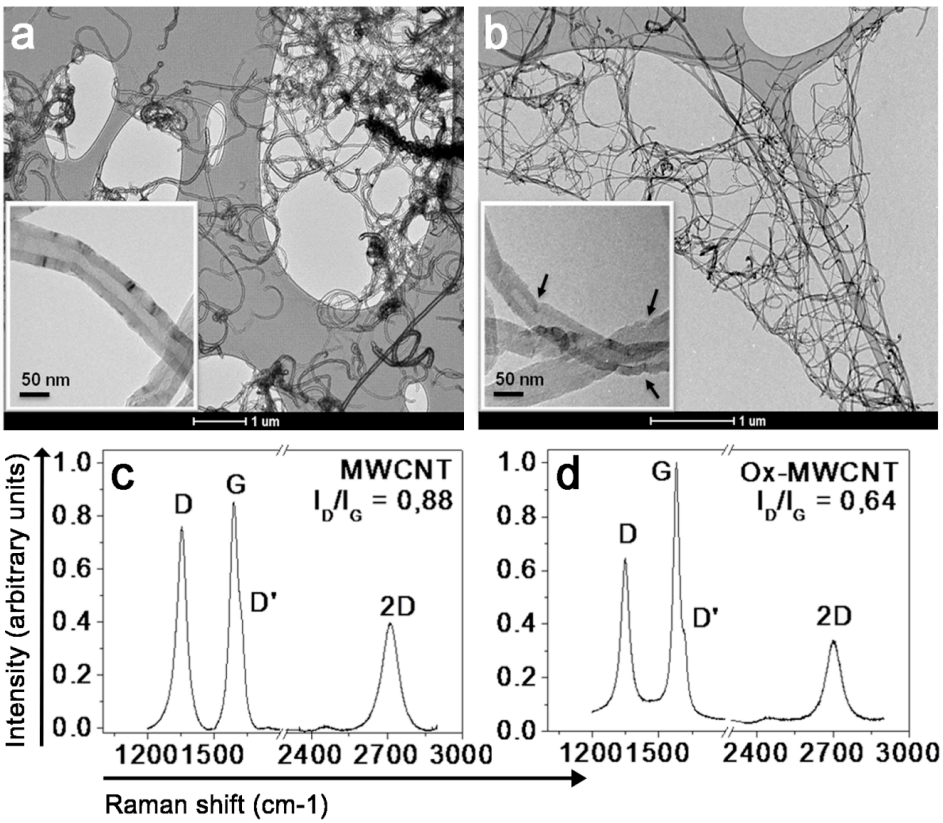

Supplementary Figure S1

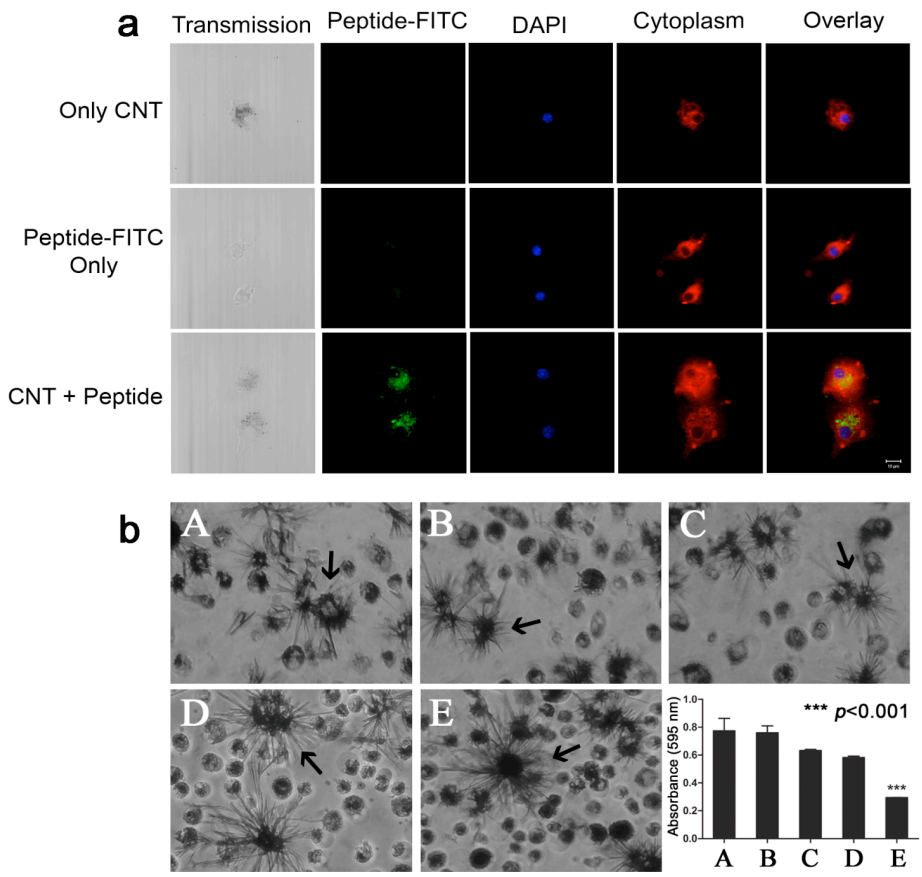

Supplementary Figure S2 |

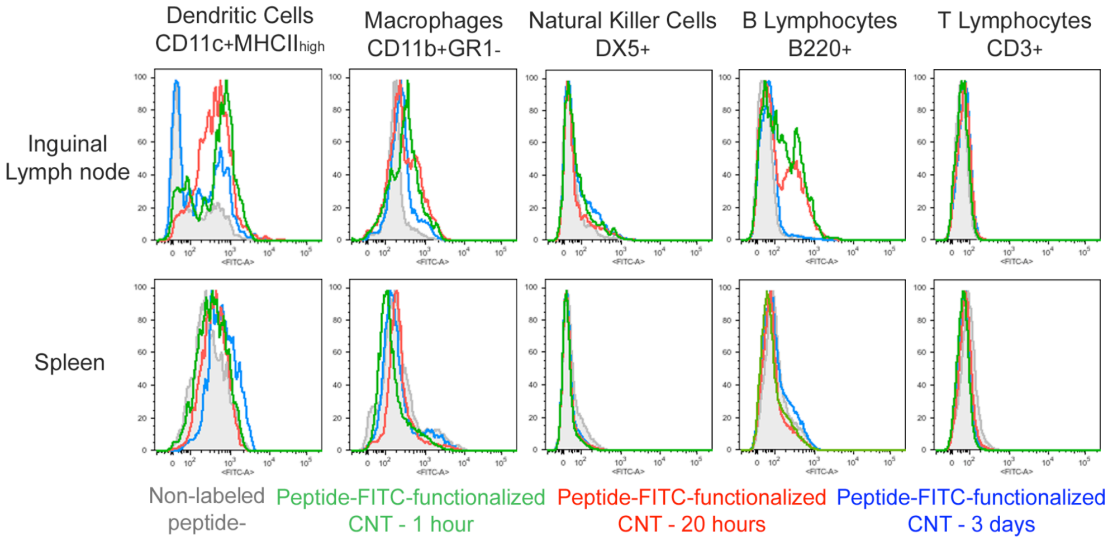

Supplementary Figure S3 |

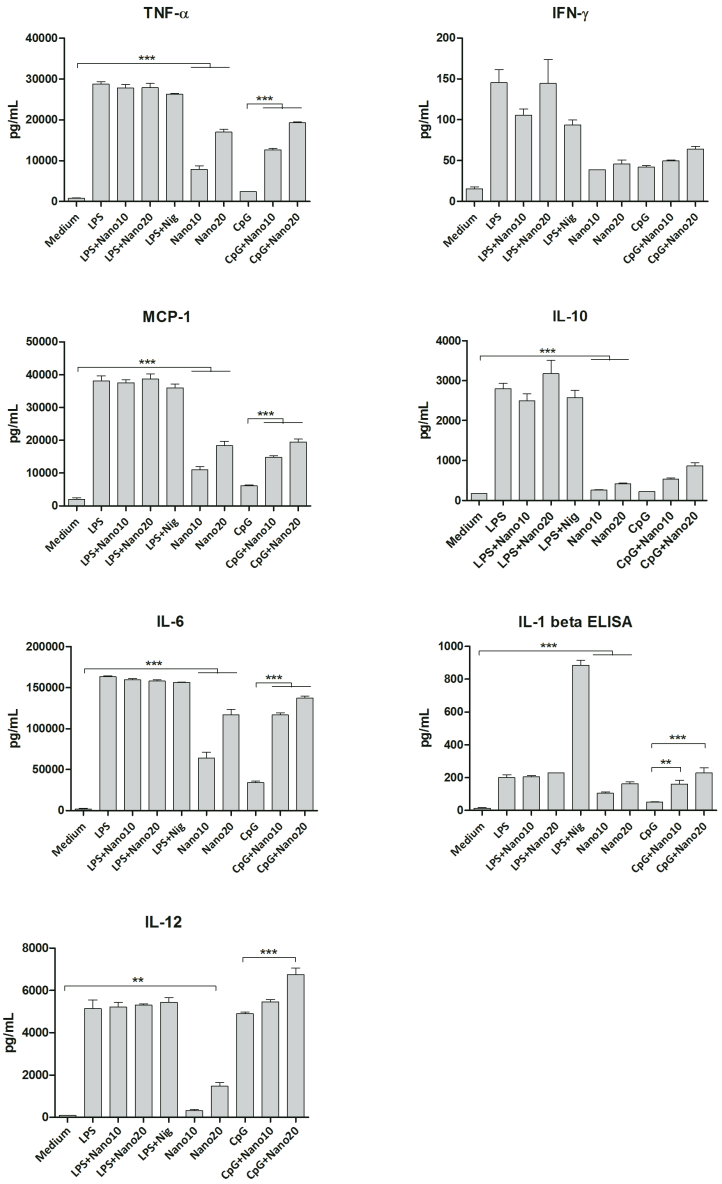

Supplementary Figure S4 |

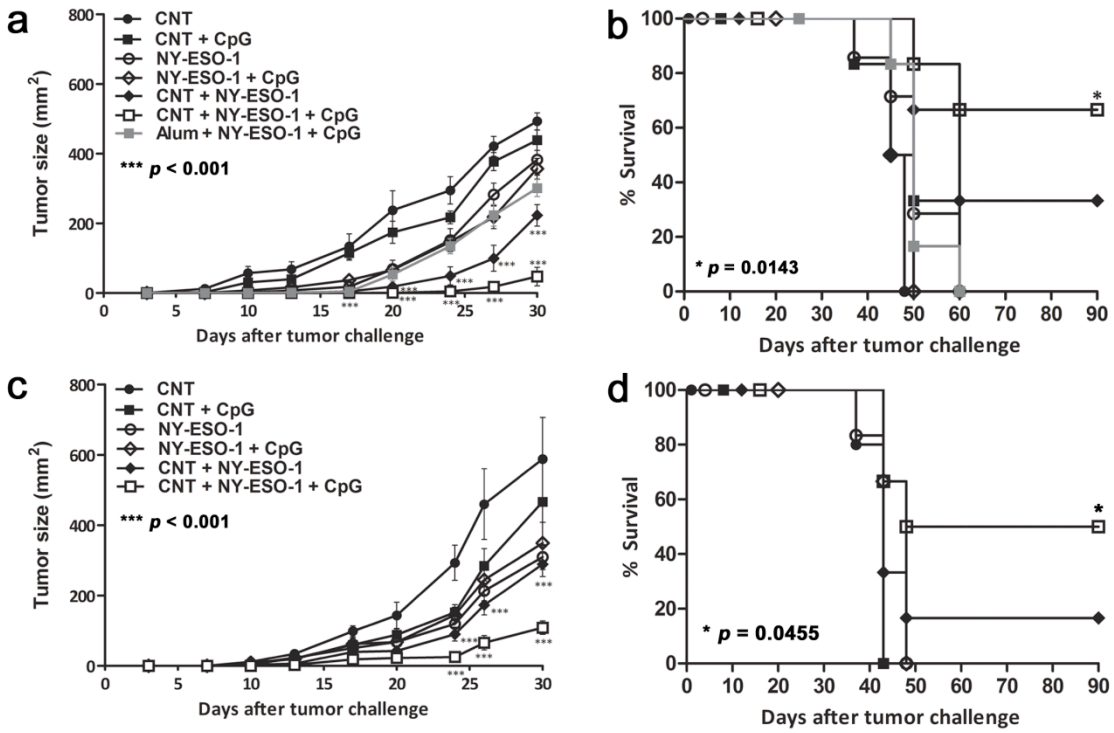

Supplementary Figure S5